Overview of Indirect Dark Matter Searches

Carsten Rott
Sungkyunkwan University, Korea

CosPA 2013
The 10th International Symposium on Cosmology and Particle Astrophysics
Nov. 12-15, 2013

Overview

- Motivation
  - WIMPs Signals
  - Strategies and Targets
- Instruments
- Indirect Searches
  - Current Status and Results
  - Future Prospects
- Conclusions

Searches for WIMPs

Searches for WIMPs

Production

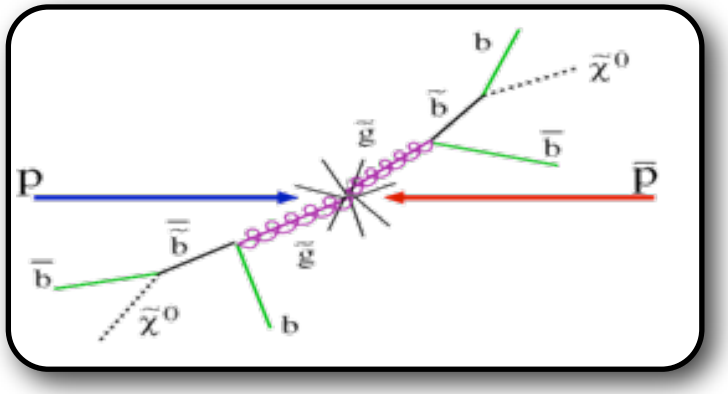

Searches for WIMPs

Production

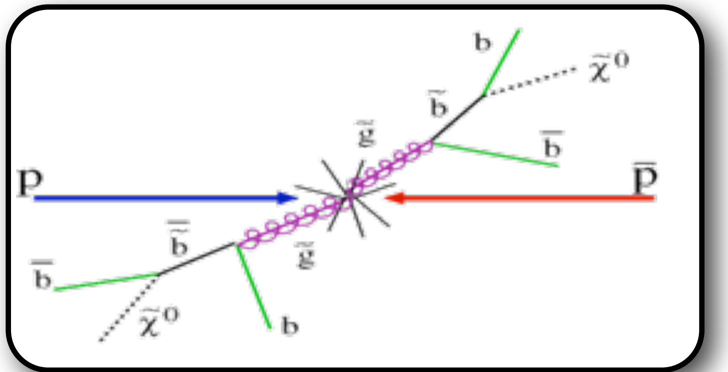

Colliders

Tuesday: Bhaskar Dutta

Searches for WIMPs

Production

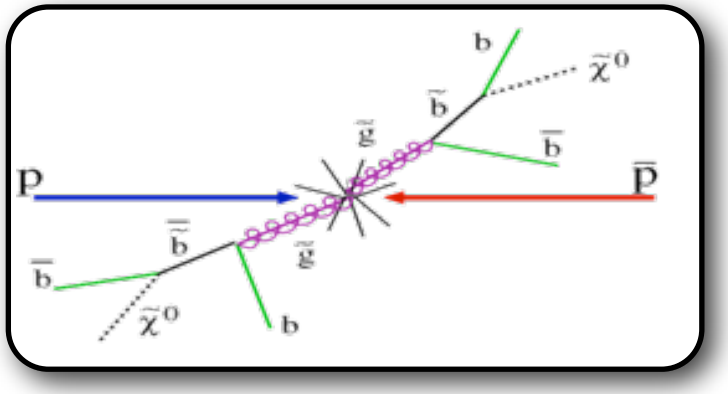

Colliders

Tuesday: Bhaskar Dutta

Scattering

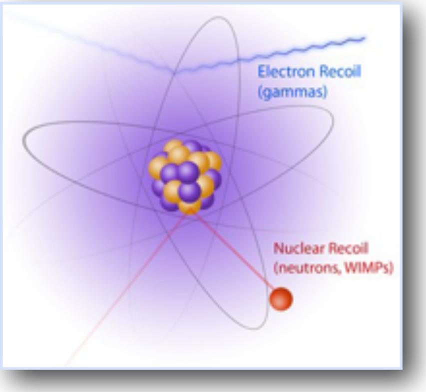

Searches for WIMPs

Production

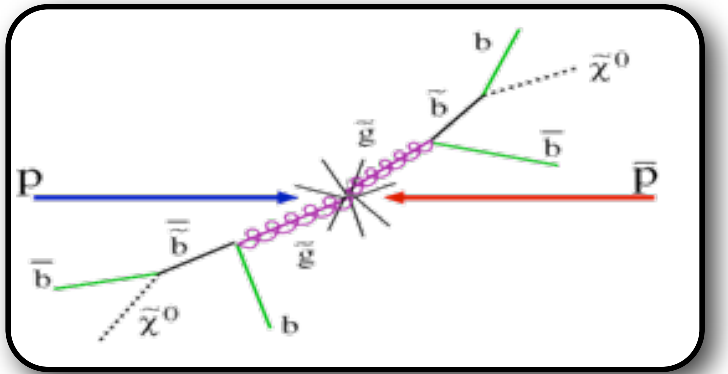

Scattering

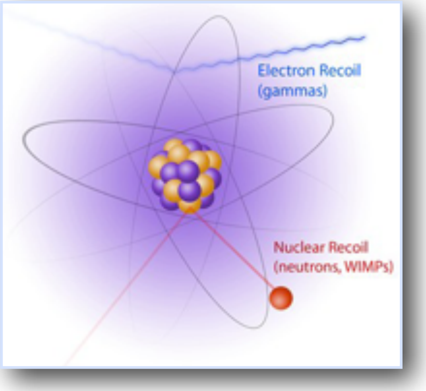

Colliders

Direct

Tuesday: Bhaskar Dutta

Tuesday: Rafael Lang

Searches for WIMPs

Production

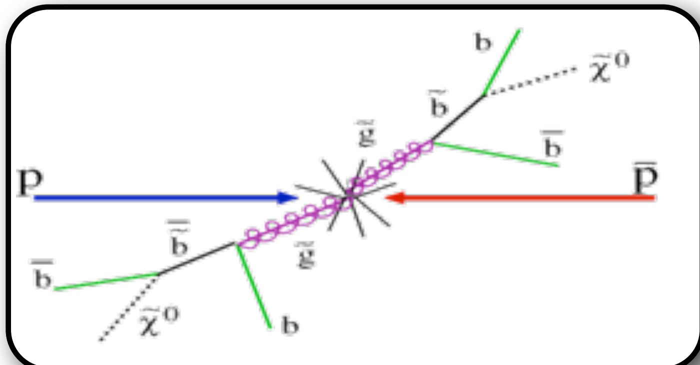

Colliders

Tuesday: Bhaskar Dutta

Scattering

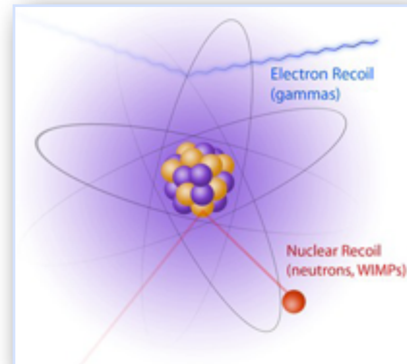

Direct

Tuesday: Rafael Lang

Annihilation

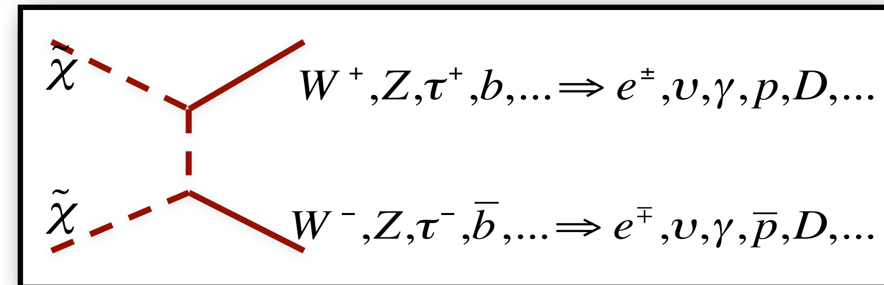

Searches for WIMPs

Production	Scattering	Annihilation

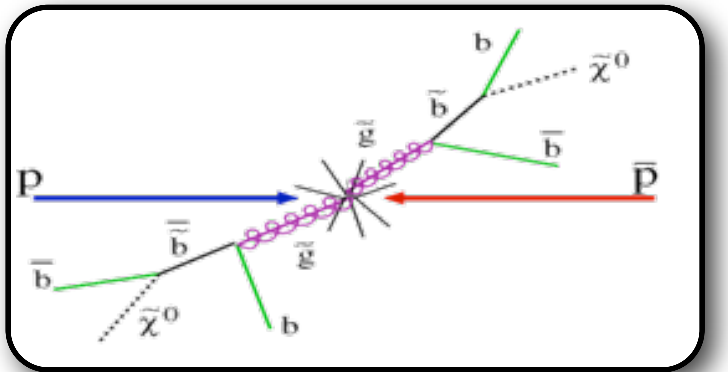

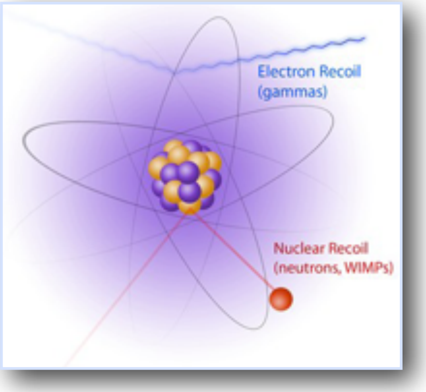

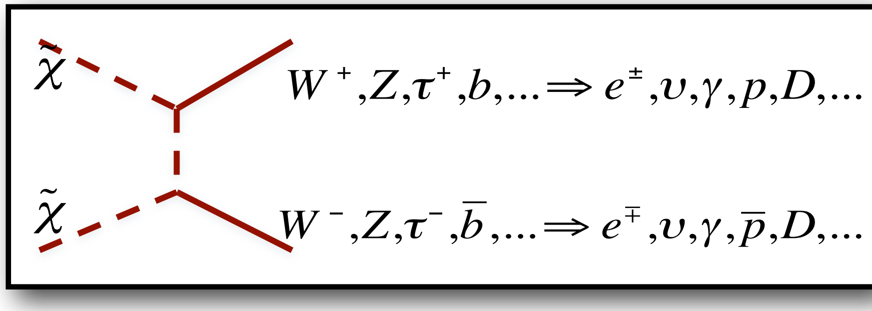

Colliders	Direct	Indirect

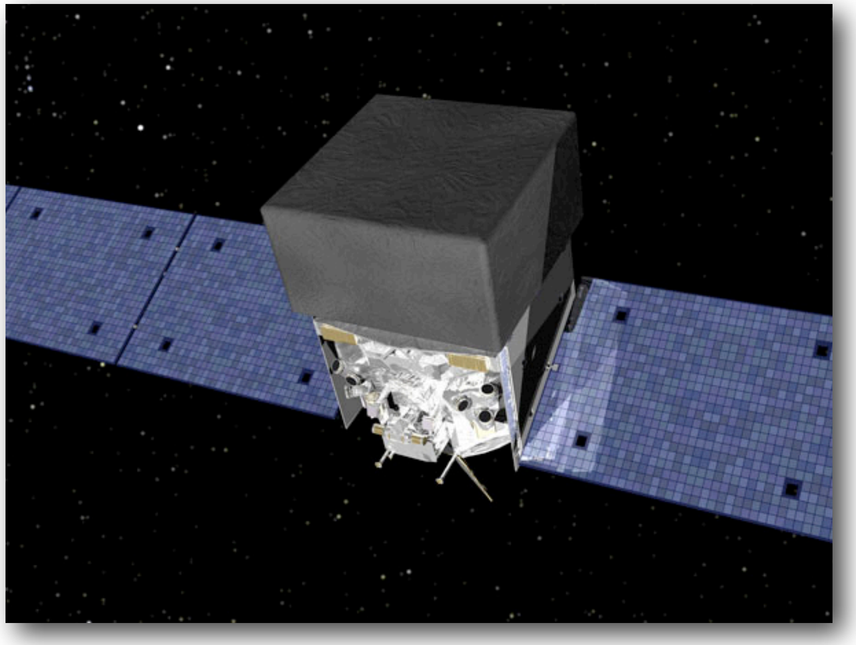

Tuesday: Bhaskar Dutta

Tuesday: Rafael Lang

Searches for WIMPs

Production

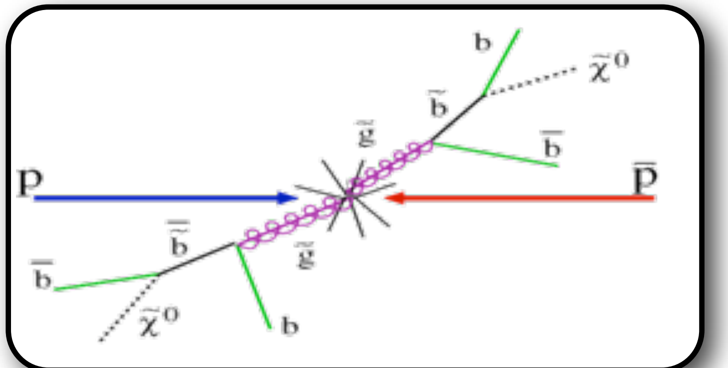

Colliders

Tuesday: Bhaskar Dutta

Scattering

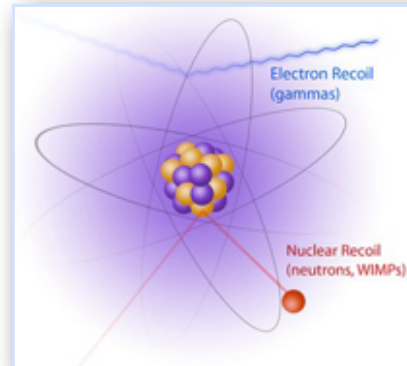

Direct

Tuesday: Rafael Lang

Annihilation

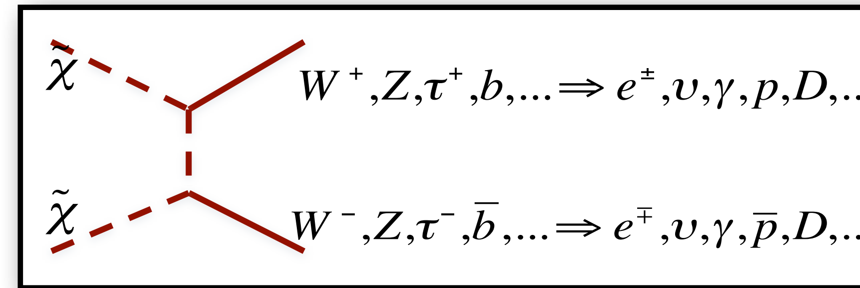

Indirect

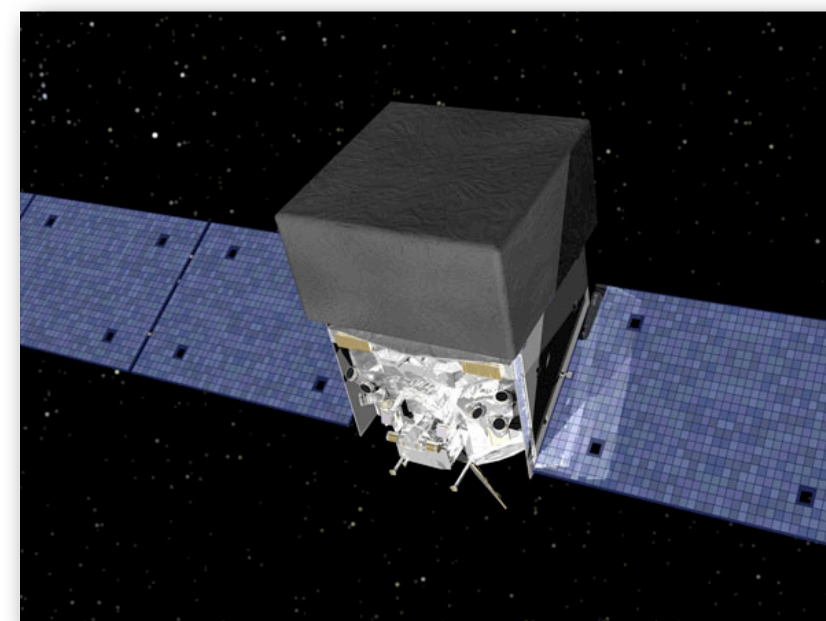

Thermal Relic

<σ_A v> - total self-annihilation cross section averaged over the relative velocity distribution

- If dark matter is a WIMP (χ) that is a thermal relic of the early Universe, then its $\langle\sigma_A v\rangle$ is revealed by its present-day mass density
- Evolution is determined by the competition between production and annihilation
- Common temperature T ($\equiv T_\gamma$)

$$\frac{dn}{dt} + 3Hn = \frac{d(na^3)}{a^3 dt} = \langle \sigma_A v \rangle \left(n_{eq}^2 - n^2 \right)$$

$$n_{eq} = g_\chi (mT/(2\pi))^{3/2} \exp(-m/T)$$

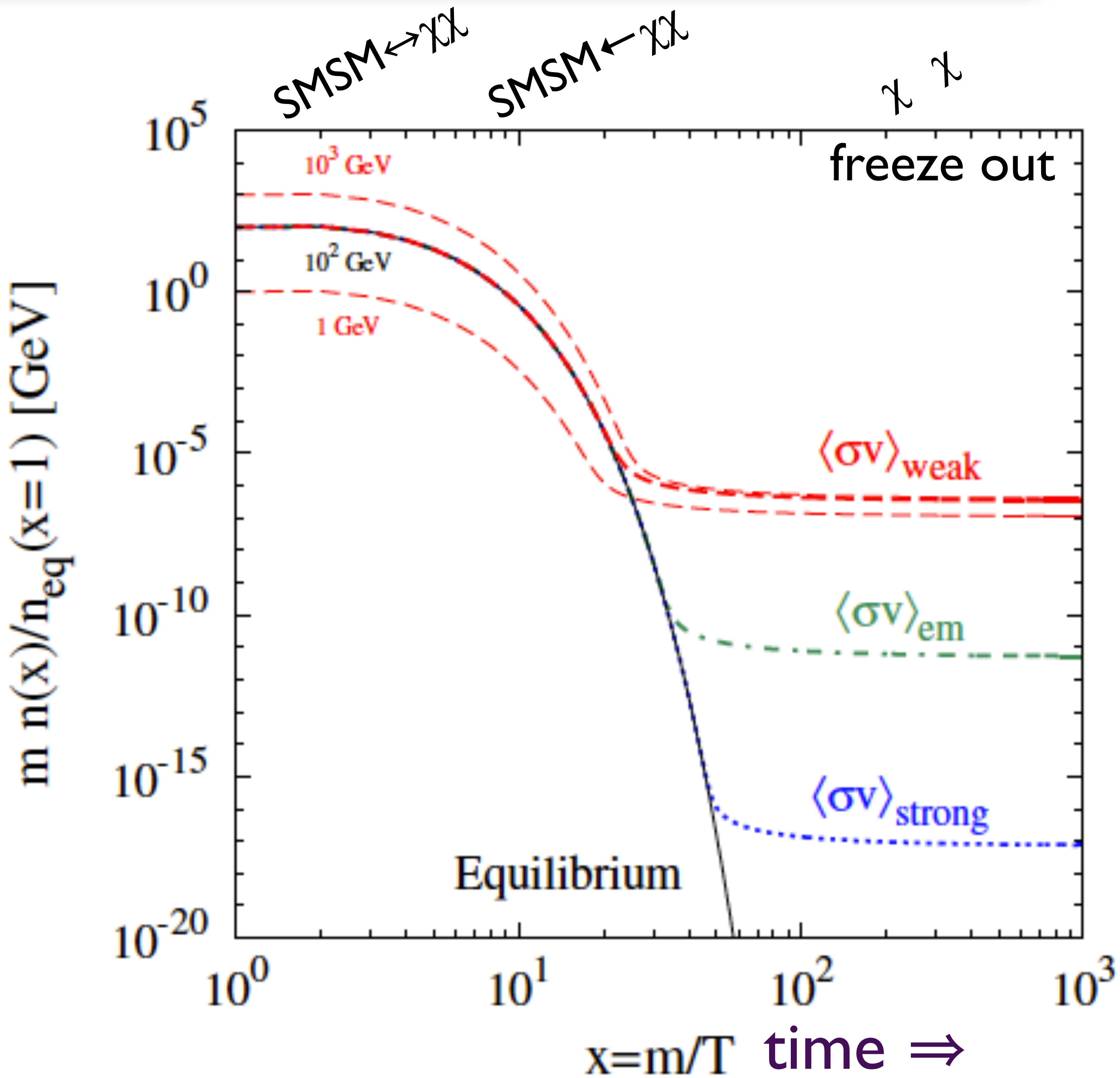

$m_\chi \approx 1\,\mathrm{GeV} \Rightarrow \langle\sigma_A v\rangle \sim 4.5 \cdot 10^{-26}\ \mathrm{cm^3 s^{-1}}$

$m_\chi > 5\,\mathrm{GeV} \Rightarrow \langle\sigma_A v\rangle \sim 2 \cdot 10^{-26}\ \mathrm{cm^3 s^{-1}}$

G. Steigman, B. Dasgupta, J.F. Beacom 1204.3622
G. Jungman, M. Kamionkowski, K. Griest, Phys. Rept., 267 (1996) 195.

Dark Matter Annihilation Signals

- Interactions that determine the WIMP relic abundance also lead to self-annihilations in the present epoch
  - Identify overdense regions of Dark Matter ⇒self-annihilation can occur at significant rates
- Pick prominent Dark Matter target
- Understand backgrounds
- Features in the signal enhance to chance distinguish backgrounds
  - Line / End-point

Annihilation Rate ~ρ^2
(Decay Rate ~ρ)

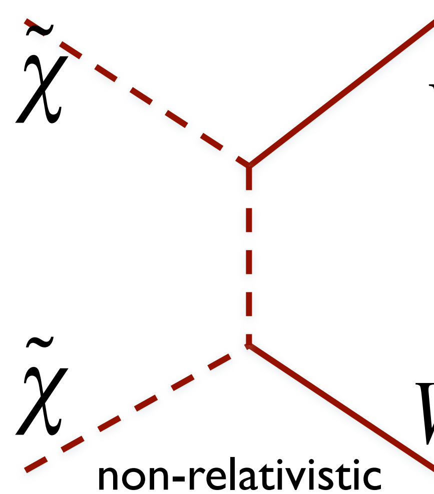

$W^+, Z, \tau^+, b, \ldots \Rightarrow e^\pm, \upsilon, \gamma, p, D, \ldots$

$W^-, Z, \tau^-, \bar{b}, \ldots \Rightarrow e^\mp, \upsilon, \gamma, \bar{p}, D, \ldots$

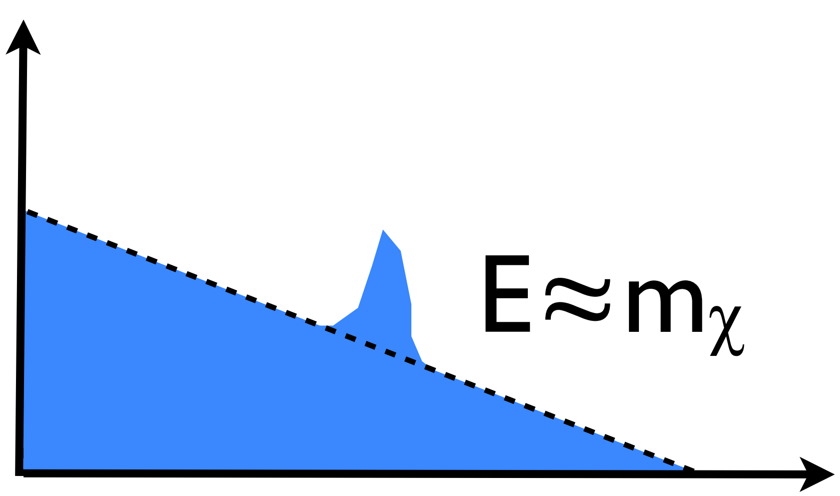

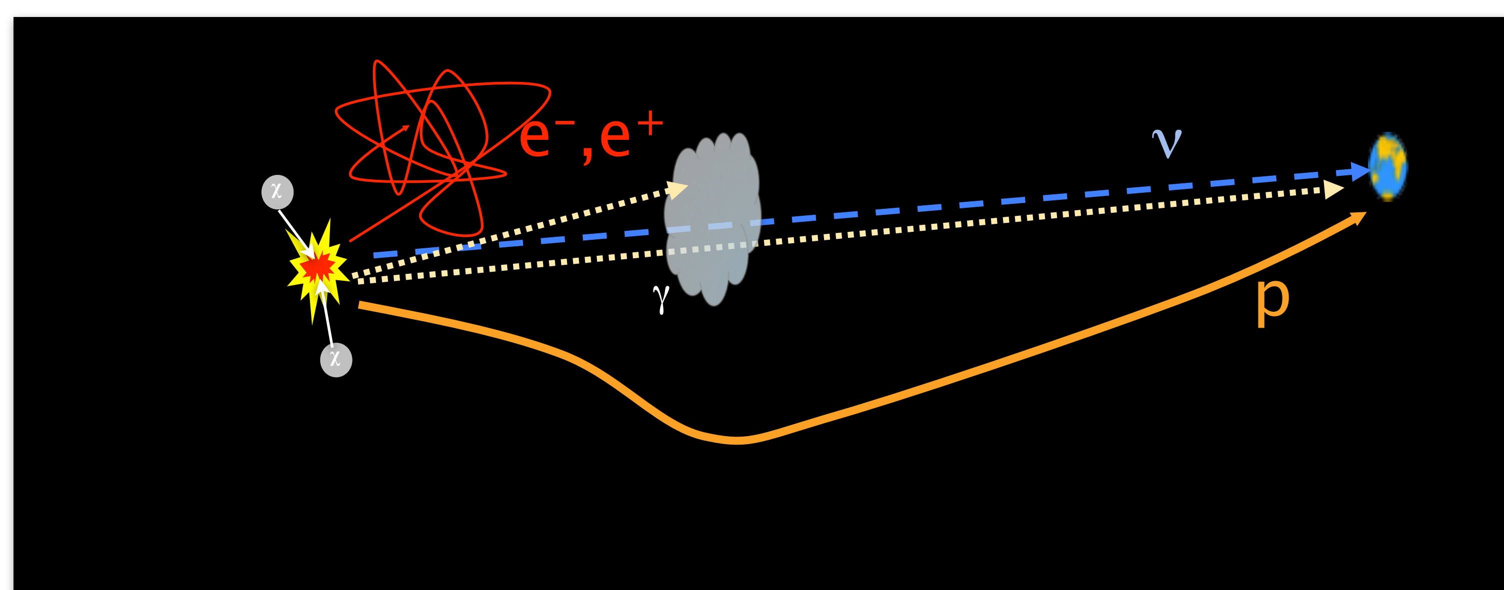

Dark Matter Annihilation Signals

- Interactions that determine the WIMP relic abundance also lead to self-annihilations in the present epoch
  - Identify overdense regions of Dark Matter ⇒self-annihilation can occur at significant rates
- Pick prominent Dark Matter target
- Understand backgrounds
- Features in the signal enhance to chance distinguish backgrounds
  - Line / End-point

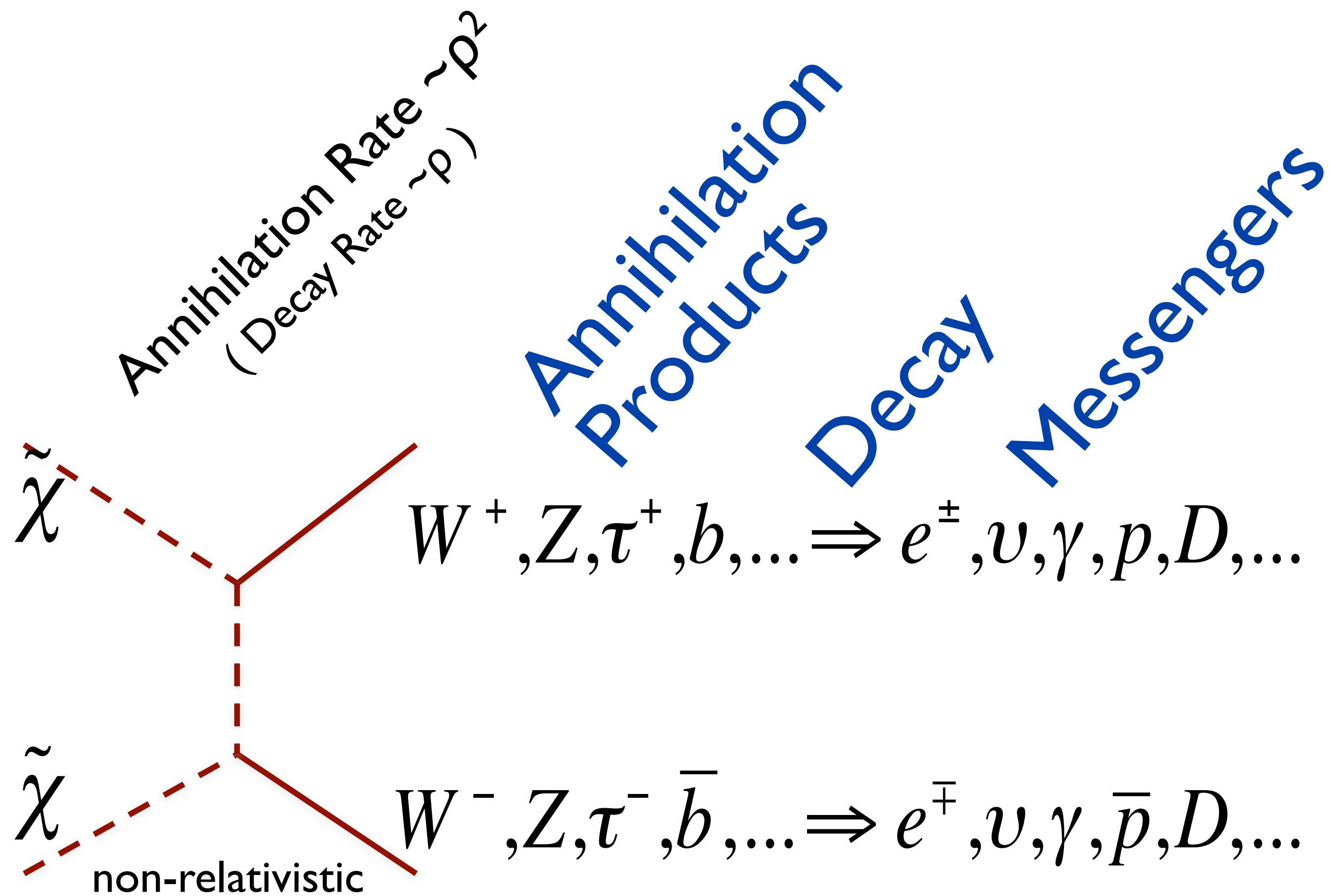

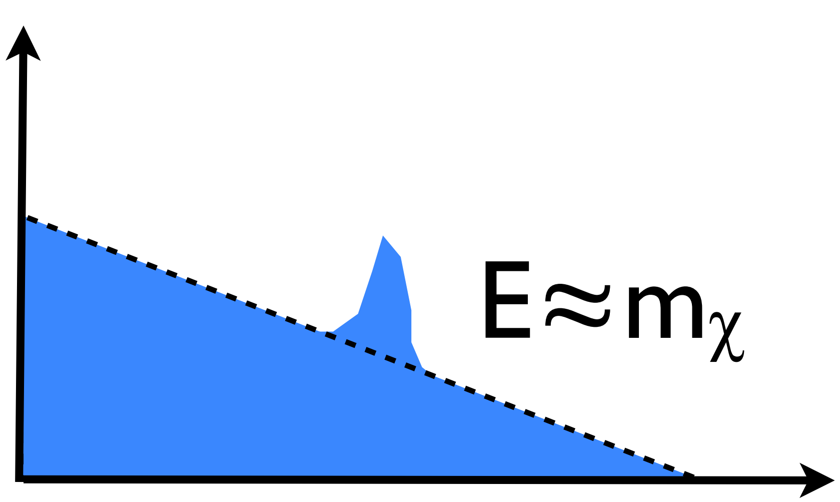

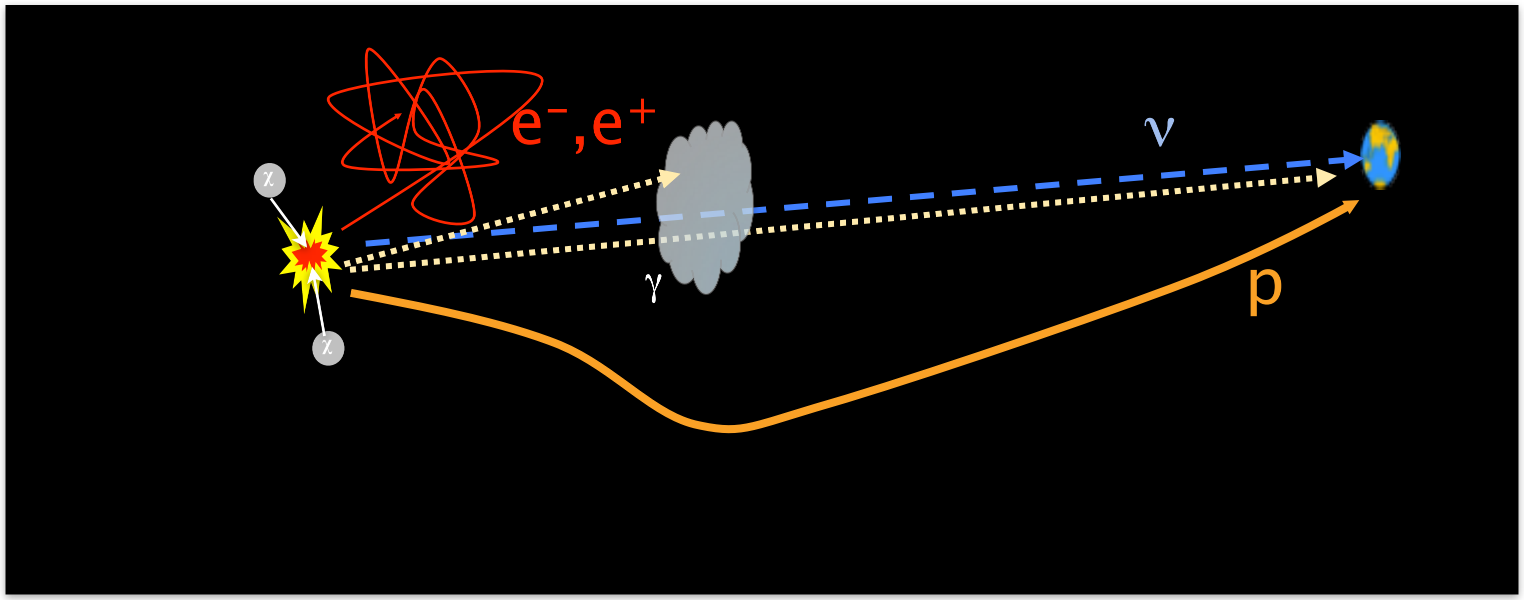

Strategies and Targets

Dark Matter at all scales

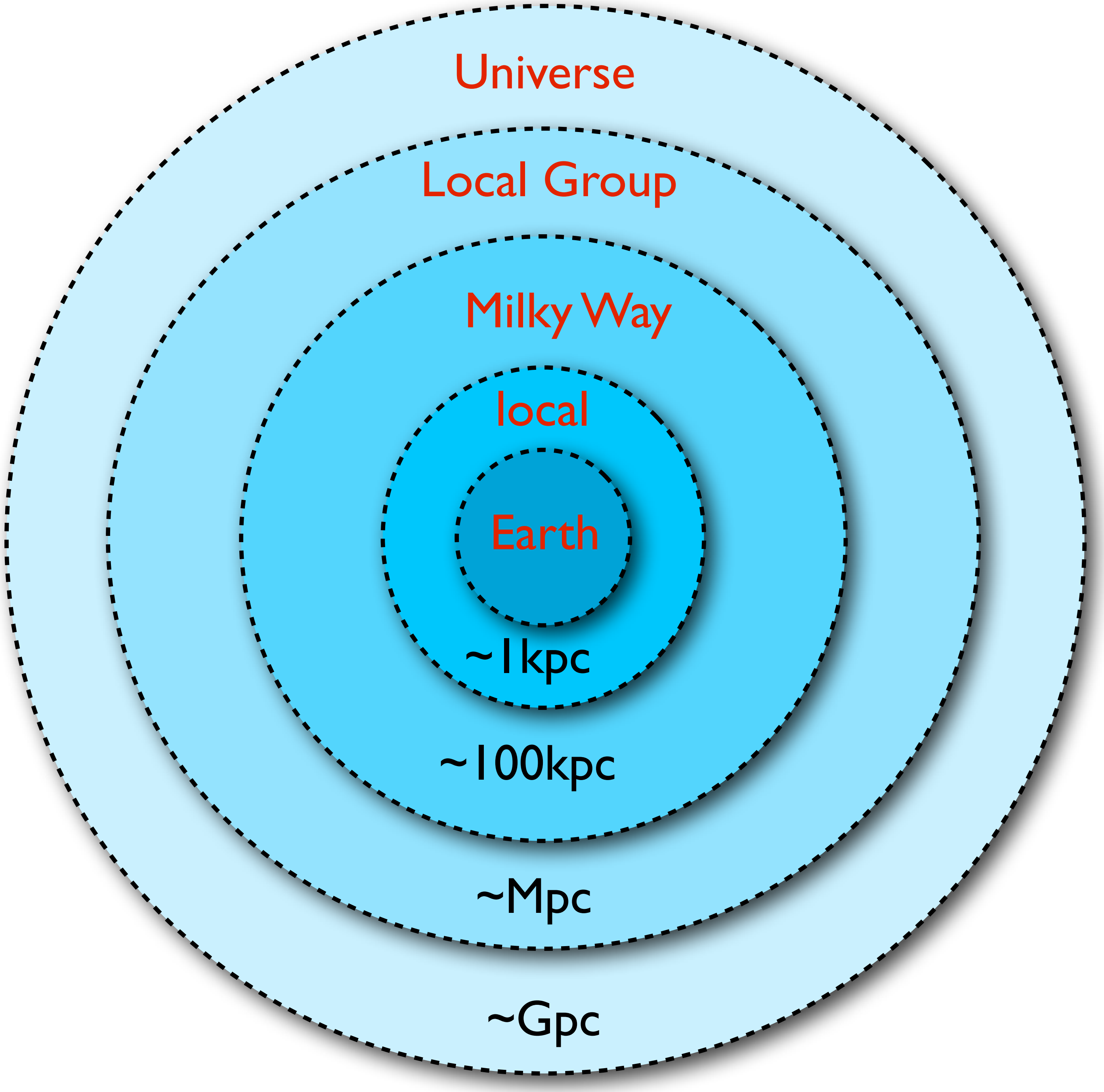

Dark Matter at all scales

“Evidence”

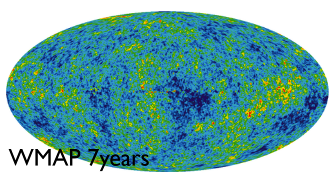

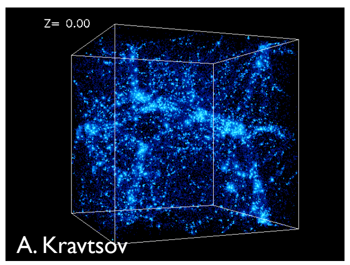

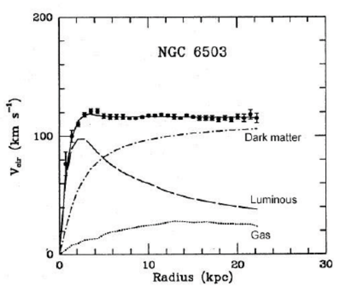

Begeman, Broels & Sanders (1991)

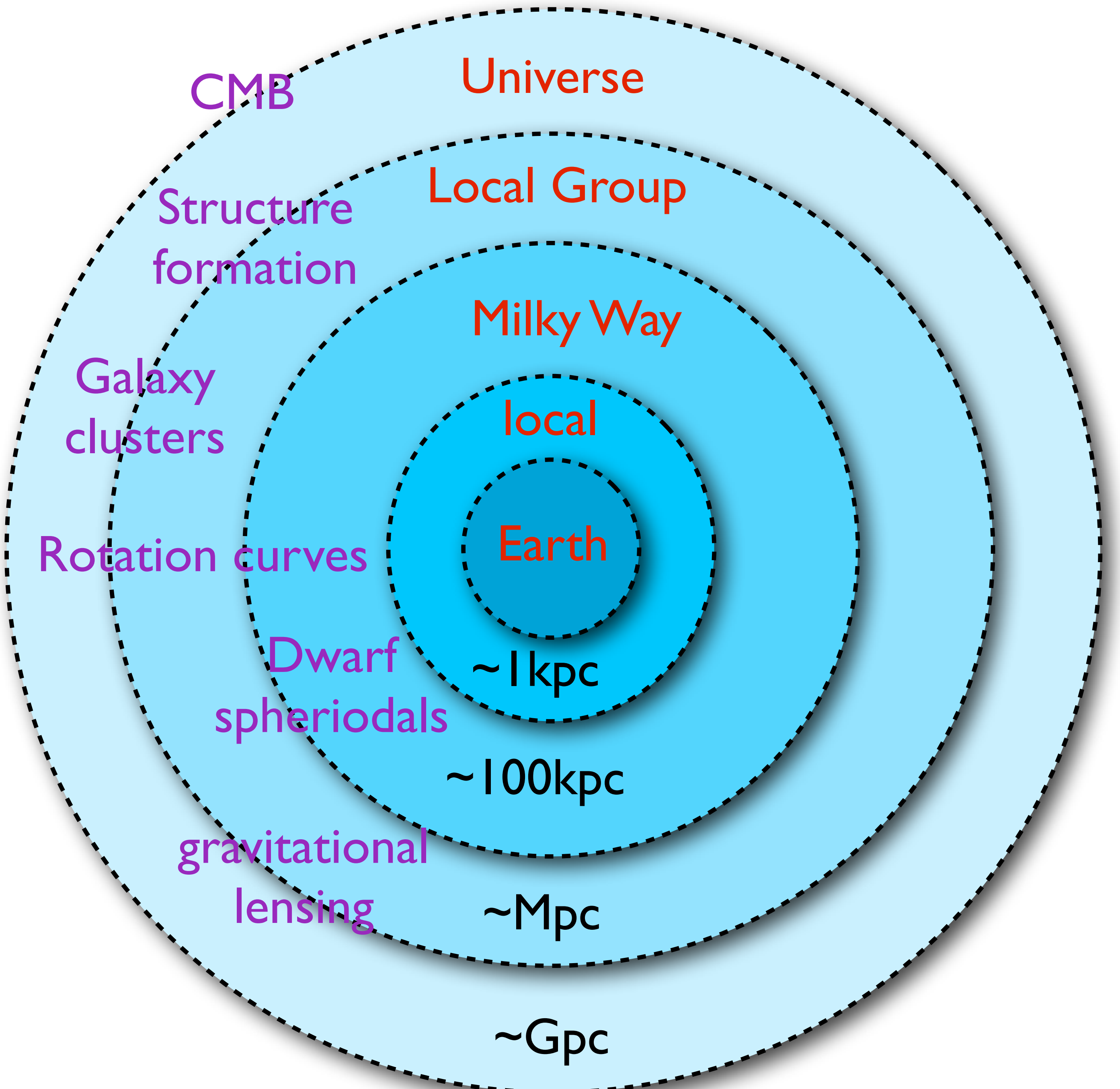

Dark Matter at all scales

“Evidence”

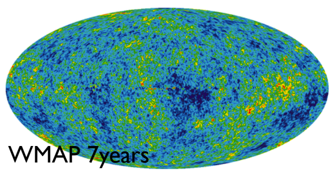

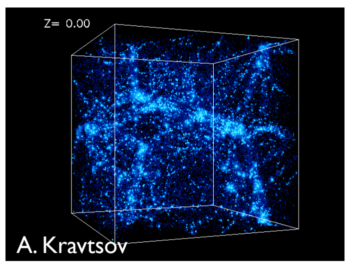

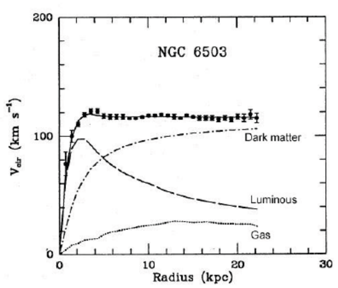

Begeman, Broels & Sanders (1991)

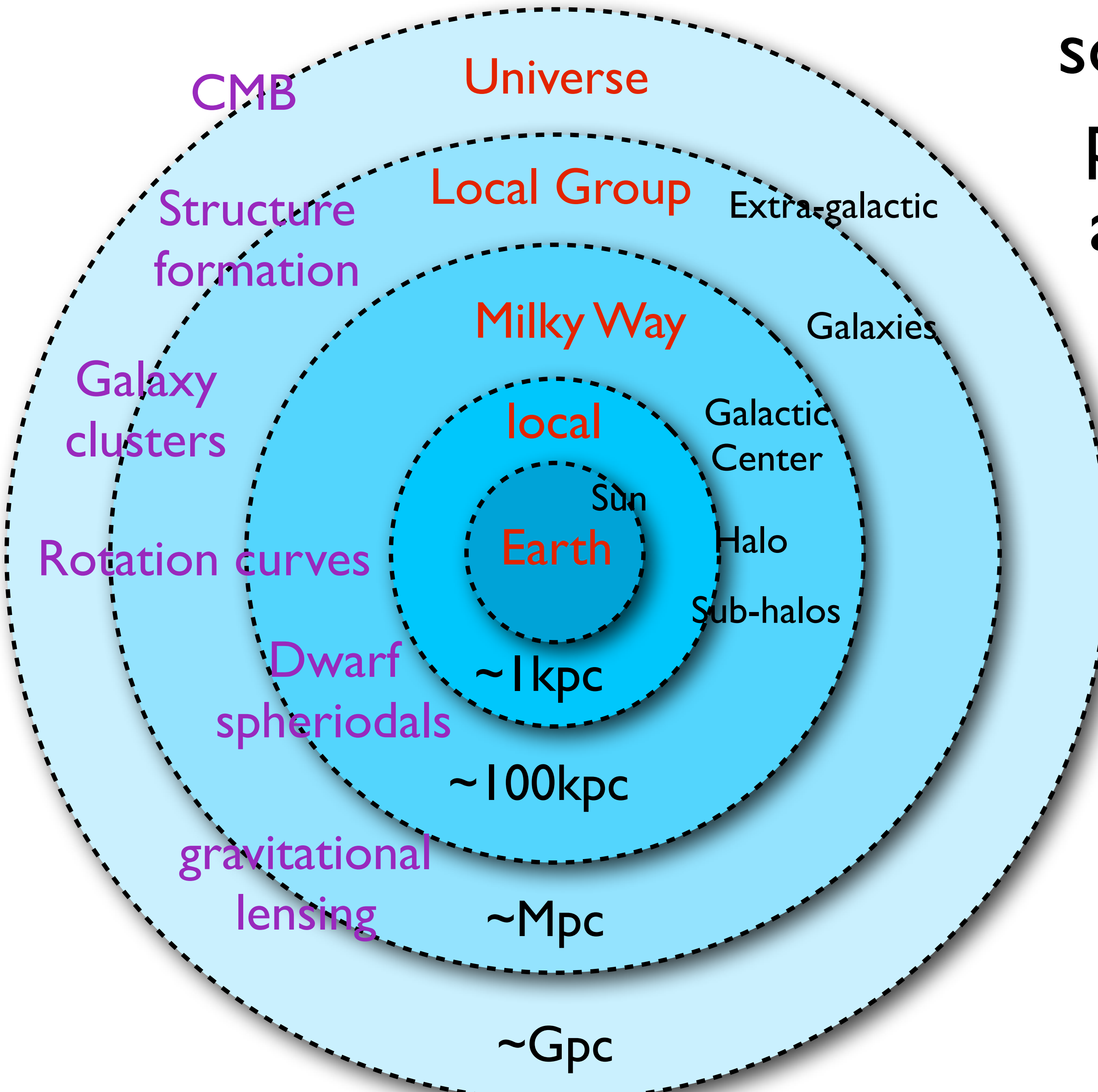

Other objects or sources expected to produce significant annihilation signals

Dark Matter at all scales

"Evidence"

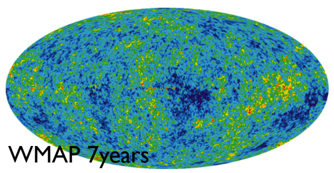

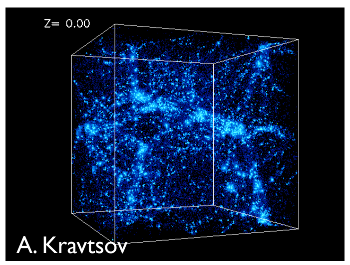

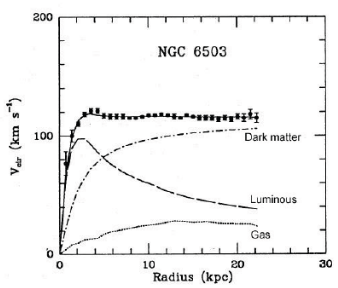

Begeman, Broels & Sanders (1991)

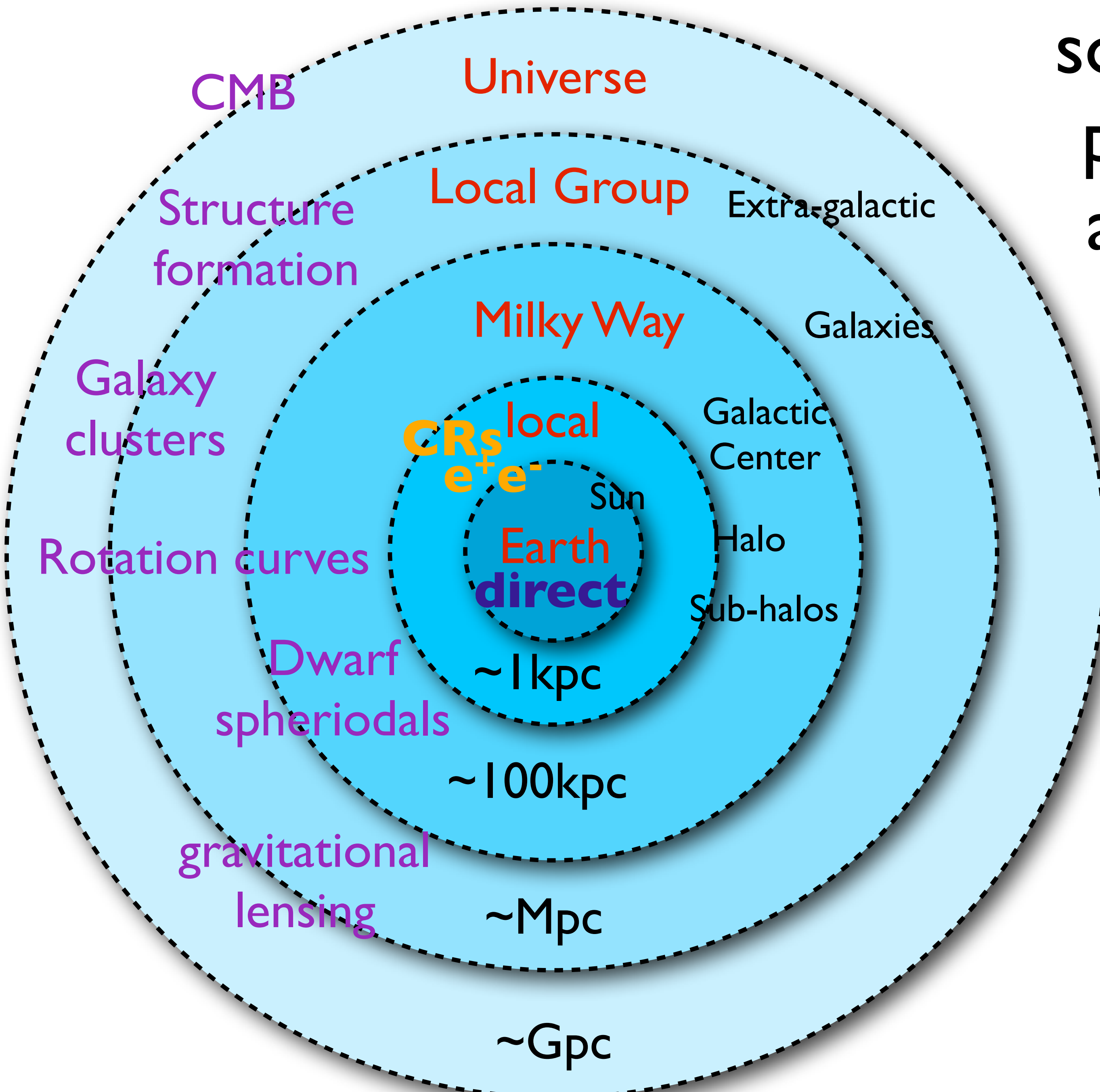

Other objects or sources expected to produce significant annihilation signals

Dark Matter at all scales

“Evidence”

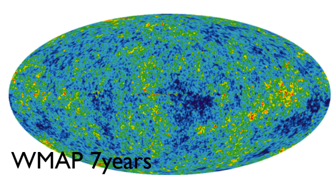

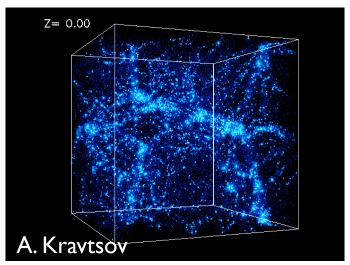

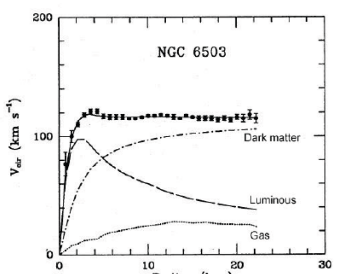

Begeman, Broels & Sanders (1991)

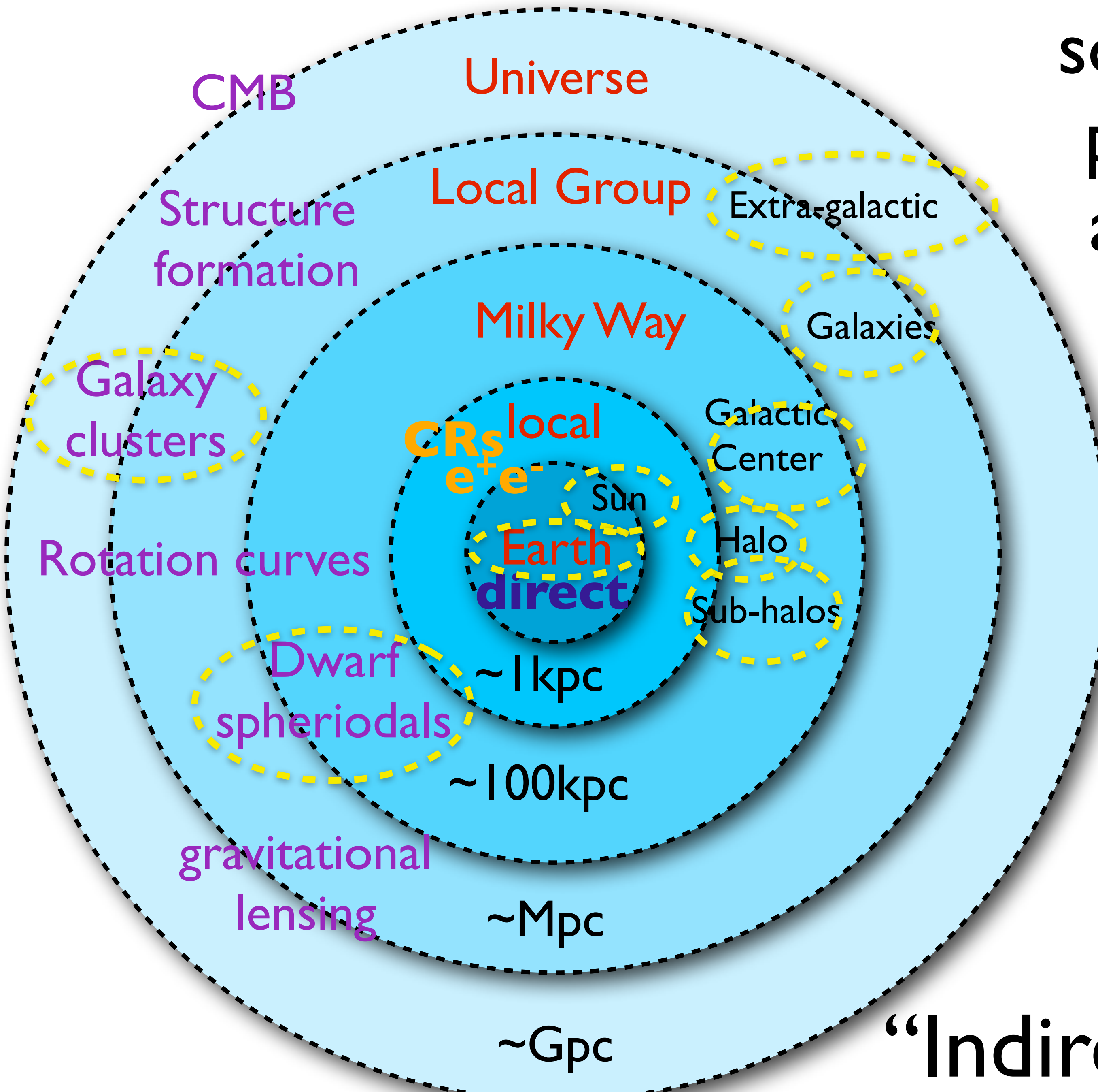

Other objects or sources expected to produce significant annihilation signals

“Indirect Targets” for ν,γ

Individual sources and diffuse

Sources of High Energy Neutrinos

Dark Matter self-annihilation or decay

Annihilation — **K_{ann}** — **$J(\Psi)_{ann}$**

$$\frac{d\Phi}{dE}(E,\phi,\theta) = \frac{1}{4\pi}\frac{\langle\sigma_A v\rangle}{2m_\chi^2}\sum_f Br(f)\frac{dN_f}{dE} \times \int_{\Delta\Omega(\phi,\theta)} d\Omega' \int_{\text{los}} \rho^2(r(l,\phi'))dl(r,\phi')$$

Measure Flux — **Particle Physics** — **Dark Matter Distribution**

$$\frac{d\Phi}{dE}(E,\phi,\theta) = \frac{1}{4\pi}\frac{1}{m_\chi \tau_\chi}\sum_f Br(f)\frac{dN_f}{dE} \times \int_{\Delta\Omega(\phi,\theta)} d\Omega' \int_{los} \rho(r(l,\phi'))dl(r,\phi')$$

Decay — **K_{decay}** — **$J(\Psi)_{decay}$**

expected prompt signal for particles propagating directly to the observer (gamma-rays, neutrinos)

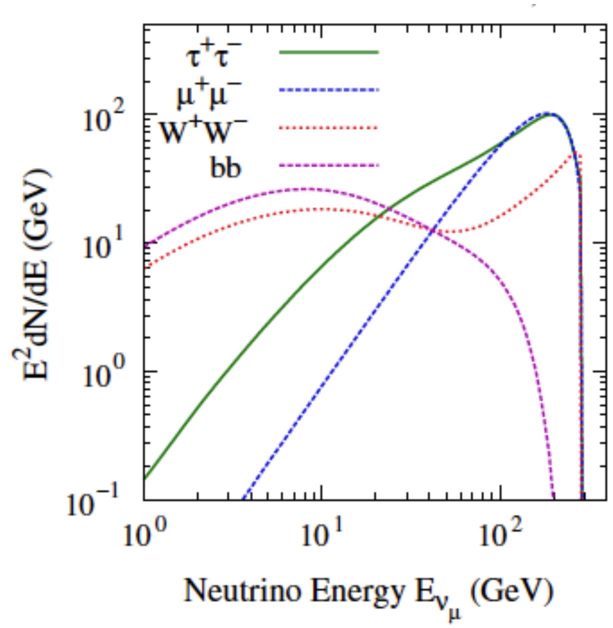

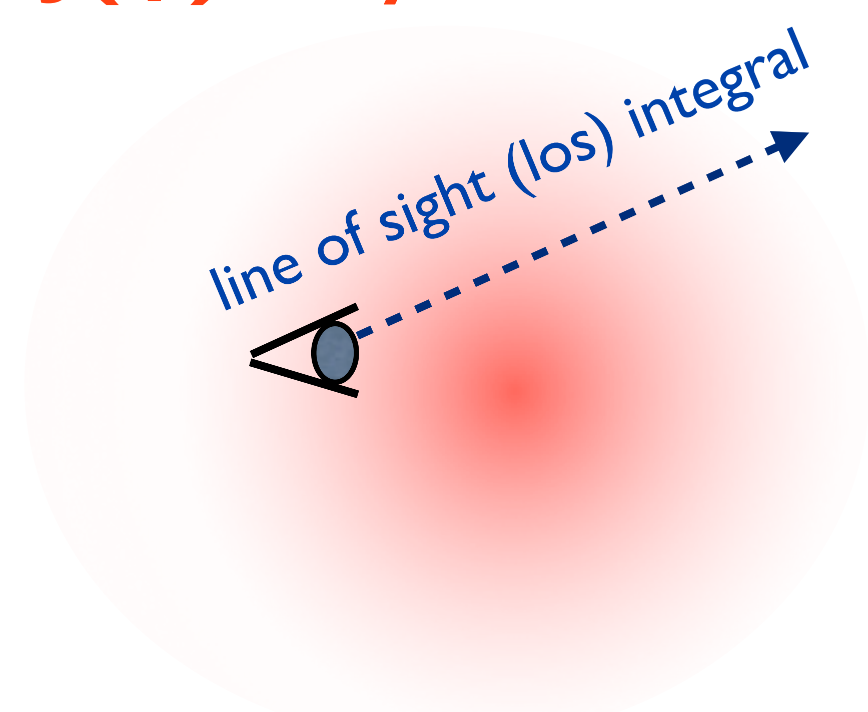

Sources of High Energy Neutrinos

Dark Matter self-annihilation or decay

Annihilation — K_{ann} — $J(\Psi)_{ann}$

$$\frac{d\Phi}{dE}(E,\phi,\theta) = \frac{1}{4\pi}\frac{\langle\sigma_A v\rangle}{2m_\chi^2}\sum_f Br(f)\frac{dN_f}{dE} \times \int_{\Delta\Omega(\phi,\theta)} d\Omega' \int_{\mathrm{los}} \rho^2(r(l,\phi'))dl(r,\phi')$$

Measure Flux — **Particle Physics** — **Dark Matter Distribution**

$$\frac{d\Phi}{dE}(E,\phi,\theta) = \frac{1}{4\pi}\frac{1}{m_\chi \tau_\chi}\sum_f Br(f)\frac{dN_f}{dE} \times \int_{\Delta\Omega(\phi,\theta)} d\Omega' \int_{los} \rho(r(l,\phi'))dl(r,\phi')$$

Decay — K_{decay} — $J(\Psi)_{decay}$

expected prompt signal for particles propagating directly to the observer (gamma-rays, neutrinos)

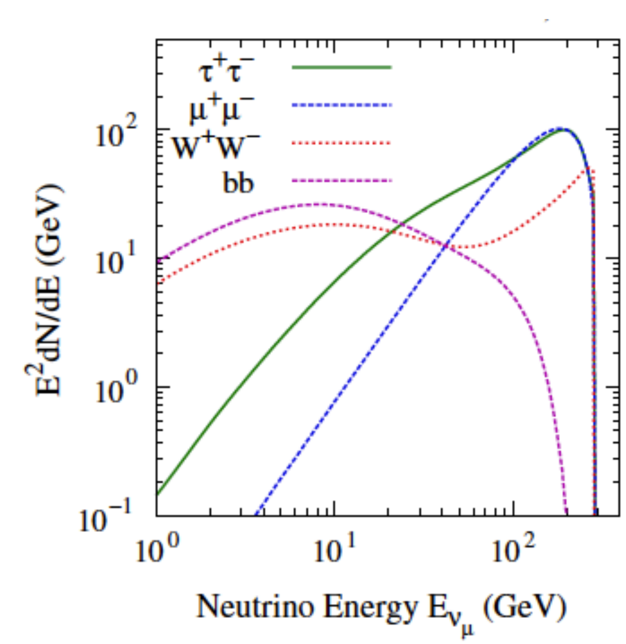

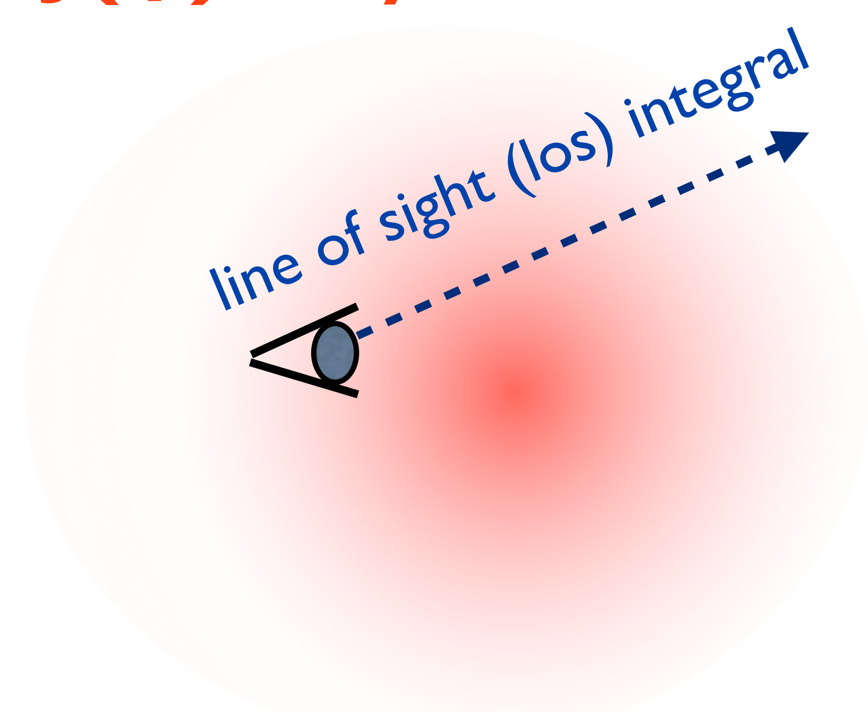

Sources of High Energy Neutrinos

Dark Matter self-annihilation or decay

Annihilation — K_{ann} — $J(\Psi)_{ann}$

$$\frac{d\Phi}{dE}(E,\phi,\theta) = \boxed{\frac{1}{4\pi}\frac{\langle\sigma_A v\rangle}{2m_\chi^2}\sum_f Br(f)\frac{dN_f}{dE}} \times \boxed{\int_{\Delta\Omega(\phi,\theta)} d\Omega' \int_{\text{los}} \rho^2(r(l,\phi'))dl(r,\phi')}$$

Measure Flux — **Particle Physics** — **Dark Matter Distribution**

$$\frac{d\Phi}{dE}(E,\phi,\theta) = \boxed{\frac{1}{4\pi}\frac{1}{m_\chi \tau_\chi}\sum_f Br(f)\frac{dN_f}{dE}} \times \boxed{\int_{\Delta\Omega(\phi,\theta)} d\Omega' \int_{los} \rho(r(l,\phi'))dl(r,\phi')}$$

Decay — K_{decay} — $J(\Psi)_{decay}$

expected prompt signal
for particles propagating
directly to the observer
(gamma-rays, neutrinos)

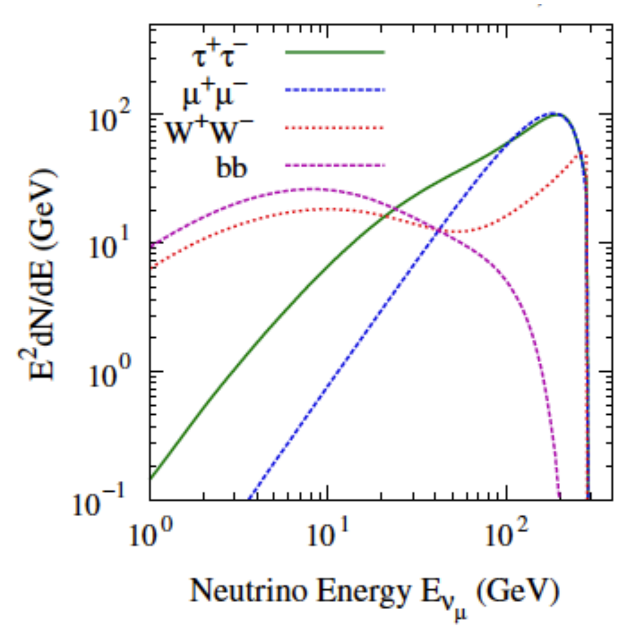

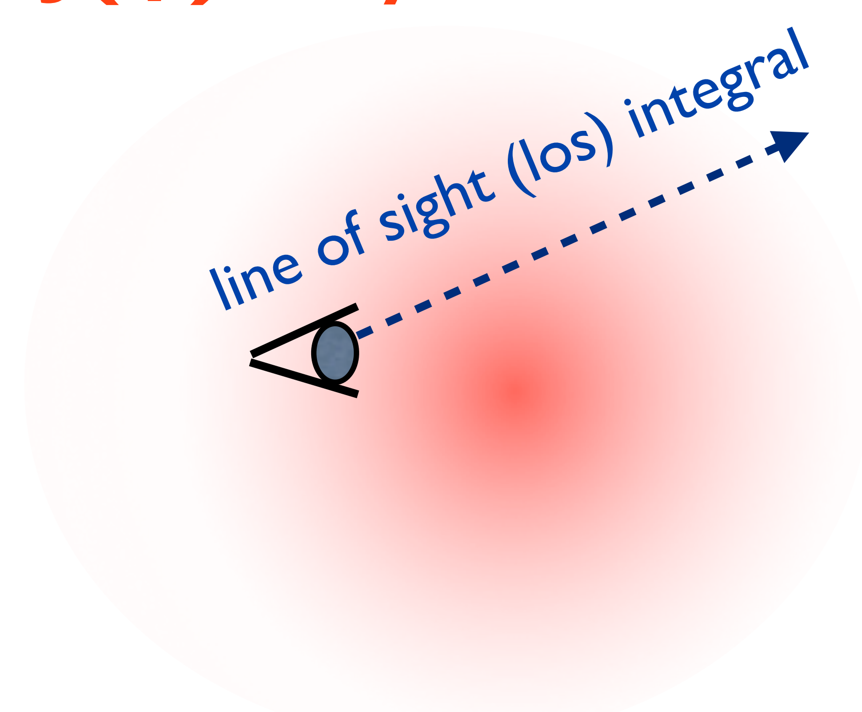

Sources of High Energy Neutrinos

Dark Matter self-annihilation or decay

Annihilation — **K_{ann}** — **$J(\Psi)_{ann}$**

$$\frac{d\Phi}{dE}(E,\phi,\theta) = \frac{1}{4\pi}\frac{\langle\sigma_A v\rangle}{2m_\chi^2}\sum_f Br(f)\frac{dN_f}{dE} \times \int_{\Delta\Omega(\phi,\theta)} d\Omega' \int_{\rm los} \rho^2(r(l,\phi'))dl(r,\phi')$$

Measure Flux — Particle Physics — Dark Matter Distribution

$$\frac{d\Phi}{dE}(E,\phi,\theta) = \frac{1}{4\pi}\frac{1}{m_\chi \tau_\chi}\sum_f Br(f)\frac{dN_f}{dE} \times \int_{\Delta\Omega(\phi,\theta)} d\Omega' \int_{los} \rho(r(l,\phi'))dl(r,\phi')$$

Decay — **K_{decay}** — **$J(\Psi)_{decay}$**

expected prompt signal
for particles propagating
directly to the observer
(gamma-rays, neutrinos)

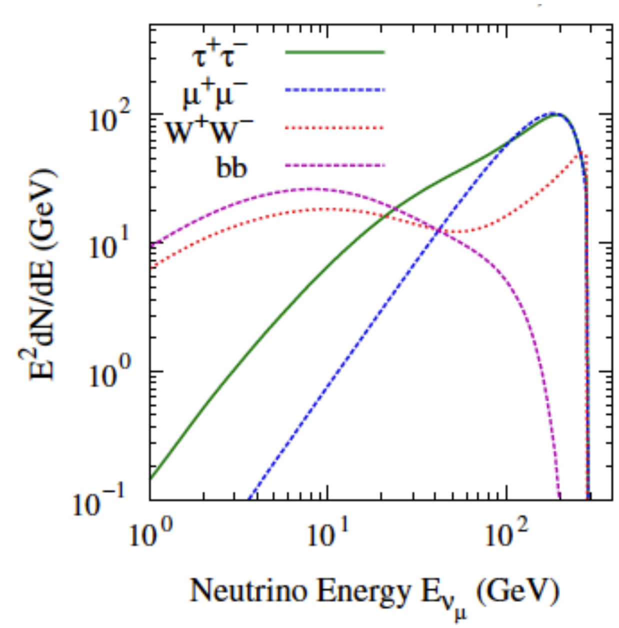

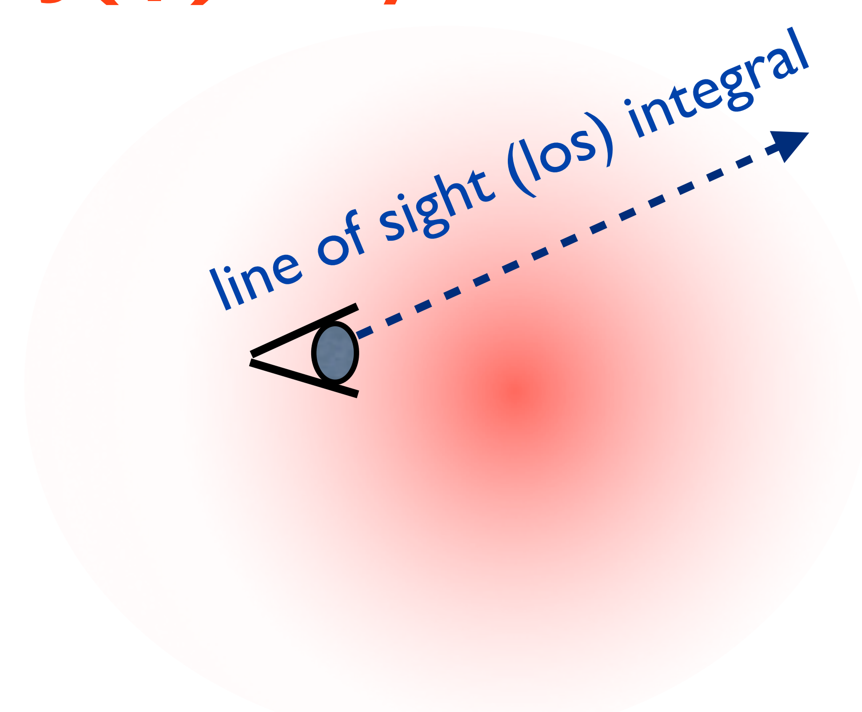

Sources of High Energy Neutrinos

Dark Matter self-annihilation or decay

Annihilation — K_{ann} — $J(\Psi)_{ann}$

$$\frac{d\Phi}{dE}(E,\phi,\theta) = \frac{1}{4\pi}\frac{\langle\sigma_A v\rangle}{2m_\chi^2}\sum_f Br(f)\frac{dN_f}{dE} \times \int_{\Delta\Omega(\phi,\theta)} d\Omega' \int_{\rm los} \rho^2(r(l,\phi'))dl(r,\phi')$$

Measure Flux — Particle Physics — Dark Matter Distribution

$$\frac{d\Phi}{dE}(E,\phi,\theta) = \frac{1}{4\pi}\frac{1}{m_\chi \tau_\chi}\sum_f Br(f)\frac{dN_f}{dE} \times \int_{\Delta\Omega(\phi,\theta)} d\Omega' \int_{los} \rho(r(l,\phi'))dl(r,\phi')$$

Decay — K_{decay} — $J(\Psi)_{decay}$

expected prompt signal for particles propagating directly to the observer (gamma-rays, neutrinos)

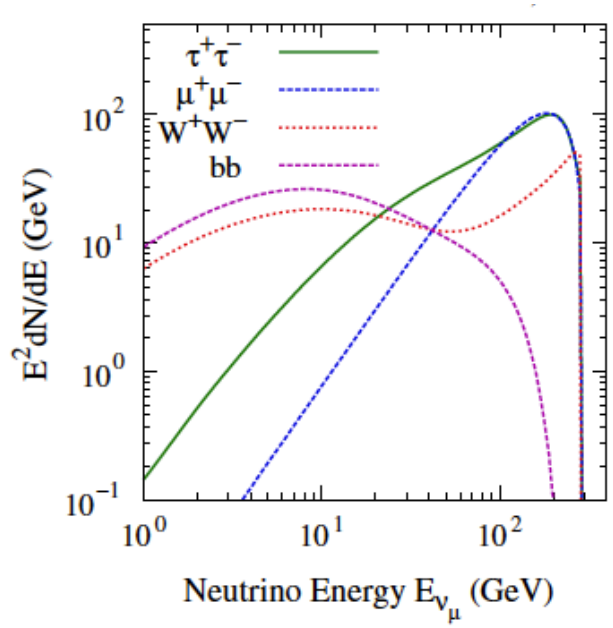

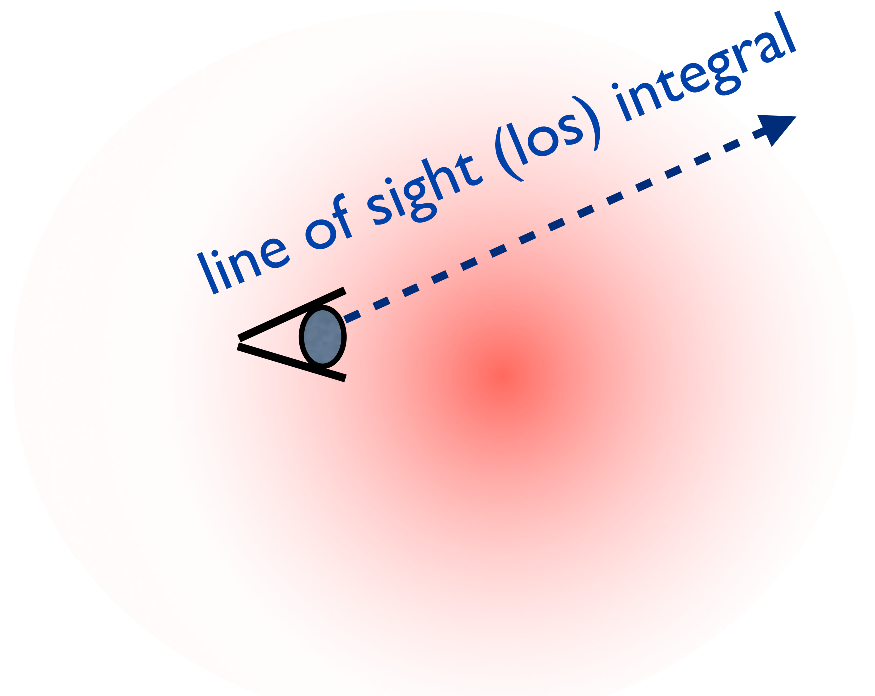

Sources of High Energy Neutrinos

Dark Matter self-annihilation or decay

Annihilation — K_{ann} — $J(\Psi)_{ann}$

$$\frac{d\Phi}{dE}(E,\phi,\theta) = \frac{1}{4\pi}\frac{\langle\sigma_A v\rangle}{2m_\chi^2}\sum_f Br(f)\frac{dN_f}{dE} \times \int_{\Delta\Omega(\phi,\theta)} d\Omega' \int_{\mathrm{los}} \rho^2(r(l,\phi'))\,dl(r,\phi')$$

Measure Flux — Particle Physics — Dark Matter Distribution

$$\frac{d\Phi}{dE}(E,\phi,\theta) = \frac{1}{4\pi}\frac{1}{m_\chi \tau_\chi}\sum_f Br(f)\frac{dN_f}{dE} \times \int_{\Delta\Omega(\phi,\theta)} d\Omega' \int_{los} \rho(r(l,\phi'))\,dl(r,\phi')$$

Decay — K_{decay} — $J(\Psi)_{decay}$

expected prompt signal for particles propagating directly to the observer (gamma-rays, neutrinos)

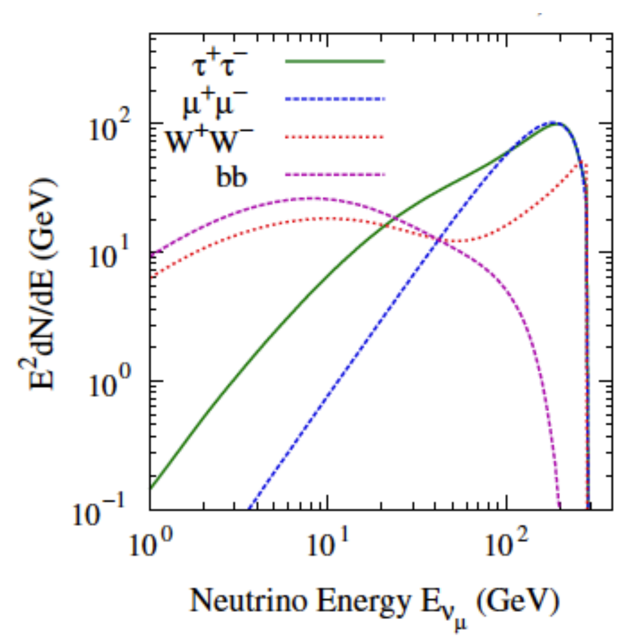

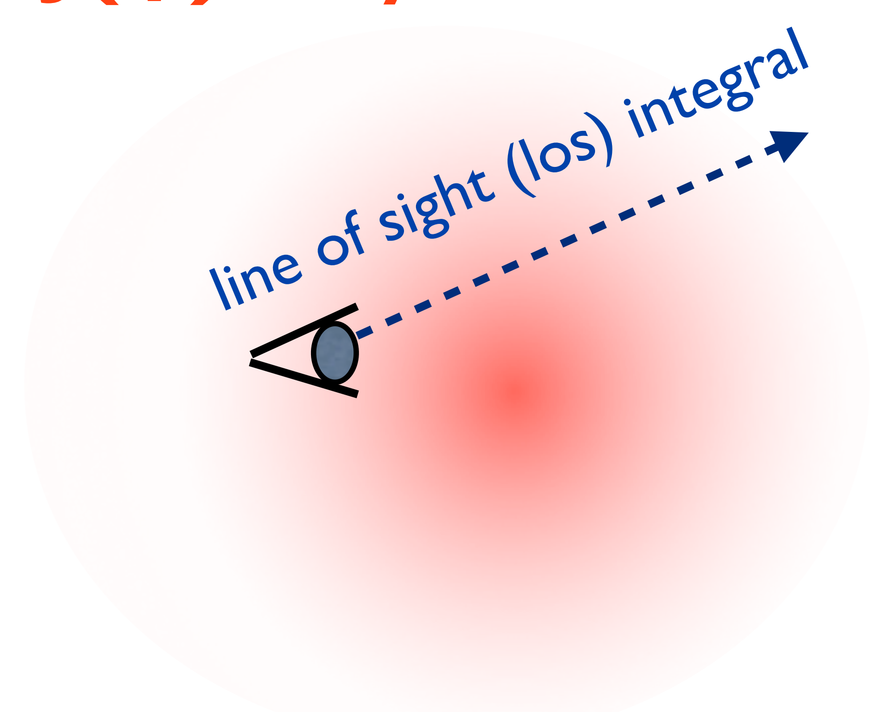

Sources of High Energy Neutrinos

Dark Matter self-annihilation or decay

Annihilation — K_{ann} — $J(\Psi)_{ann}$

$$\frac{d\Phi}{dE}(E,\phi,\theta) = \frac{1}{4\pi}\frac{\langle\sigma_A v\rangle}{2m_\chi^2}\sum_f Br(f)\frac{dN_f}{dE} \times \int_{\Delta\Omega(\phi,\theta)} d\Omega' \int_{\mathrm{los}} \rho^2(r(l,\phi'))dl(r,\phi')$$

Measure Flux — **Particle Physics** — **Dark Matter Distribution**

$$\frac{d\Phi}{dE}(E,\phi,\theta) = \frac{1}{4\pi}\frac{1}{m_\chi \tau_\chi}\sum_f Br(f)\frac{dN_f}{dE} \times \int_{\Delta\Omega(\phi,\theta)} d\Omega' \int_{los} \rho(r(l,\phi'))dl(r,\phi')$$

Decay — K_{decay} — $J(\Psi)_{decay}$

expected prompt signal
for particles propagating
directly to the observer
(gamma-rays, neutrinos)

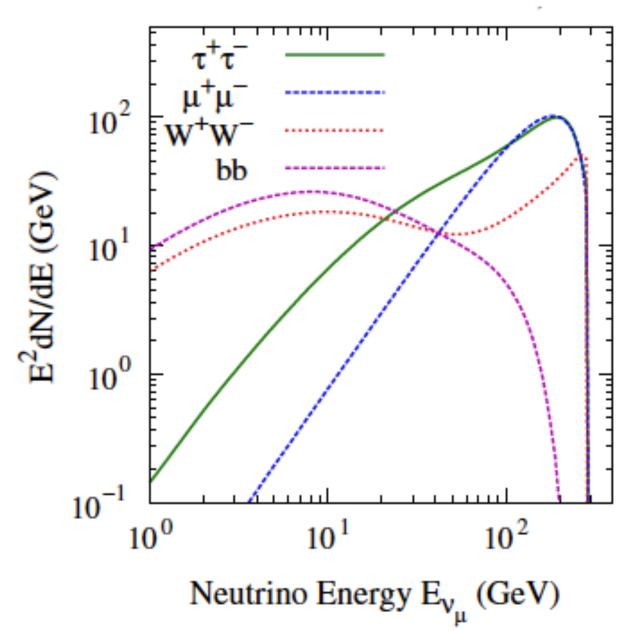

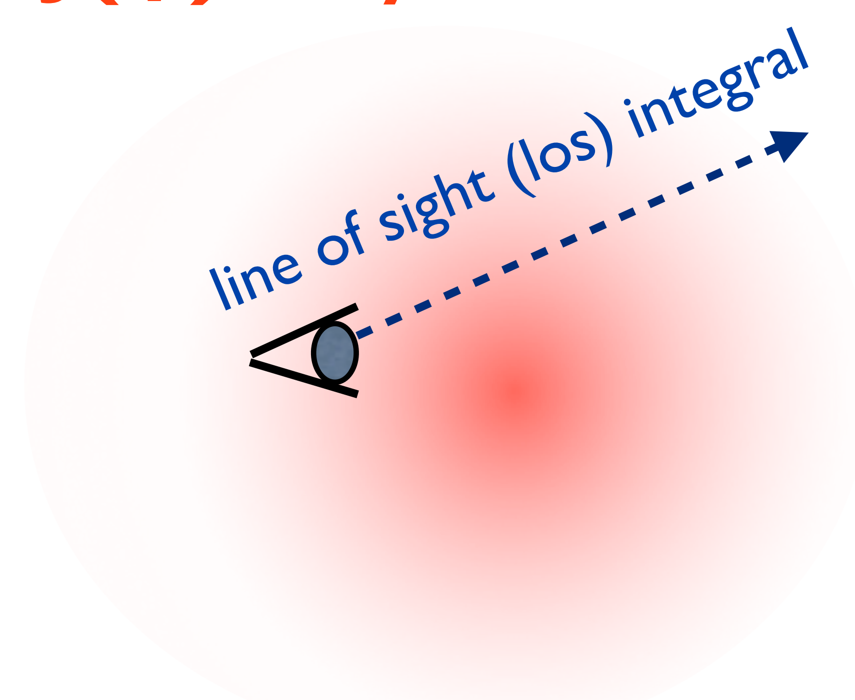

How Dark Matter is distributed

The Astrophysical Journal, 742:20 (19pp), 2011 November 20

- N-body simulations of Milky Way like galaxies yield halo profiles ρ(r). Halo profiles described the average dark matter density (smooth)
- <u>Two major difficulties</u>
  - Inner halo shape (cuspy or cored ?)
  - Sub-structure in outer halo

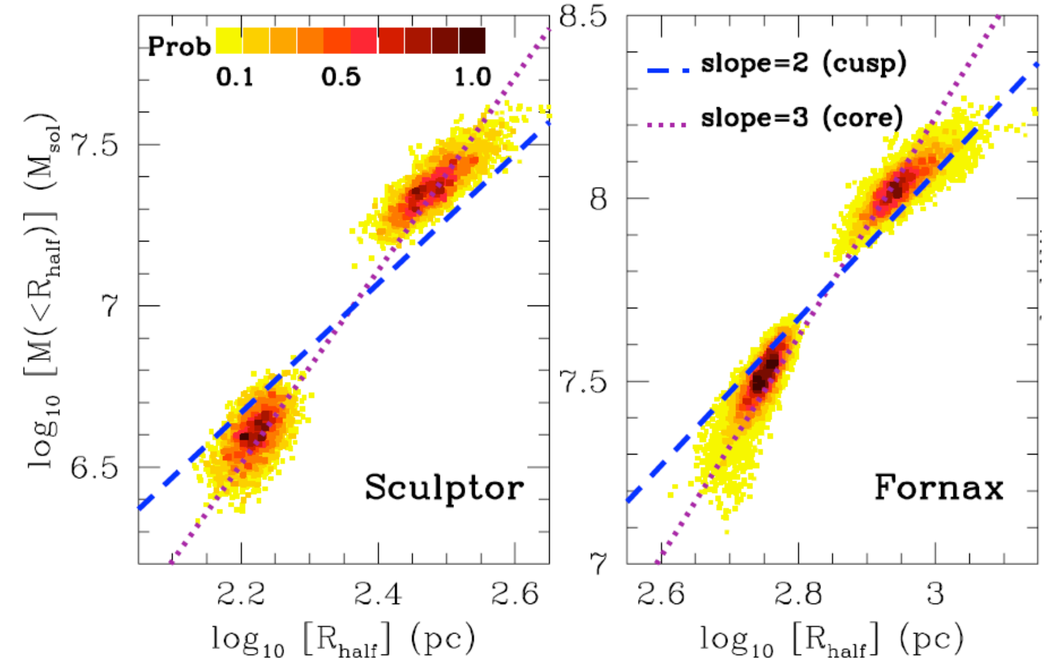

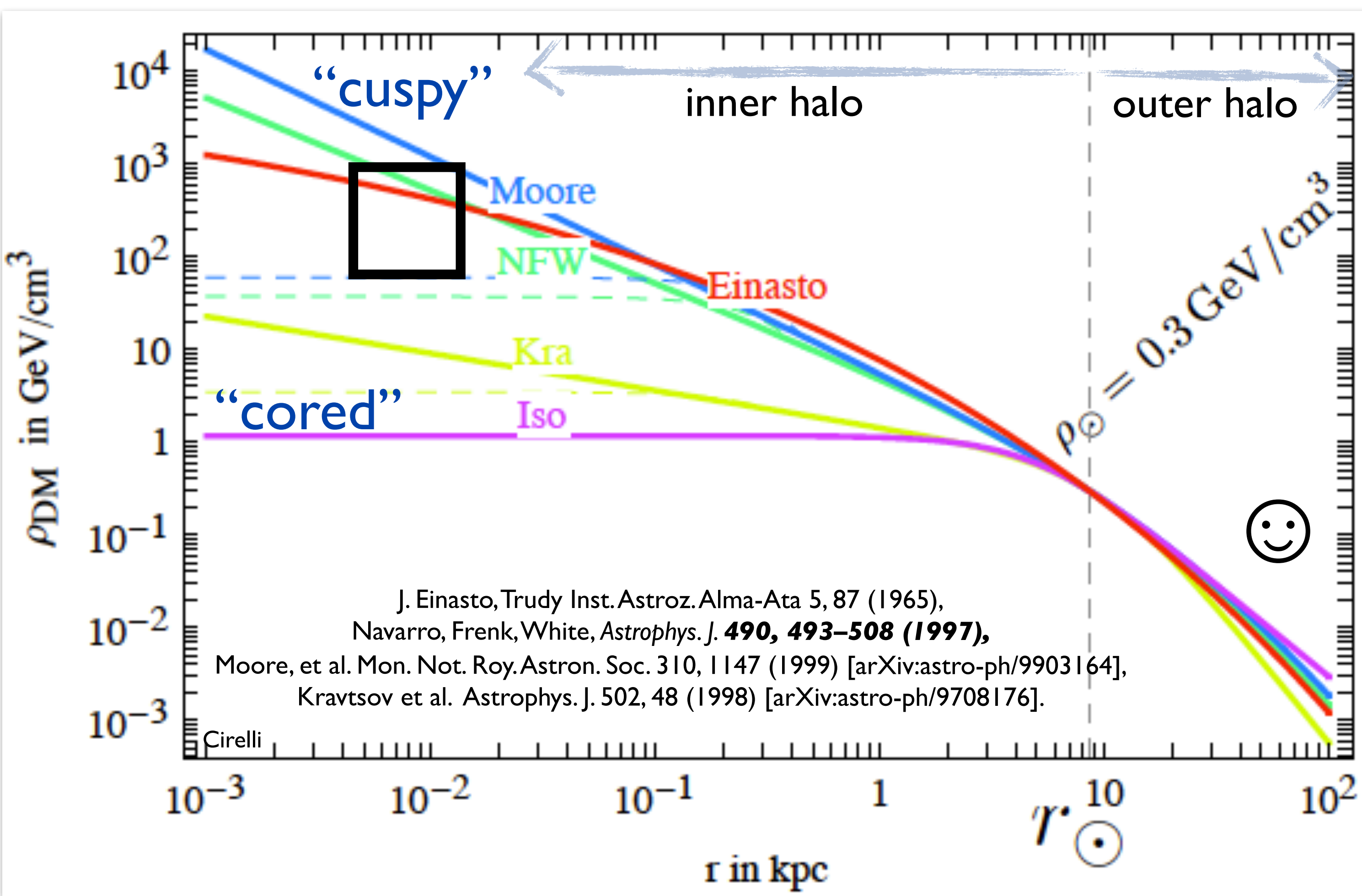

Sources of High Energy Neutrinos

Dark Matter self-annihilation or decay

Annihilation — **K_{ann}** — **$J(\Psi)_{ann}$**

$$\frac{d\Phi}{dE}(E,\phi,\theta) = \frac{1}{4\pi}\frac{\langle\sigma_A v\rangle}{2m_\chi^2}\sum_f Br(f)\frac{dN_f}{dE} \times \int_{\Delta\Omega(\phi,\theta)} d\Omega' \int_{\text{los}} \rho^2(r(l,\phi'))dl(r,\phi')$$

Measure Flux — **Particle Physics** — **Dark Matter Distribution**

$$\frac{d\Phi}{dE}(E,\phi,\theta) = \frac{1}{4\pi}\frac{1}{m_\chi\tau_\chi}\sum_f Br(f)\frac{dN_f}{dE} \times \int_{\Delta\Omega(\phi,\theta)} d\Omega' \int_{los} \rho(r(l,\phi'))dl(r,\phi')$$

Decay — **K_{decay}** — **$J(\Psi)_{decay}$**

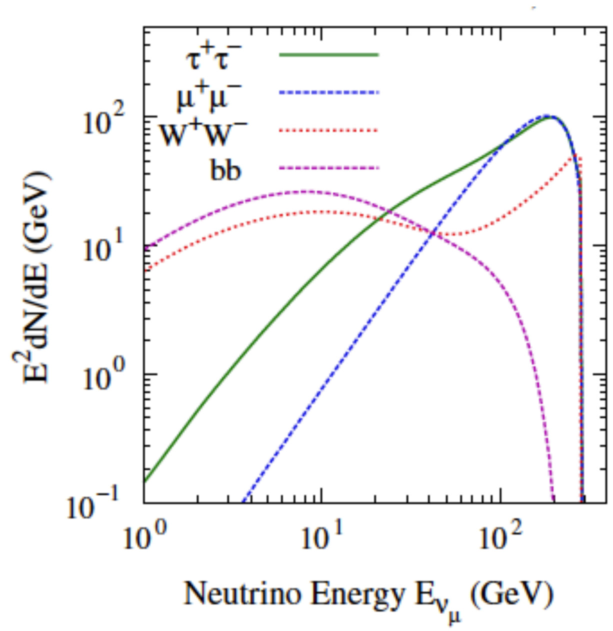

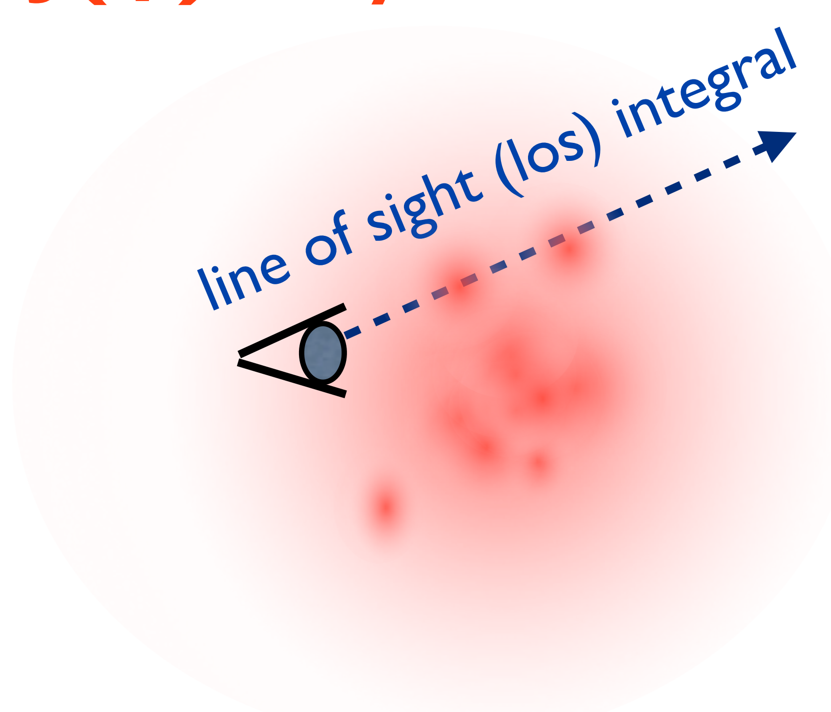

Boost factor

Astro-physical boost factor

- Local clumps in the DM halo enhance the density and boost the flux from annihilations:
  - Boost $B = \frac{\phi^{actual}(\vec{r})}{\phi^{smooth}(\vec{r})}$
- Typical boost factors are B~ 1-20 (simulations)
- Boost factor ~ 1 (for central halo region <10kpc) tidal stripping

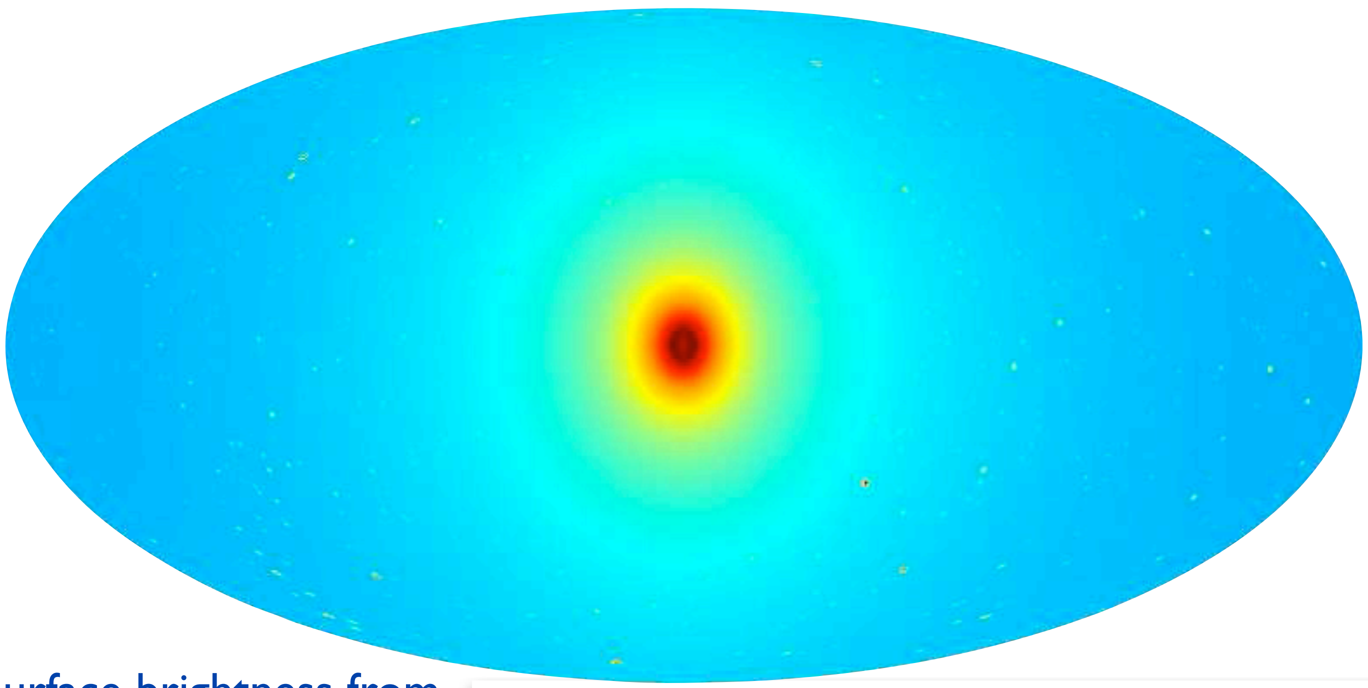

Surface brightness from dark matter annihilation at the position of the Sun, calculated directly from the Aq-A-1 simulation.

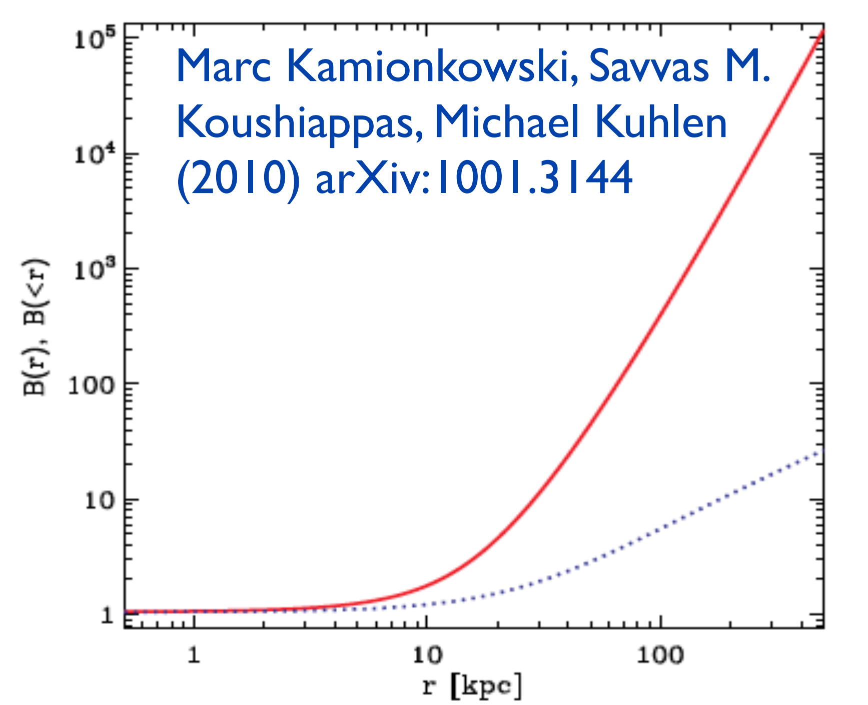

FIG. 4. The local substructure boost $B(r)$ (*solid*) and the cumulative luminosity boost $B(<r)$ (*dotted*), as a function of radius.

- Boost factor important for:
  - Galaxy clusters, Diffuse extra galactic, ...
- Not important for:
  - Galactic Center, Solar circle, ...

Sources of High Energy Neutrinos

Dark Matter self-annihilation or decay

Annihilation | **K_{ann}** | **Boost x $J_{smooth}(\Psi)_{ann}$**

$$\frac{d\Phi}{dE}(E,\phi,\theta) = \frac{1}{4\pi}\frac{\langle\sigma_A v\rangle}{2m_\chi^2}\sum_f Br(f)\frac{dN_f}{dE} \times \int_{\Delta\Omega(\phi,\theta)} d\Omega' \int_{los} b \times \rho^2_{smooth}(r(l,\phi'))dl(r,\phi')$$

Measure Flux | Particle Physics | Dark Matter Distribution

$$\frac{d\Phi}{dE}(E,\phi,\theta) = \frac{1}{4\pi}\frac{1}{m_\chi \tau_\chi}\sum_f Br(f)\frac{dN_f}{dE} \times \int_{\Delta\Omega(\phi,\theta)} d\Omega' \int_{los} \rho_{smooth}(r(l,\phi'))dl(r,\phi')$$

Decay | **K_{decay}** | **$J_{smooth}(\Psi)_{decay}$**

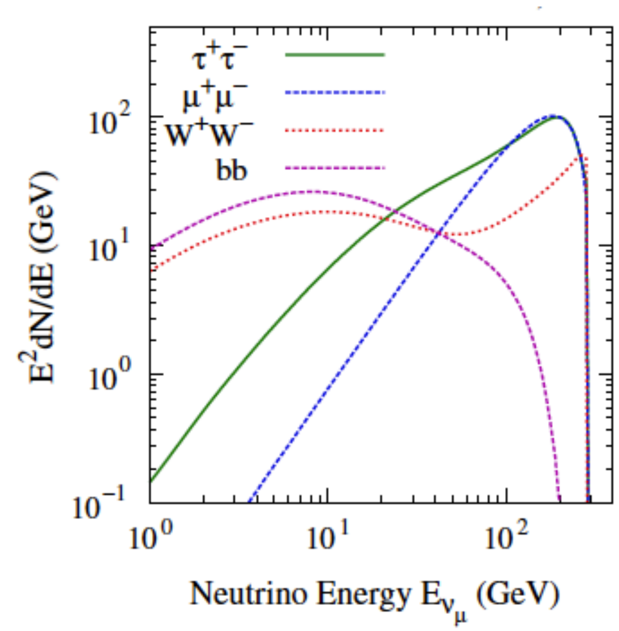

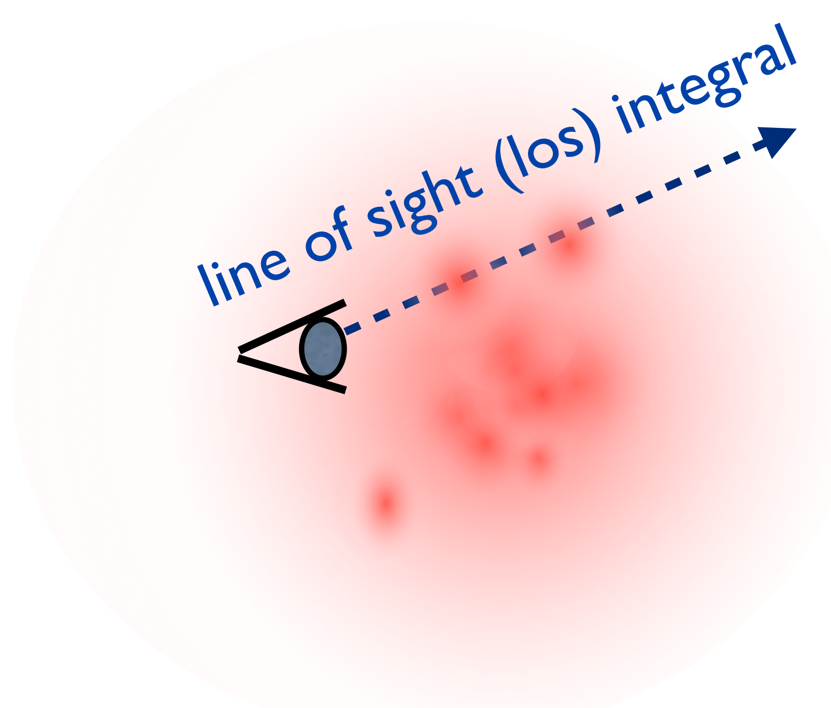

Instruments

Indirect Searches - Instruments

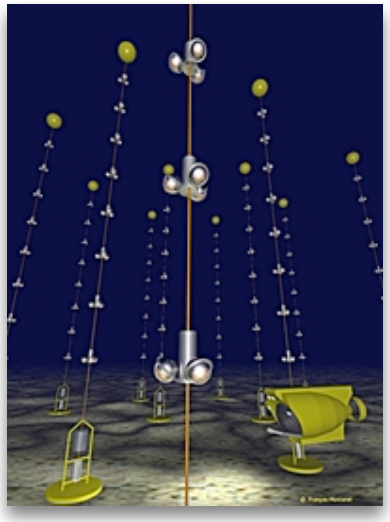

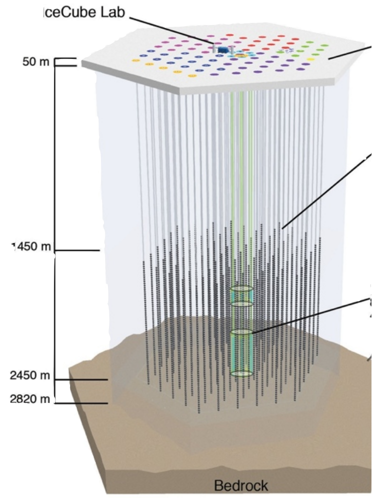

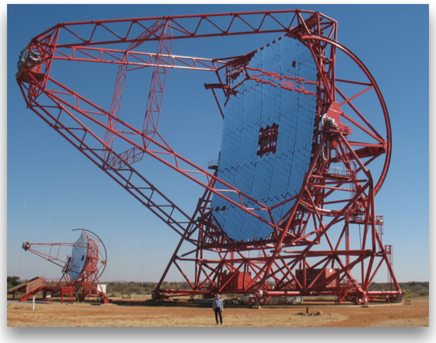

Neutrino Detectors

- ANTARES, NESTOR, NEMO, KM3Net...
- IceCube, PINGU, ORCA, ...
- Baikal, ...
- Super-K, KamLAND, Laguna-LBNO, Hyper-K, ...

Gamma Ray Telescopes

- MAGIC, H.E.S.S., VERITAS, ...
- Fermi, ...
- CTA, Gamma-400,...

Anti-Matter Satellites

- PAMELA, ATIC, PPB-Bets, ...
- AMS-02

Others

- x-ray, radio, ...

Cosmic Rays

Cosmic-Ray detection

PAMELA – Payload for Anti-Matter Exploration and Light-nuclei Astrophysics

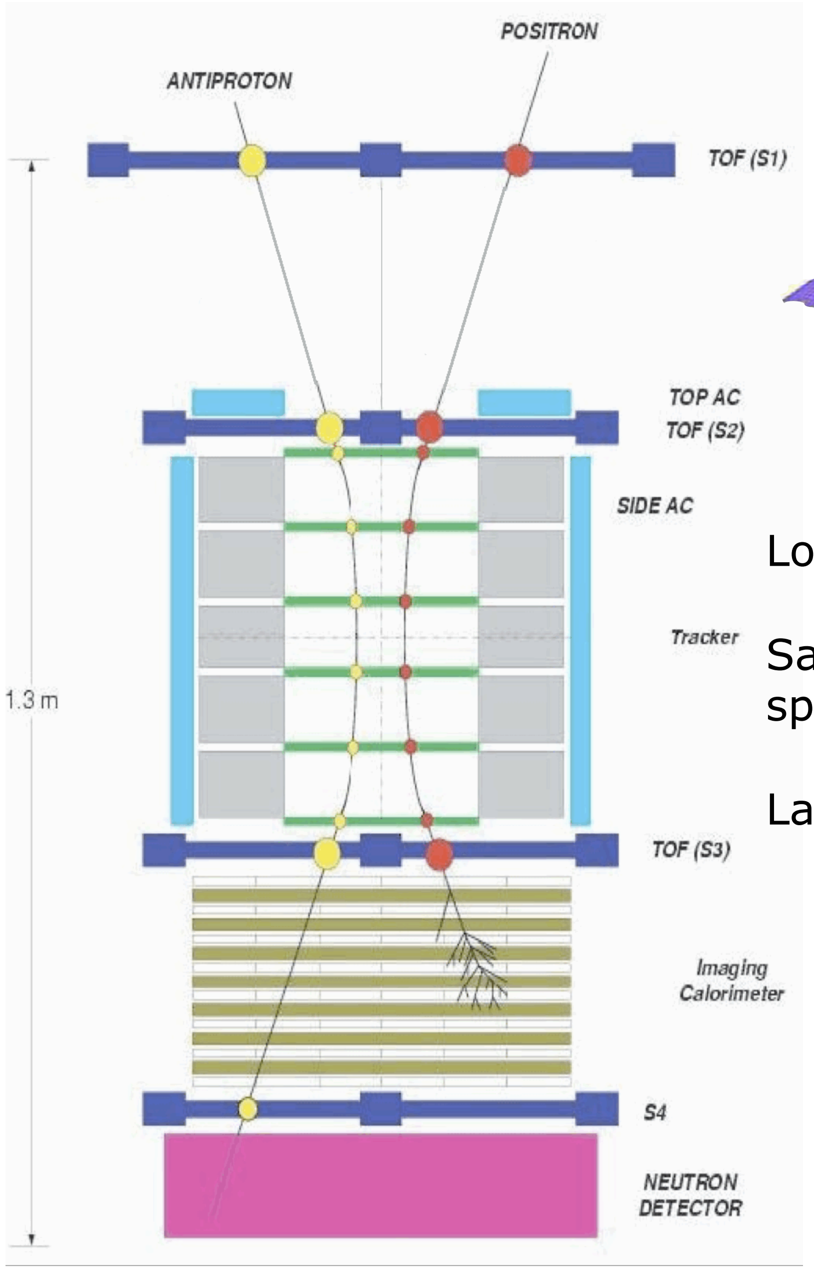

Low-earth elliptical orbit

Satellite-born Magnetic spectrometer

Launched 2006

- Size 70x70x130cm^3
- $e^+(e^-)$ - 50 MeV –300GeV (600GeV)
- Protons up to ~1TeV

Astropart.Phys. 27 (2007) 296-315

The AMS-02 Detector

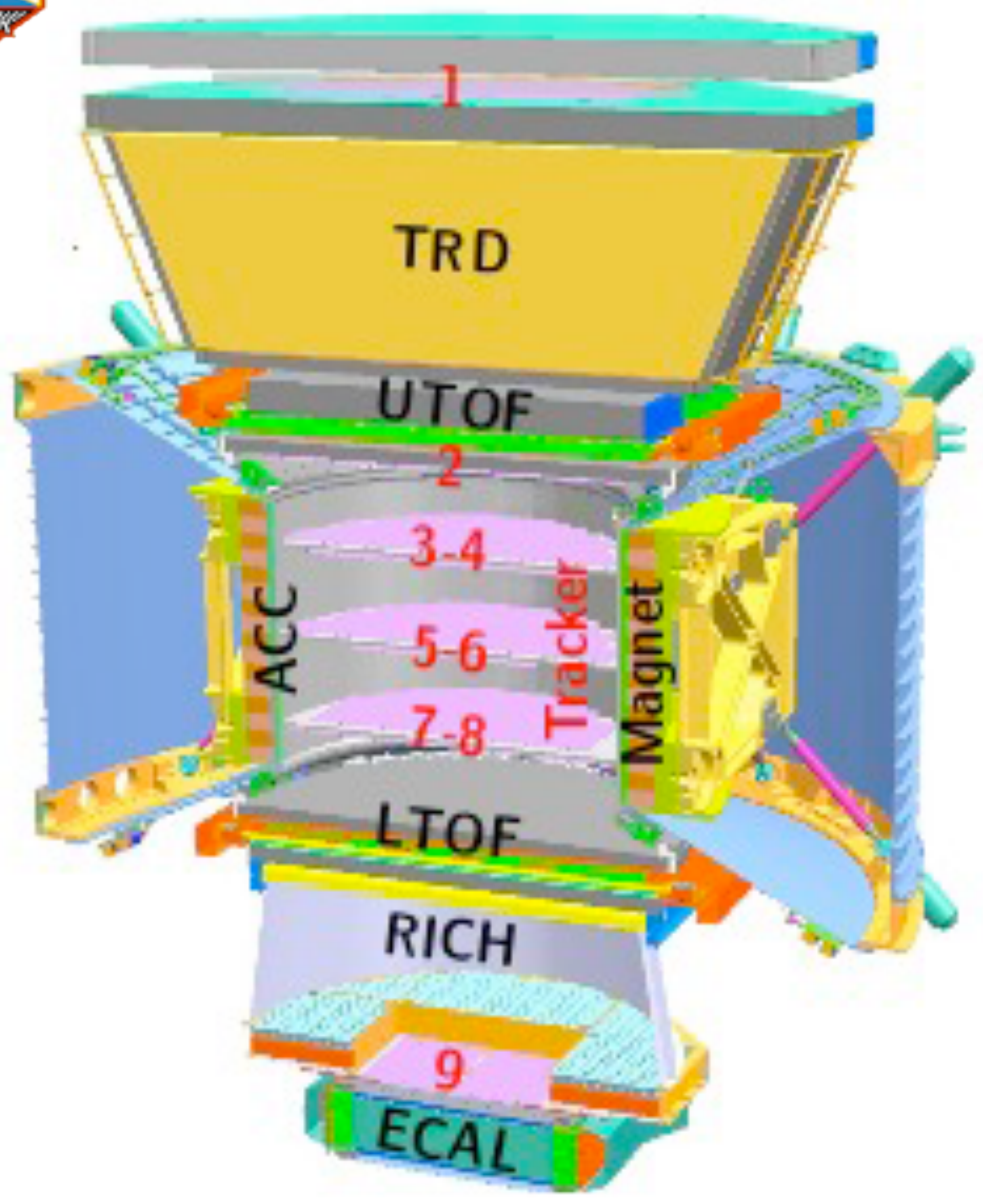

installed on the International Space Station on May 19th 2011

Tuesday: Veronica Bindi

Cosmic e^+e^-

$\Phi(e^+)/\Phi(e^++e^-)$

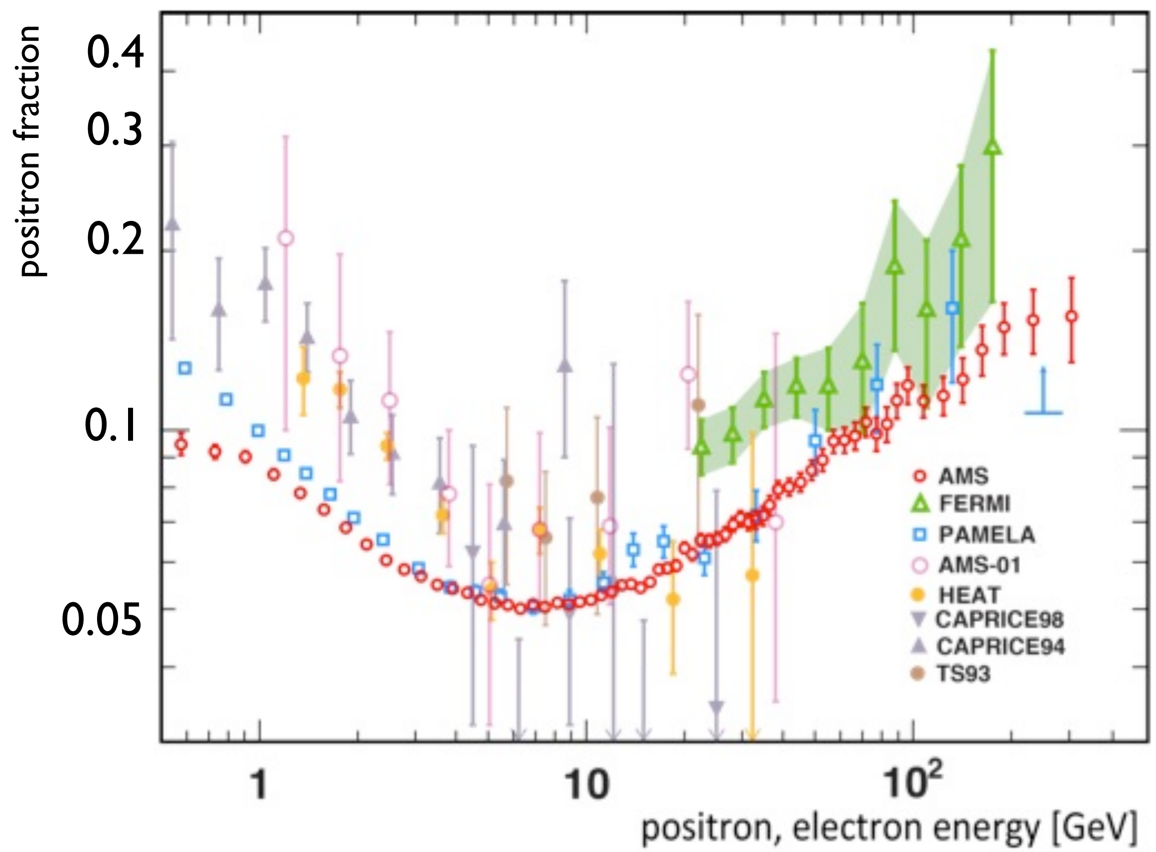

Ackermann et al. [Fermi LAT Collaboration] 2011
M. Boezio, UCLA Dark Matter 2012
Aguilar et al. [AMS-02 Collaboration] 2013

$\Phi(e^++e^-)$

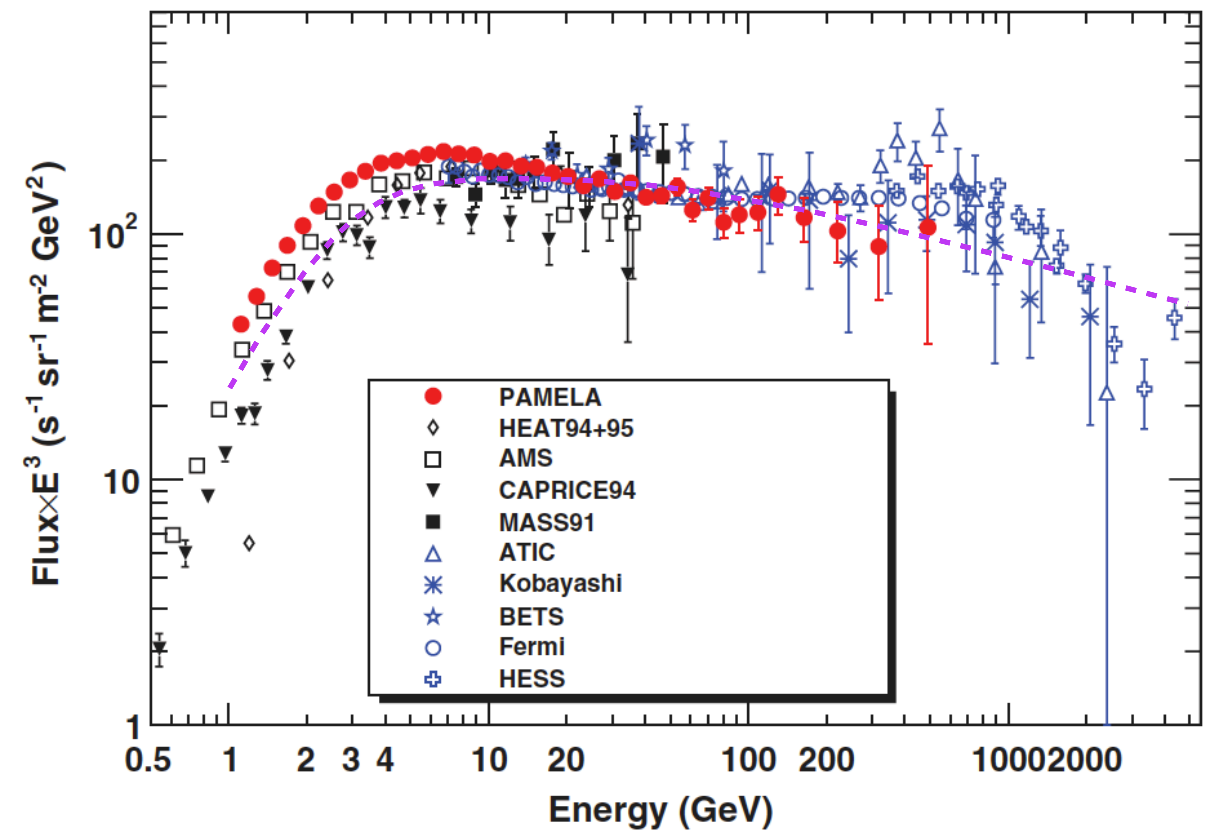

Phys. Rev. Lett. 106, 201101 (2011)

Anomaly could be hint of dark matter
see for example:
Strumia & Cirelli 2009
P. Meade, M. Papucci, A. Strumia, and T. Volansky, Nucl. Phys. B831, 178 (2010)

Alternatively one or more near by sources could explain excess.
see for example:
H. Yuksel, M. D. Kistler, and T. Stanev, Phys. Rev. Lett. 103, 051101 (2009).
Hooper, Blasi, Serpico JCAP 0901 (2009) 025

Arrival direction isotropic -- local origin ~ 1kpc

Self-annihilating or decaying dark matter requires high boost factors

Gamma Rays

Gamma-rays

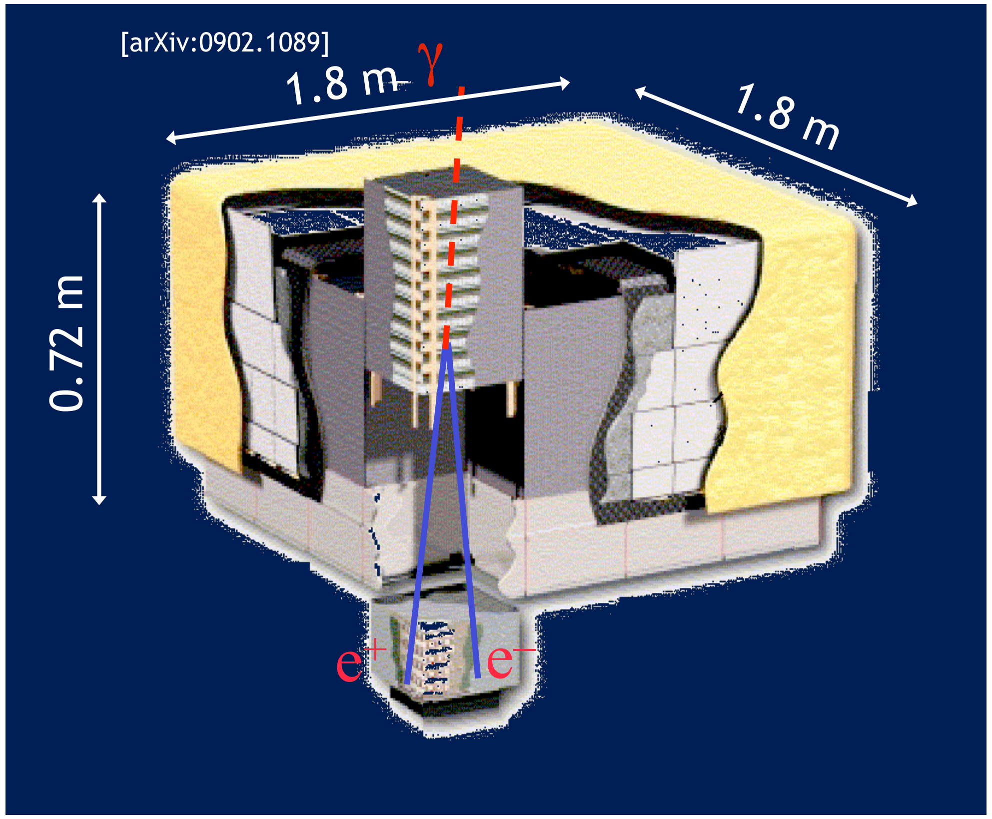

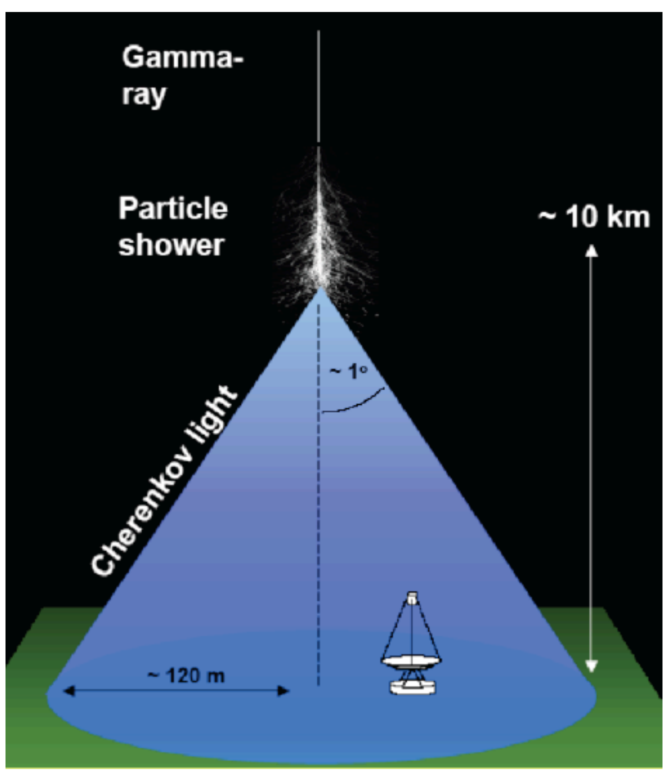

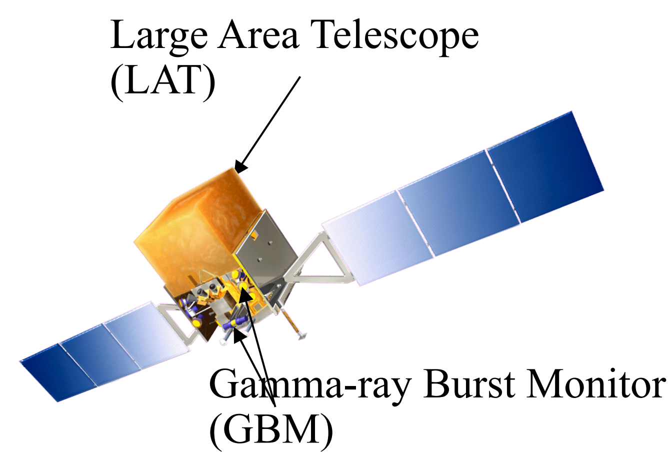

	Fermi-LAT	Imaging Air Cherenkov Telescopes
Detection Method	Pair conversion	Cherenkov light from particle shower
Effective Area	$1 m^2$	~400-$500 m^2$
Field of View (FOV)	2.5sr	3.5° - 5.0°
Duty cycle	~100%	~15%
Energy range	20MeV - 300GeV	>100GeV
Energy resolution	4% (@5GeV) 2% (@200GeV)	10% - 20%
Angular resolution	~0.1° (@10GeV) ~3.5°(@100MeV)	0.1° at 100 GeV

Individual Sources: Dwarfs / Clusters of Galaxies

H.E.S.S.

Lamanna et al, ICRC 2013, arXiv:1307.4918v1

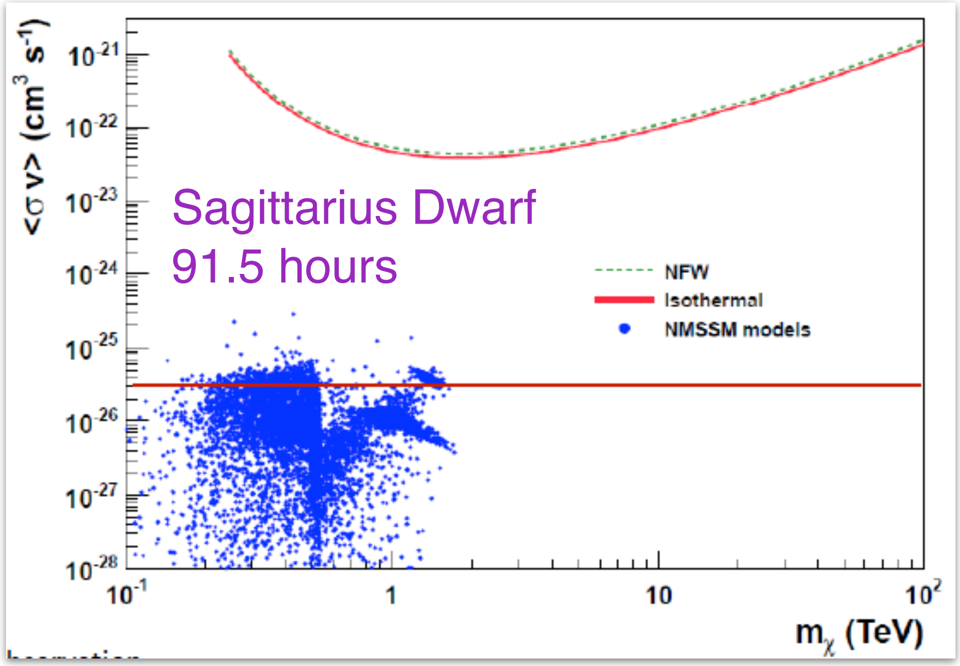

MAGIC

JCAP 1106 (2011) 035 arXiv:1103.0477 ; Jelena Aleksic, EPS HEP 2013

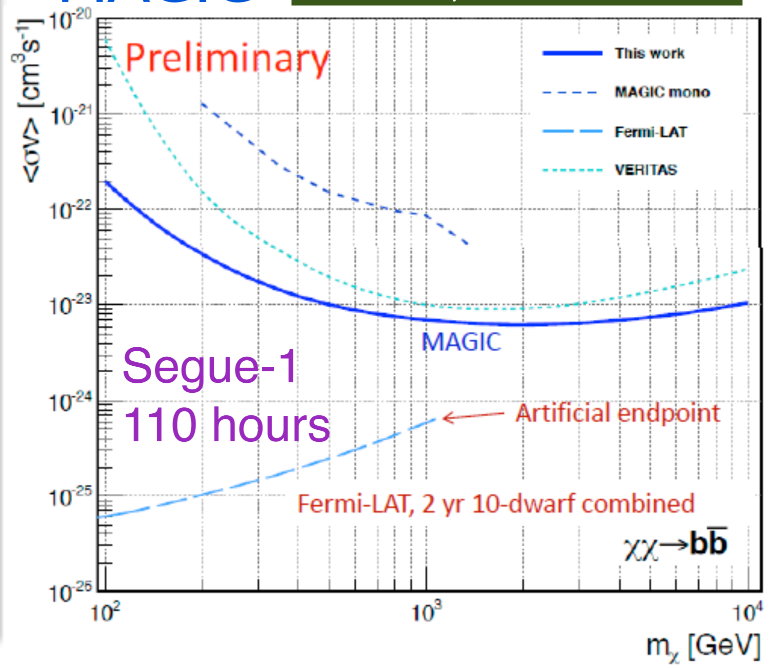

Veritas

E. Aliu et al. arXiv 1202.2144
B. Zitzer, ICRC 2013, arXiv:1307.8367

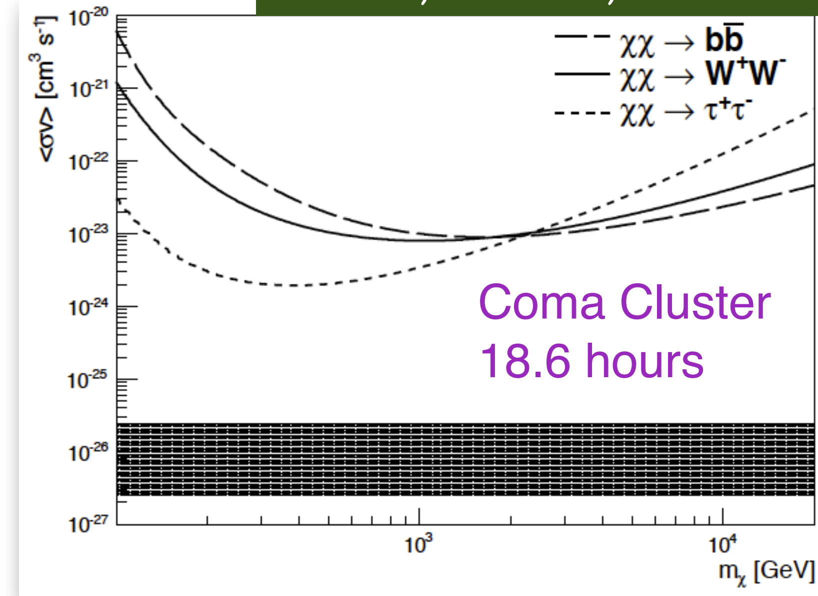

- Roughly two dozen known dwarf spheroidal satellite galaxies in the Milky Way
- Dwarfs: Some of the most dark matter dominated objects in the Universe
- No astrophysical gamma-ray production expected

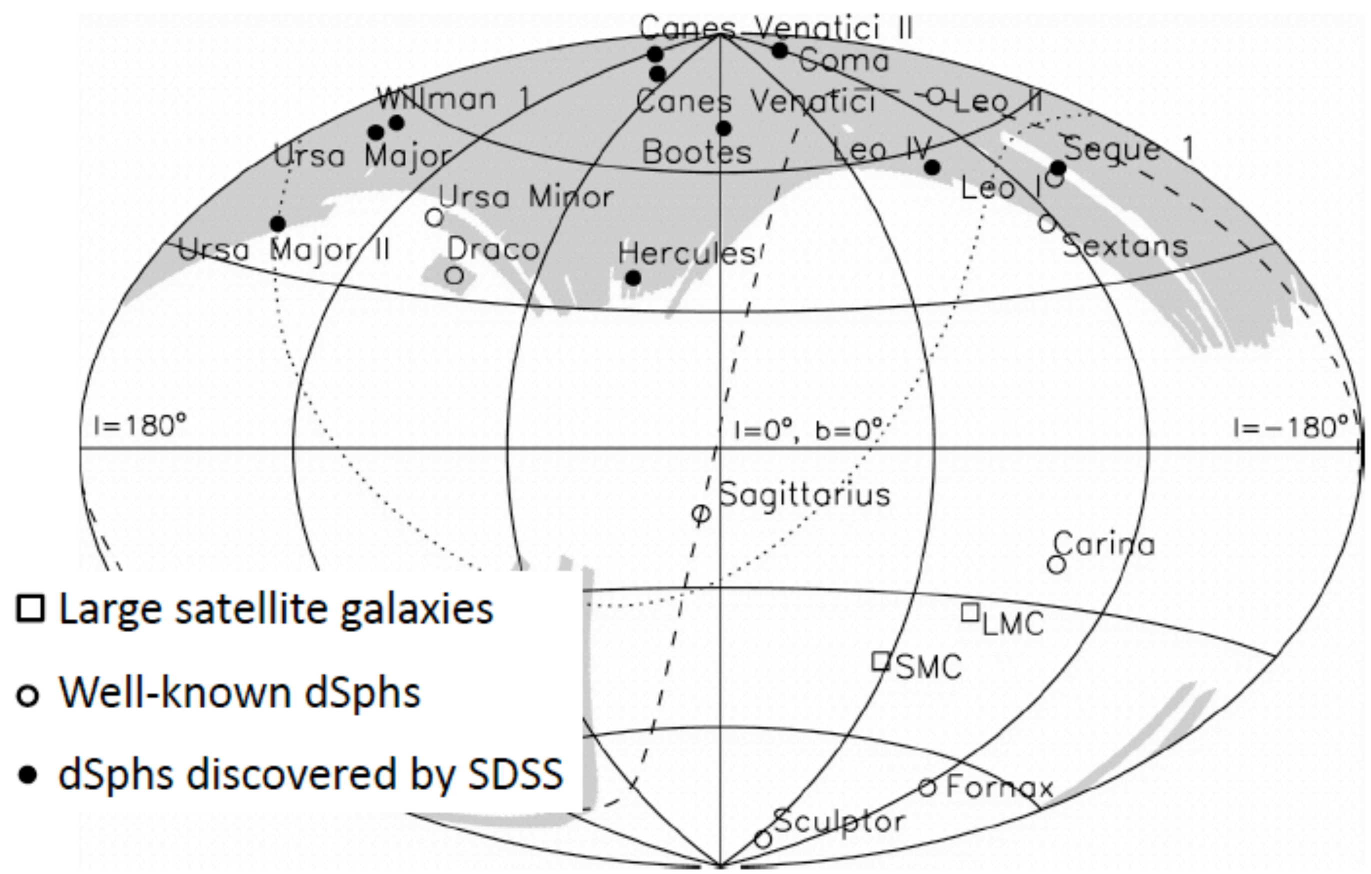

Belokurov, V., et al. 2007, ApJ, 654, 897

Fermi-LAT Searches

Galactic Halo

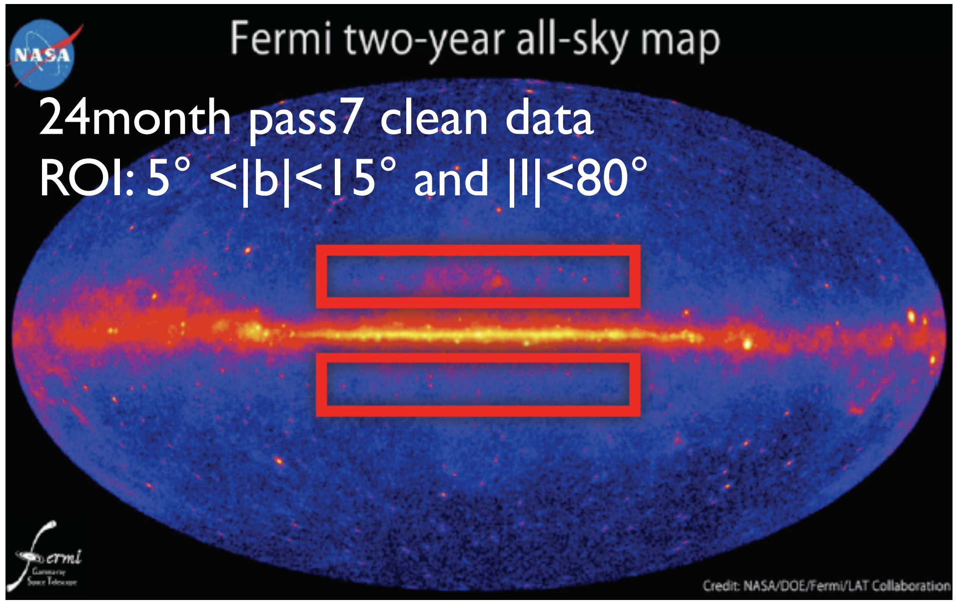

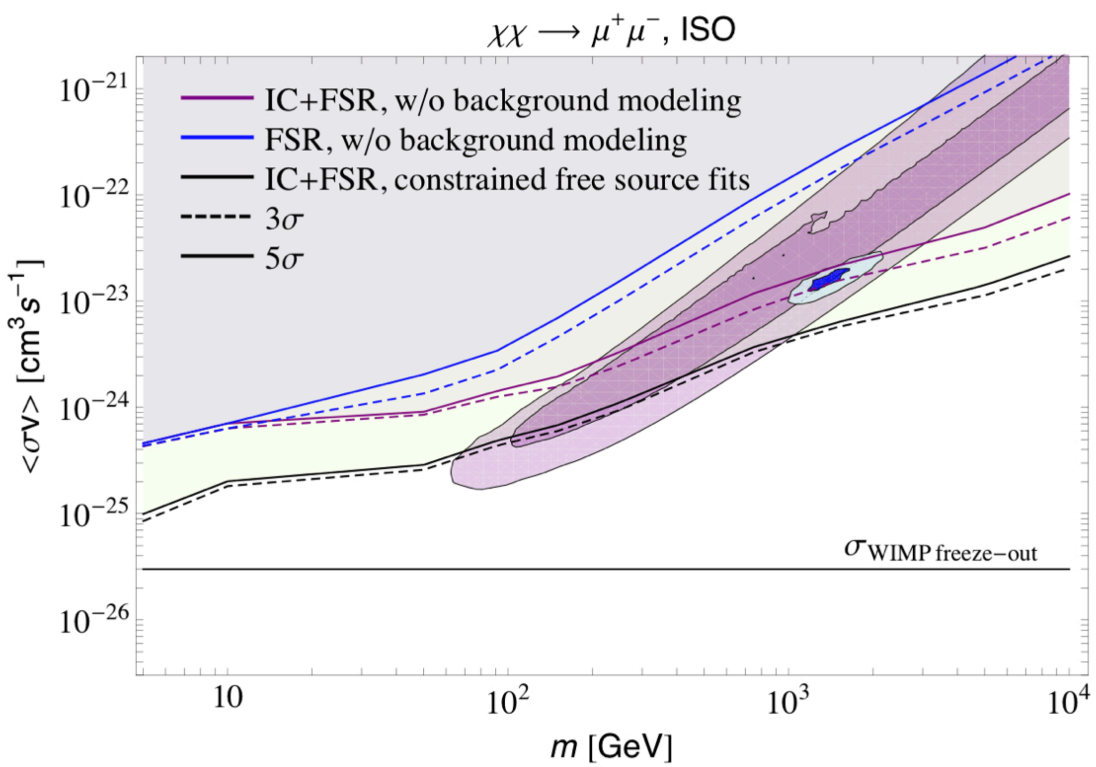

Dwarf Limits from 24 Months of Data

Phys. Rev. Lett. 107 (2011) 241302 and 241303.

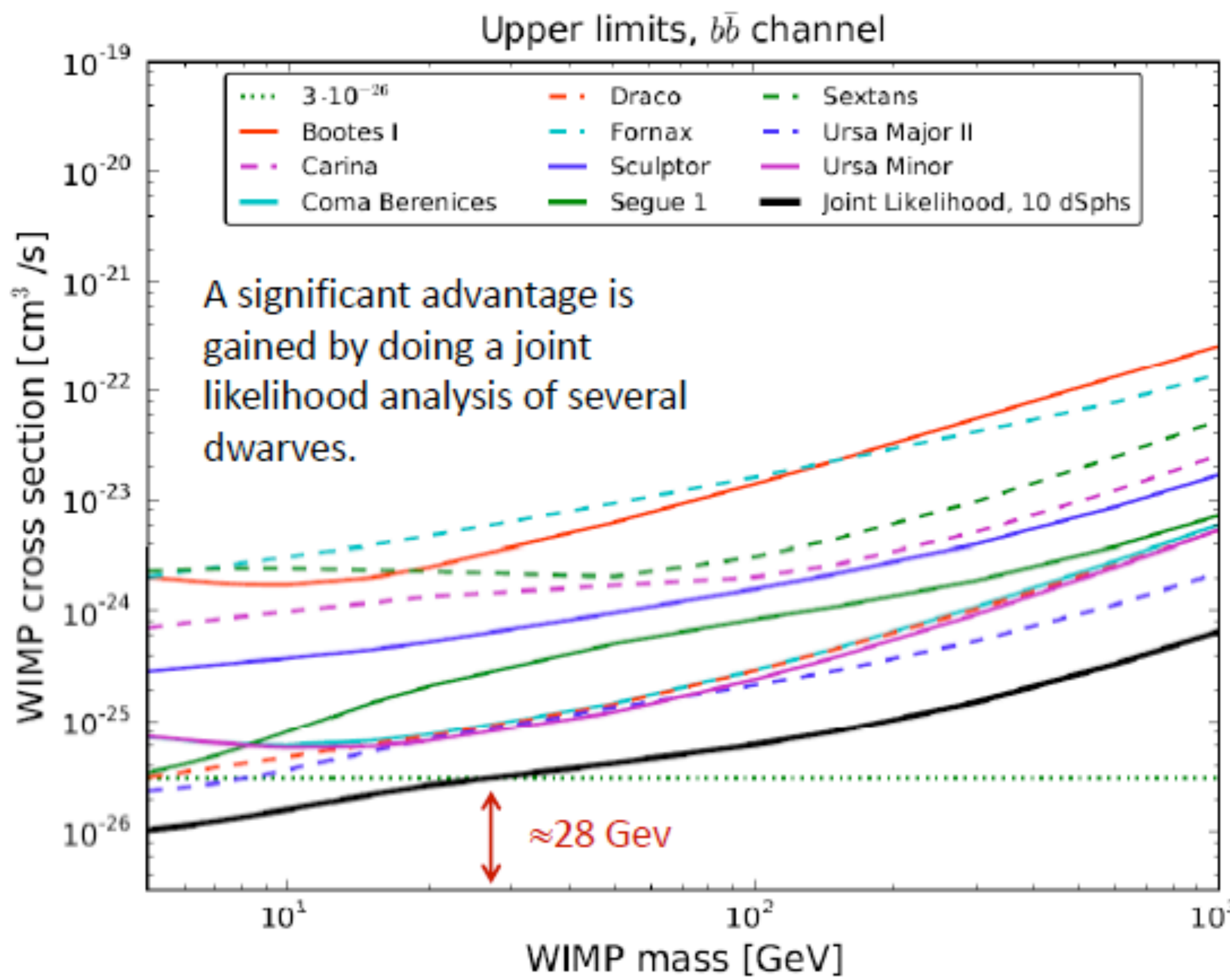

$<\sigma_A v>$ - total self-annihilation cross section averaged over the relative velocity distribution

Dark Matter interpretation of PAMELA/Fermi CR anomalies strongly disfavored (for annihilating DM)

4yrs Combined Fermi-LAT dSphs

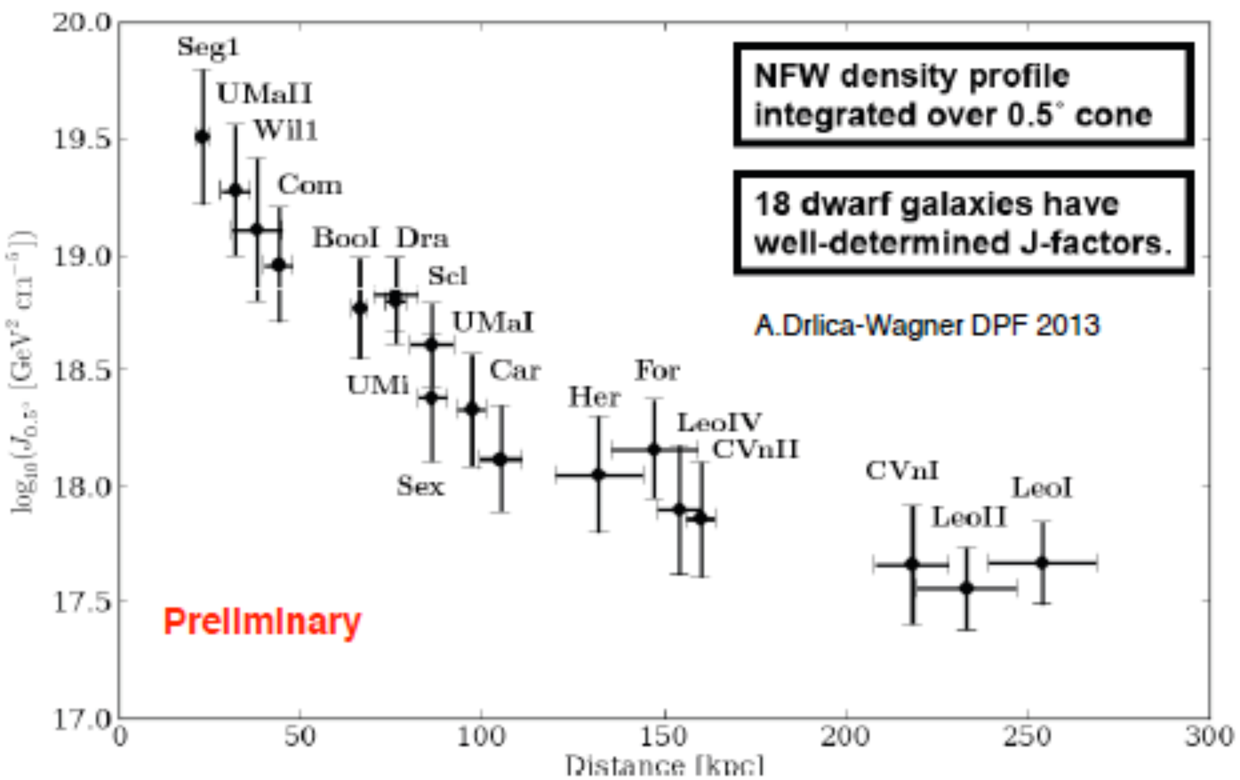

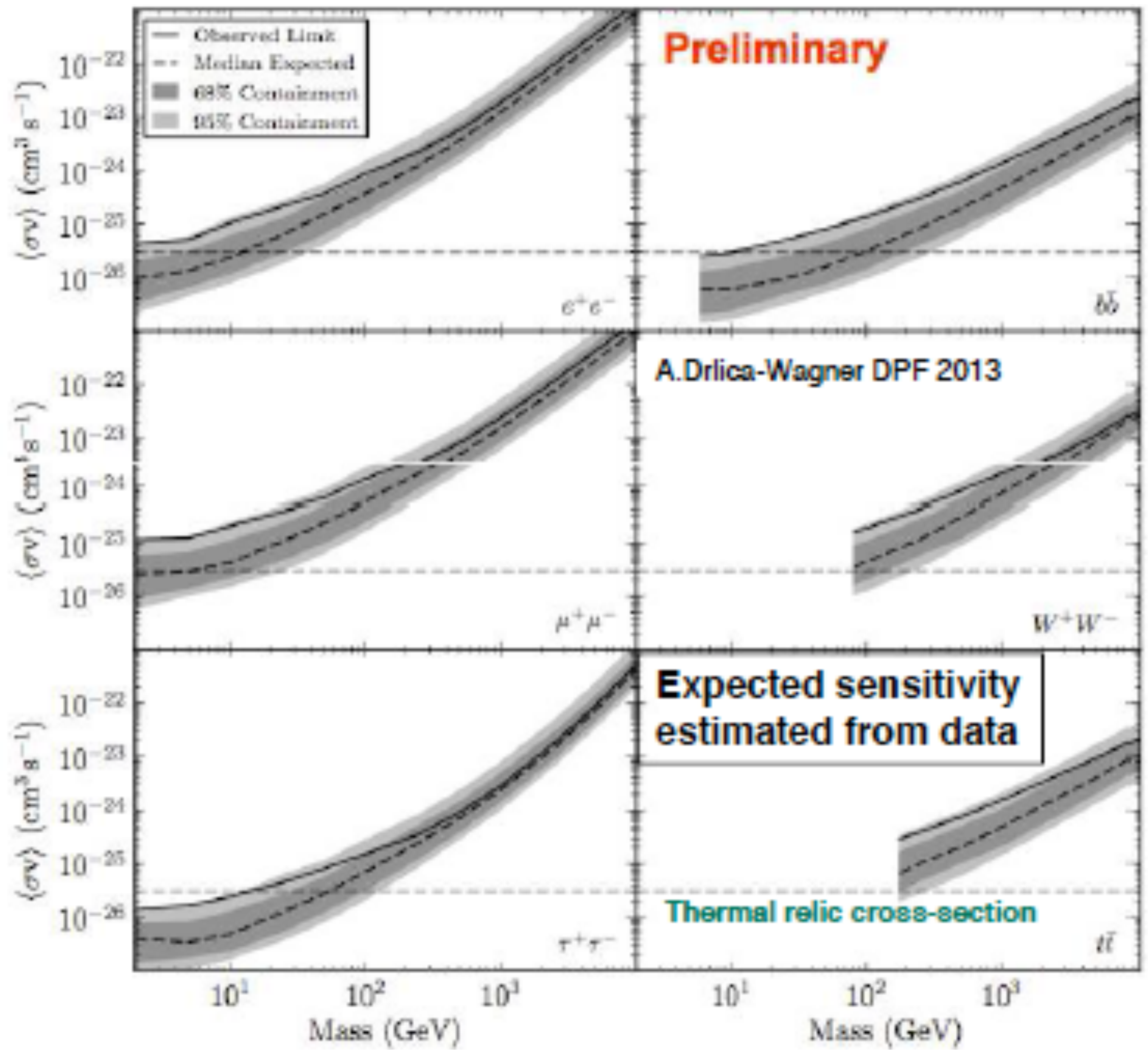

- Joint likelihood analysis of 15 dwarfs
- 4 years of data covering 500MeV - 0.5TeV
- Account for J-factor uncertainties
  - Determined using observed stellar velocities
- No DM signal seen
  - Exclude canonical thermal relic cross-section for m_x<10GeV (for bb and tau-channel)

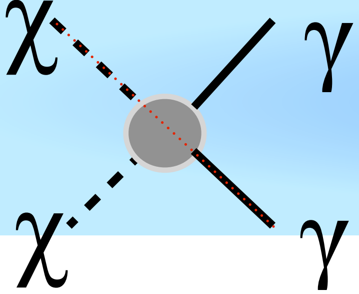

Fermi-LAT: Line Search (2yrs)

M. Ackermann [Fermi-LAT] arXiv:1205.2739v1

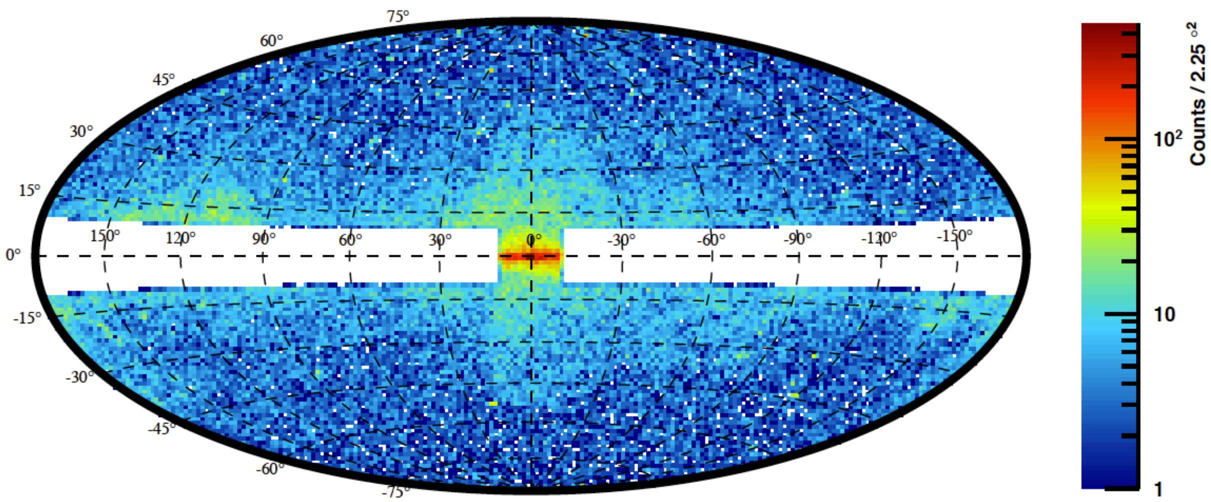

ROI: Exclude galactic plane and sources (1FGL)

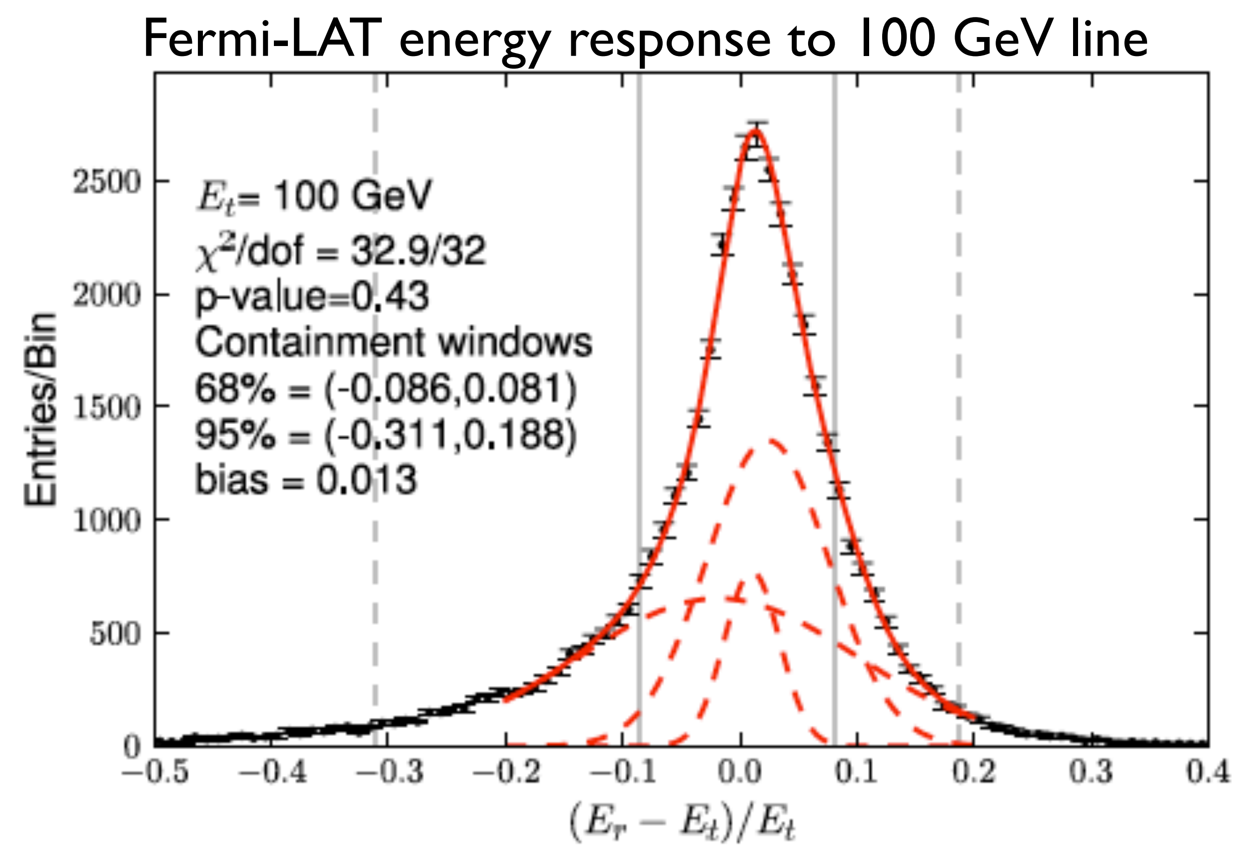

Fermi-LAT analysis based on 2yrs of data

Search for line from dark matter annihilation or decay to γγ or Zγ

Assume power-law background (spectral index free to vary)

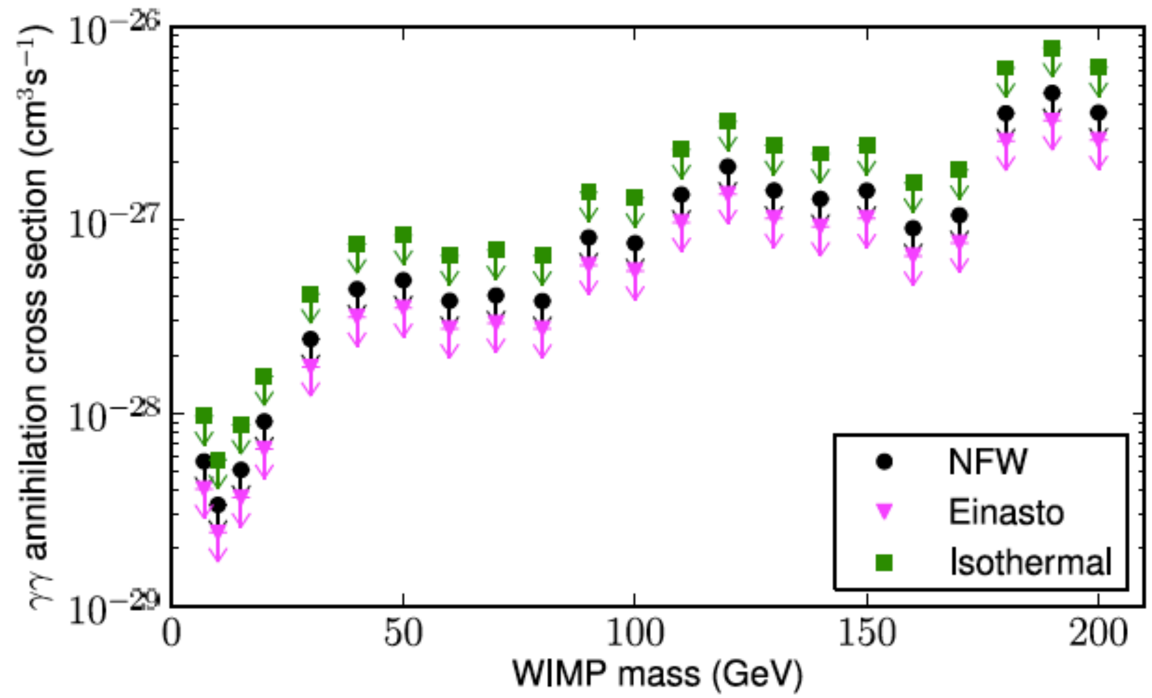

130GeV Line

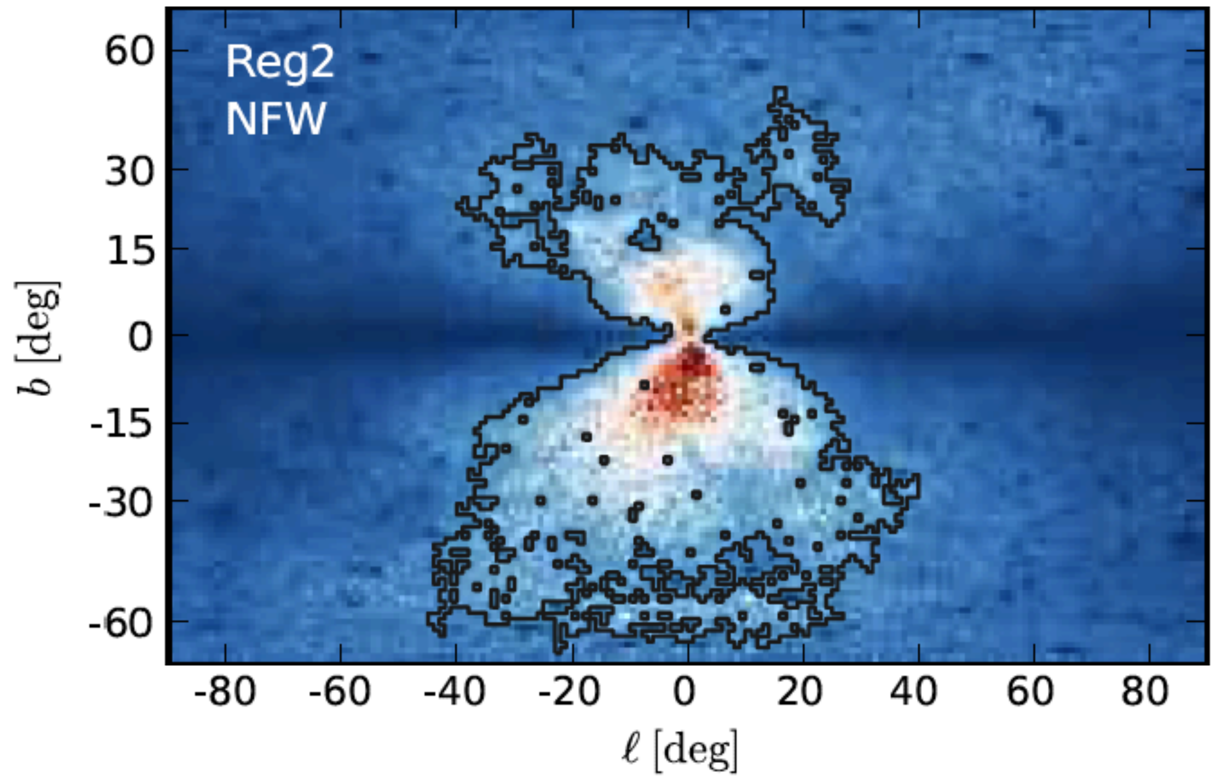

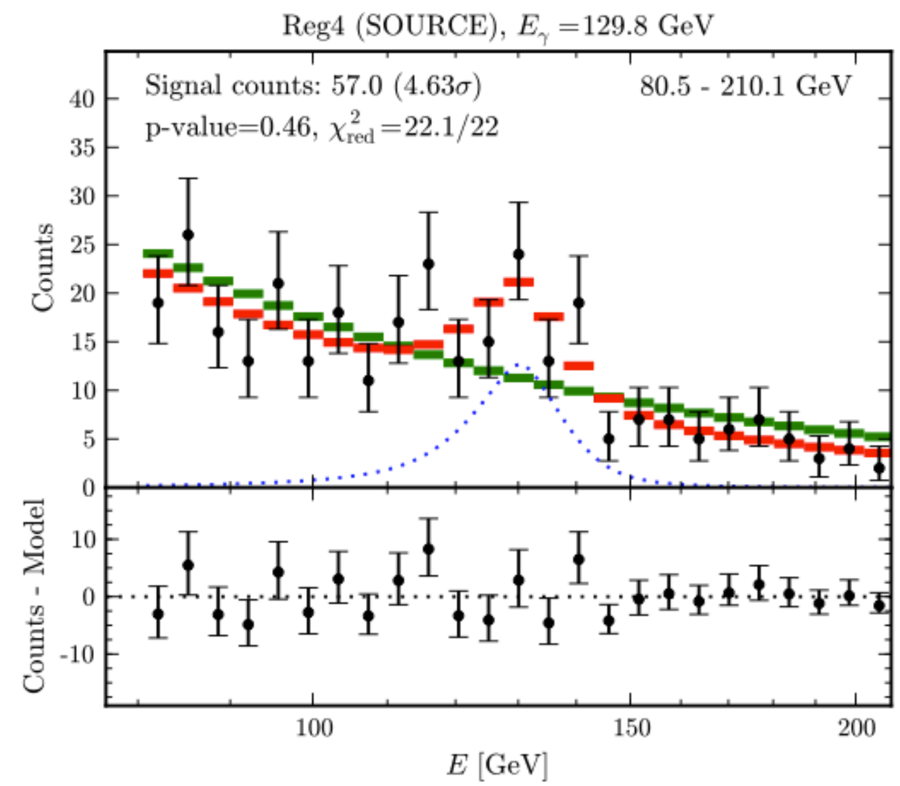

Weniger (2012)

- Pass 7 data used for these analyses, while initial Fermi Collaboration line search used pass 6 data.
- Line confirmed in various follow-up papers (Su & Finkbeiner find 2 lines)
- Statistical fluctuation ?
- Astrophysical explanations are difficult to find
- Instrumental effect ? Same feature seen in Earth Limb data

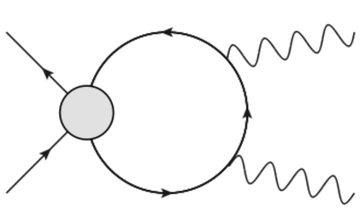

$$\langle \sigma v \rangle_{\gamma\gamma} \sim 10^{-27}\ \mathrm{cm}^3/\mathrm{s}$$

see also:
Lars Bergström, Gianfranco Bertone, Jan Conrad, Christian Farnier, Christoph Weniger 1207.6773
Meng Su, Douglas P. Finkbeiner 1207.7060
Timothy Cohen, Mariangela Lisanti, Tracy R. Slatyer, Jay G. Wacker 1207.0800
Buchmueller and Garny 1206.7056
Meng Su, Douglas P. Finkbeiner 1206.1616
Christoph Weniger 1204.2797 / JCAP 1208 (2012) 007
Torsten Bringmann, Xiaoyuan Huang, Alejandro Ibarra, Stefan Vogl, Christoph Weniger 1203.1312 / JCAP 1207 (2012) 054

Fermi-LAT: Search for Spectral Lines

Fermi count map 3.7years

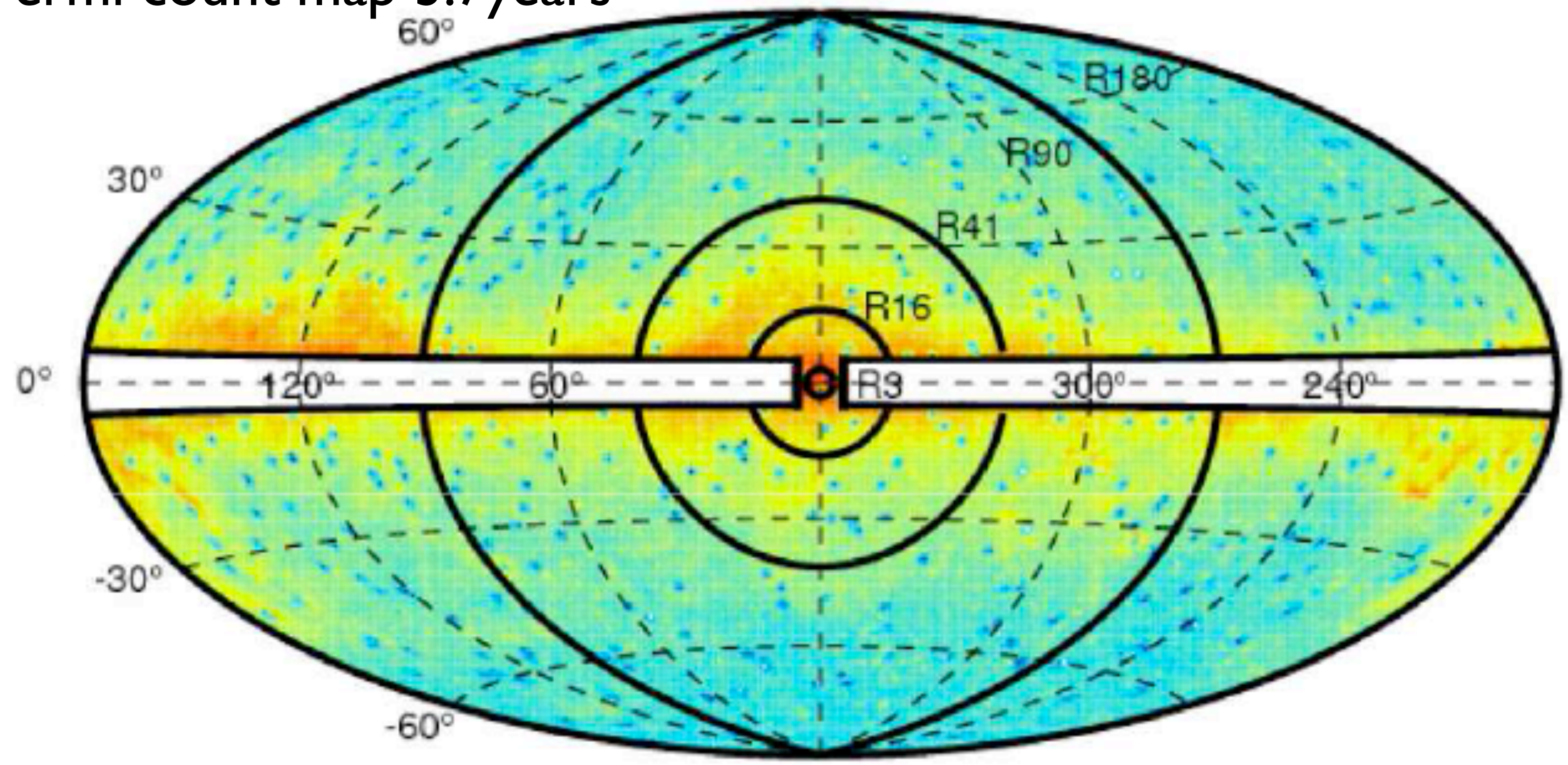

R3 - (contracted NFW, no source masking)

R16 - (Einasto)

R41 - (NFW)

R90 - (Isothermal)

R180 - (Dark Matter Decay)

- Search for lines from 5-300 GeV with 3.7 years of data
  - Maximum likelihood fit with improved energy dispersion model
- Use P7REP_CLEAN event selection
  - Reprocessed data with updated calorimeter calibration constants
  - Clean cuts are recommended for faint diffuse emission analysis
- Mask bright (>10σ for E>1GeV) 2FGL sources

Region of Interest (ROI) optimization is motivated by:
Bringmann et al 2012 arXiv:1203.1312
Weniger 2012 arXiv:1204.2797

95% CL $\langle\sigma_A v\rangle$upper limits

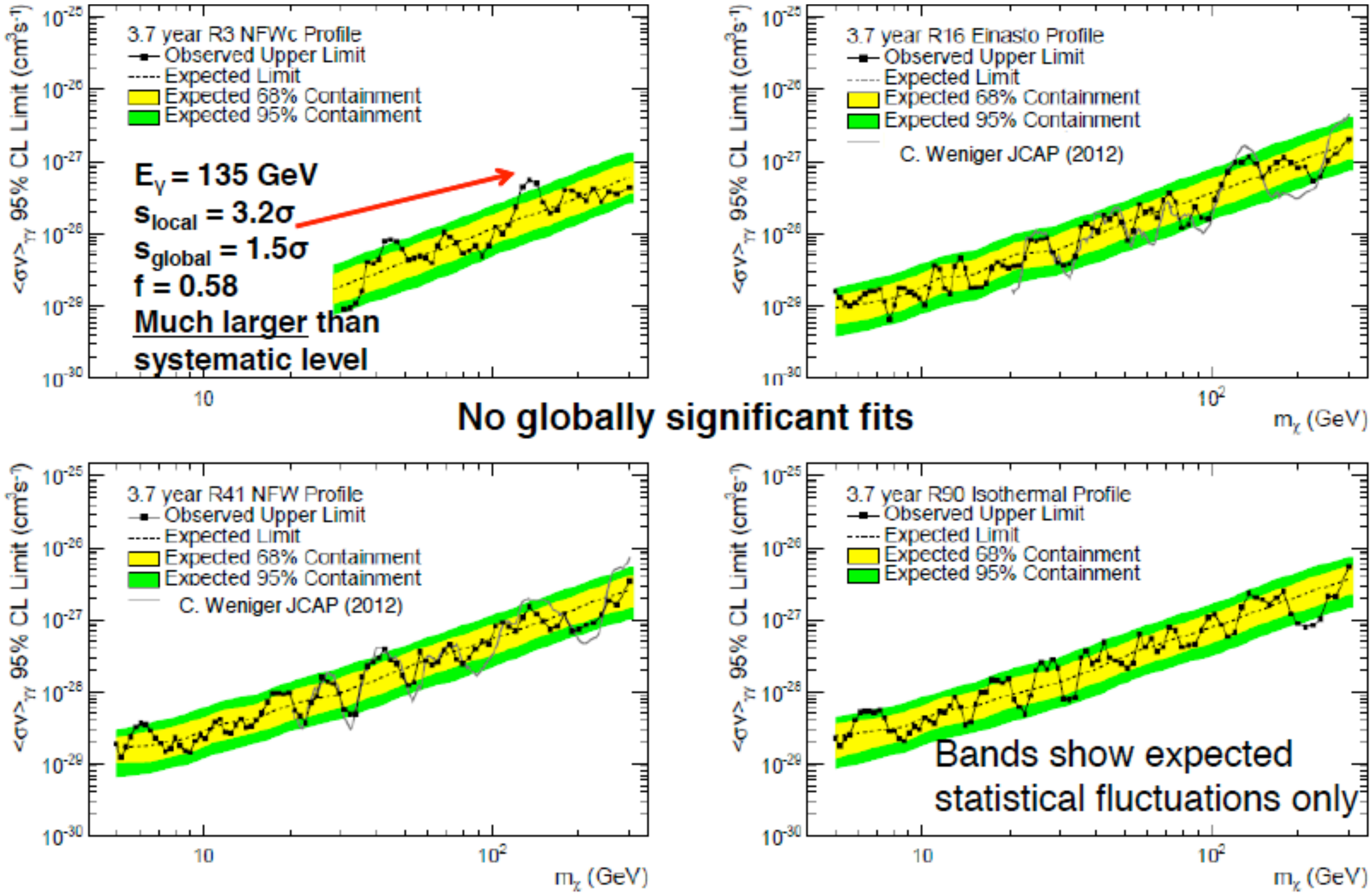

The Line-like Feature near 133 GeV

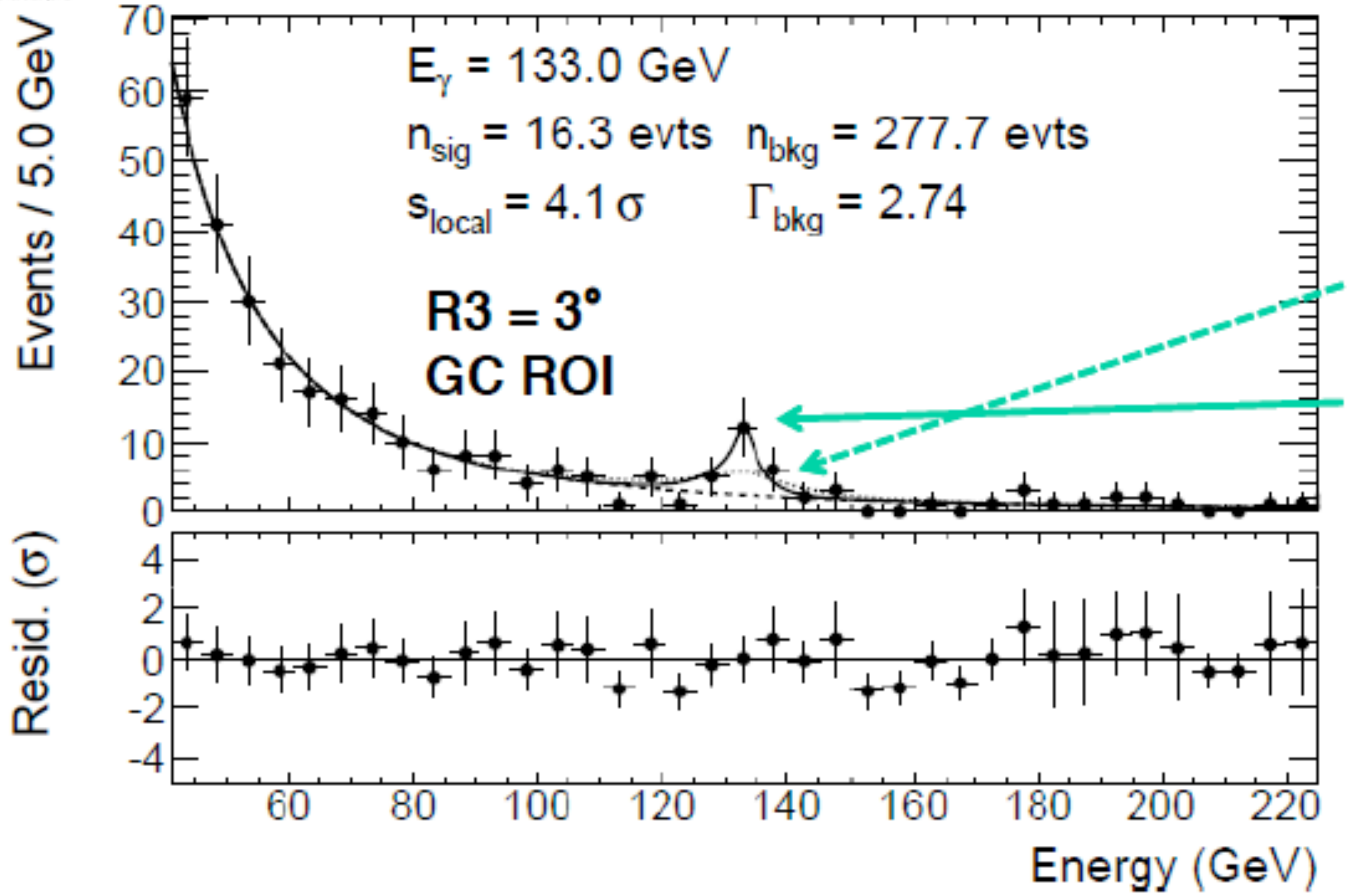

Dashed is fit with s_σ=1

Solid is fit with best fit s_σ

Unbinned fit, binning is for visualization only

- 3.2σ (local) 2D fit at 133 GeV with reprocessed data
  - Fit with energy dispersion model that includes event-by-event energy recon. quality estimator P_E ("2D" model)
- Let width scale factor float in fit (while preserving shape)
  - $s_\sigma = 0.32^{+0.22}_{-0.07} (95\% CL) \quad \Delta TS = 9.4$
  - Feature in data is narrower than expected energy resolution (s_σ=1)

9/12/2013 Andrea Albert (SLAC) 12

Line Search Summary

- Weniger's observation of "bump" is real, confirmed many times including Fermi-LAT collaboration
  - Seen also in simpler, geometric ROI selections
- No "signal" seen from search in dwarfs (Geringer–Sameth & Koushiappas, PRD 021302(R) (2012))
- 130 GeV line also seen in Earth limb data, however magnitude is not large enough to explain GC excess fully.
- "Pass–8" will include new reconstruction code for gamma-rays that do not convert in the Si-tracker and will enhance the effective area and performance.
- Fermi-LAT will switch to Modified Observing Strategy at the end of this year.

H.E.S.S. Line Search

van Eldik and Nekrassov, AIP Conf. Proc. 1505, pp. 474-477, Gamma 2012

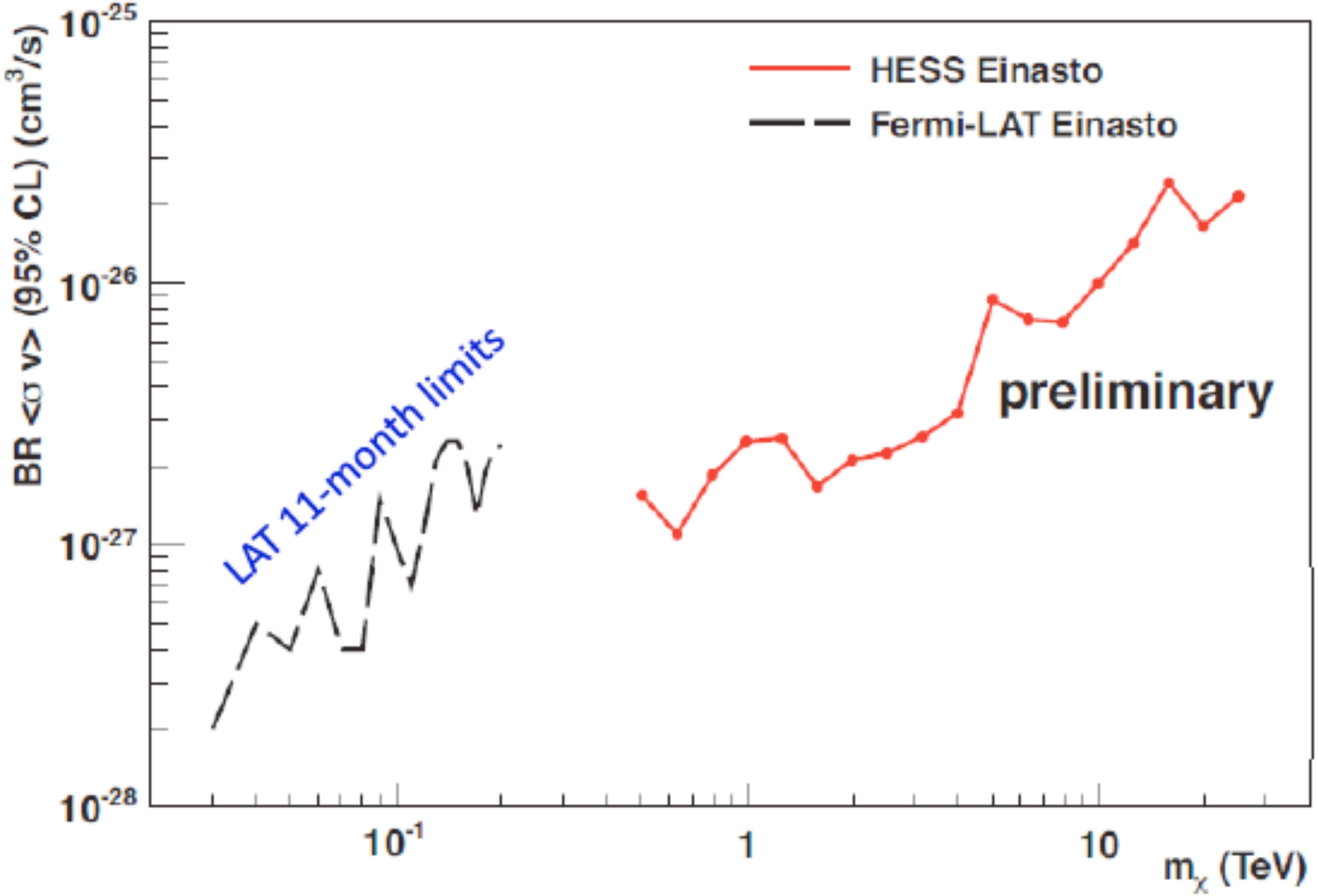

- 112 hours of H.E.S.S. I observations of a 1deg radius circle around the Galactic center
- H.E.S.S. II extends reach to lower energies and 130GeV line might be in sight

Neutrinos

Neutrino Telescopes / Detectors

- **ANTARES** is located at a depth of 2475 m in the Mediterranean Sea, 40 km offshore from Toulon
- Consists 885 10”PMTs on 12 lines with 25 storeys each.
- Detector was competed in May 2008

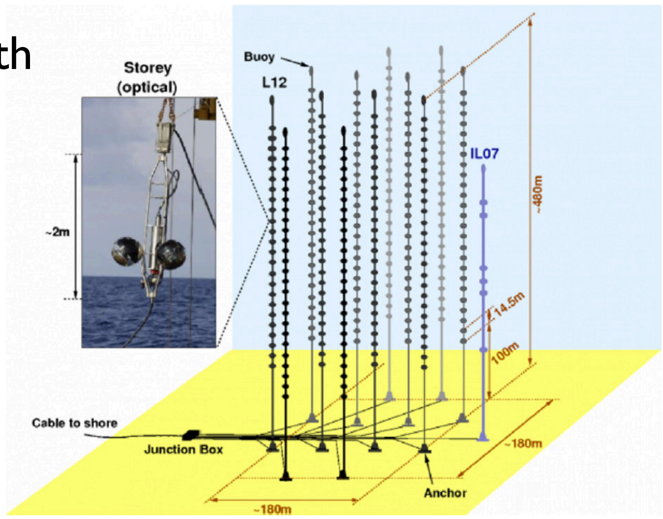

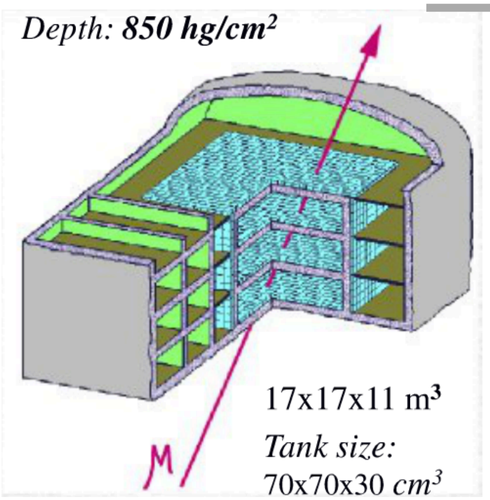

- **Baksan** Underground Scintillator Telescope with muon energy threshold about 1 GeV using 3,150 liquid scintillation counters
- Operating since Dec 1978 ; More than 34 years of continuous operation

- Lake **Baikal**, Siberia, at a depth 1.1 km NT36 in 1993
- NT200 (since Apr 1998) consists of one central and seven peripheral strings of 70m length

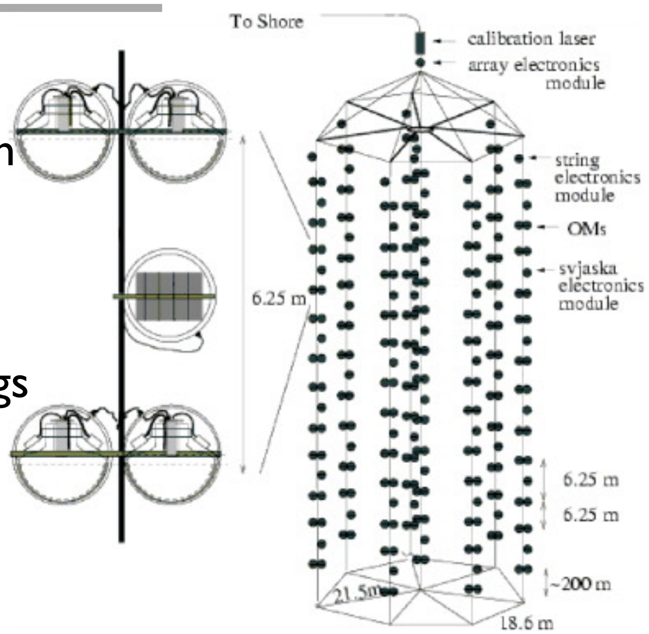

- **IceCube** at the Geographic South Pole
- 5160 10”PMTs in Digital optical modules distributed over 86 strings instrumenting ~1km^3
- Physics data taking since 2007 ; Completed in December 2010, including **DeepCore** low-energy extension

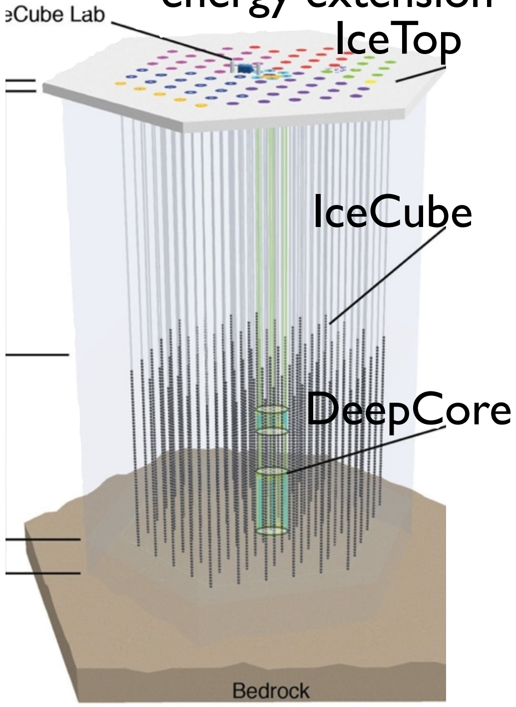

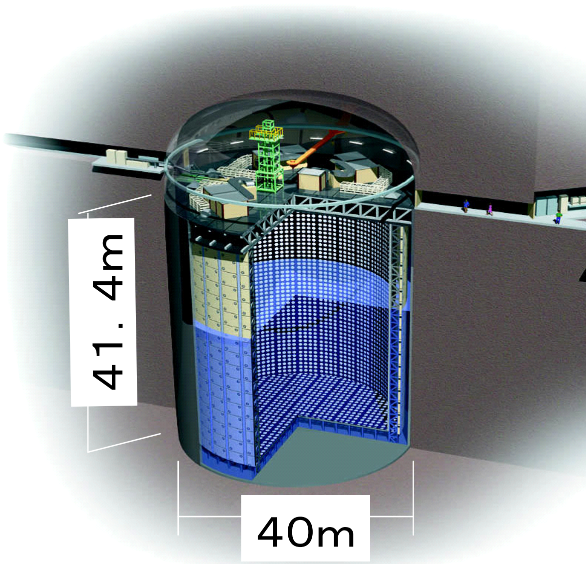

- **Super-Kamiokande** at Kamioka uses 11K 20” PMTs
- 50kt pure water (22.5kt fiducial) water-cherenkov detector
- Operating since 1996

IceCube Anisotropies in the Galactic Halo

IC22 Halo Analysis

high-purity neutrino sample (up-going muon events)

276 days of data from the IceCube 22-string configuration detector acquired during 2007 and 2008

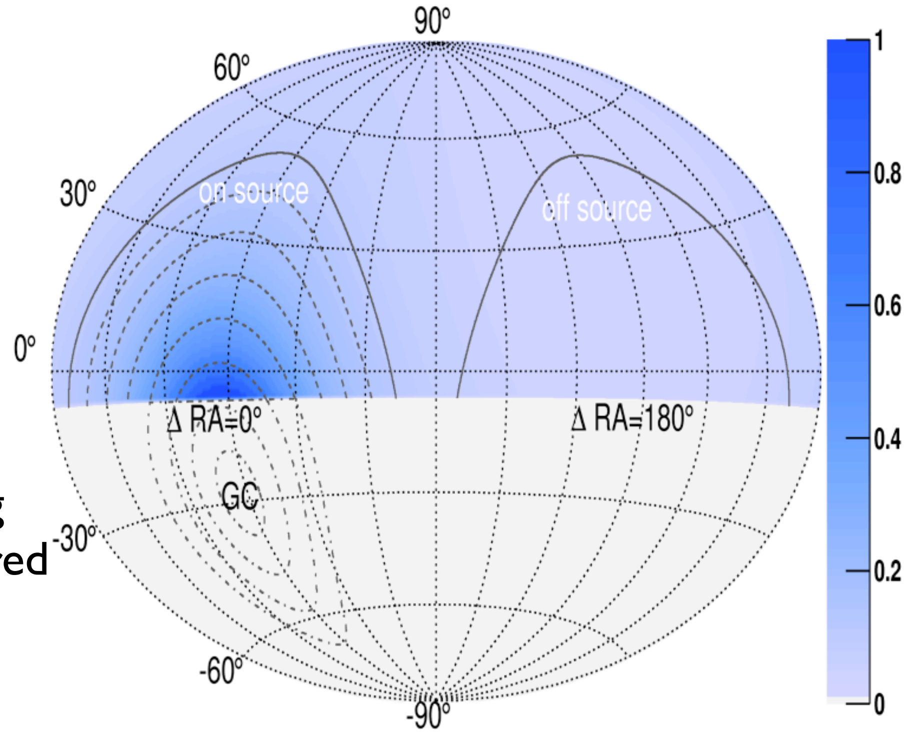

Phys.Rev.D84:022004,2011

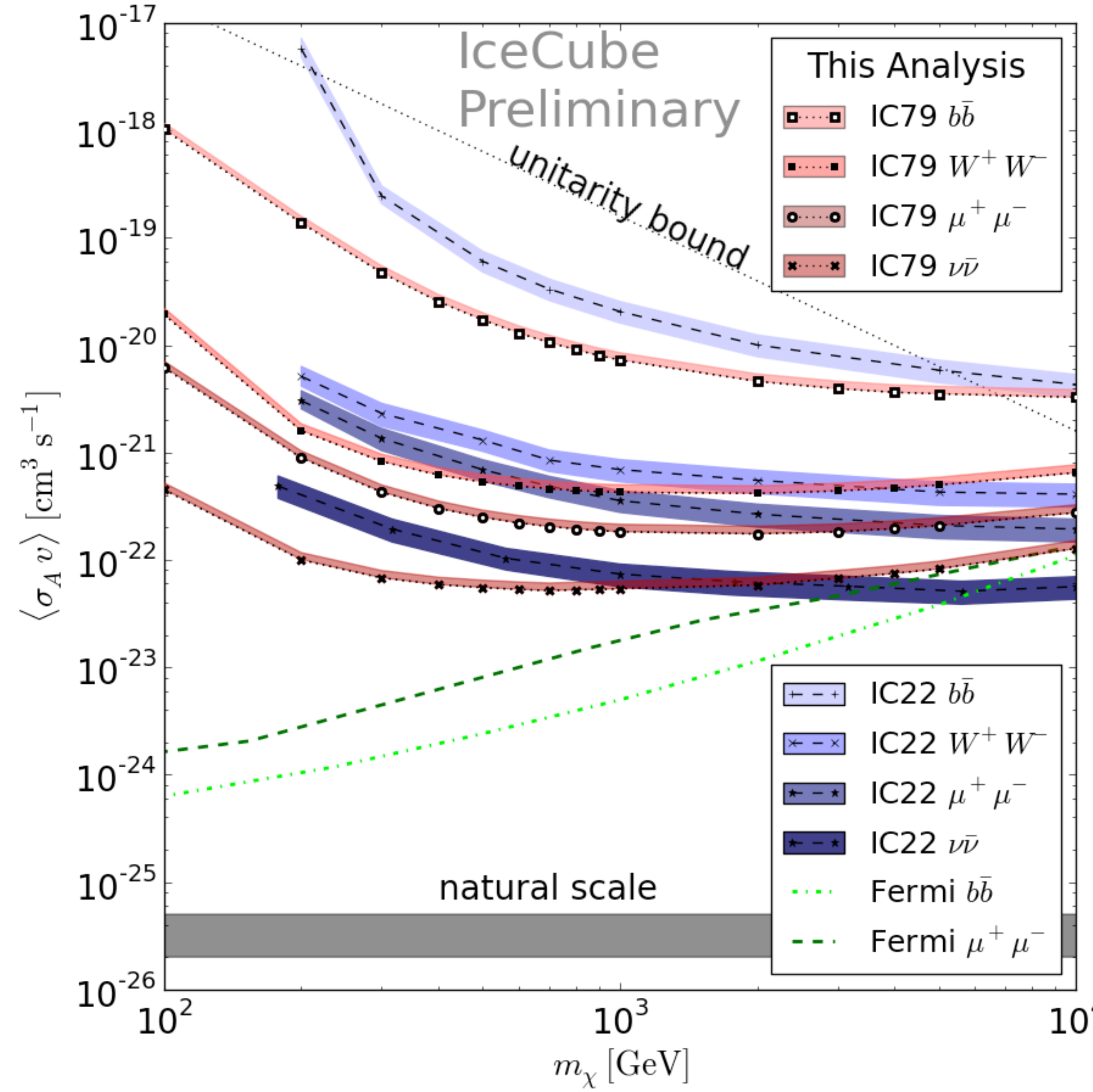

IC79 multipole analysis

ICRC 2013

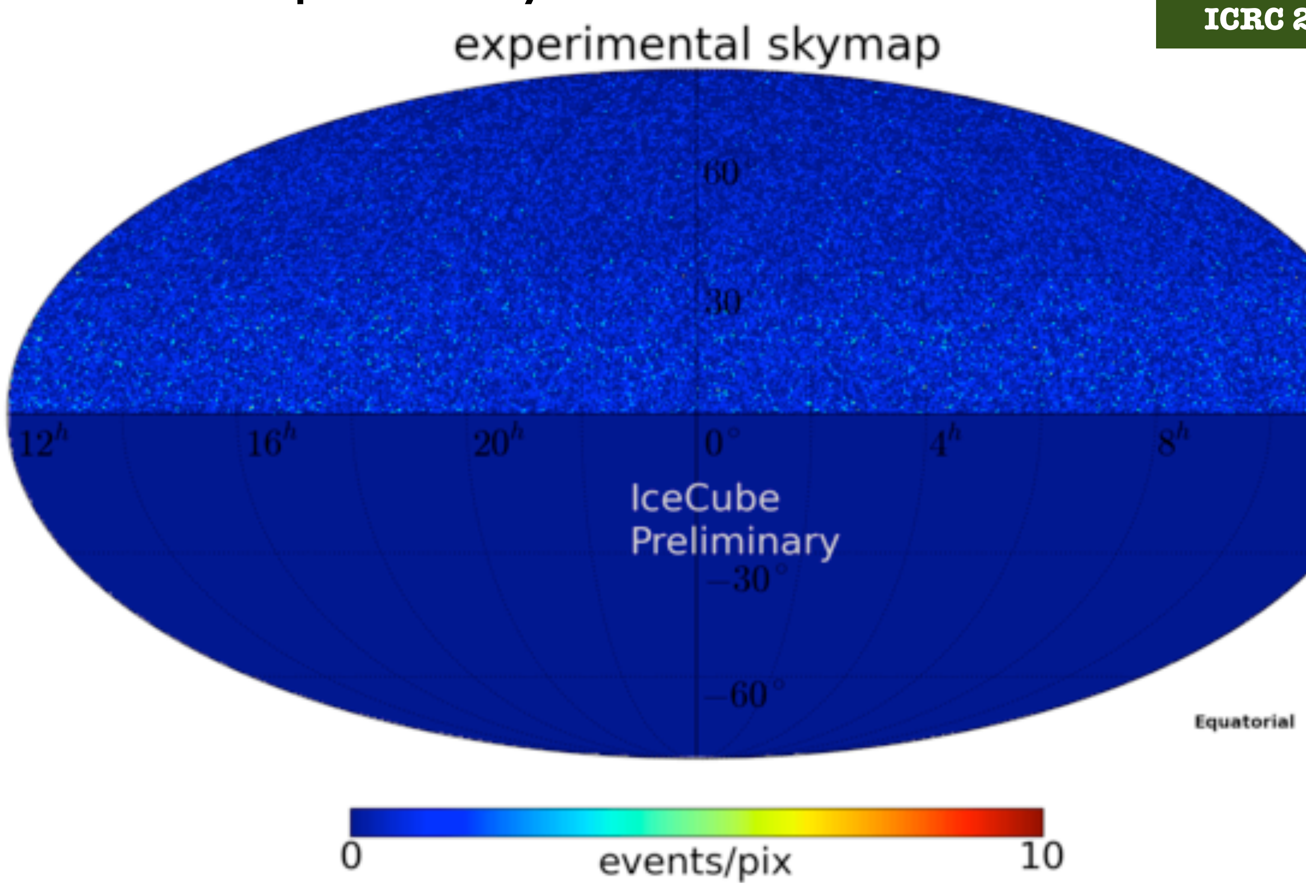

Super-K - Galactic Search

- Search for a diffuse signal from Milky Way halo
  - Assume annihilation into νν, bb, or WW
- Use all samples e-like + mu-like FC + PC (2806 days)+UPMU (3109 days)
- Use all neutrino flavors and topologies

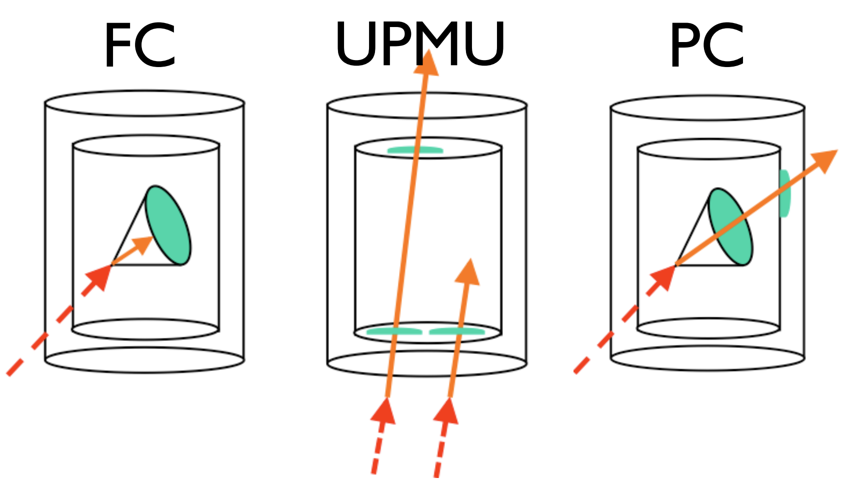

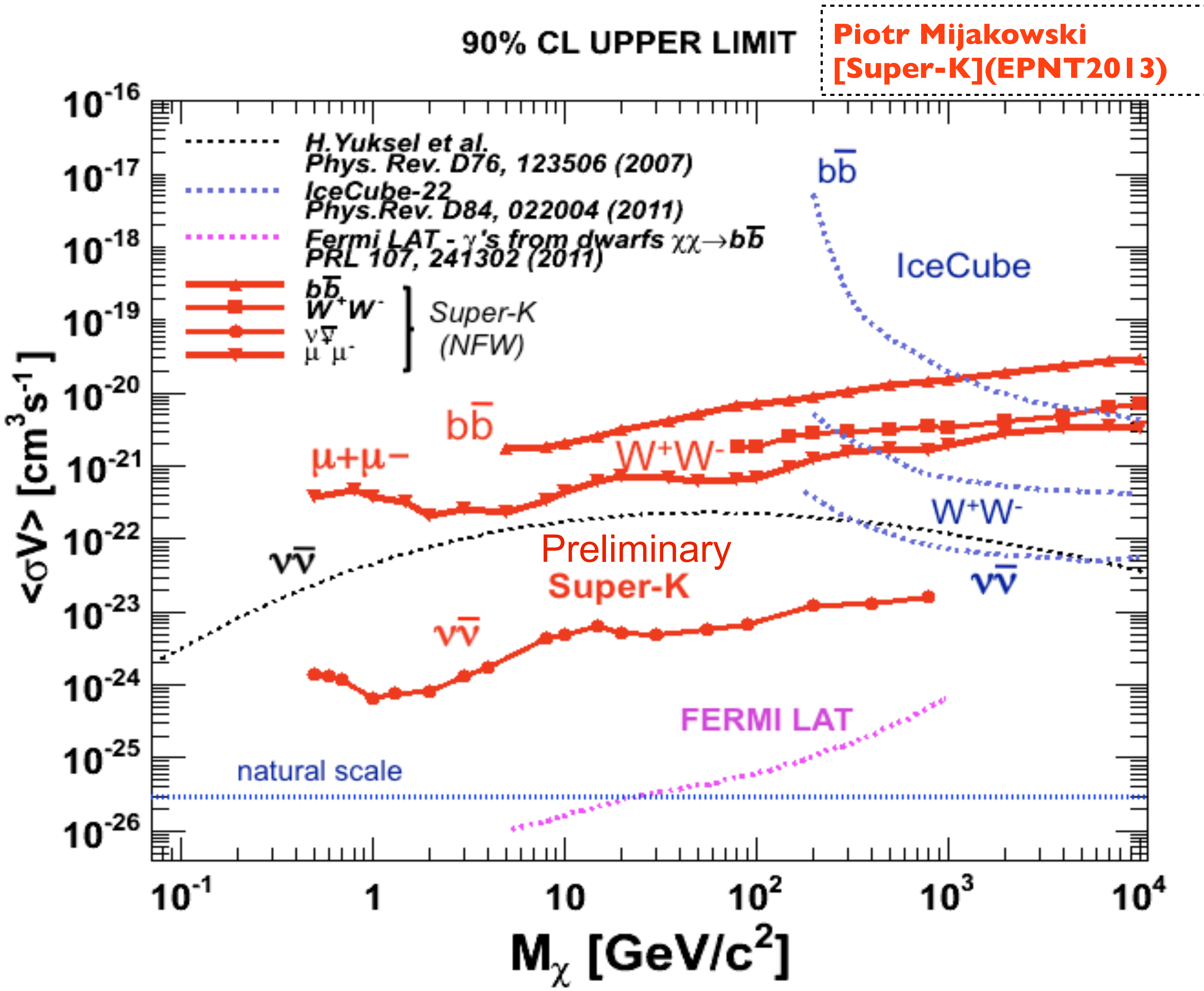

IceCube Search for Dark Matter at the Galactic Center

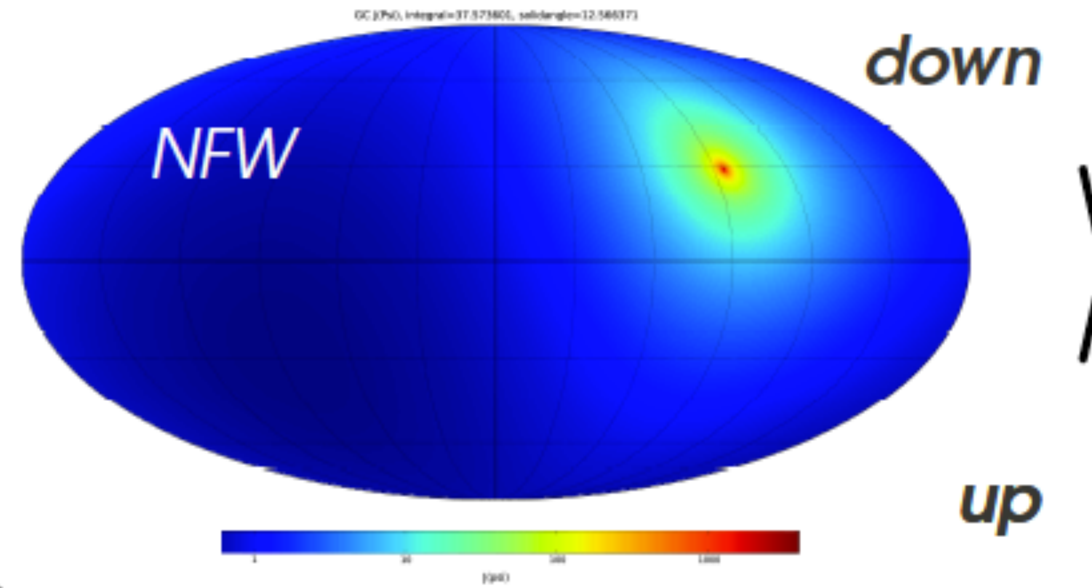

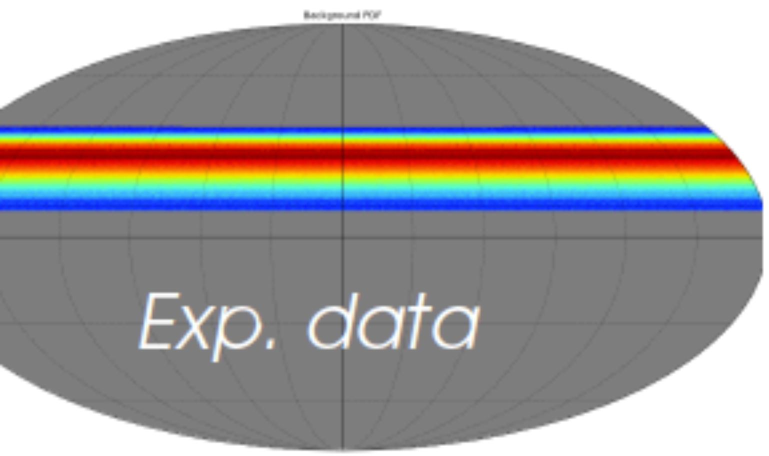

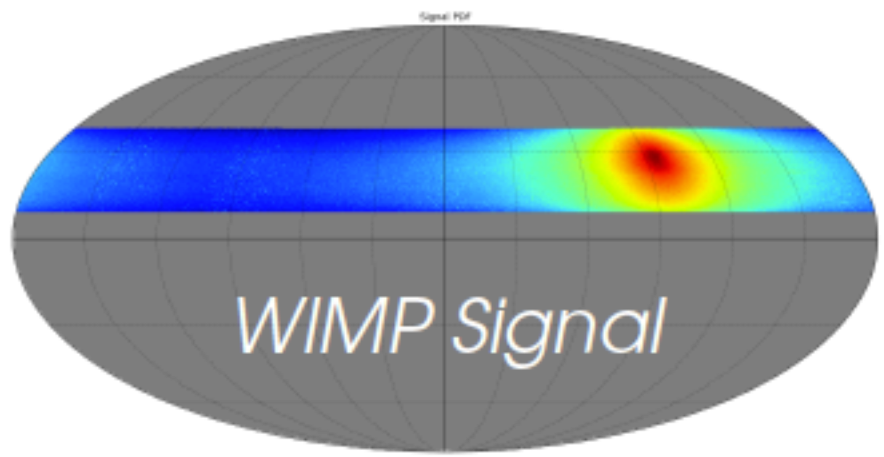

2D PDFs generated with healpix

- IceCube achieves sensitivity to reach down to WIMP masses of 30GeV

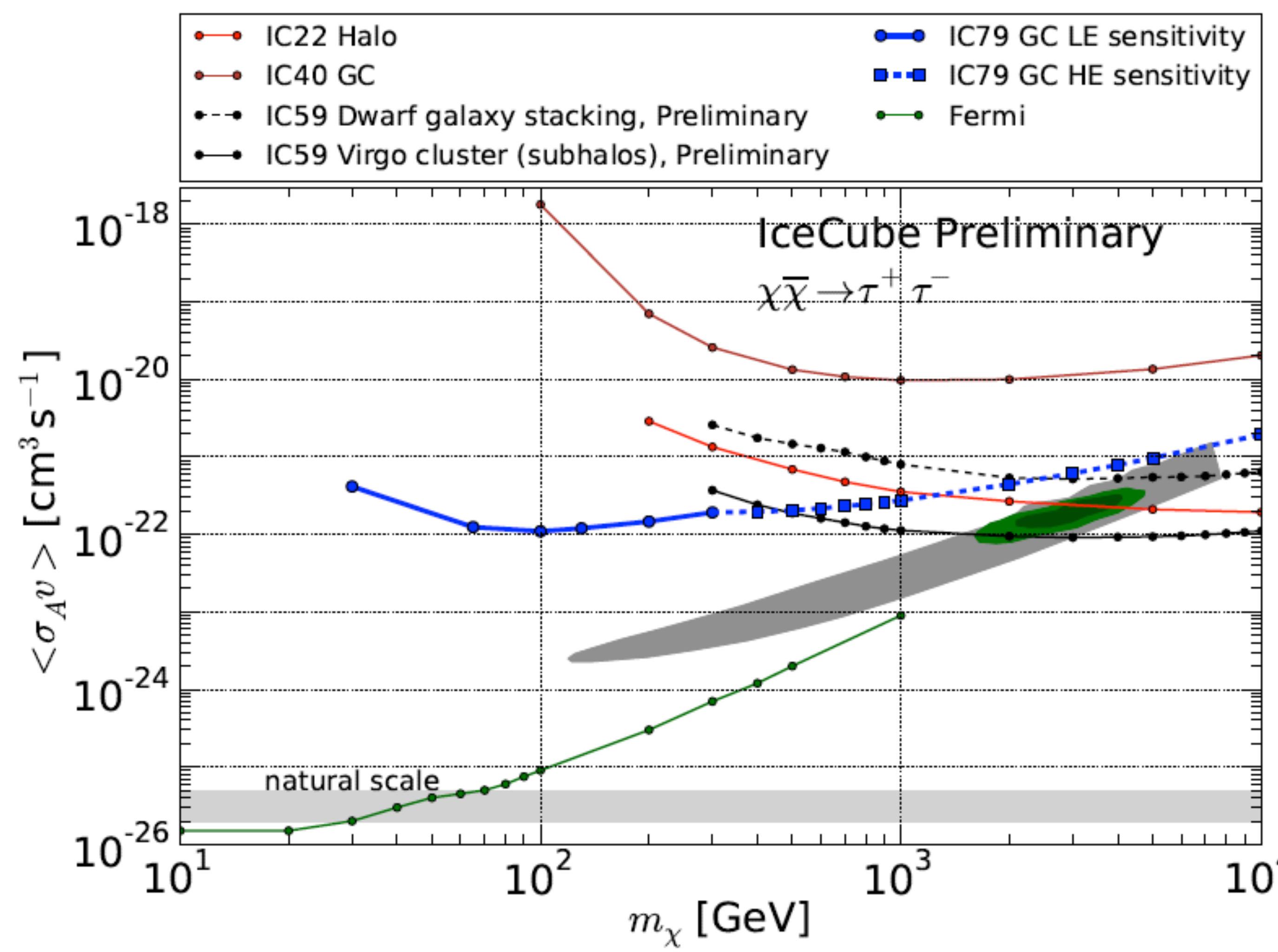

IceCube Search for Dark Matter at the Galactic Center

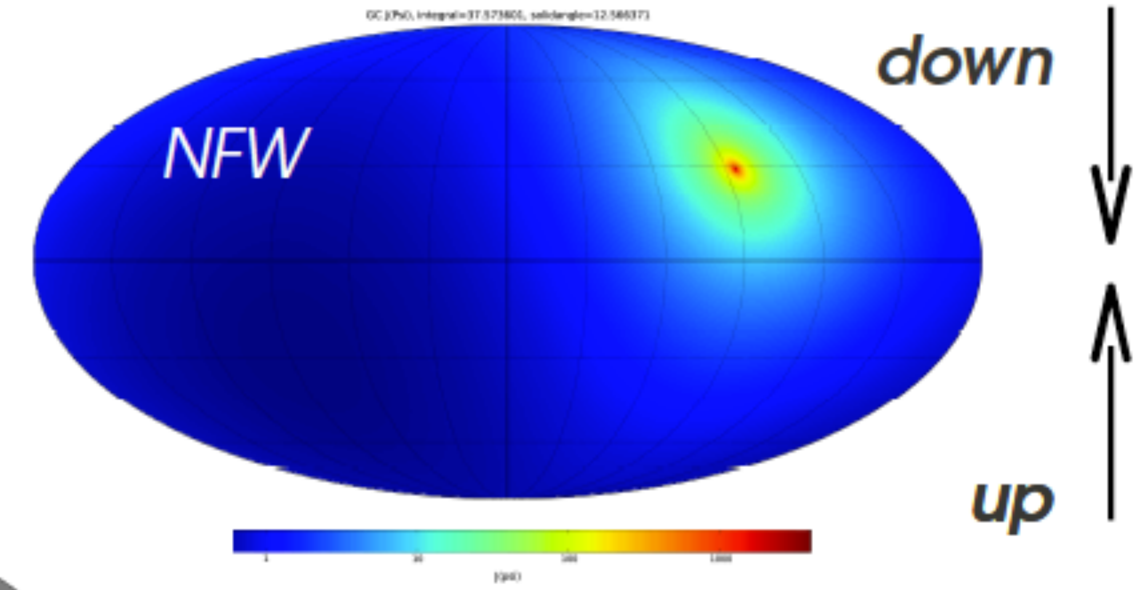

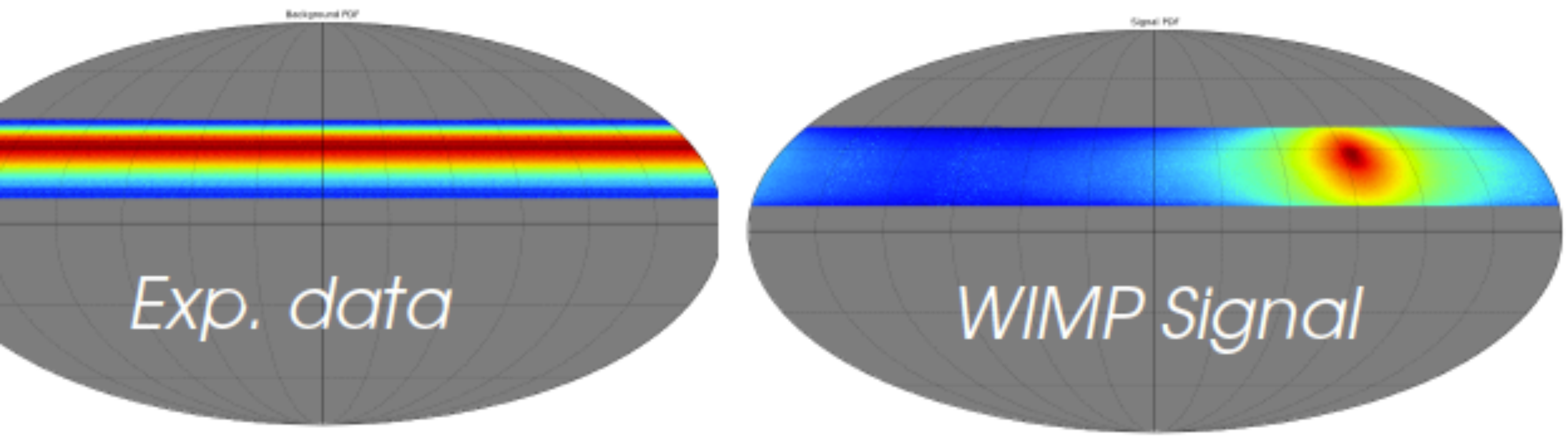

2D PDFs generated with healpix

- IceCube achieves sensitivity to reach down to WIMP masses of 30GeV

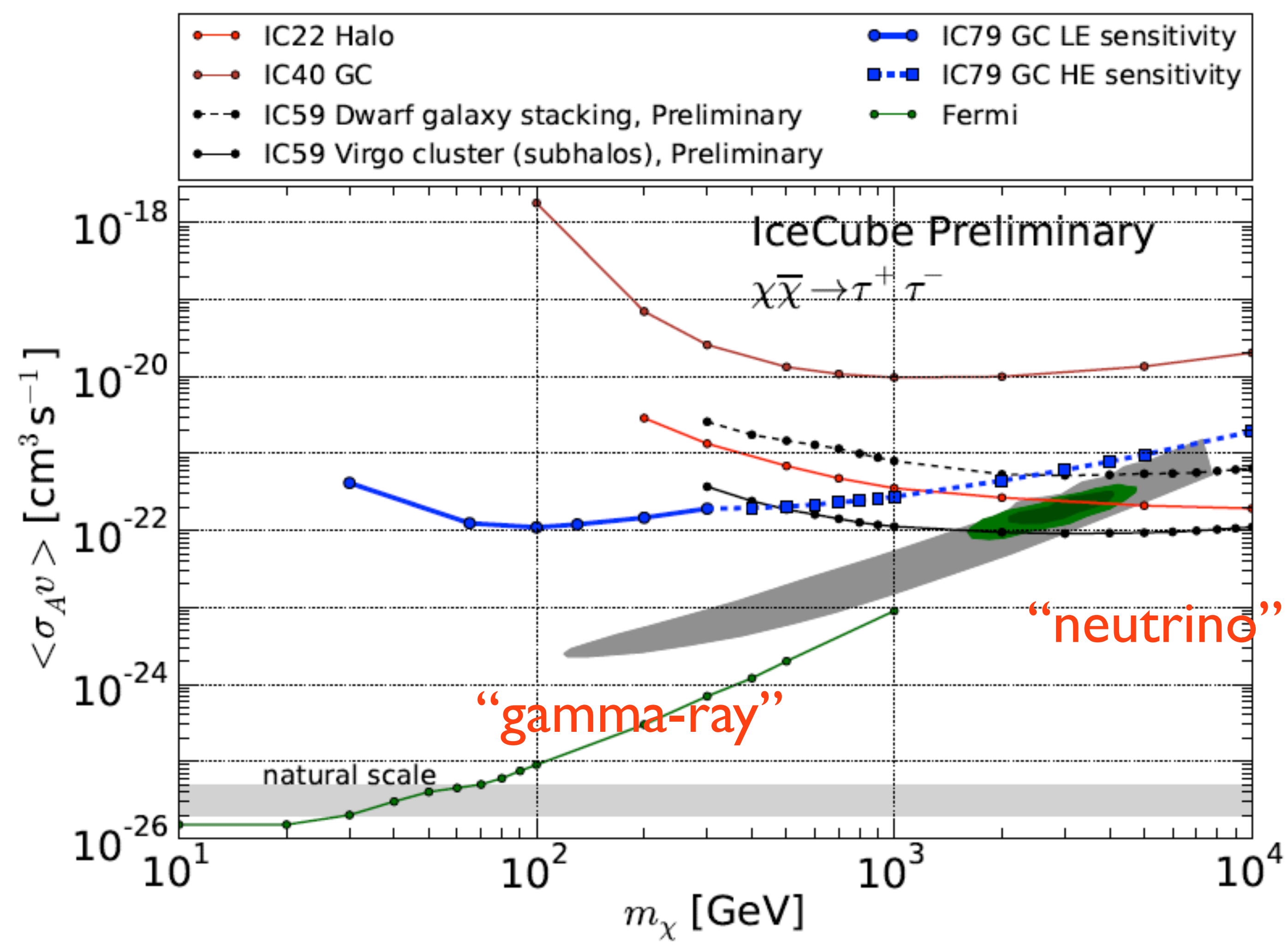

IceCube Search for Dark Matter at the Galactic Center

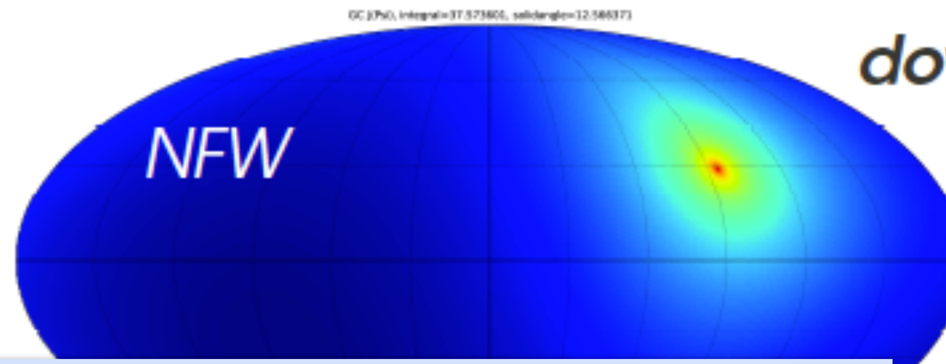

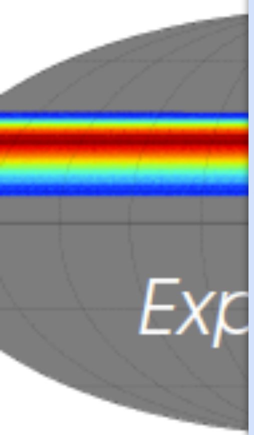

Status of interpretation of positron excess + electron spectrum as originating from Dark Matter only (for NFW profile):

Excluded	Tension	Possible
$\chi\chi \rightarrow \mu^+\mu^-$	$\chi\chi \rightarrow e^+e^-$	$\chi \rightarrow \mu^+\mu^-$
$\chi\chi \rightarrow \tau^+\tau^-$	$\chi\chi \rightarrow e^+e^-e^+e^-$	$\chi \rightarrow \mu^+\mu^-\mu^+\mu^-$
$\chi\chi \rightarrow \tau^+\tau^-\tau^+\tau^-$	$\chi\chi \rightarrow \mu^+\mu^-\mu^+\mu^-$	
	$\chi \rightarrow \tau^+\tau^-$	

- WIMP masses of 30GeV

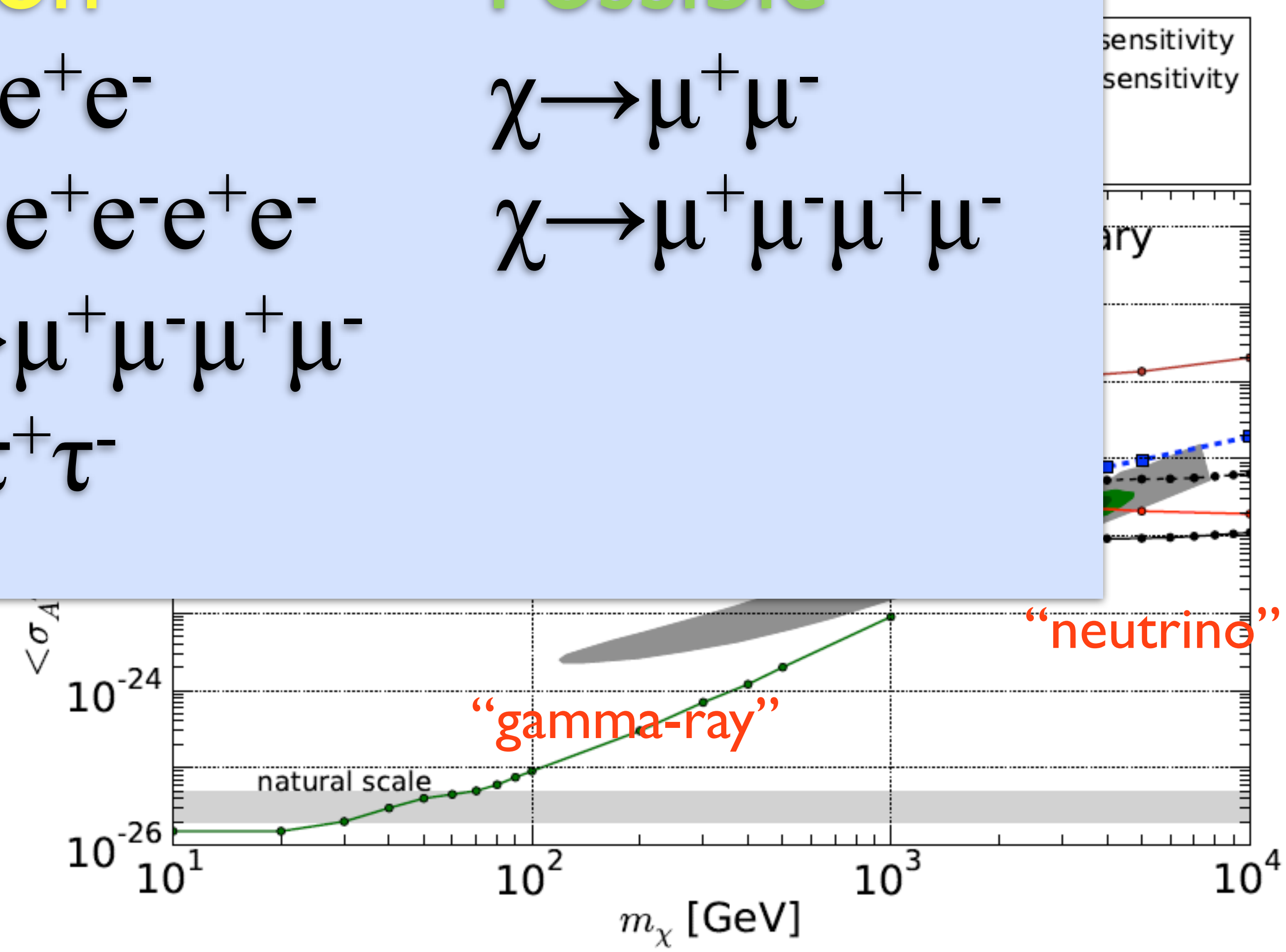

Origin of the PeV events

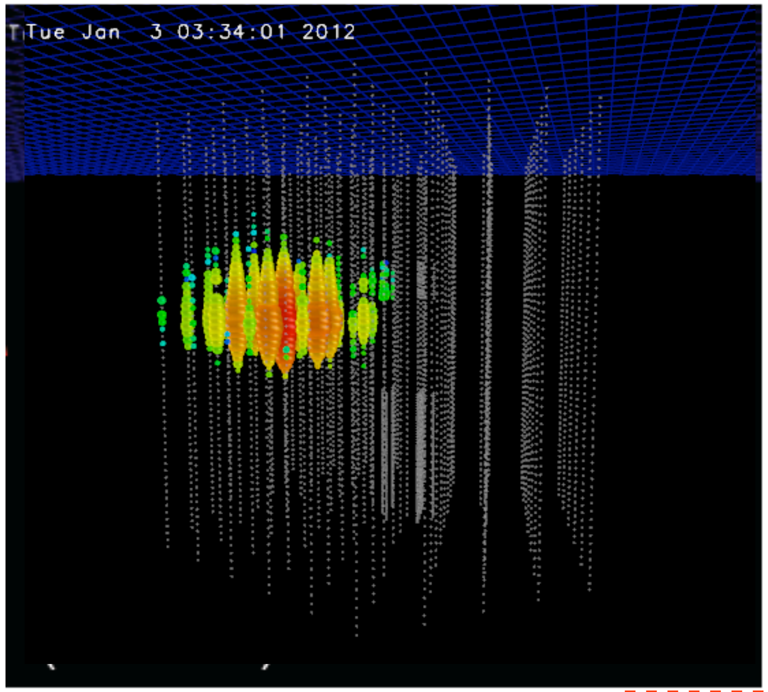

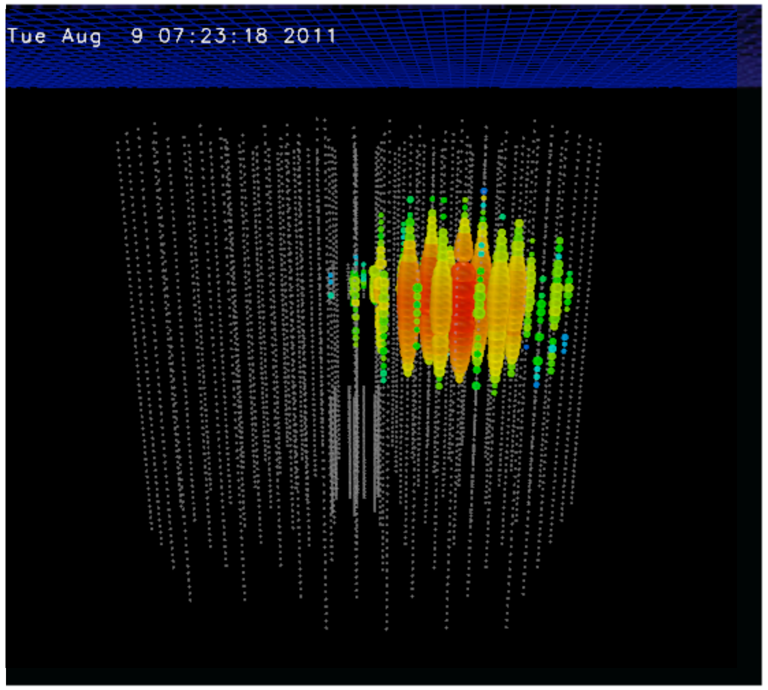

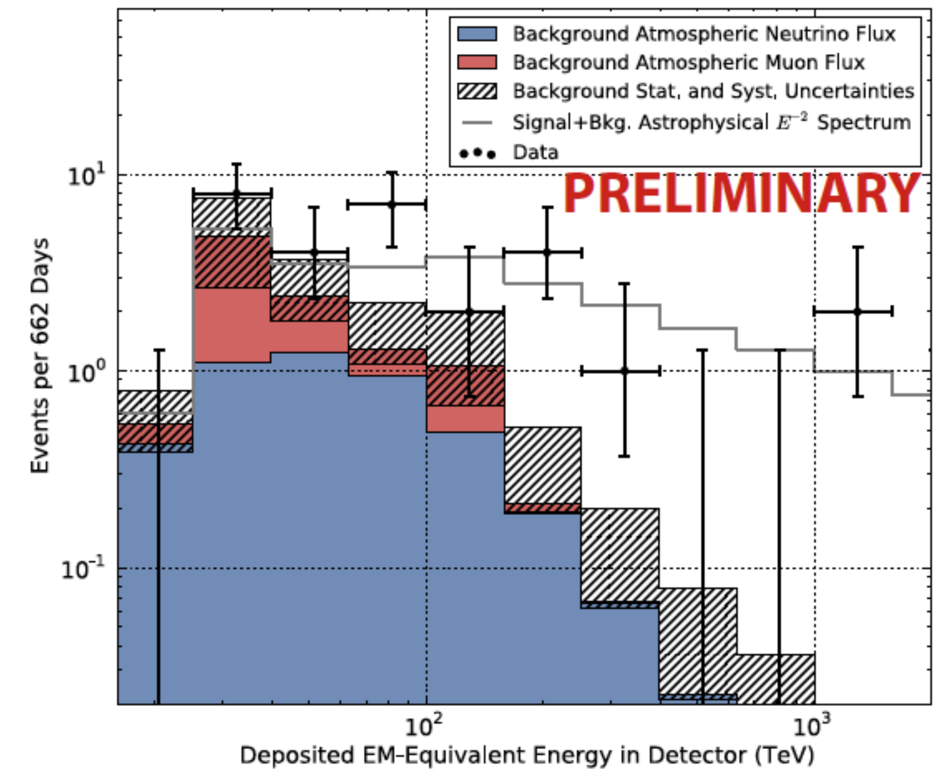

IceCube arXiv:1304.5356

This afternoon: Naoko Kurahashi Neilson

- What do the two IceCube events tell us ? and the additional 26 events ?

Papers based on the 2 IceCube Events [Phys.Rev.Lett. 111 (2013) 021103)]: so far 48
<u>Comprehensive discussion (example):</u>
R.Laha et al. Phys. Rev. D 88, 043009

GZK neutrinos	a few events at ~ 100 TeV - 1 PeV implies many more events at higher energies	***Impossible***
Conventional atm. neutrinos	Very low flux predictions. Flavor ratio favors strongly favors muon neutrinos	***Implausible***
Prompt	Coincidence in down-going events. Possible only if proton composition; upward statistical fluctuation needed	***Unlikely***
Astrophysical	Most natural. Events are isotropic. Cannot be continuum spectrum. power law with break at ~ 2 PeV ?	***Plausible***
Dark Matter	2 events overlap in energy	**Intriguing**

Heavy Dark Matter

- IceCube has reported 2 high-energy cascade events in 2 years of IceCube 79 + 86-string data
  - consistent with electron neutrino interactions at about 1PeV
    - reported events are intriguingly close in energy

Could this be dark matter ?

Evidence:

B. Feldstein, A. Kusenko, S. Matsumoto, and T. Yanagida arXiv:1303.7320v1 [hep-ph]

- 2.4PeV Dark Matter Particle mass
- Flux can be related to the lifetime τ_{DM}

$$\tau_{\mathrm{DM}} \simeq 1.9 N_\nu \times 10^{28}\ \mathrm{s}$$

- Models
  - Singlet fermion in an extra dimension
  - Hidden Sector Gauge Boson
  - Gravitino Dark Matter with R-Parity Violation

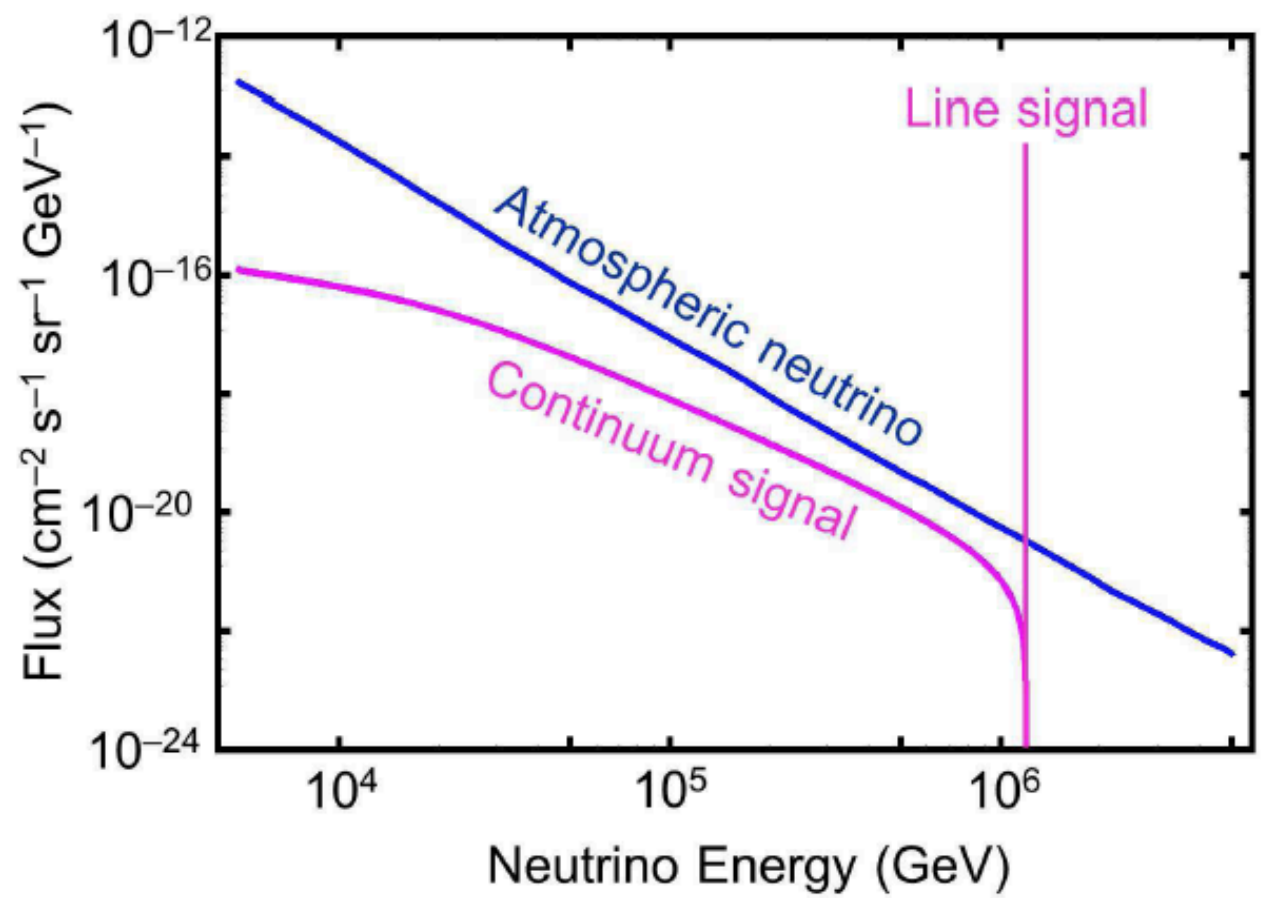

NFW Profile [Kohri, Park, Rott (in prep.)]

Decay **Annihilation**

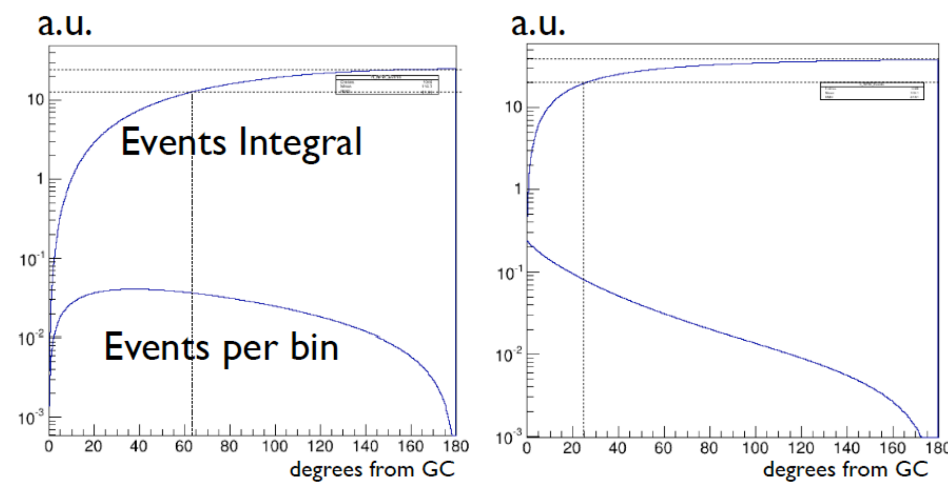

50% of events within 65°

50% of events within 25°

Heavy Dark Matter

- IceCube has reported 2 high-energy cascade events in 2 years of IceCube 79 + 86-string data
  - consistent wi
    interactions a
    - reported
      intriguingl

Could this be (

B. Felds
and T. Y

Evidence:
- 2.4PeV Dark Matte
- Flux can be related

$\tau_{\mathrm{DM}} \simeq 1.9$

- Models
  - Singlet fermion i
  - Hidden Sector (
  - Gravitino Dark
    Violation

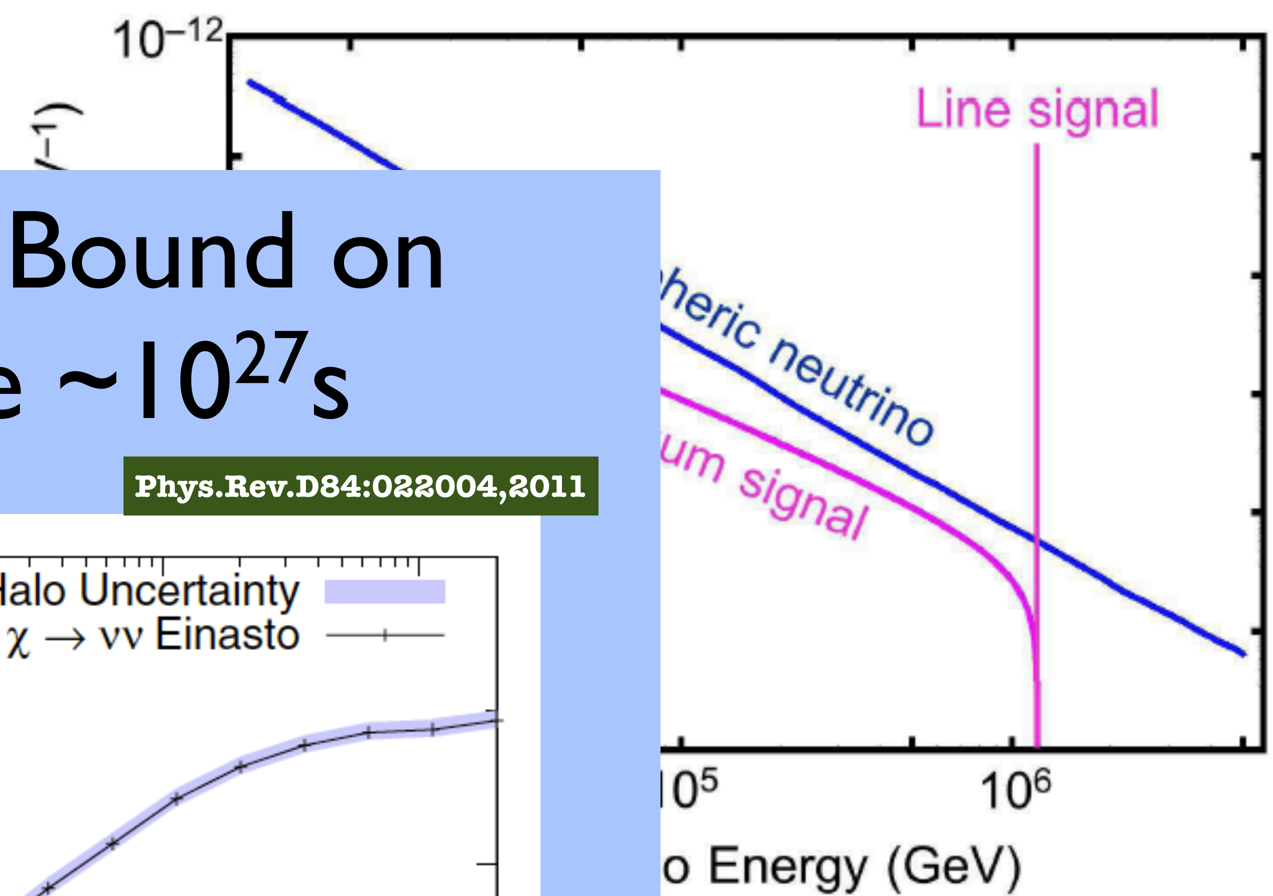

V Profile

[Kohri, Park, Rott (in prep.)]

Annihilation

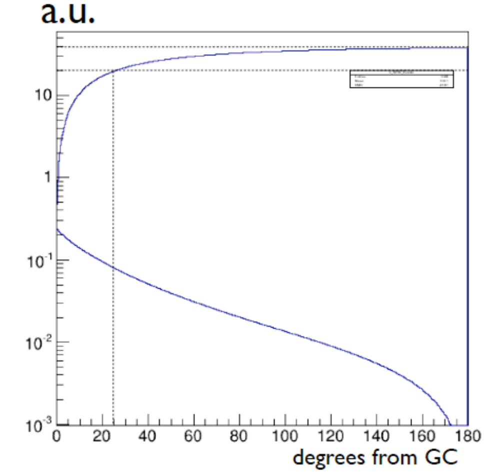

50% of events within 65°

50% of events within 25°

IceCube Bound on lifetime ~10^{27}s

Phys.Rev.D84:022004,2011

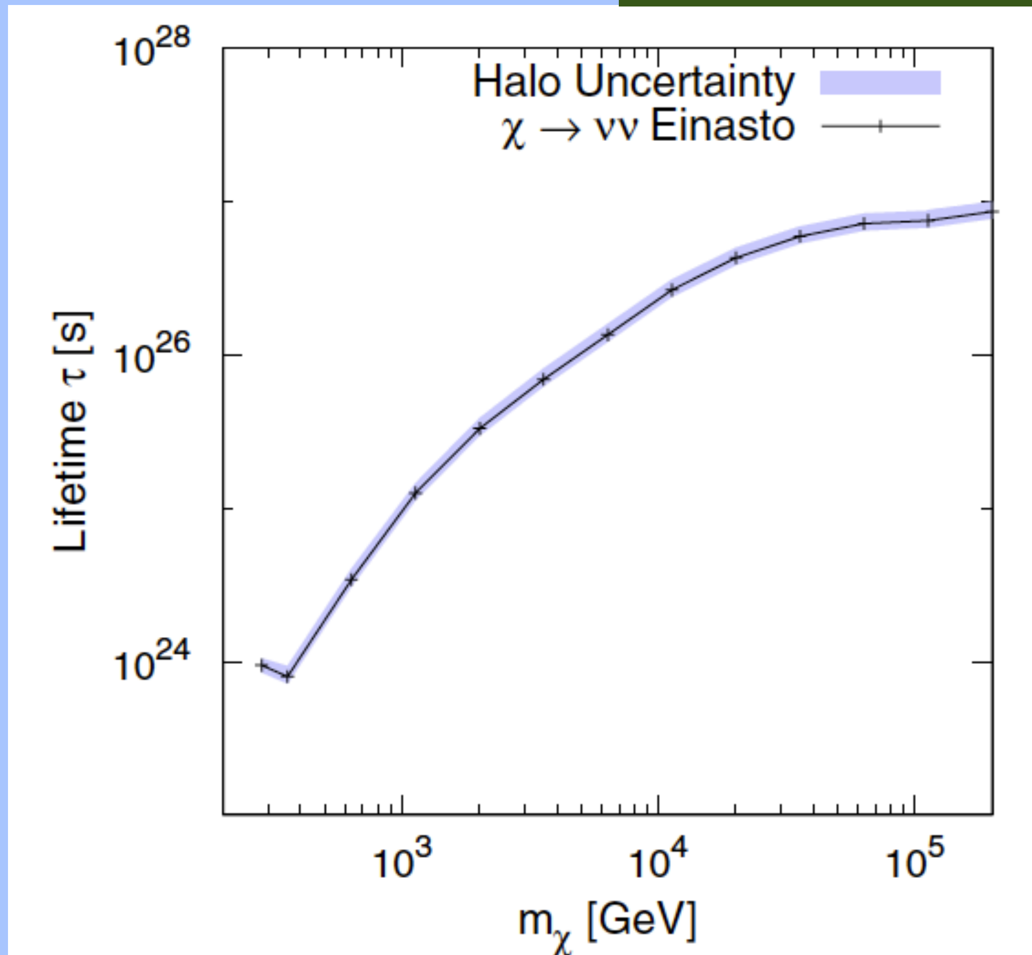

Solar WIMPs

σ_{scatt}

Solar WIMPs

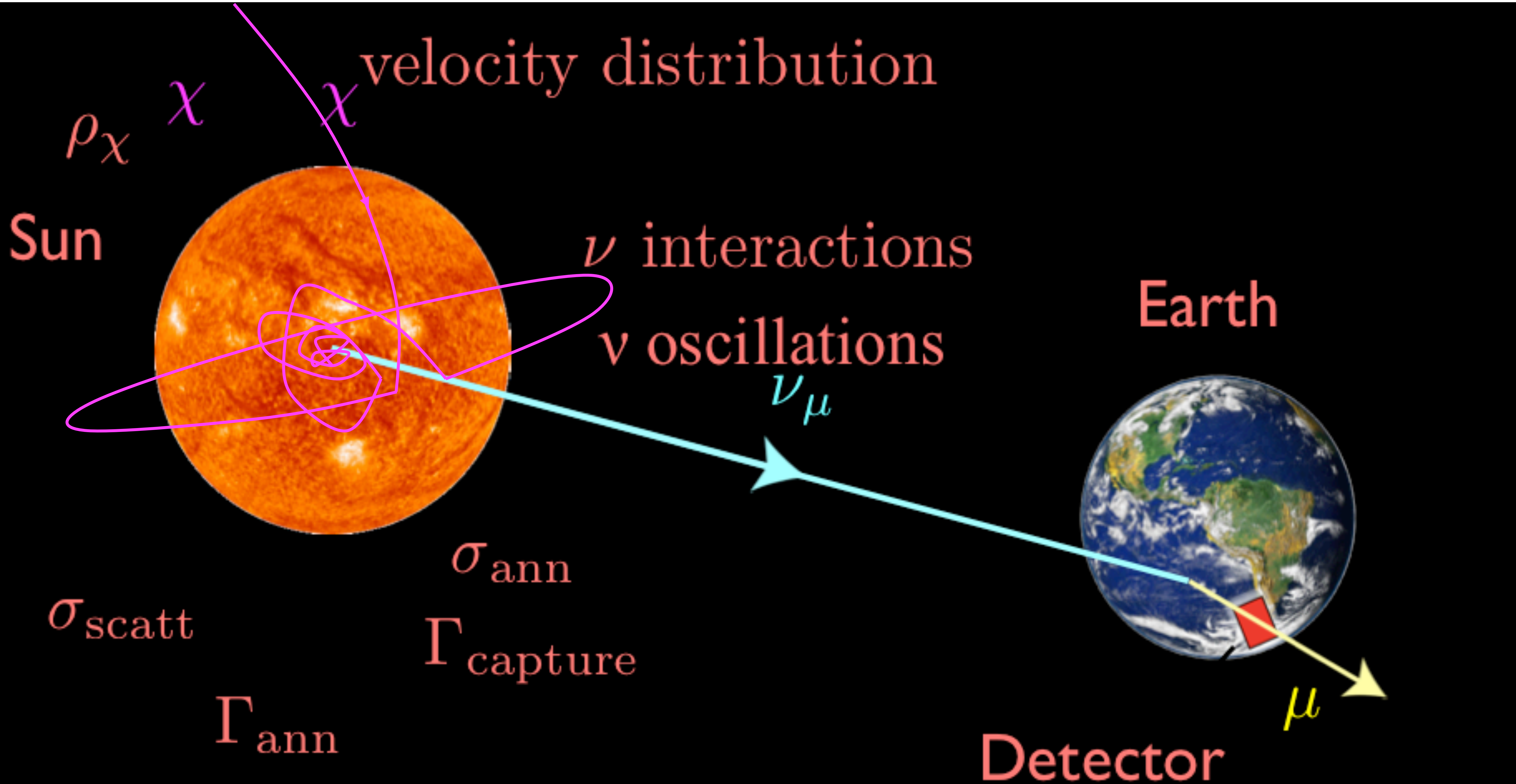

Freese '86
Krauss, Srednicki & Wilczek '86
Gaisser, Steigman & Tilav '86

Silk, Olive and Srednicki '85
Gaisser, Steigman & Tilav '86

Solar WIMP Capture

- WIMPs can get gravitationally captured by the Sun
  - Capture rate, Γ_C ,depends on WIMP-nucleon scattering cross section
- Dark Matter accumulates and starts annihilating
  - → Only neutrinos can make it out
- Equilibrium: The capture rate regulates the annihilation rate ($\Gamma_A=\Gamma_C/2$)
  - The neutrino flux only depends on the WIMP-Nucleon scattering cross section

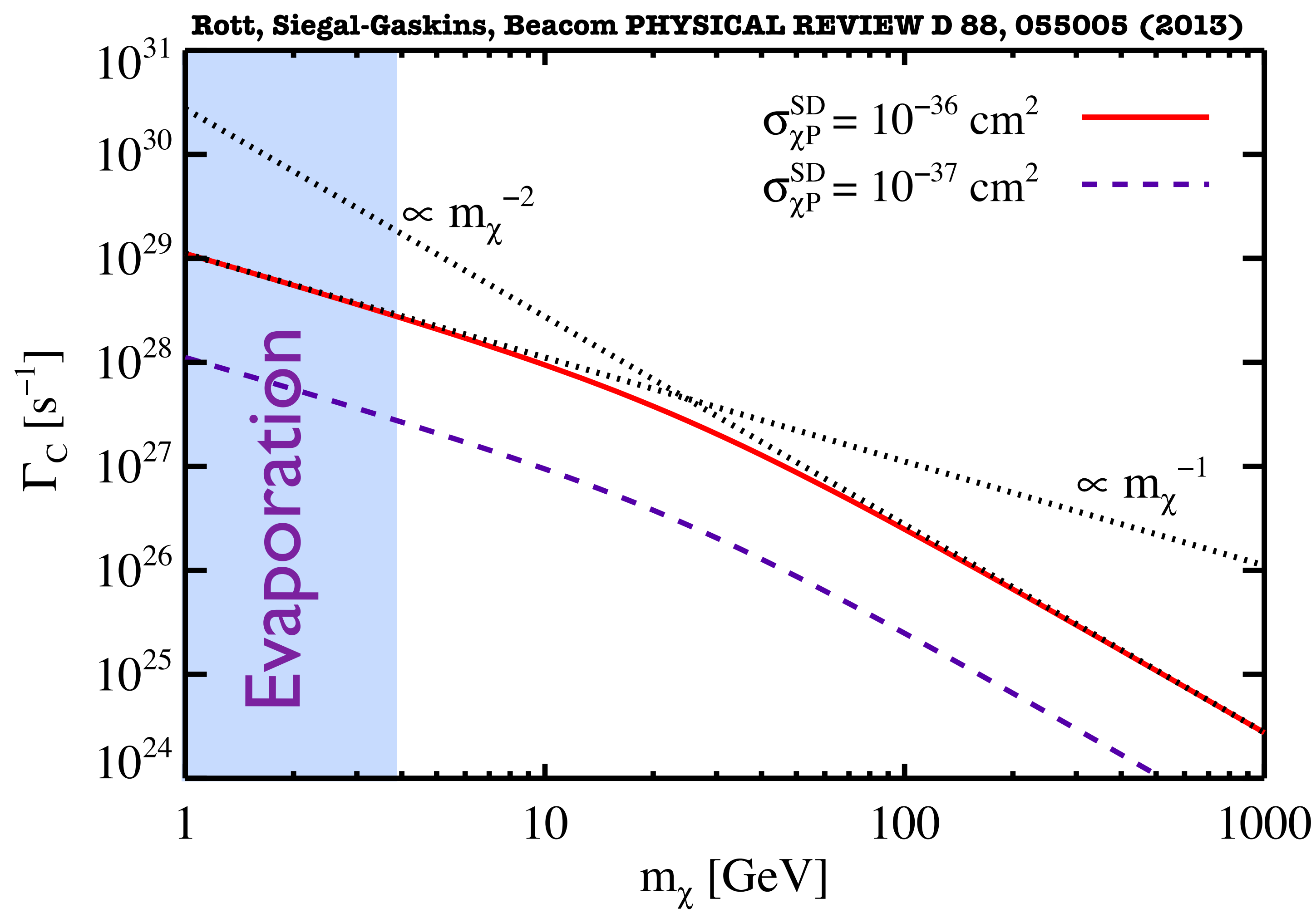

The capture rates scales as:

$\Gamma_C \sim \rho_\chi m_\chi^{-1} \sigma_A$ for $m_\chi \sim m_A$

$\Gamma_C \sim \rho_\chi m_\chi^{-2} \sigma_A$ for $m_\chi >> m_A$

number density + kinematic suppression

m_A - is the target mass

Local Dark Matter Density / Velocity

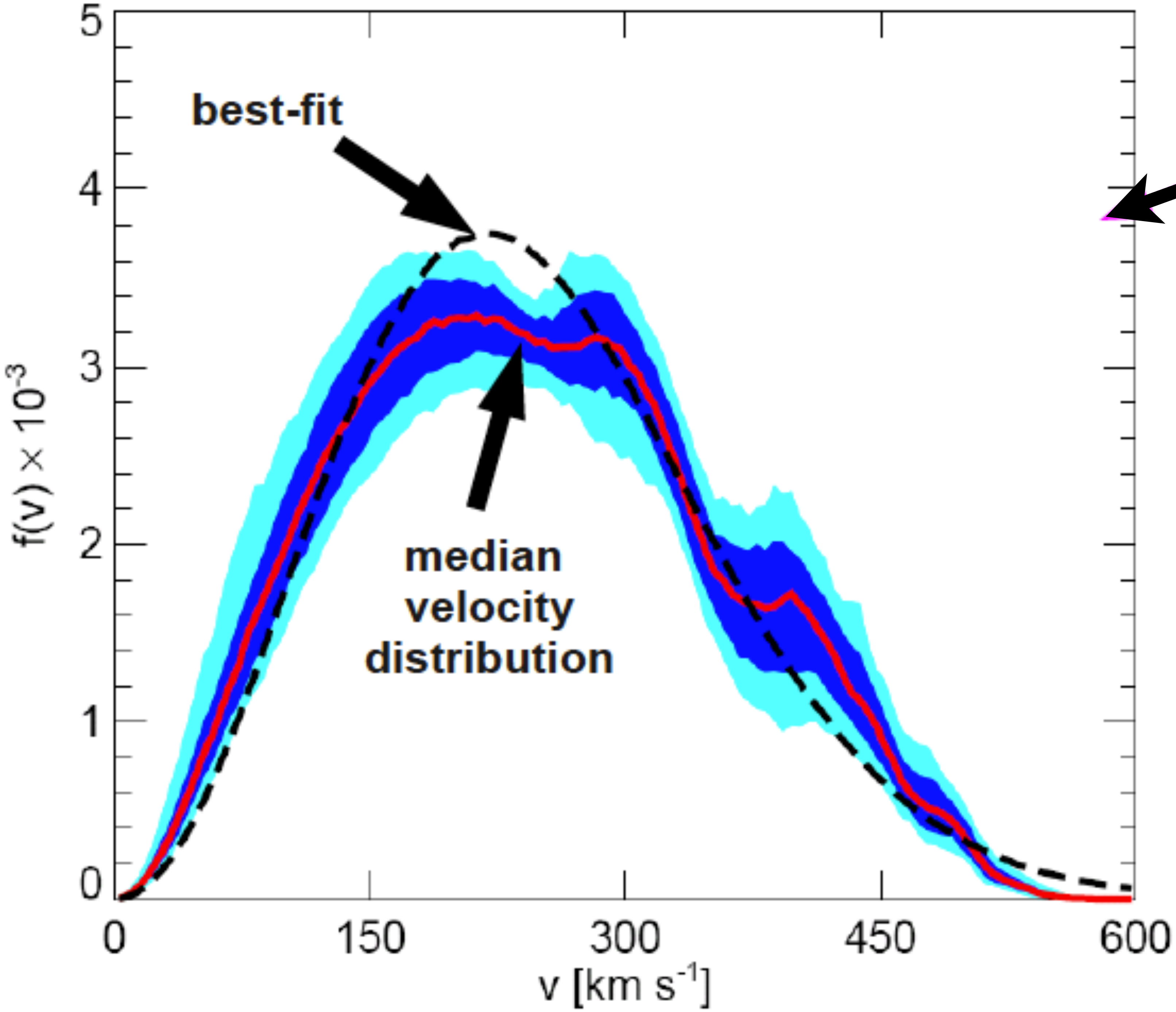

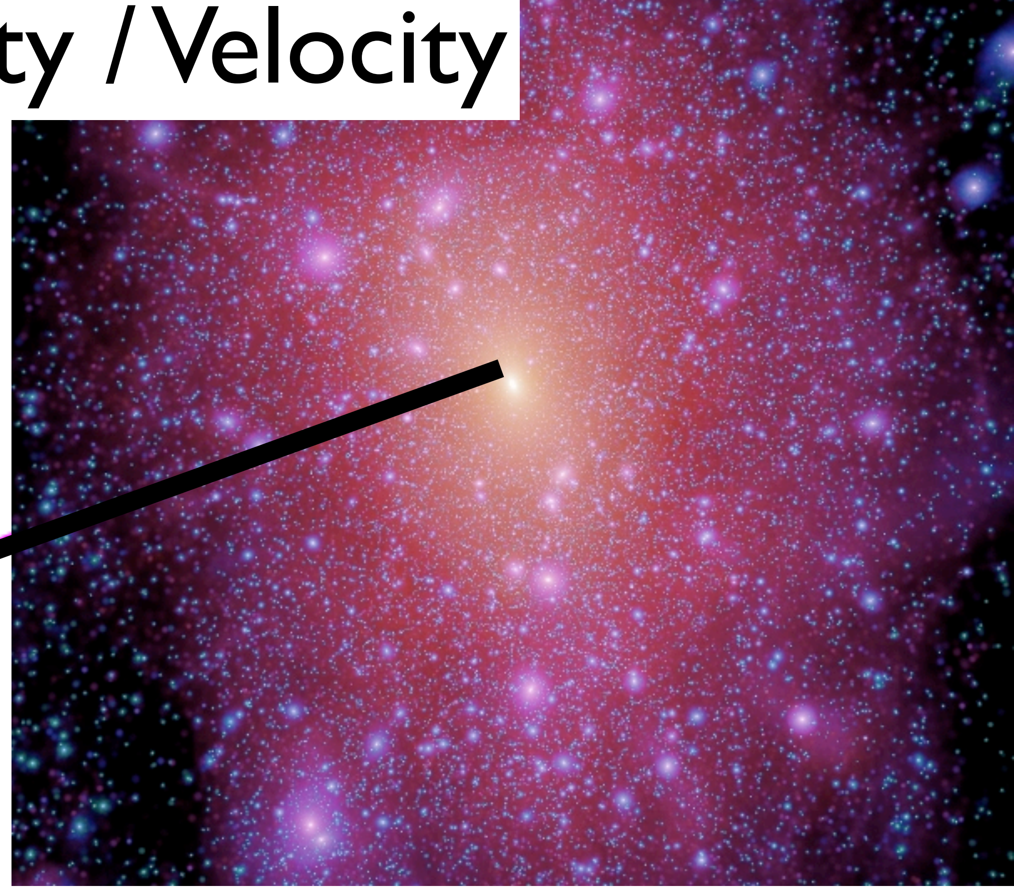

Velocity distribution still not very well understood

Maxwellian is reasonable

Local dark matter density ~0.3GeV/cm^3

Local Dark Matter Density / Velocity

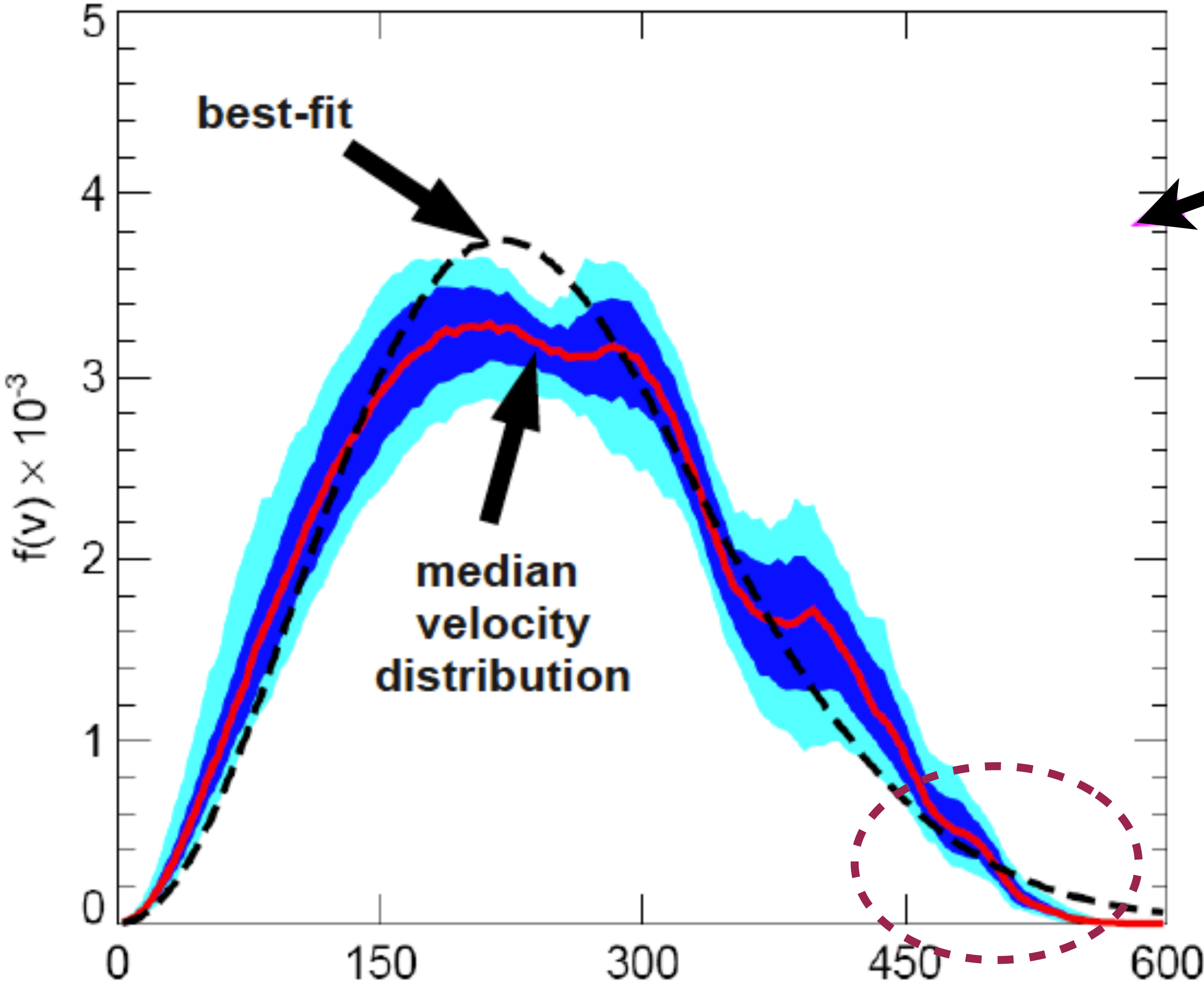

large recoils
"best sensitivity" with
direct detection

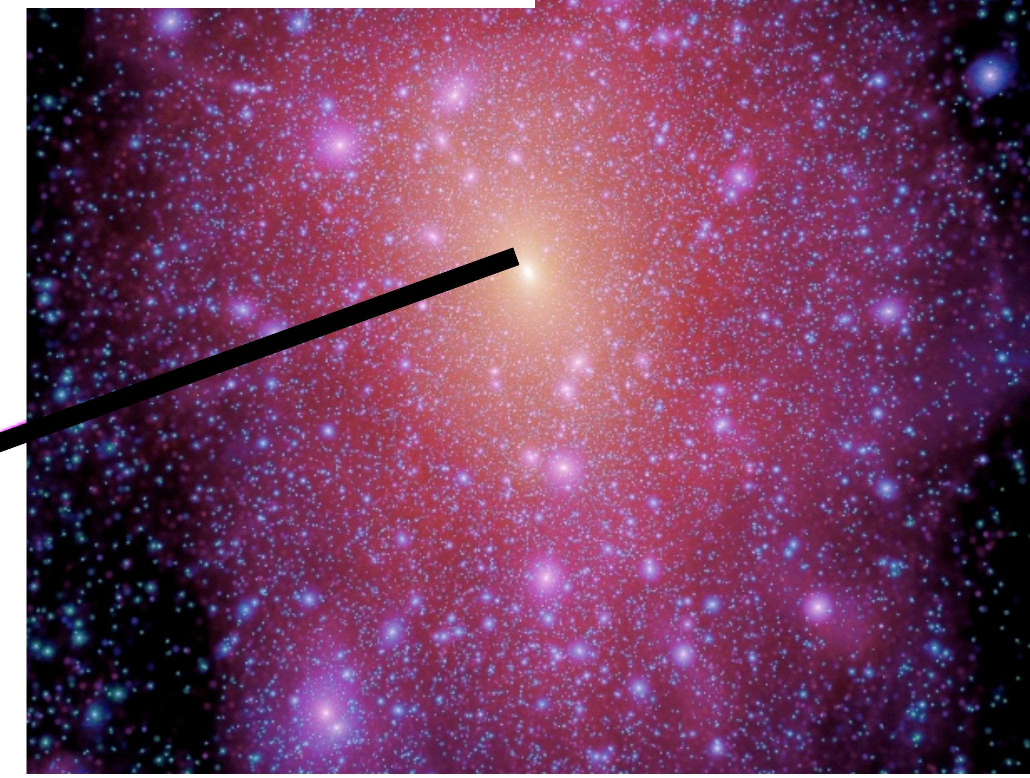

Velocity distribution still not very well understood

Maxwellian is reasonable

Local dark matter density ~0.3GeV/cm^3

Local Dark Matter Density / Velocity

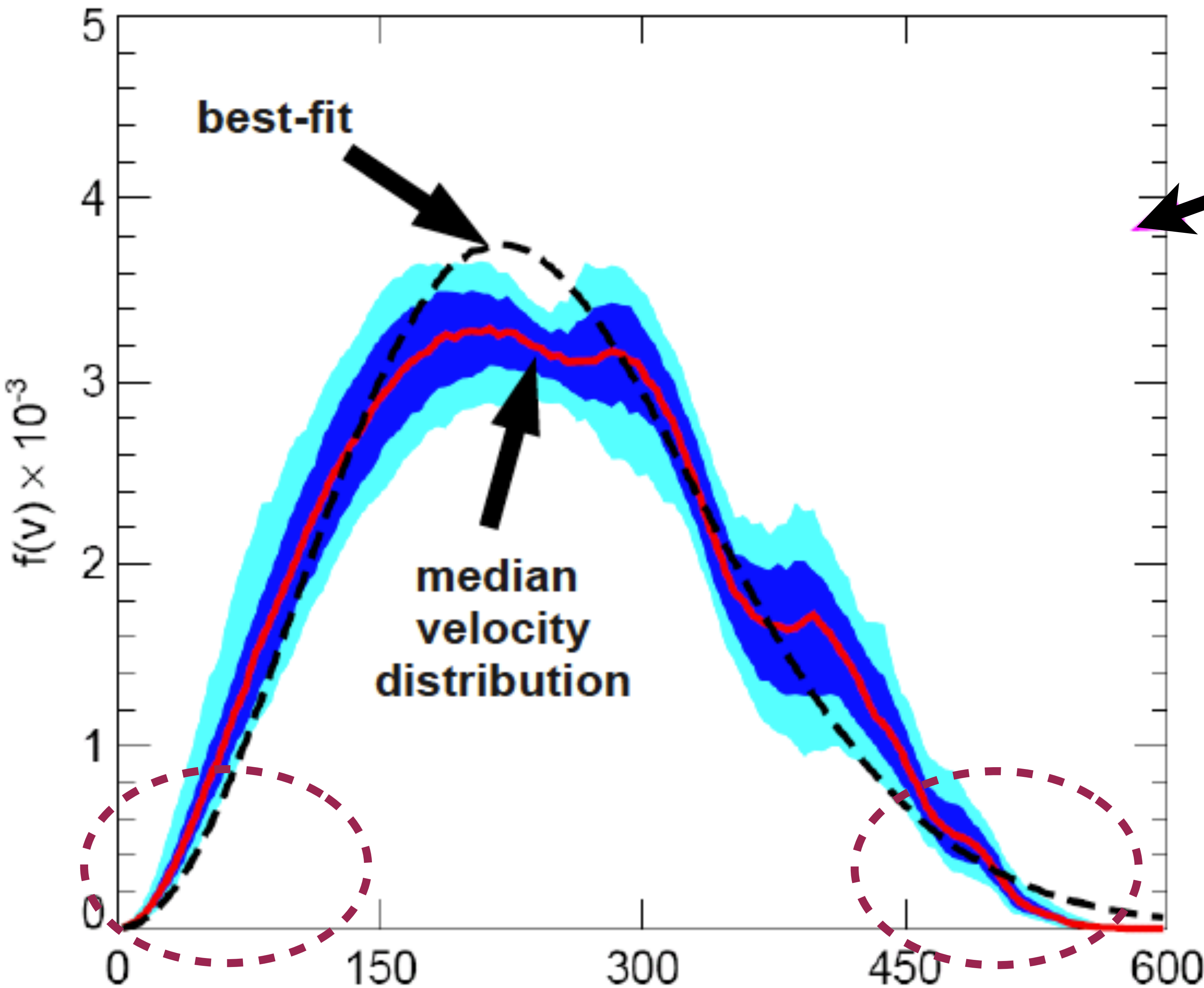

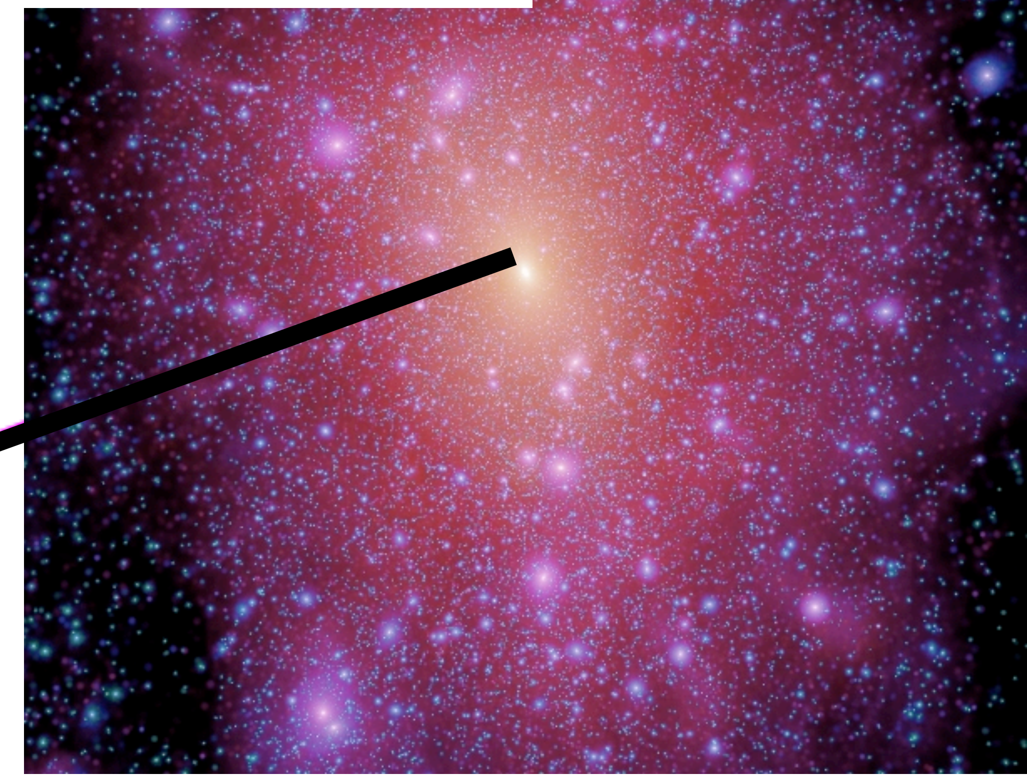

small recoils
“easiest” to be captured
in the Sun/Earth -
indirect searches

large recoils
“best sensitivity” with
direct detection

Velocity distribution still not very well understood

Maxwellian is reasonable

Local dark matter density $\sim 0.3 GeV/cm^3$

Impact of velocity distribution

- Explore the change in capture rate using different velocity distributions obtained from dark matter simulations

Choi, Rott, Itow to be submitted

f(v) in Galactic frame at solar circle

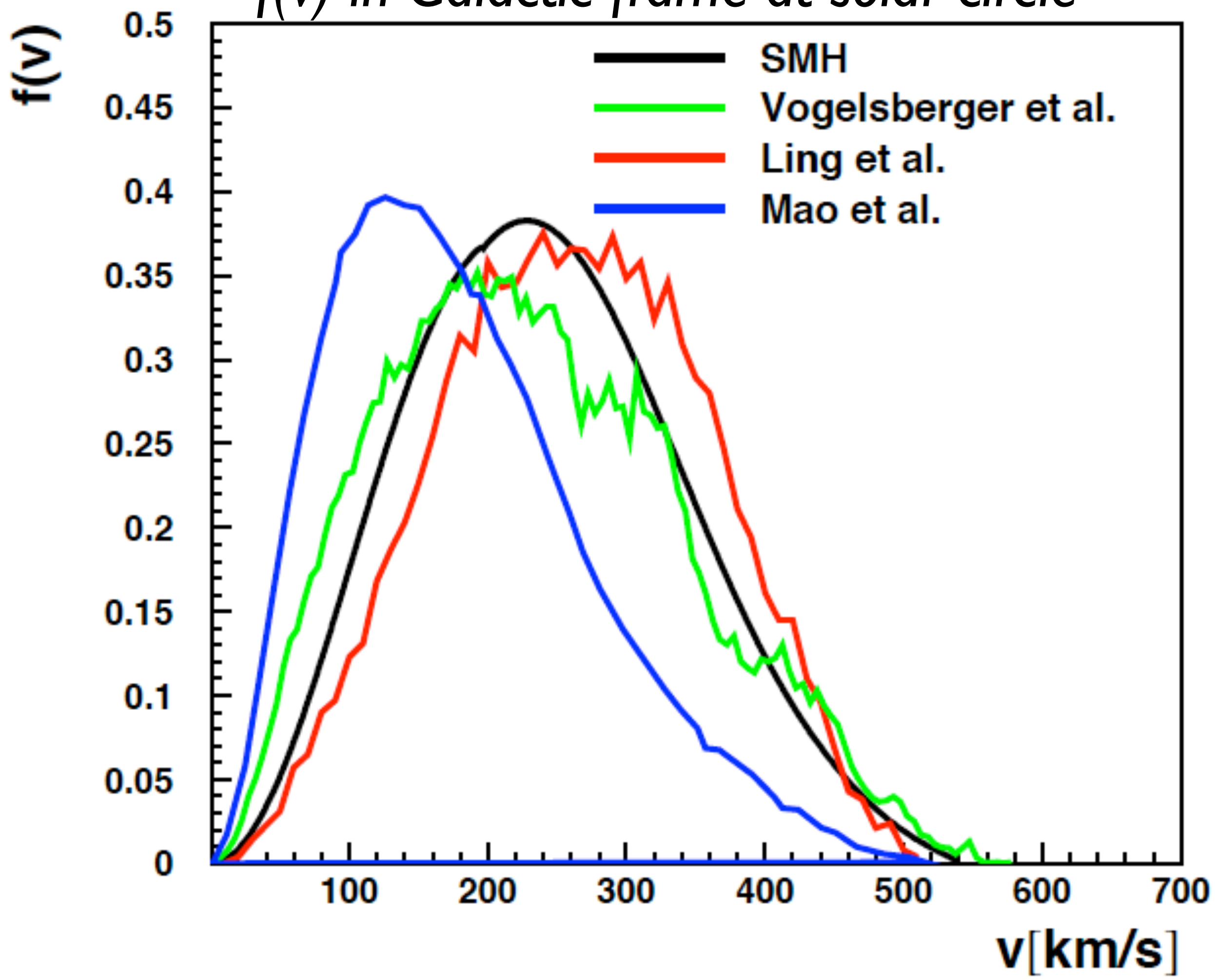

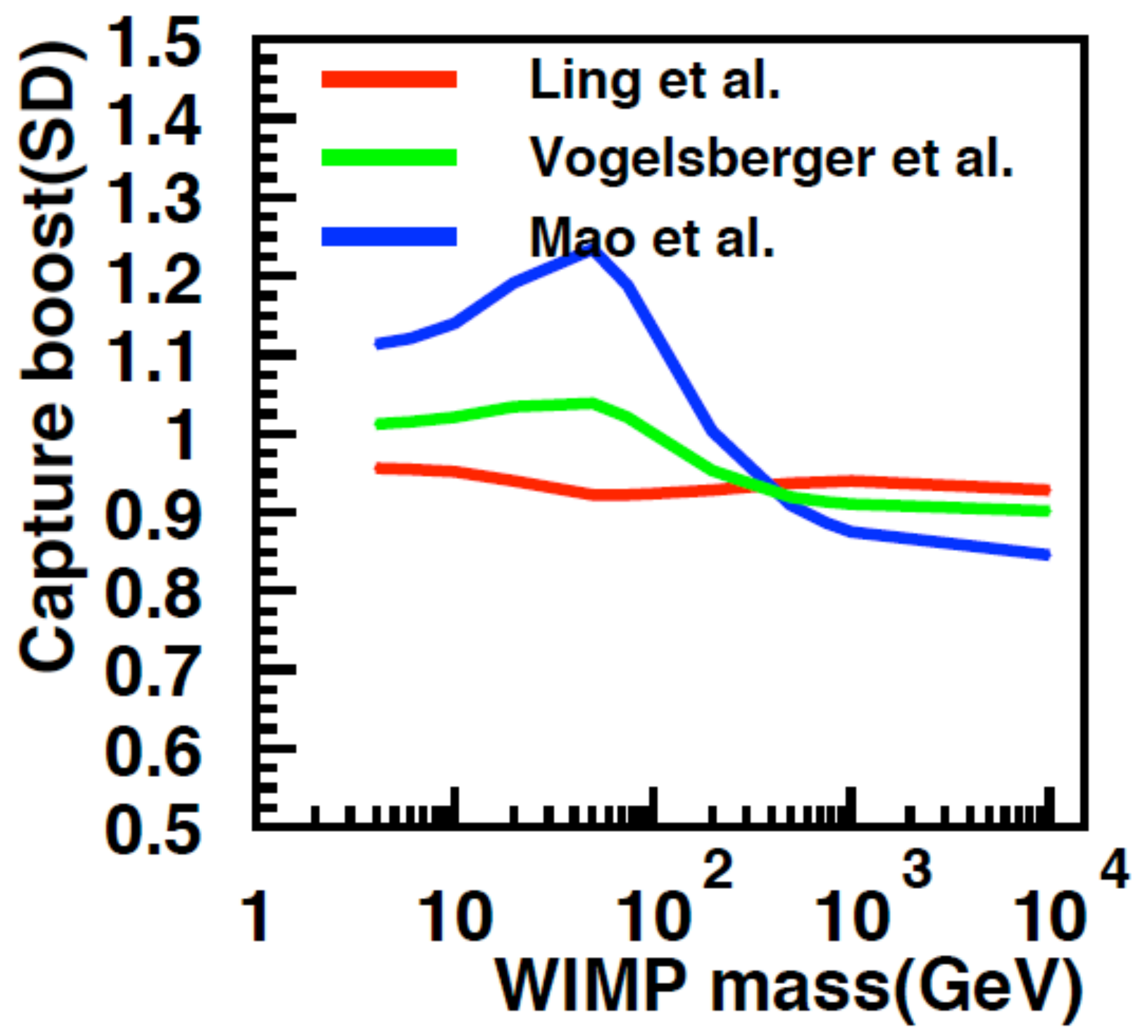

- A comparison of captures rates for different WIMP velocity distributions show that overall changes in the capture rate are smaller than 20%

Dark Matter Annihilation in the Sun

Model i: $Br(\tau\tau)_i + Br(WW)_i + Br(bb)_i + Br(qq)_i + ... = 1$

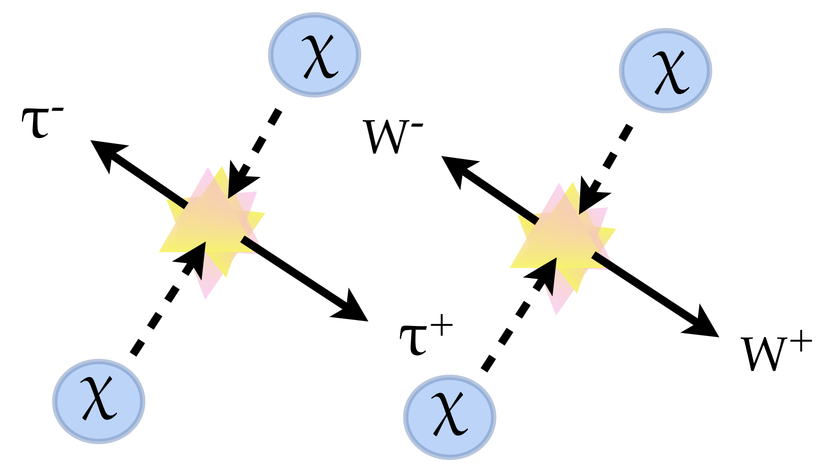

Hard channel

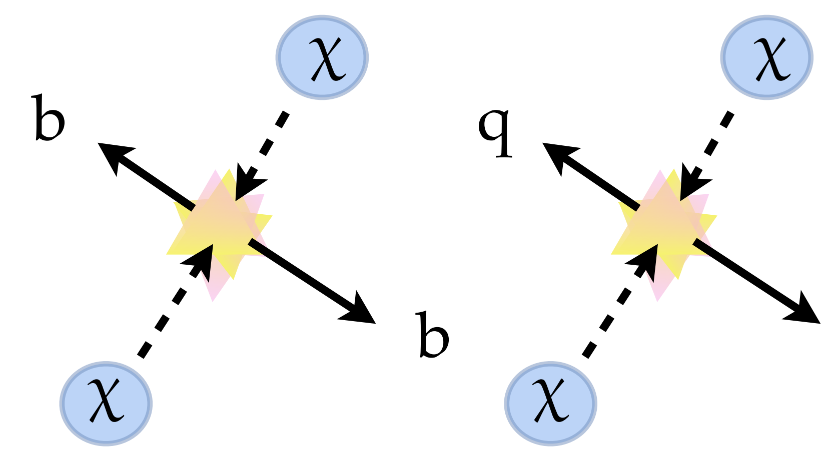

Soft channel

high energy neutrinos from annihilation / decay products

$\nu\nu$ $\tau^-\tau^+$ W^-W^+ bb qq e^+e^-

highest energy neutrinos

fewest neutrinos

low energy neutrinos from hadronic shower

see: Rott, Siegal-Gaskins, Beacom arXiv1208.0827
N. Bernal, J. Martin-Albo and S. Palomares-Ruiz, arXiv:1208.0834

$$\tau^- \rightarrow \bar{\nu}_\mu \nu_\tau \mu^-$$
$$\tau^- \rightarrow \bar{\nu}_e \nu_\tau e^-$$
$$\tau^- \rightarrow hadrons$$

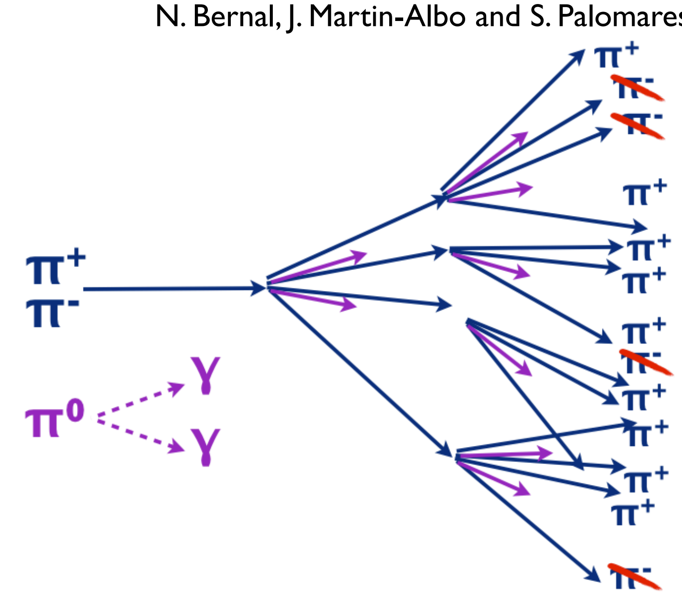

Charged pions decay at rest producing neutrinos up to E=52.8MeV

$$\pi^+ \rightarrow \mu^+ \nu_\mu$$
$$\mu^+ \rightarrow e^+ \nu_e \bar{\nu}_\mu$$

IceCube Solar WIMP Limits

PRL 110, 131302 (2013)

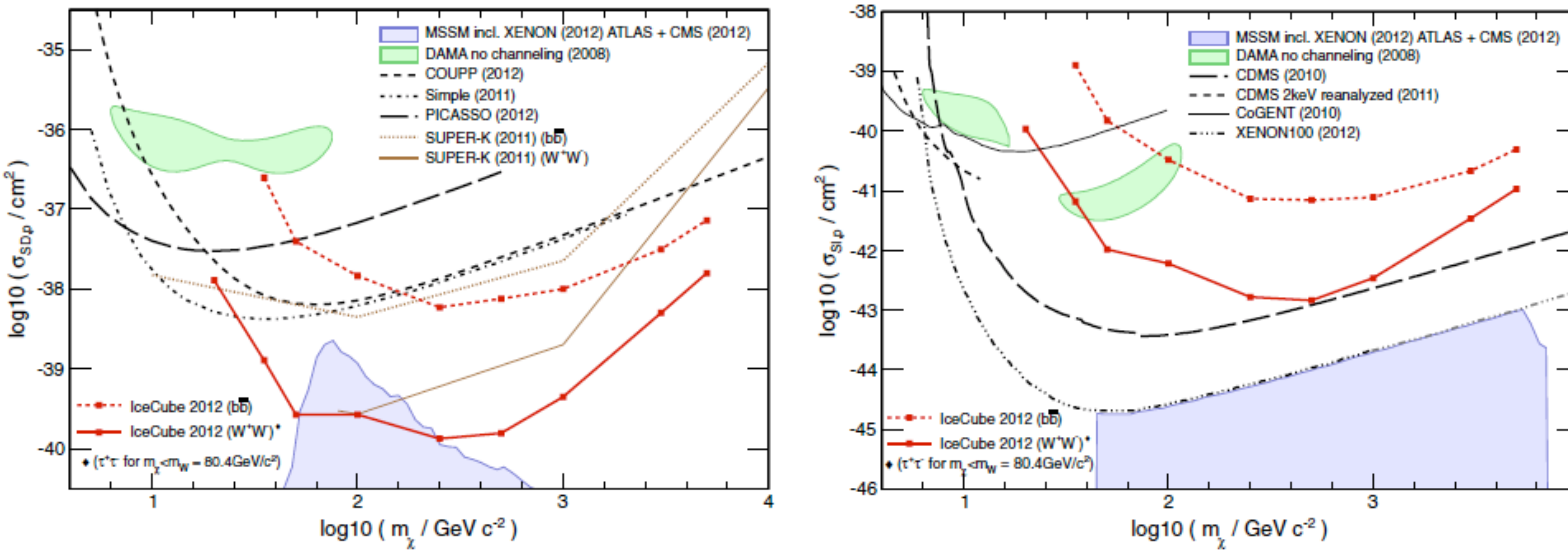

- 1 year of data with the detector in the IC79 string configuration (partially completed DeepCore)

Other Preliminary Results

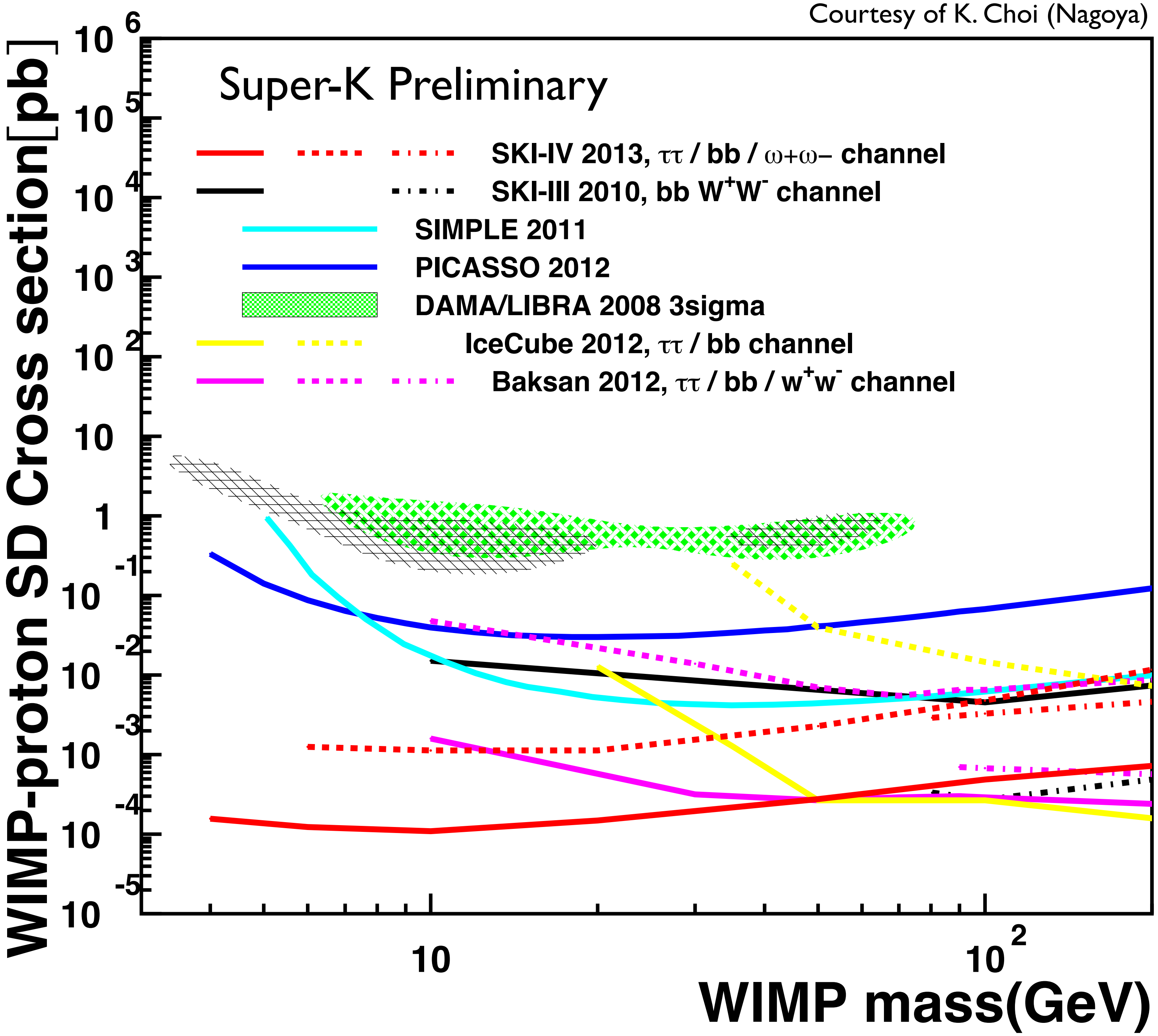

Neutrino Telescopes provide world best limits on SD WIMP proton scattering

Future Prospects

Gamma-rays future

Cherenkov Telescope Array (CTA)

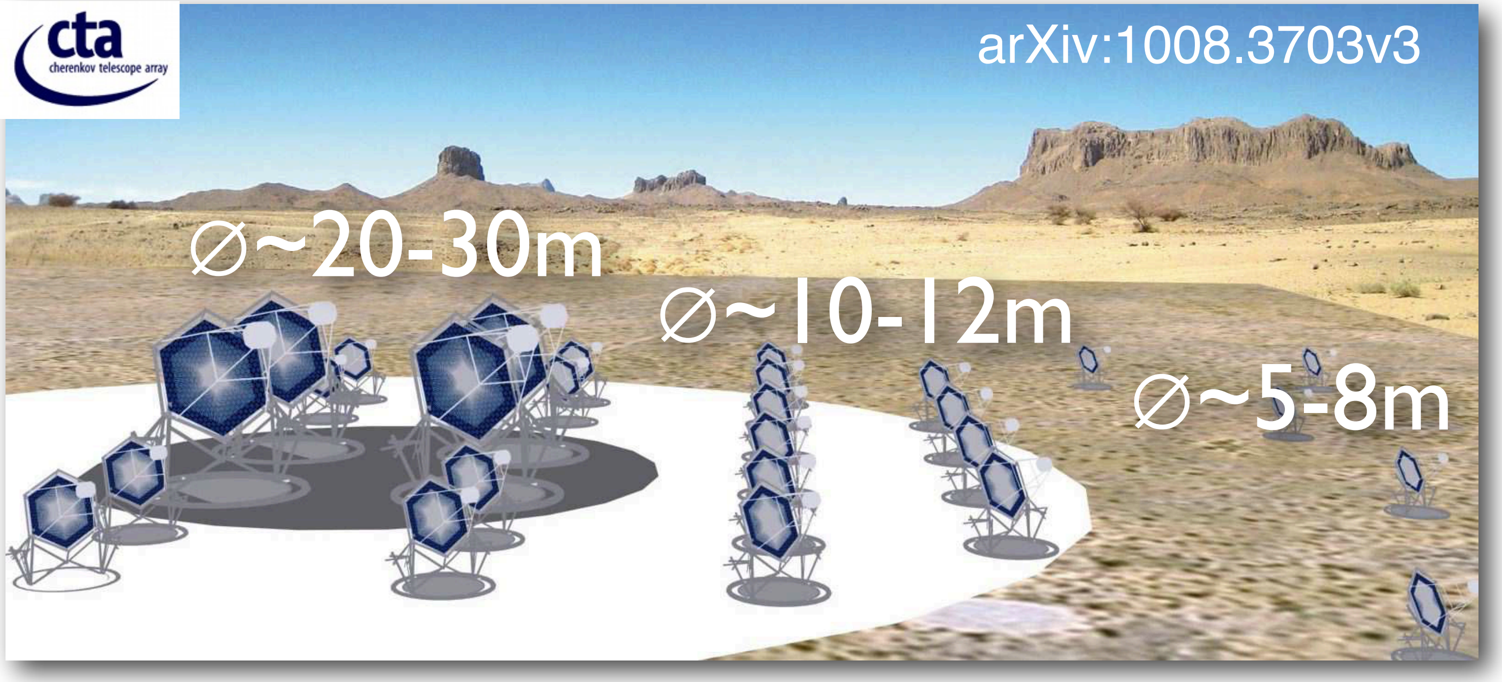

- Energy range: a few tens of GeV to above 100 TeV)
- Baseline design consists of three single-mirror telescopes: Small/Medium/Large size telescopes.
- Improvement in flux sensitivity of 1-2 orders of magnitude over current instruments is expected

See also Special issue of Astroparticle Physics (arXiv1208.5356)

Gamma-400

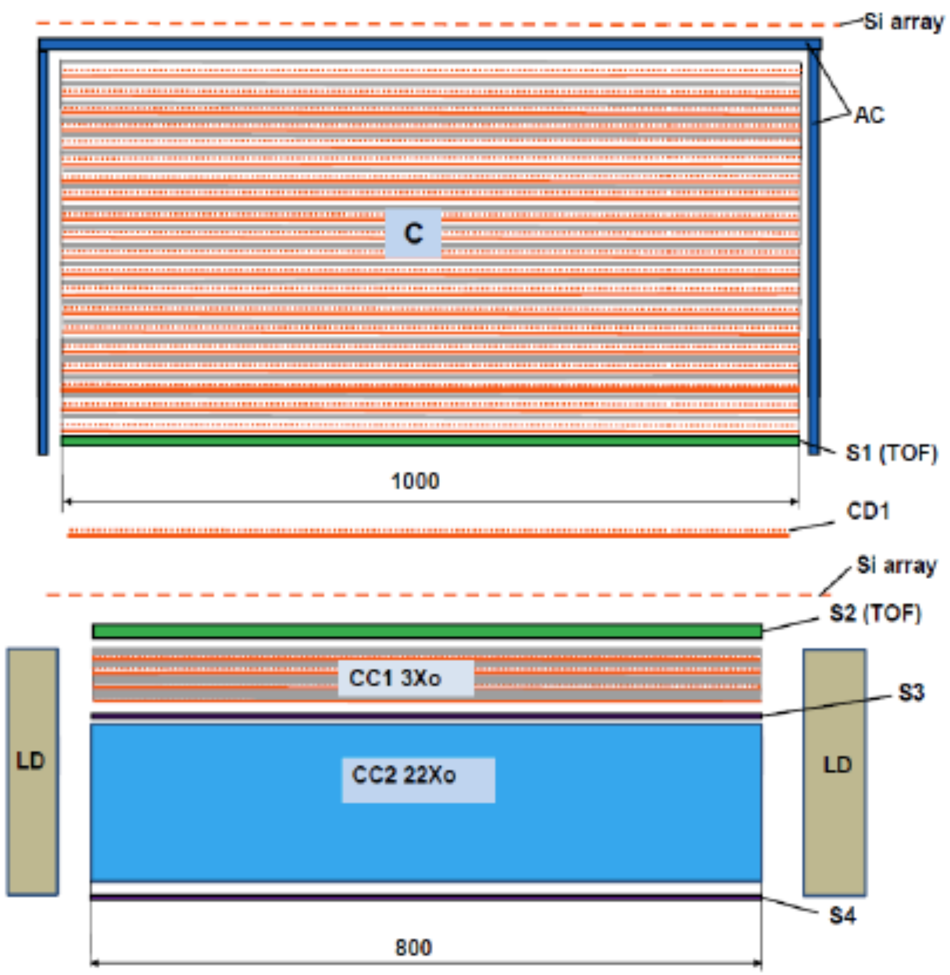

- Follow up to Fermi
- extend energy range to 3TeV
- Improve angular resolution
- Launch of the GAMMA-400 space observatory is planned in 2018

Galper, A., et al., 2012. Design and Performance of the GAMMA-400 Gamma-Ray Telescope for the Dark Matter Searches. arXiv:1201.2490

Gamma-ray outlook

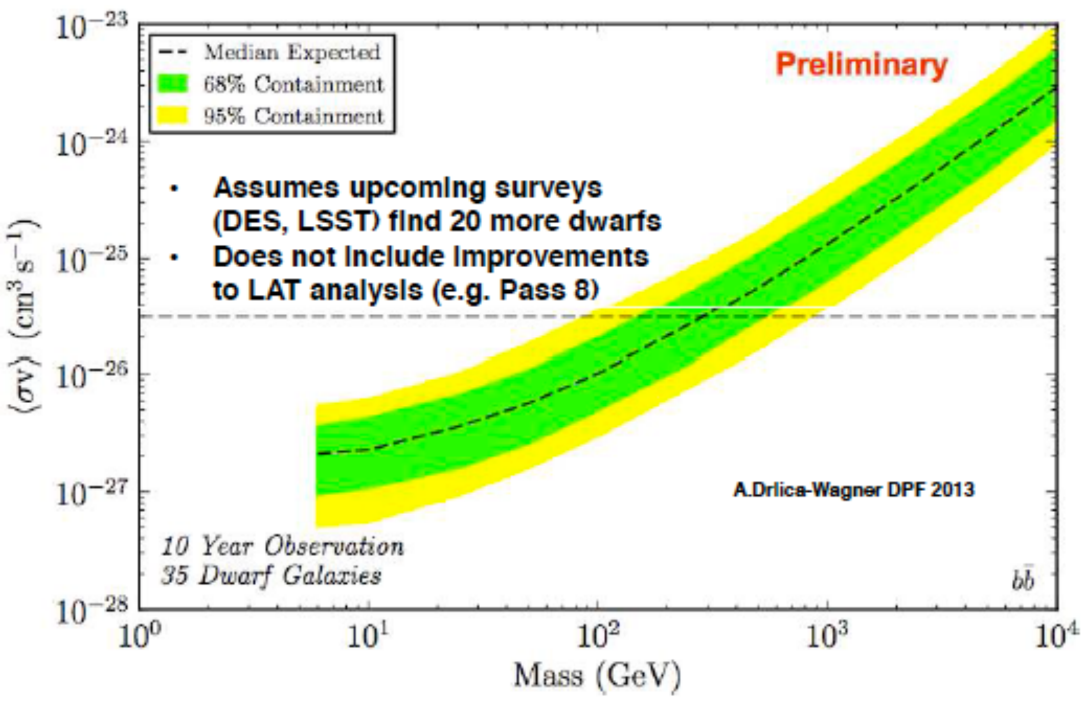

[CF2 Working Group: arXiv1310.7040]

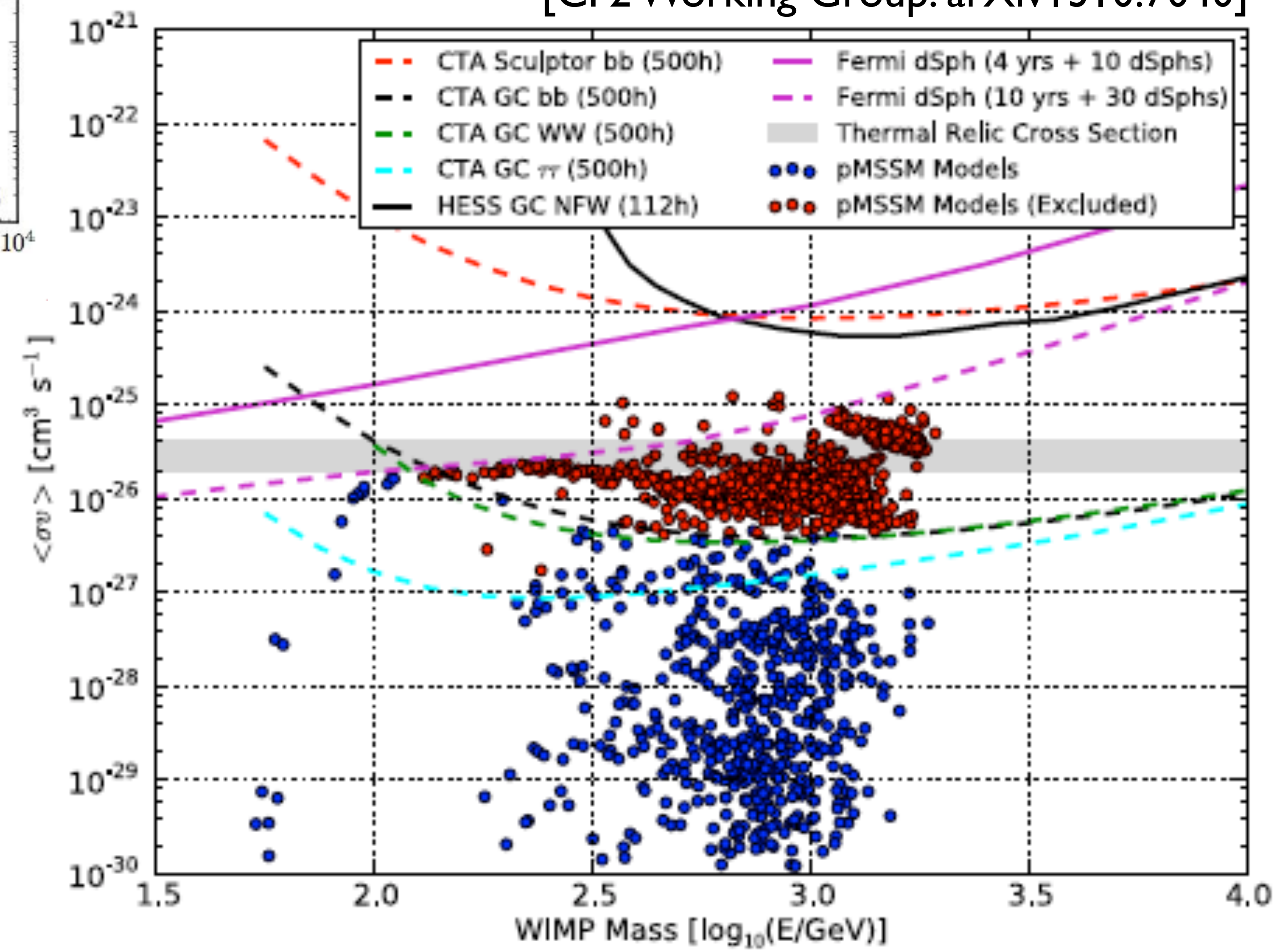

CTA and Fermi-LAT will be able to "cover" the thermal relic cross

See also Special issue of Astroparticle Physics (arXiv1208.5356)

PINGU WIMP sensitivity - neutrinos from decays of WIMP annihilation products

Solar WIMPs -- $\sigma_{\chi p}$

- Preliminary solar WIMP sensitivity based on adapted version of JCAP09(2011)029 to PINGU.
- Assume that atmospheric muon backgrounds can be effectively rejected (as demonstrated by DeepCore analyses)

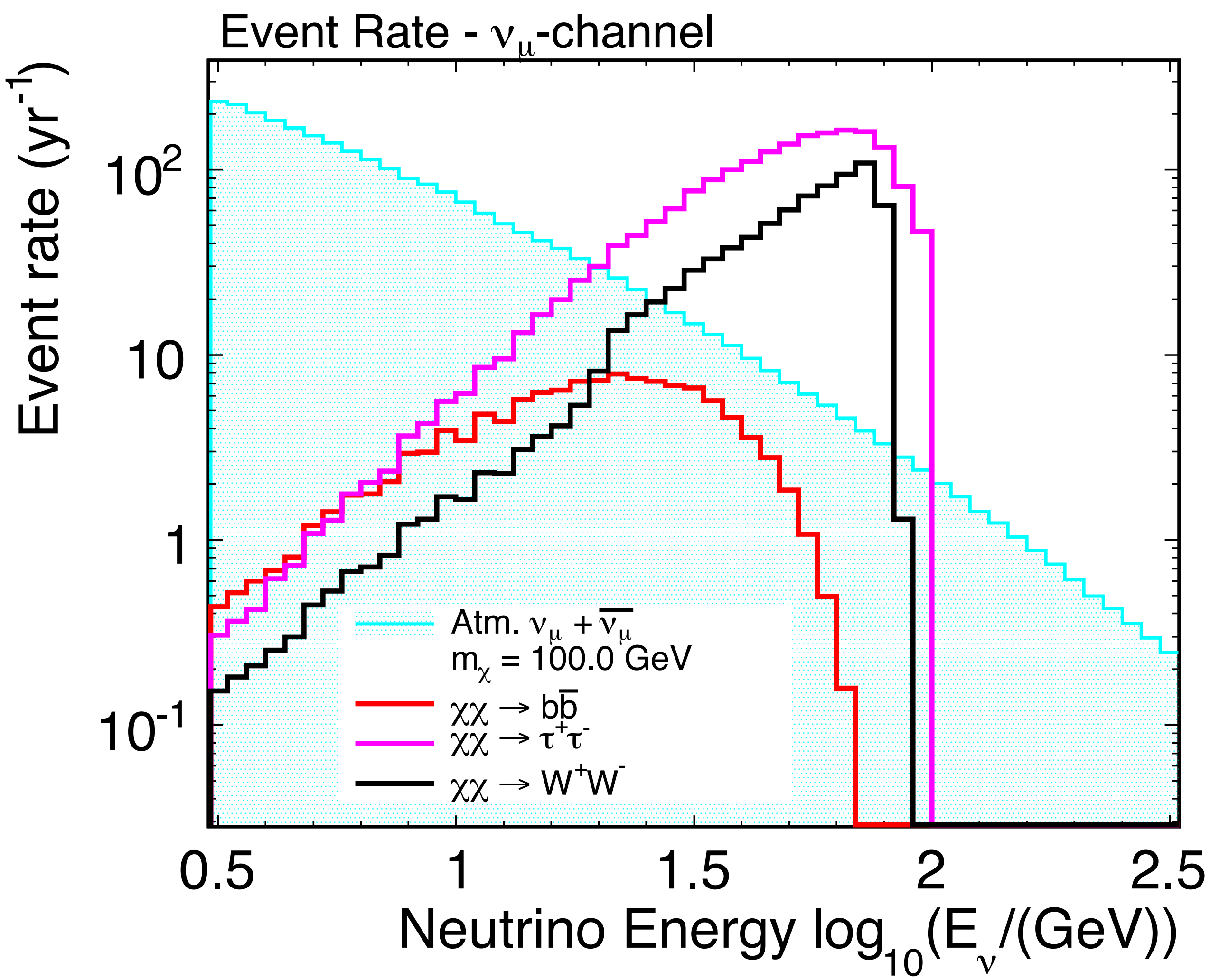

[Rott prepared for CF2]

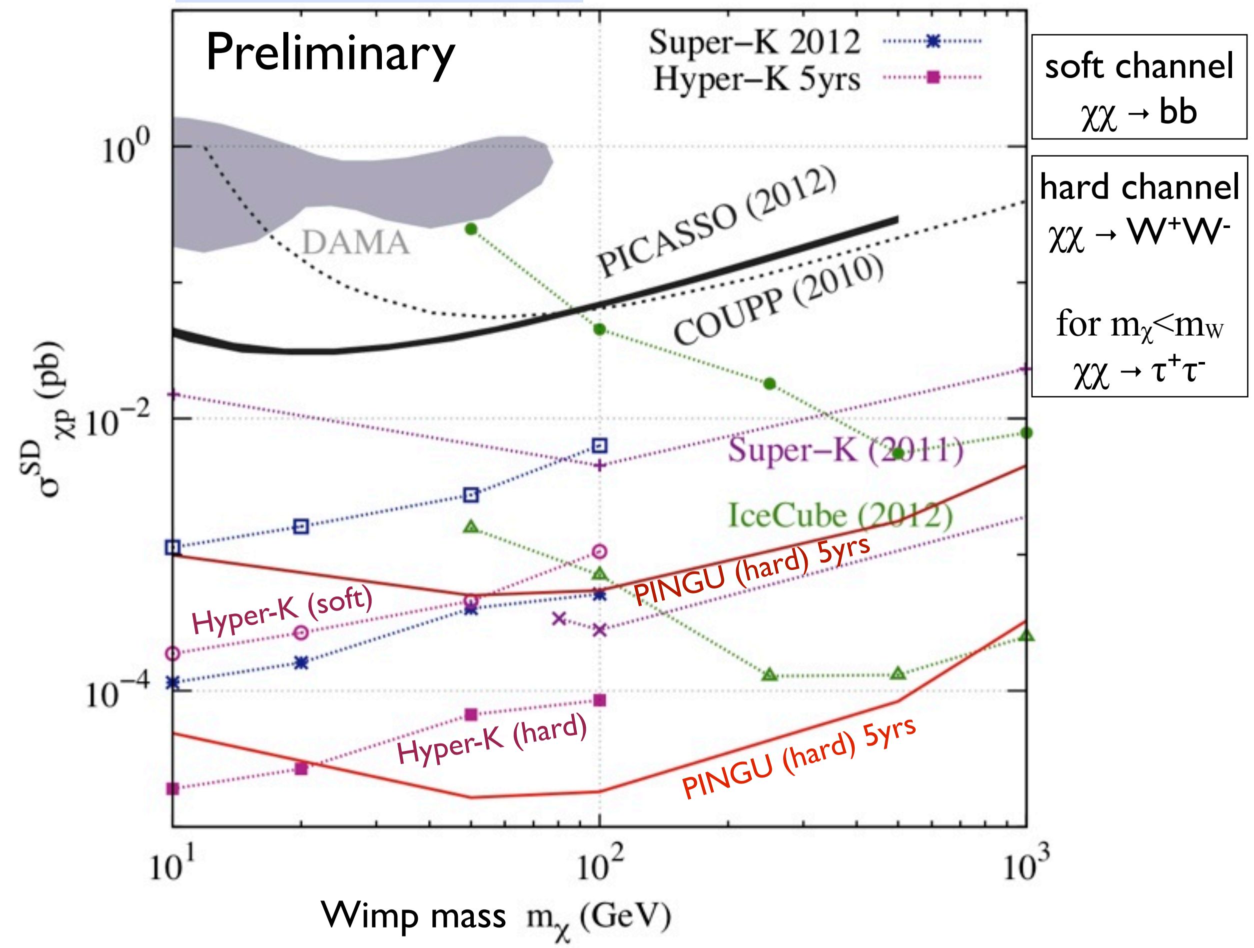

- Benchmark high-energy neutrino channels can comfortably test DAMA/Libra

PINGU WIMP sensitivity - neutrinos from decays of WIMP annihilation products

Solar WIMPs -- $\sigma_{\chi p}$

- Preliminary solar WIMP sensitivity based on adapted version of JCAP09(2011)029 to PINGU.
- Assume that atmospheric muon backgrounds can be effectively rejected (as demonstrated by DeepCore analyses)

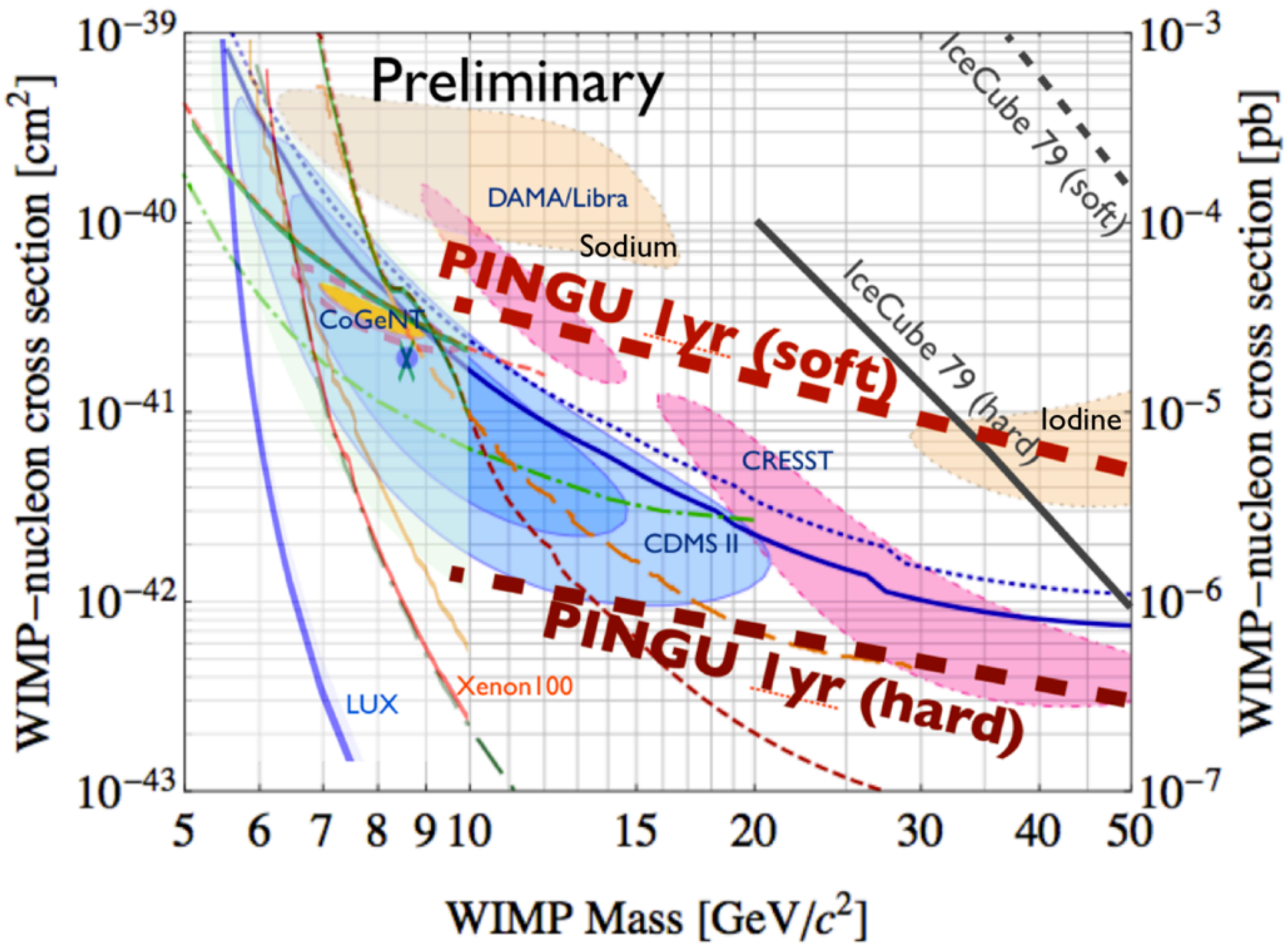

[Rott prepared for CF2]

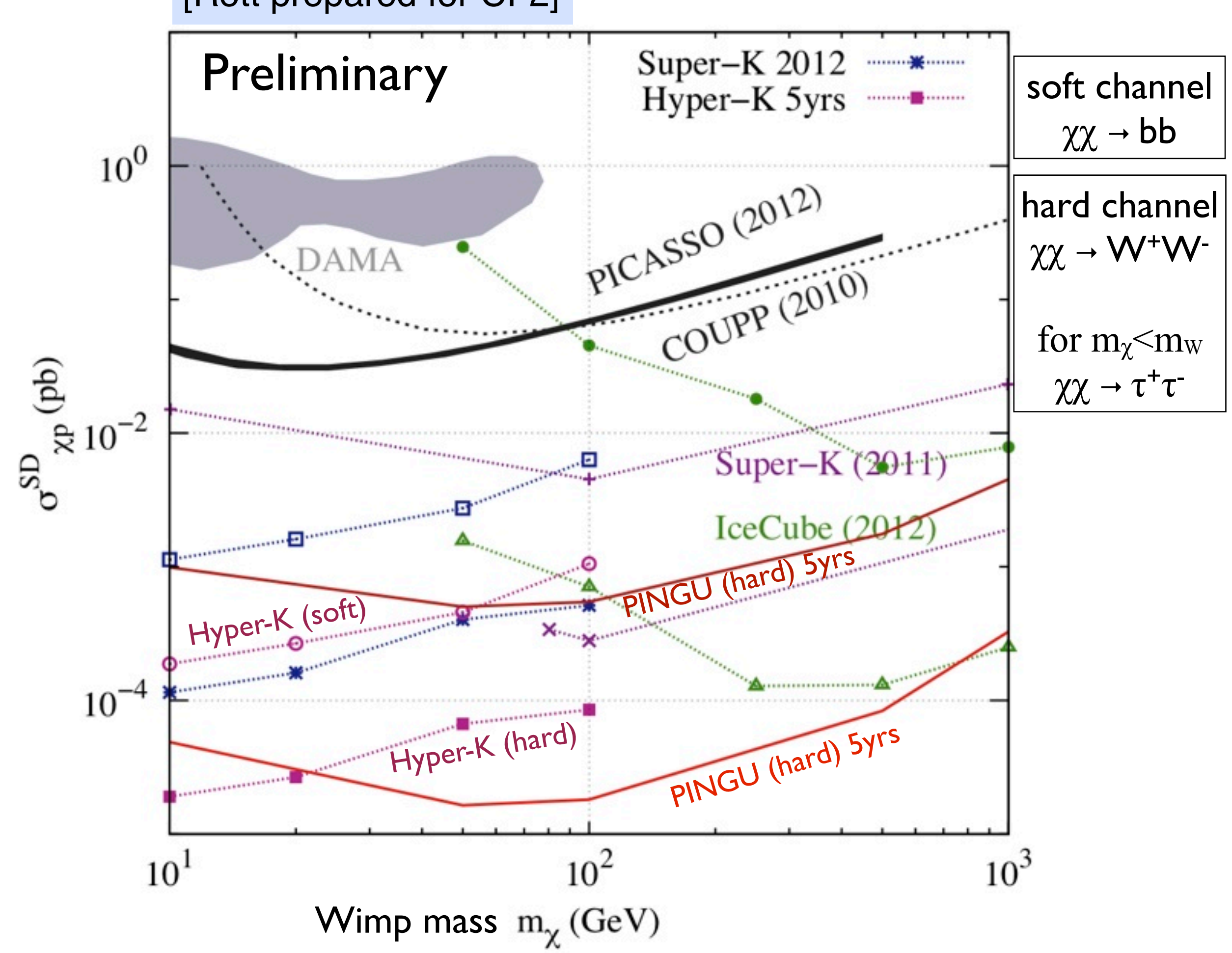

- Benchmark high-energy neutrino channels can comfortably test DAMA/Libra

WIMP Sensitivity Super-K / Hyper-K

Neutrinos from stopped π^+ decay at rest in the Sun:

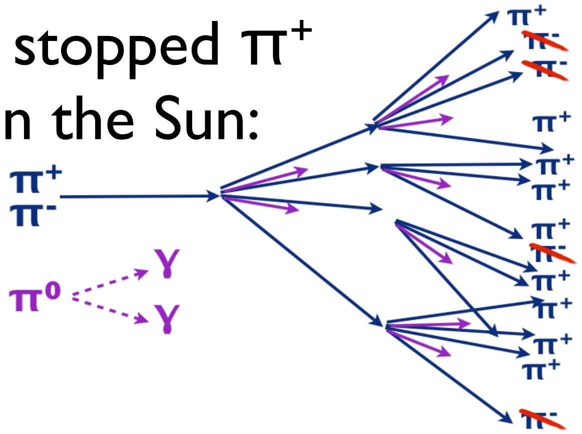

Rott, Siegal-Gaskins, Beacom PHYSICAL REVIEW D 88, 055005 (2013)

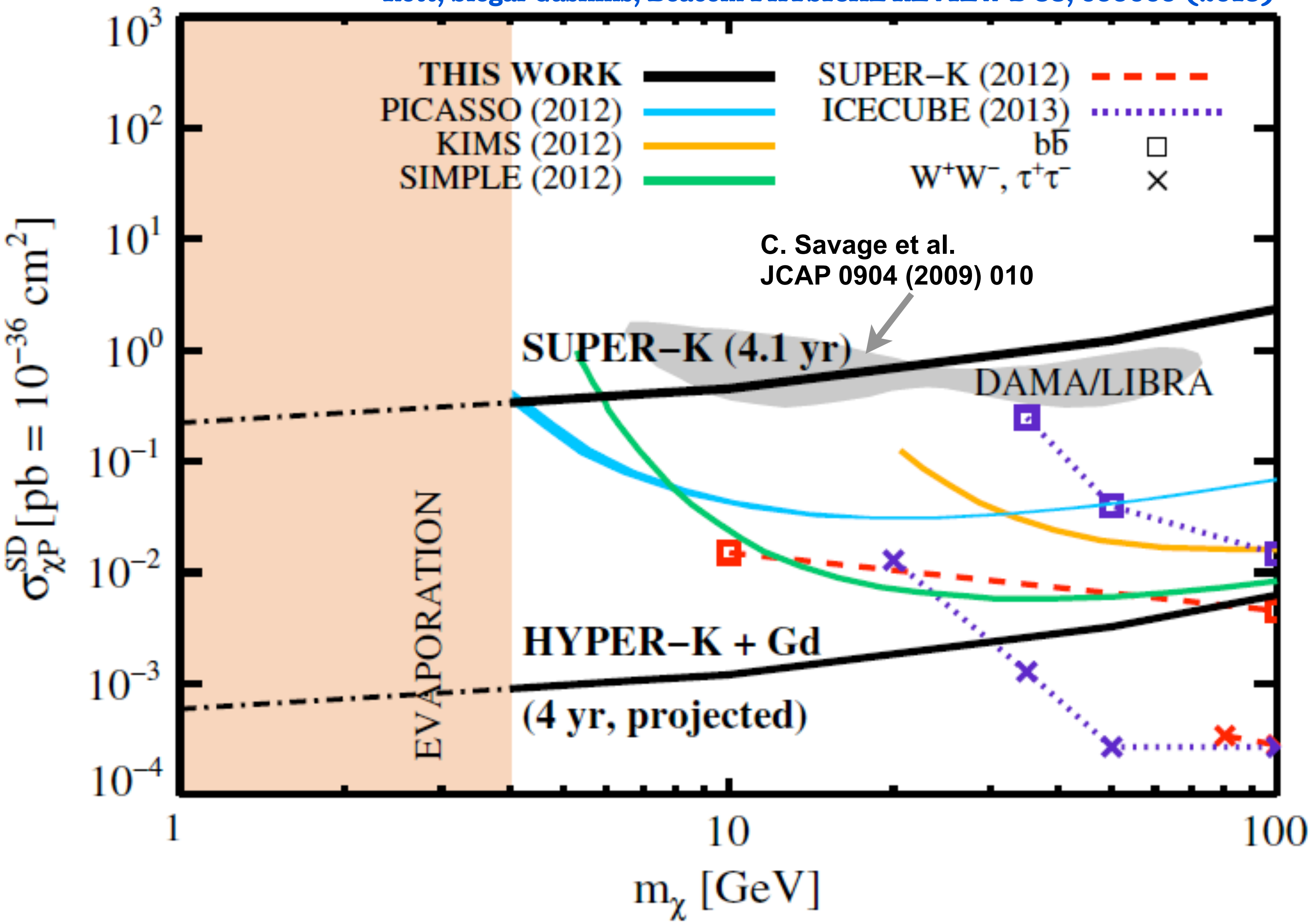

Previous searches relied on high energy neutrinos directly from the decays of annihilation products

Model the full hadronic shower in the Sun

WIMP sensitivity continues to improve for low masses

Minimal dependence on mix annihilation channels

New key detection channel to compliment other searches

Super-K data can already be used to test DAMA/Libra

Great Prospect for future detectors

Conclusions

- We are in an exciting data driven era
- No signs of SUSY or Dark Matter at LHC, yet
- Tight constraints from gamma-rays can exclude the WIMP paradigm for some masses and branching fractions
  - CTA & Fermi-LAT can cover thermal relic cross section in future
- Line search near the Galactic center remains controversial
- Neutrino Telescopes provide world best limits on SD WIMP-Proton scattering cross section
  - PINGU & Hyper-K can further increase sensitivity

Thanks !

130GeV Line

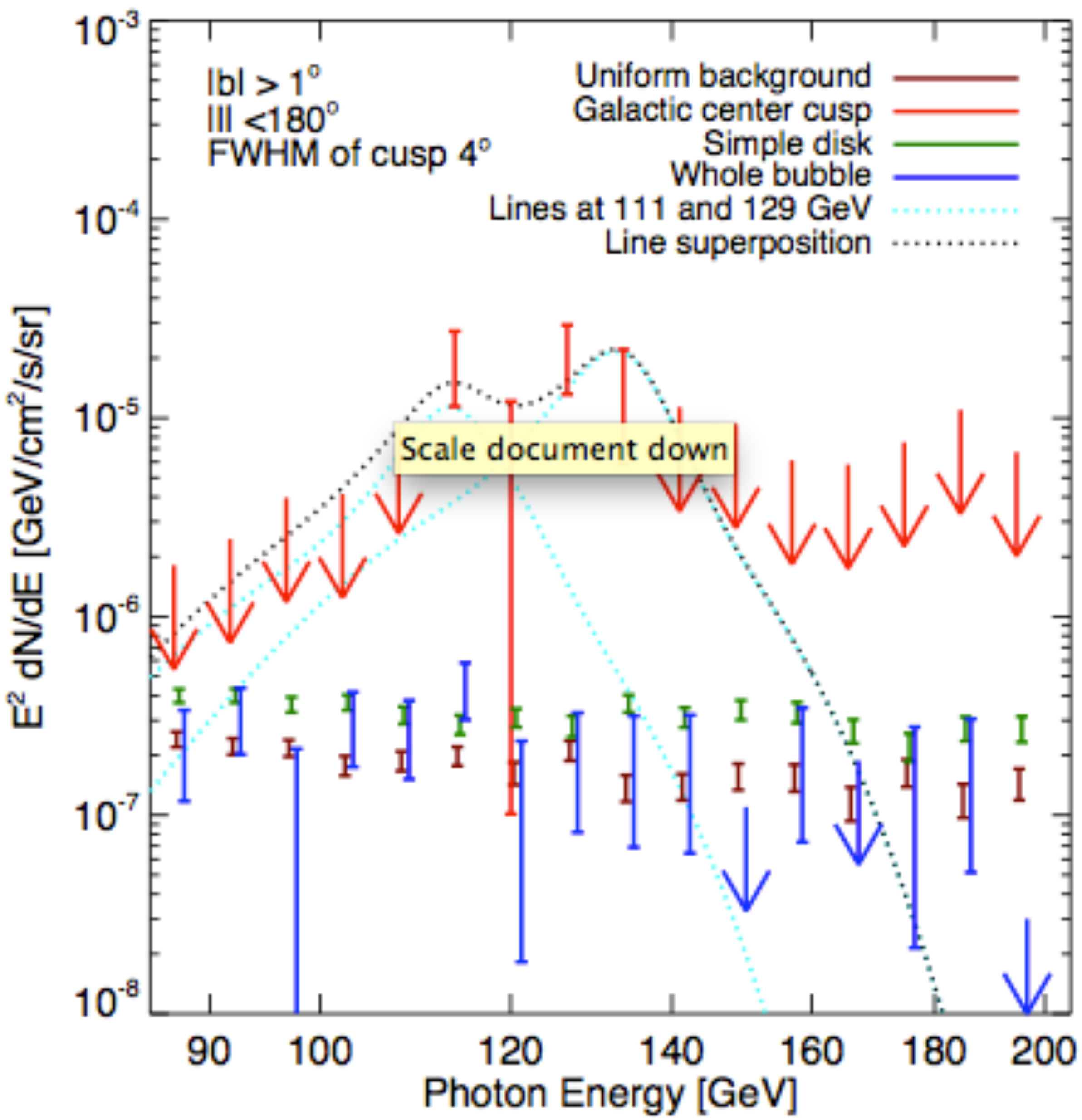

Su, Finkbeiner (2012)

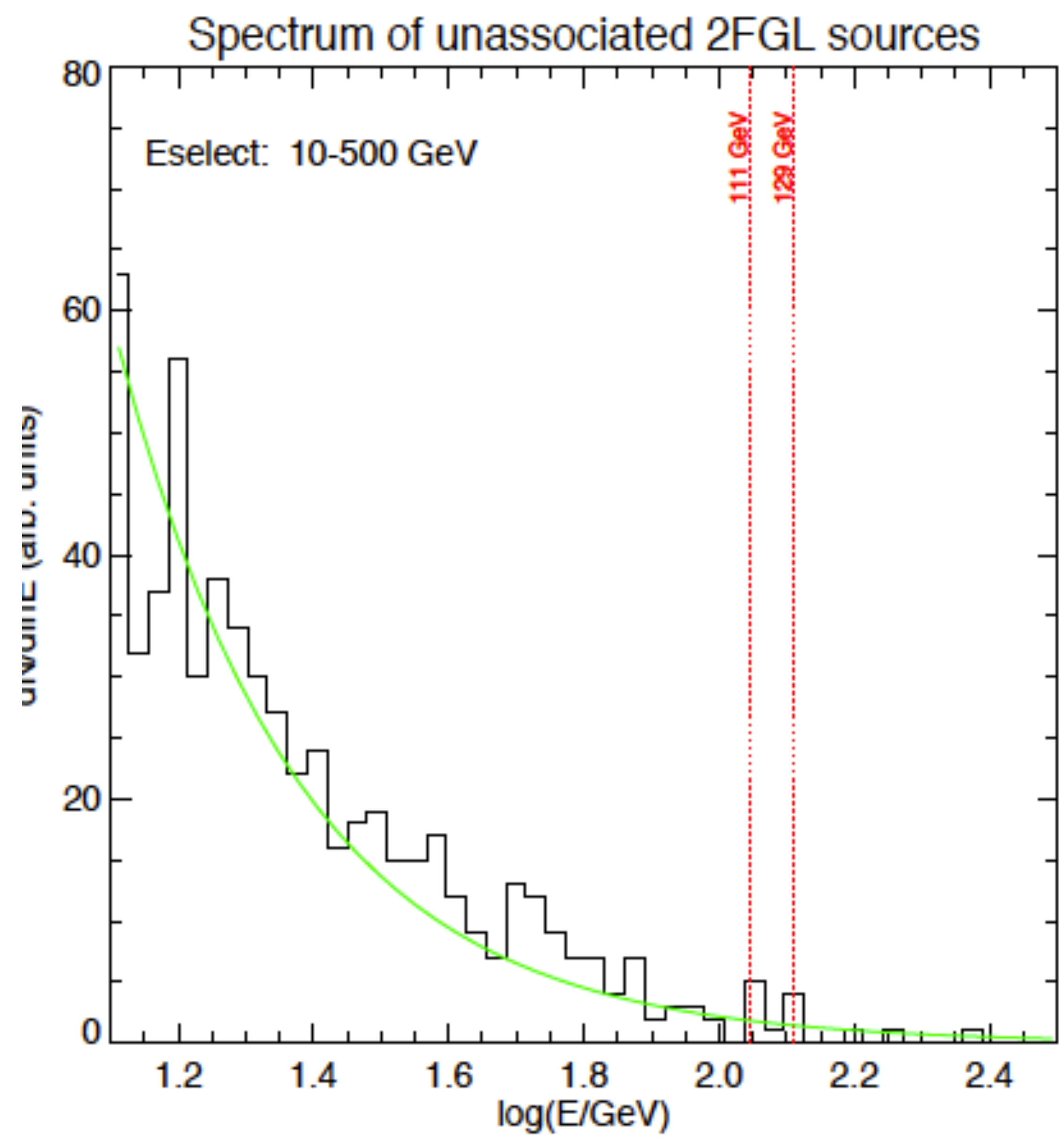

Su, Finkbeiner (2012)

Galactic Distribution of DM

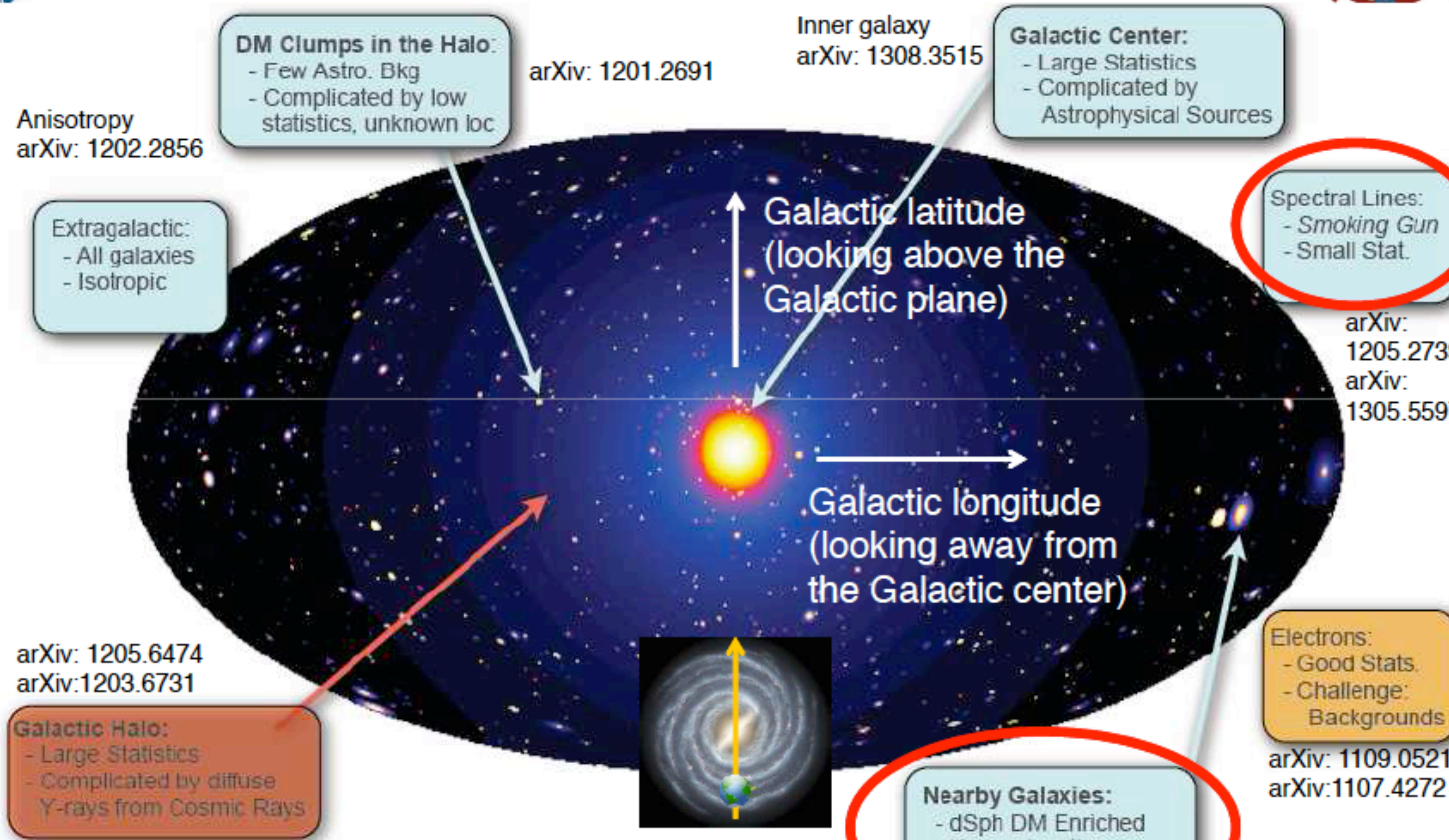

Milky Way Halo simulated by Taylor & Babul (2005)

All-sky map of DM gamma ray emission (Baltz 2006)

Low-Energy Neutrinos - Solar WIMPs

Rott, Siegal-Gaskins, Beacom 2012

Previous searches relied on high energy neutrinos directly from the decays of annihilation products

Model the full hadronic shower in the Sun

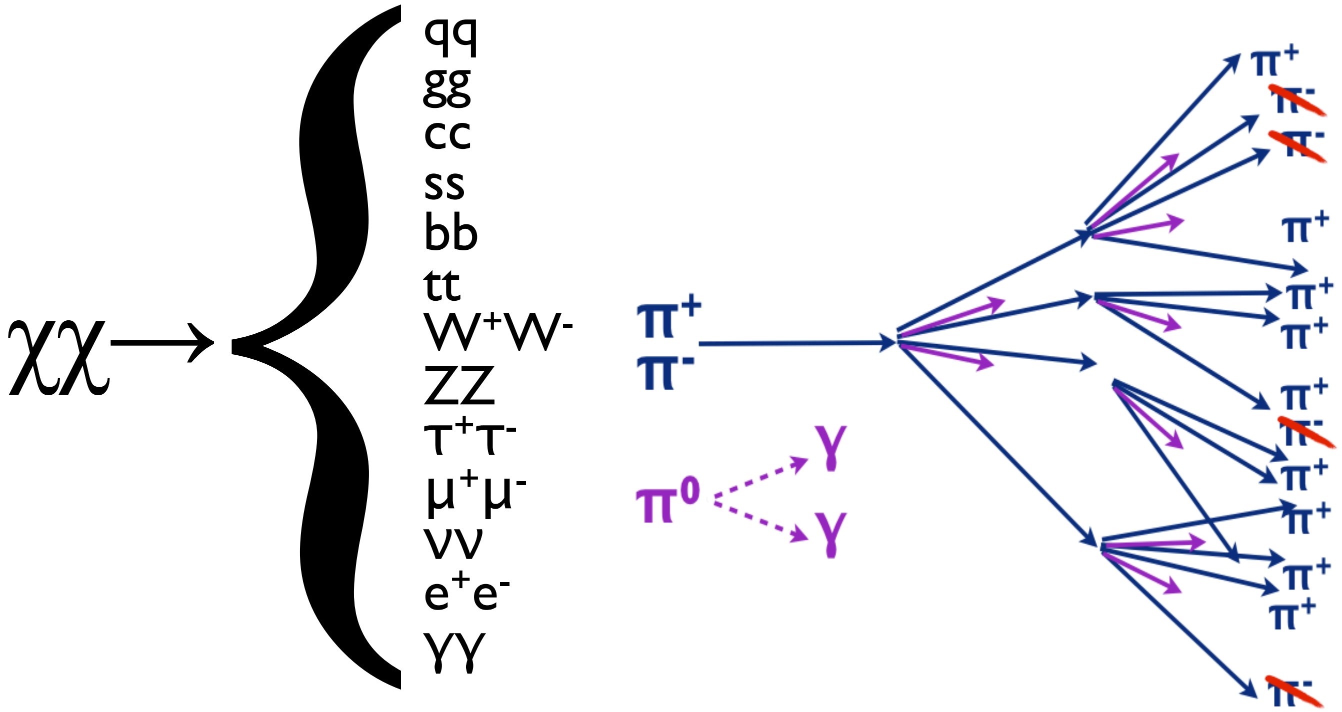

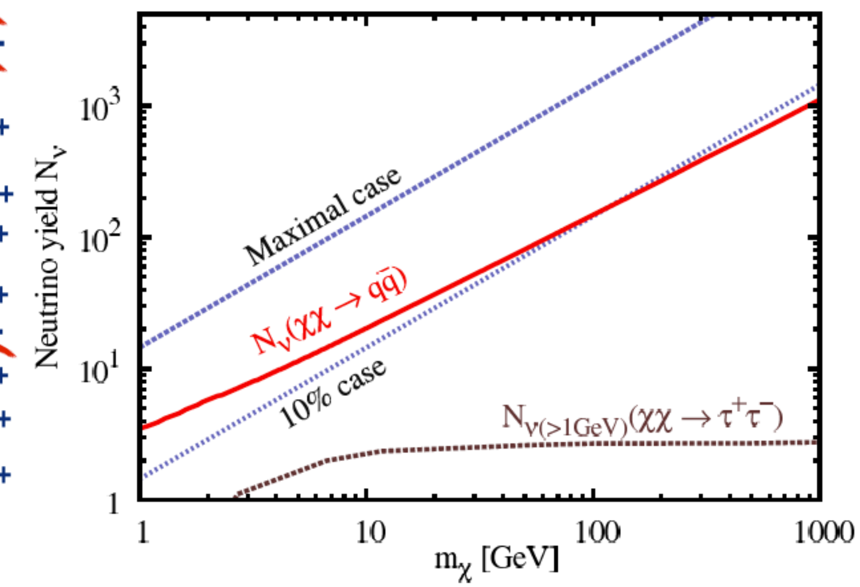

New key detection channel to compliment other searches; Super-K data can already be used to test DAMA

Interesting signatures for future neutrino detectors (LENA, Hyper-K, ...), other nuclear final states could provide additional sensitivity

Example detection with inverse beta-decay

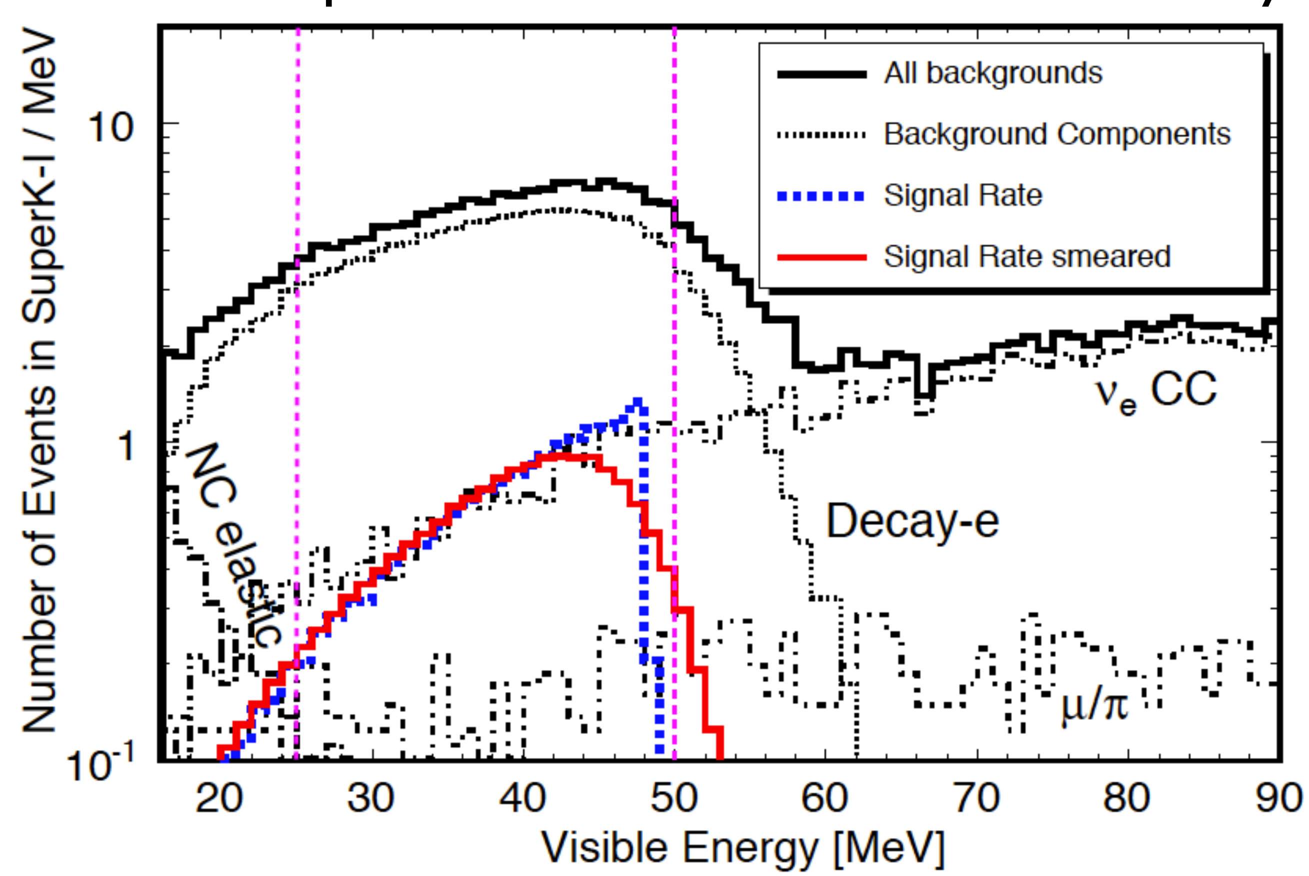

Neutrino Analyses

K. Murase and J. F. Beacom 2012 (in prep)

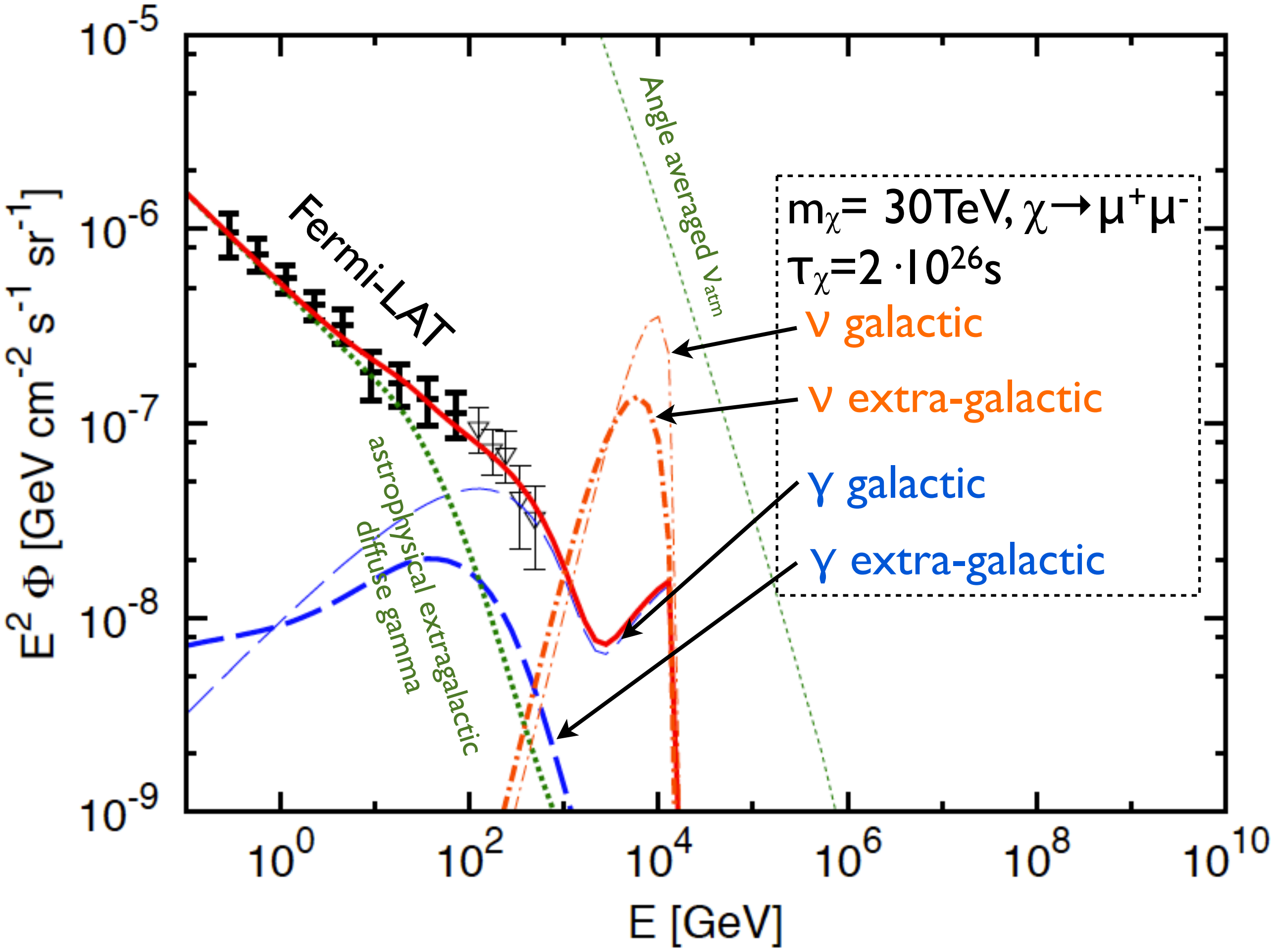

Mandal et al. PRD 81:043508 (2010)

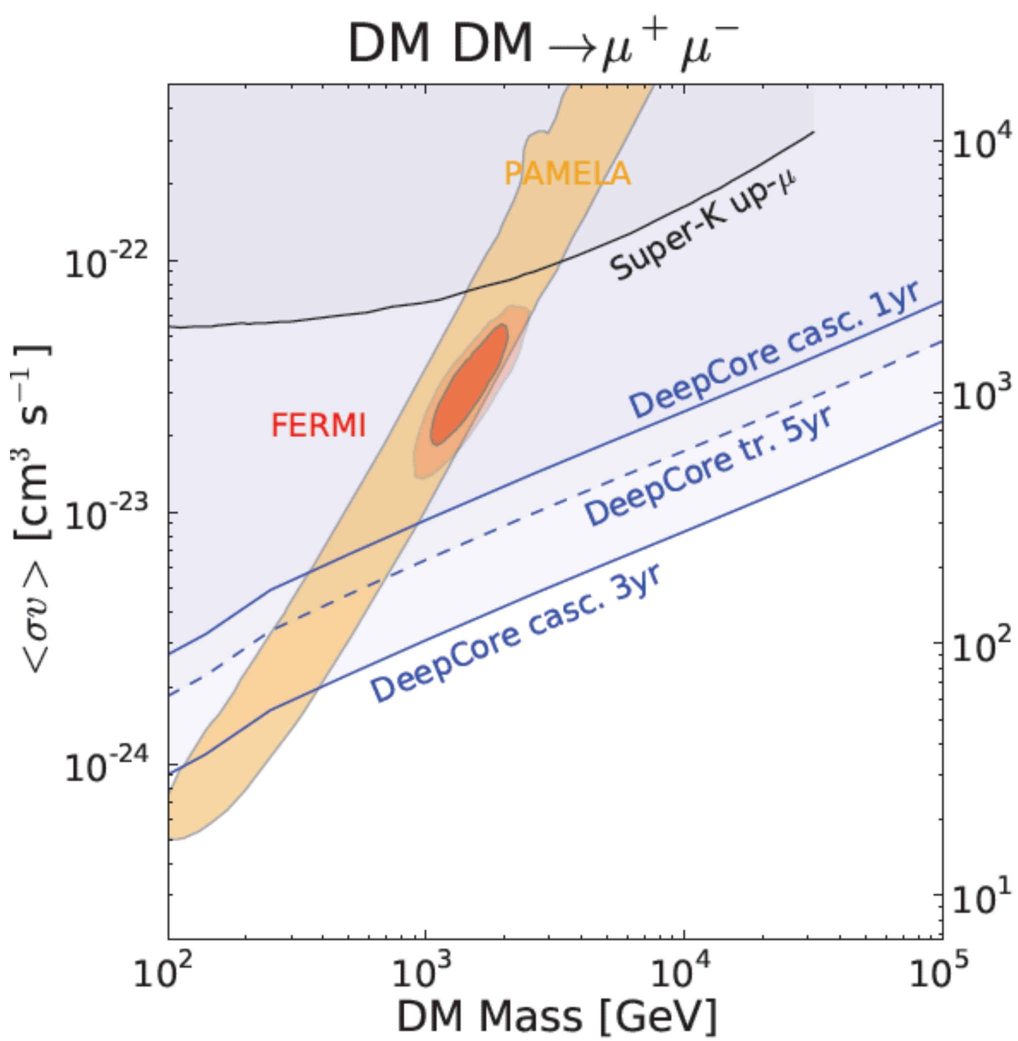

- Already with existing detectors high mass WIMP scenarios and those motivated by anomalous lepton signals can be tested

130 GeV Line

Instrument Effects?

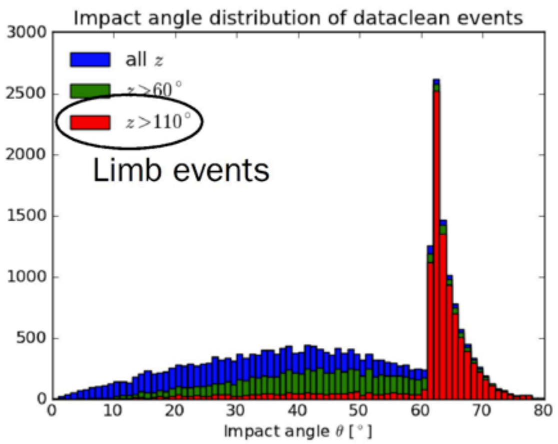

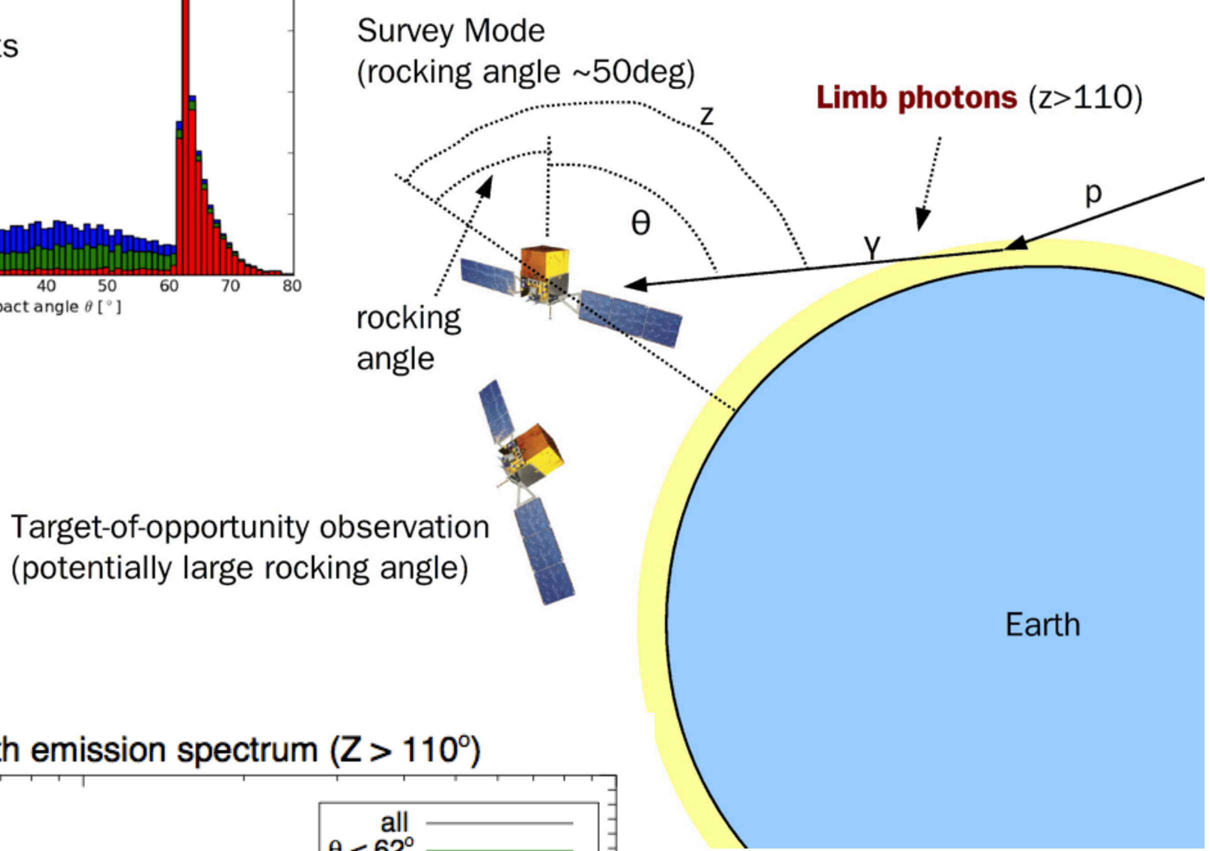

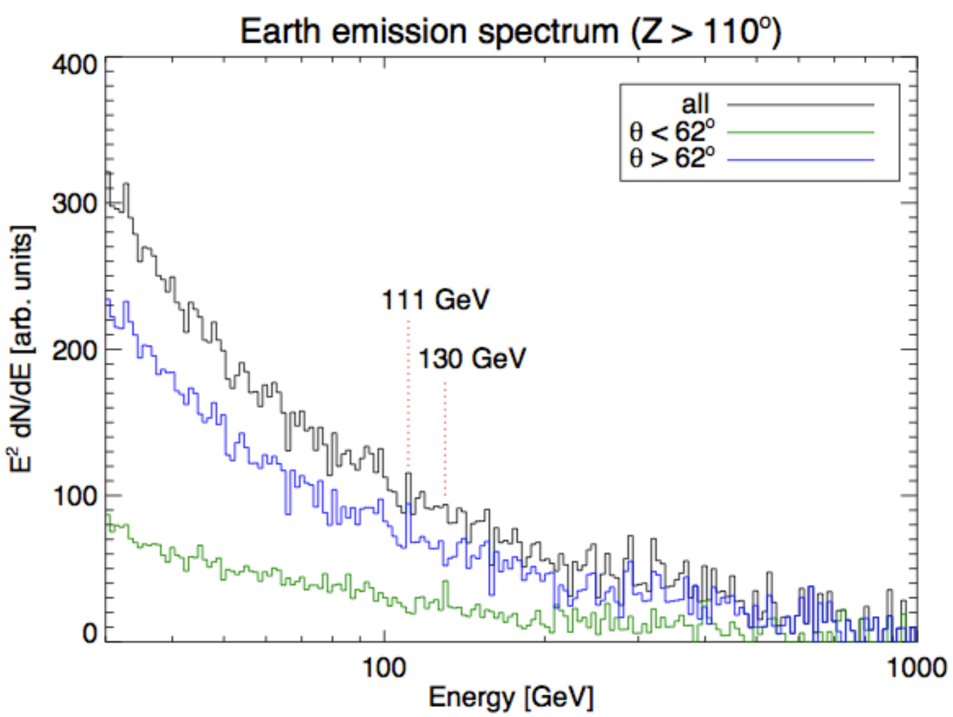

Dark Matter ?

$$\langle \sigma v \rangle_{\gamma\gamma} \sim 10^{-27}\ \mathrm{cm}^3/\mathrm{s}$$

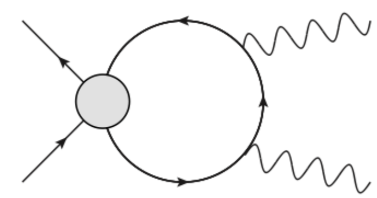

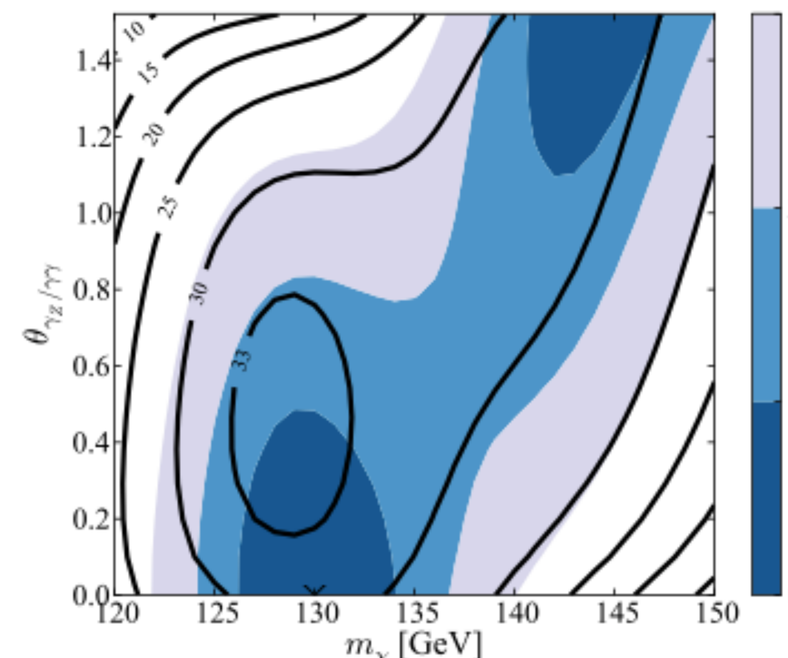

Cohen, Lisanti, Slatyer, Wacker (2012)

130 GeV Line

Instrument Effects?

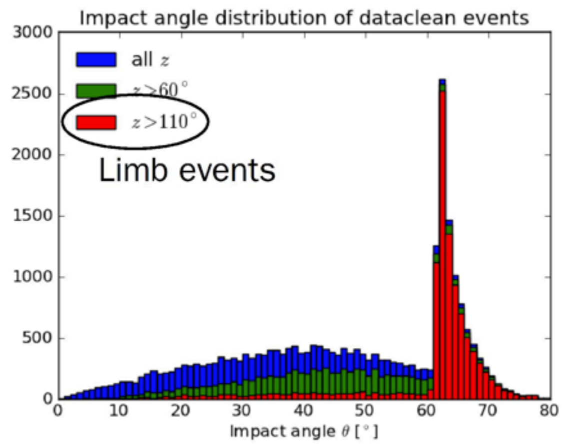

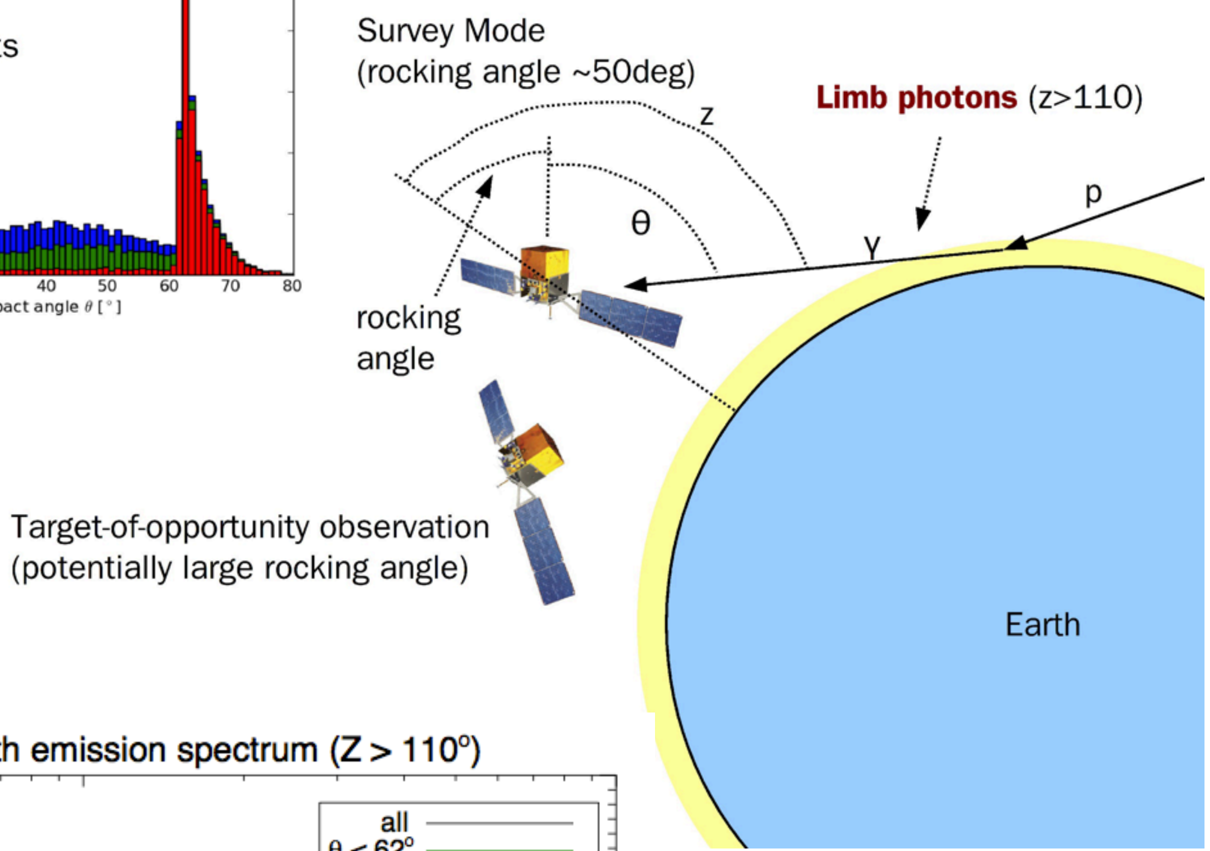

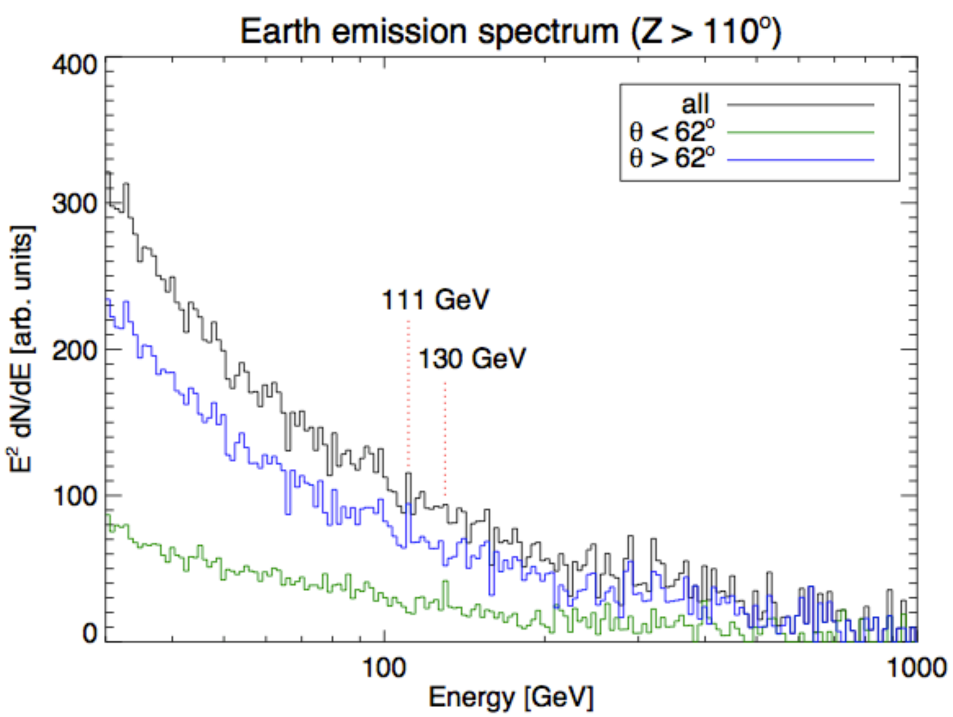

Dark Matter ?

$$\langle \sigma v \rangle_{\gamma\gamma} \sim 10^{-27}\ \mathrm{cm}^3/\mathrm{s}$$

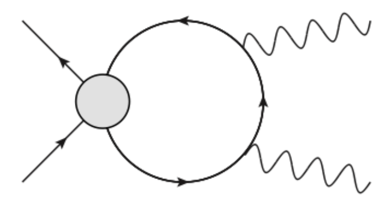

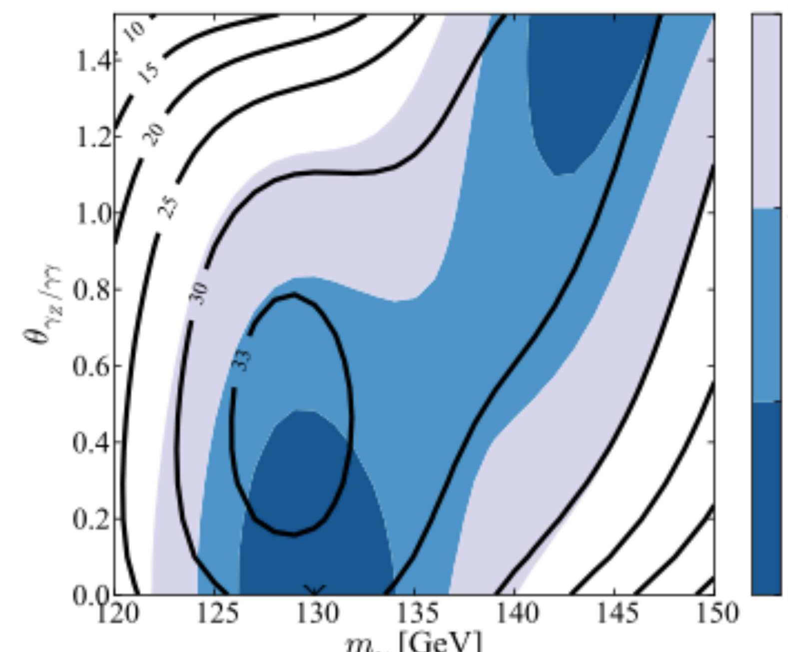

Cohen, Lisanti, Slatyer, Wacker (2012)

<u>How to resolve this ?</u>

Next Fermi Symposium ?

new data: H.E.S.S. II, Fermi-LAT, CTA, GAMMA-400, Neutrinos

Fermi-LAT Pass 6 / 7 / 8

arXiv:1206.1896

- Pass 6 indicates the event analysis scheme designed prior to launch. As such, it was based exclusively on our informed estimates of the cosmic-ray environment at the orbit of *Fermi* and a MC-based evaluation of the LAT performance. After the commissioning phase, as data started accumulating, we observed phenomena that were not reproduced in the MC simulations (see § 2.5 and § 5.2). Without modifying the event analysis in any way, we opted to reduce systematic errors by adding these effects to the MC simulations, and we re-evaluated the LAT performance (in particular we calculated new IRFs, see § 5.2). While this did not allow us to recover any of the lost LAT performance, it ensured that real and simulated data were subject to the same effects and the MC-estimated performance was therefore adequate for science analysis. We have described the initial Pass 6 release (P6_V1) in Atwood et al. (2009), and the corrected IRFs (P6_V3) in Rando & the Fermi LAT Collaboration (2009). We will discuss some improvements that were incorporated into the later P6_V11 IRFs in § 5.4 and § 6.2.

- Pass 7 indicates an improved version of the event analysis, for which we updated parts of the data reduction process to account for known on-orbit effects by making use of the large number of real events the LAT collected in 2 years of operation. The event reconstruction and the overall analysis design were not modified, but the event classification was re-optimized on simulated data-sets including all known on-orbit effects. Large samples of real events were used to assess the efficiency of each step and the systematics involved. Particular attention was paid to increasing effective area below ~ 300 MeV where the impact of on-orbit effects was large, while maintaining tolerable rates of CR contamination at those energies. Event class definitions were optimized based on comparisons of MC events and selected samples of real LAT data. See § 3 for a description of Pass 7.

Pass 8: being developed; redoing everything from the event reconstruction up

Summary <σAV>

Galactic Center

Fermi-LAT: TeVPA 2009, arXiv:0912.3828
Fermi: Goodenough & Hooper. arXiv:0910.2998
Fermi: Dobler et al., arXiv:0910.4583 (Fermi-data)

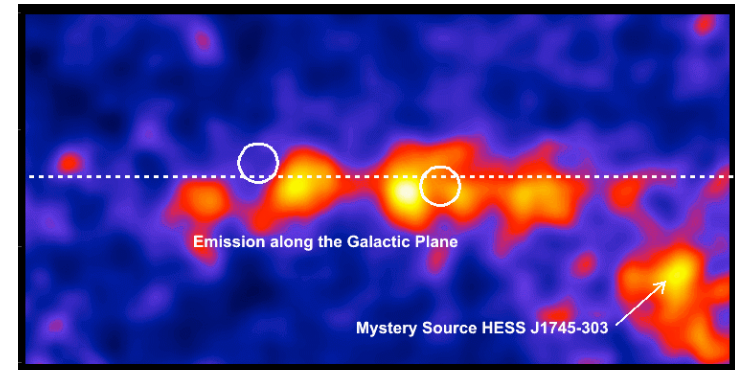

Milky Way Halo

Fermi: Cirelli et. al. Nucl.Phys.B840:284-303,2010
H.E.S.S. Phys.Rev.Lett. 106 (2011) 161301
IceCube: Phys.Rev. D84 (2011) 022004

Dwarf Galaxies and Galaxy Clusters

Fermi-LAT: Astrophys.J.712:147-158,2010
Fermi-LAT: JCAP 1005:025,2010
Fermi: Scott, J.C. et al.: JCAP 1001:031, 2010
H.E.S.S.: Astropart.Phys. 34 (2011) 608-616
MAGIC: Astrophys.J. 697 (2009) 1299-1304
VERITAS: Astrophys.J. 720 (2010) 1174-1180

Extra Galactic

Fermi-LAT: JCAP 1004:014,2010
Fermi: Akorvazian et al. JCAP 1011:041,2010
Fermi: Huetsi et. al. arXiv:1004.2036 (JCAP)

Lines

Fermi-LAT: Phys.Rev.Lett. 104:091302,2010
Fermi: Vertongen & Weniger, JCAP1105(2011)027;
Fermi: Bringmann et al., arXiv:1203.1312
Fermi: Weniger, arXiv:1204.2797
Fermi-LAT: arXiv:1205.2739v1

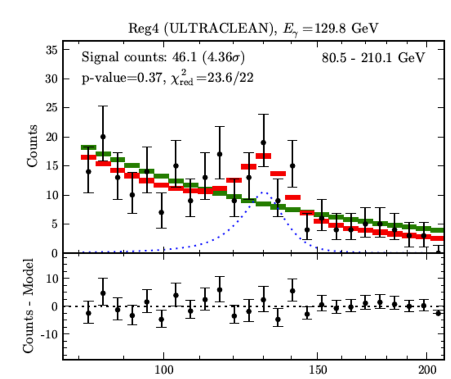

An Effective Theory of Dark Matter

Example for Dirac; similar for Majorana, Real, Complex

Name	Operator		Coefficient
D1	$\bar{\chi}\chi\bar{q}q$	scalar	m_q/M_*^3
D2	$\bar{\chi}\gamma^5\chi\bar{q}q$		im_q/M_*^3
D3	$\bar{\chi}\chi\bar{q}\gamma^5 q$		im_q/M_*^3
D4	$\bar{\chi}\gamma^5\chi\bar{q}\gamma^5 q$		m_q/M_*^3
D5	$\bar{\chi}\gamma^\mu\chi\bar{q}\gamma_\mu q$	vector	$1/M_*^2$
D6	$\bar{\chi}\gamma^\mu\gamma^5\chi\bar{q}\gamma_\mu q$		$1/M_*^2$
D7	$\bar{\chi}\gamma^\mu\chi\bar{q}\gamma_\mu\gamma^5 q$		$1/M_*^2$
D8	$\bar{\chi}\gamma^\mu\gamma^5\chi\bar{q}\gamma_\mu\gamma^5 q$	axial-vector	$1/M_*^2$
D9	$\bar{\chi}\sigma^{\mu\nu}\chi\bar{q}\sigma_{\mu\nu} q$	tensor	$1/M_*^2$
D10	$\bar{\chi}\sigma_{\mu\nu}\gamma^5\chi\bar{q}\sigma_{\alpha\beta} q$		i/M_*^2
D11	$\bar{\chi}\chi G_{\mu\nu}G^{\mu\nu}$	scalar	$\alpha_s/4M_*^3$
D12	$\bar{\chi}\gamma^5\chi G_{\mu\nu}G^{\mu\nu}$		$i\alpha_s/4M_*^3$
D13	$\bar{\chi}\chi G_{\mu\nu}\tilde{G}^{\mu\nu}$		$i\alpha_s/4M_*^3$
D14	$\bar{\chi}\gamma^5\chi G_{\mu\nu}\tilde{G}^{\mu\nu}$		$\alpha_s/4M_*^3$

Invariant under Lorentz symmetry and U(1)em

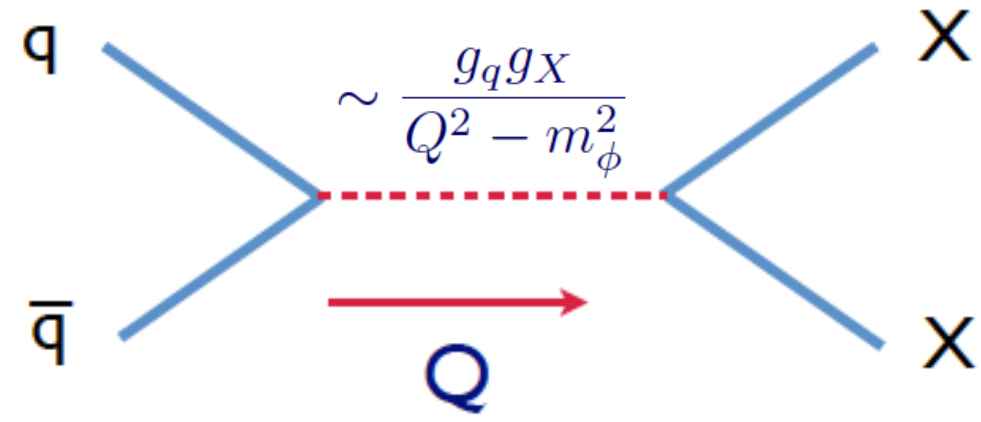

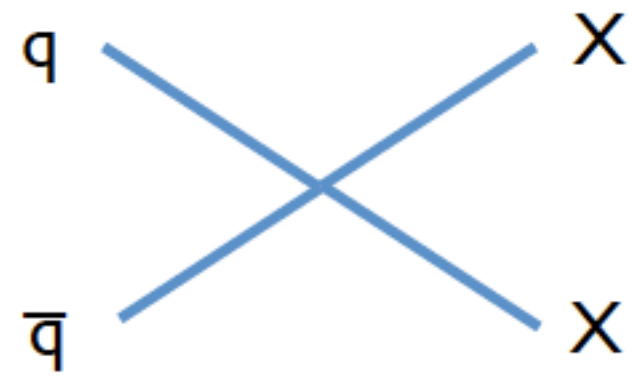

$$Q \ll m_\phi$$

$$M_* = m_\phi/\sqrt{g_q g_X}$$

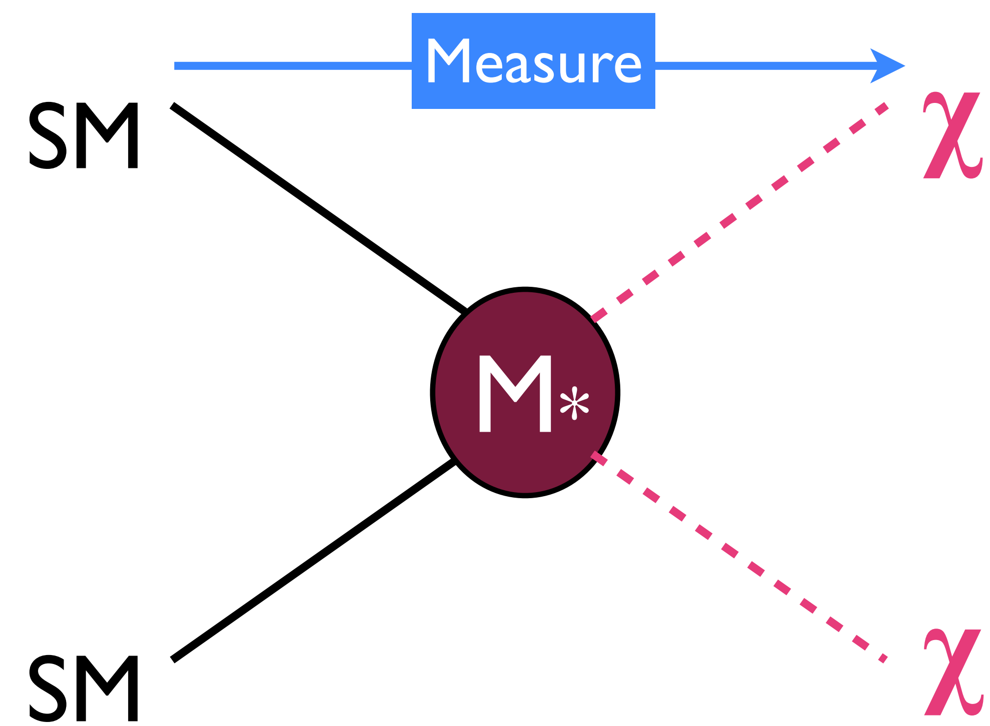

An Effective Theory of Dark Matter

Example for Dirac; similar for Majorana, Real, Complex

Name	Operator		Coefficient
D1	$\bar{\chi}\chi\bar{q}q$	scalar	m_q/M_*^3
D2	$\bar{\chi}\gamma^5\chi\bar{q}q$		im_q/M_*^3
D3	$\bar{\chi}\chi\bar{q}\gamma^5 q$		im_q/M_*^3
D4	$\bar{\chi}\gamma^5\chi\bar{q}\gamma^5 q$		m_q/M_*^3
D5	$\bar{\chi}\gamma^\mu\chi\bar{q}\gamma_\mu q$	vector	$1/M_*^2$
D6	$\bar{\chi}\gamma^\mu\gamma^5\chi\bar{q}\gamma_\mu q$		$1/M_*^2$
D7	$\bar{\chi}\gamma^\mu\chi\bar{q}\gamma_\mu\gamma^5 q$		$1/M_*^2$
D8	$\bar{\chi}\gamma^\mu\gamma^5\chi\bar{q}\gamma_\mu\gamma^5 q$	axial-vector	$1/M_*^2$
D9	$\bar{\chi}\sigma^{\mu\nu}\chi\bar{q}\sigma_{\mu\nu}q$	tensor	$1/M_*^2$
D10	$\bar{\chi}\sigma_{\mu\nu}\gamma^5\chi\bar{q}\sigma_{\alpha\beta}q$		i/M_*^2
D11	$\bar{\chi}\chi G_{\mu\nu}G^{\mu\nu}$	scalar	$\alpha_s/4M_*^3$
D12	$\bar{\chi}\gamma^5\chi G_{\mu\nu}G^{\mu\nu}$		$i\alpha_s/4M_*^3$
D13	$\bar{\chi}\chi G_{\mu\nu}\tilde{G}^{\mu\nu}$		$i\alpha_s/4M_*^3$
D14	$\bar{\chi}\gamma^5\chi G_{\mu\nu}\tilde{G}^{\mu\nu}$		$\alpha_s/4M_*^3$

Invariant under Lorentz symmetry and U(1)$_{em}$

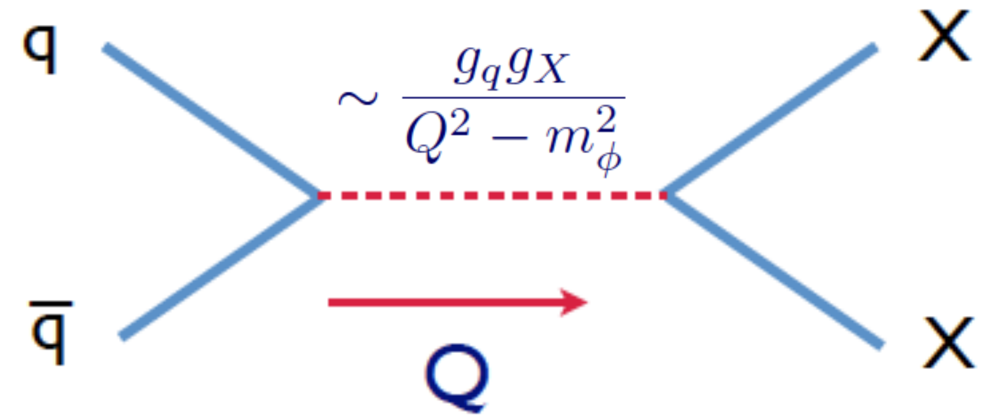

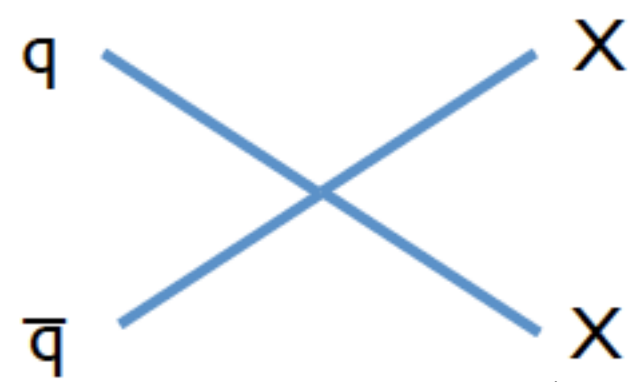

$Q \ll m_\phi$

$M_* = m_\phi / \sqrt{g_q g_\chi}$

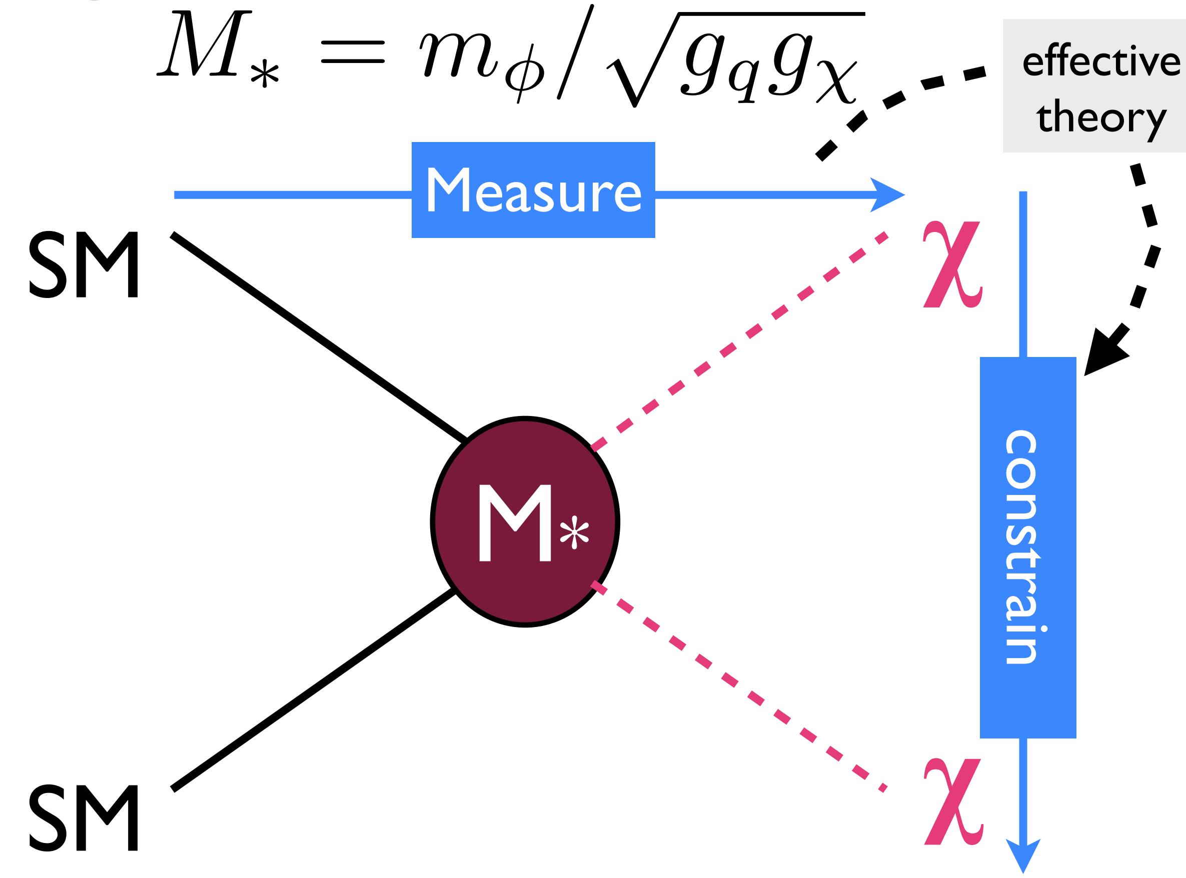

Accelerator Bounds - Monojets

Bai et.al. JHEP1012

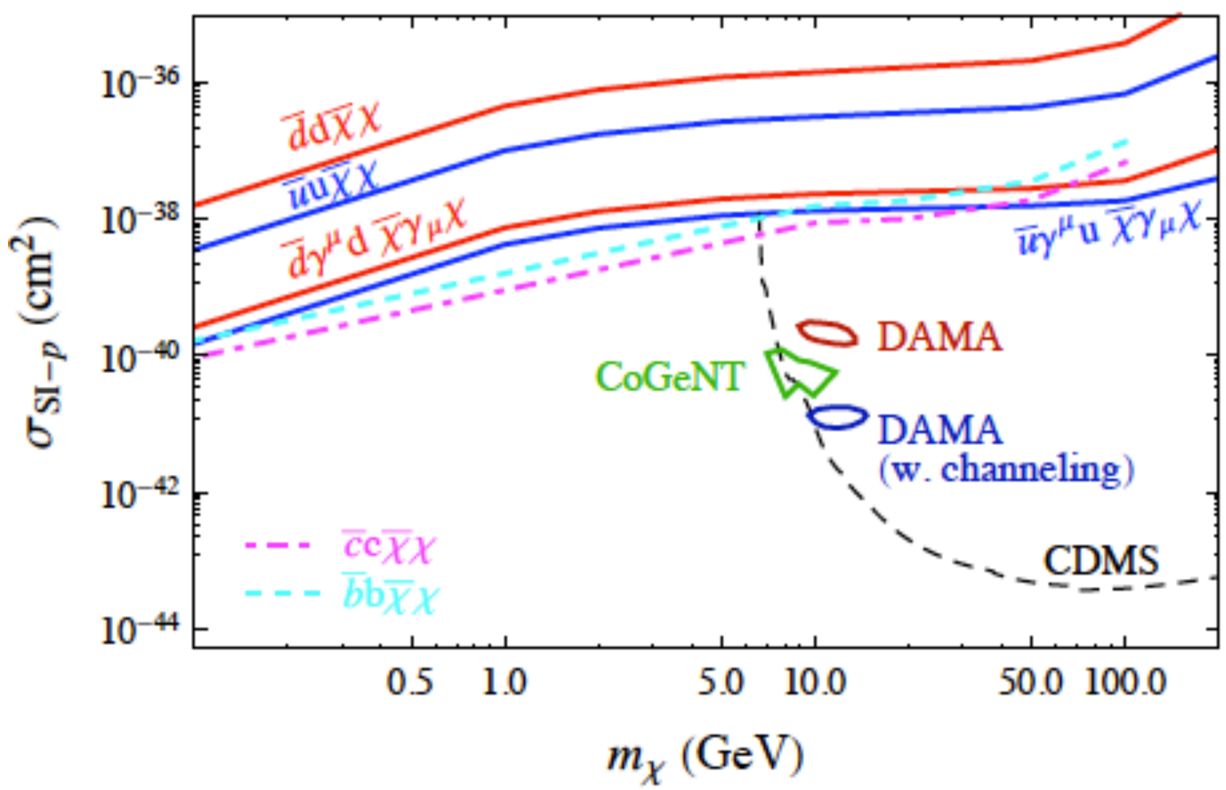

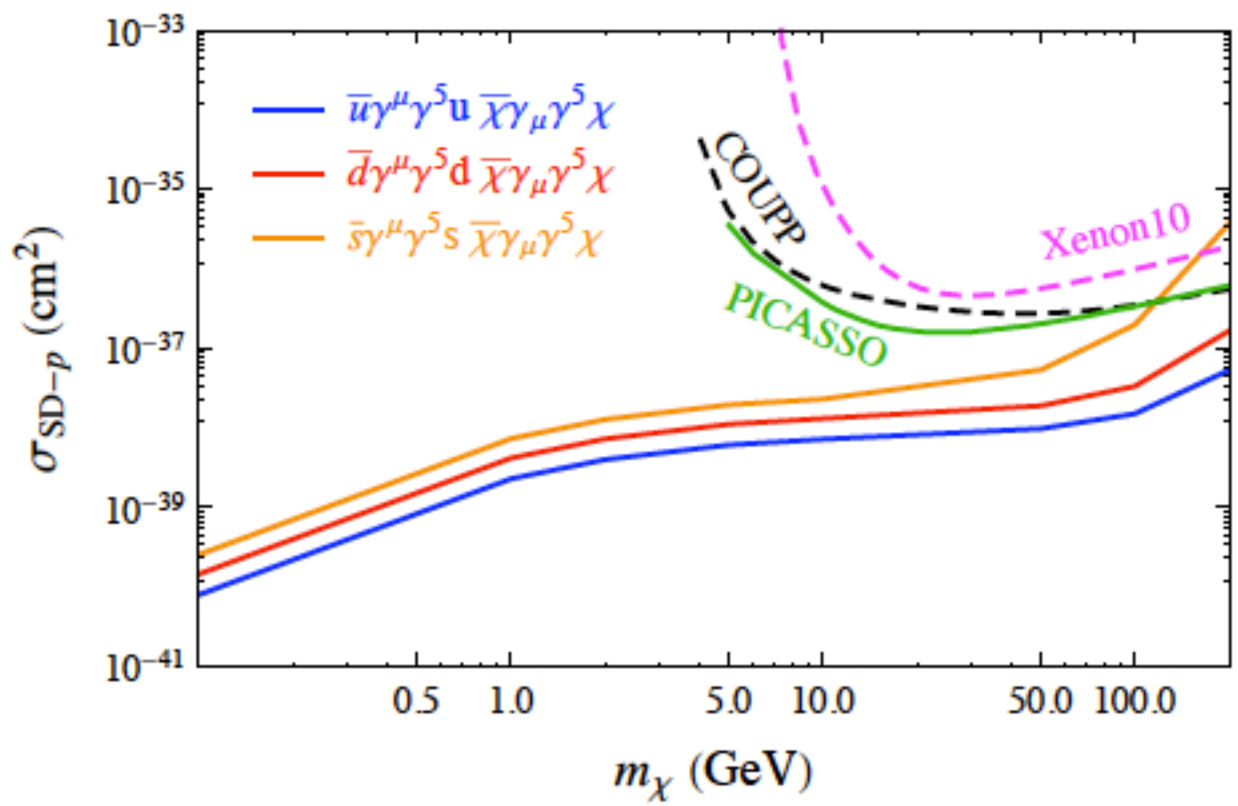

Paper analyzed implications of CDF monojet search in "direct detection" plane

Accelerator Bounds

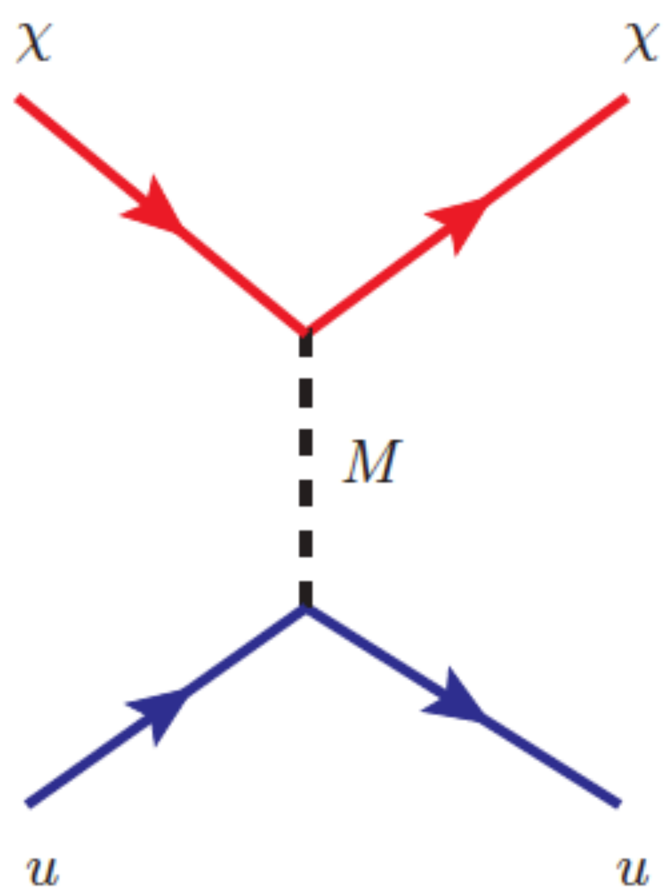

Bai et.al. JHEP1012

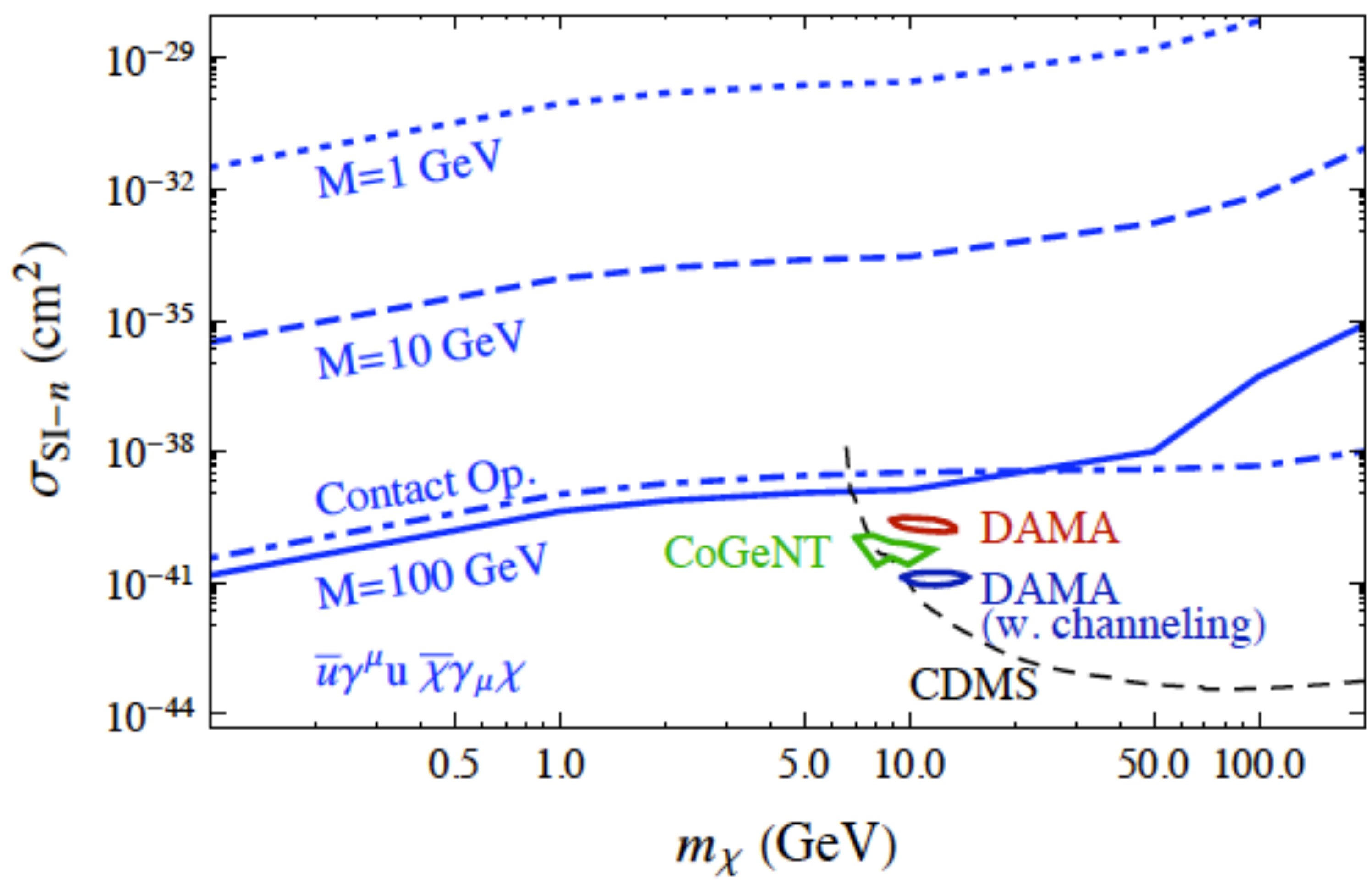

Direct detection enhanced over collider production if exchange has light mediator

M < p_T(1jet)

ATLAS Monojet + MET

Name	Initial state	Type	Operator
D1	qq	scalar	$\frac{m_q}{M_\star^3}\bar{\chi}\chi\bar{q}q$
D5	qq	vector	$\frac{1}{M_\star^2}\bar{\chi}\gamma^\mu\chi\bar{q}\gamma_\mu q$
D8	qq	axial-vector	$\frac{1}{M_\star^2}\bar{\chi}\gamma^\mu\gamma^5\chi\bar{q}\gamma$
D9	qq	tensor	$\frac{1}{M_\star^2}\bar{\chi}\sigma^{\mu\nu}\chi\bar{q}$
D11	gg	scalar	$\frac{1}{4M_\star^3}\bar{\chi}\chi\alpha_s($

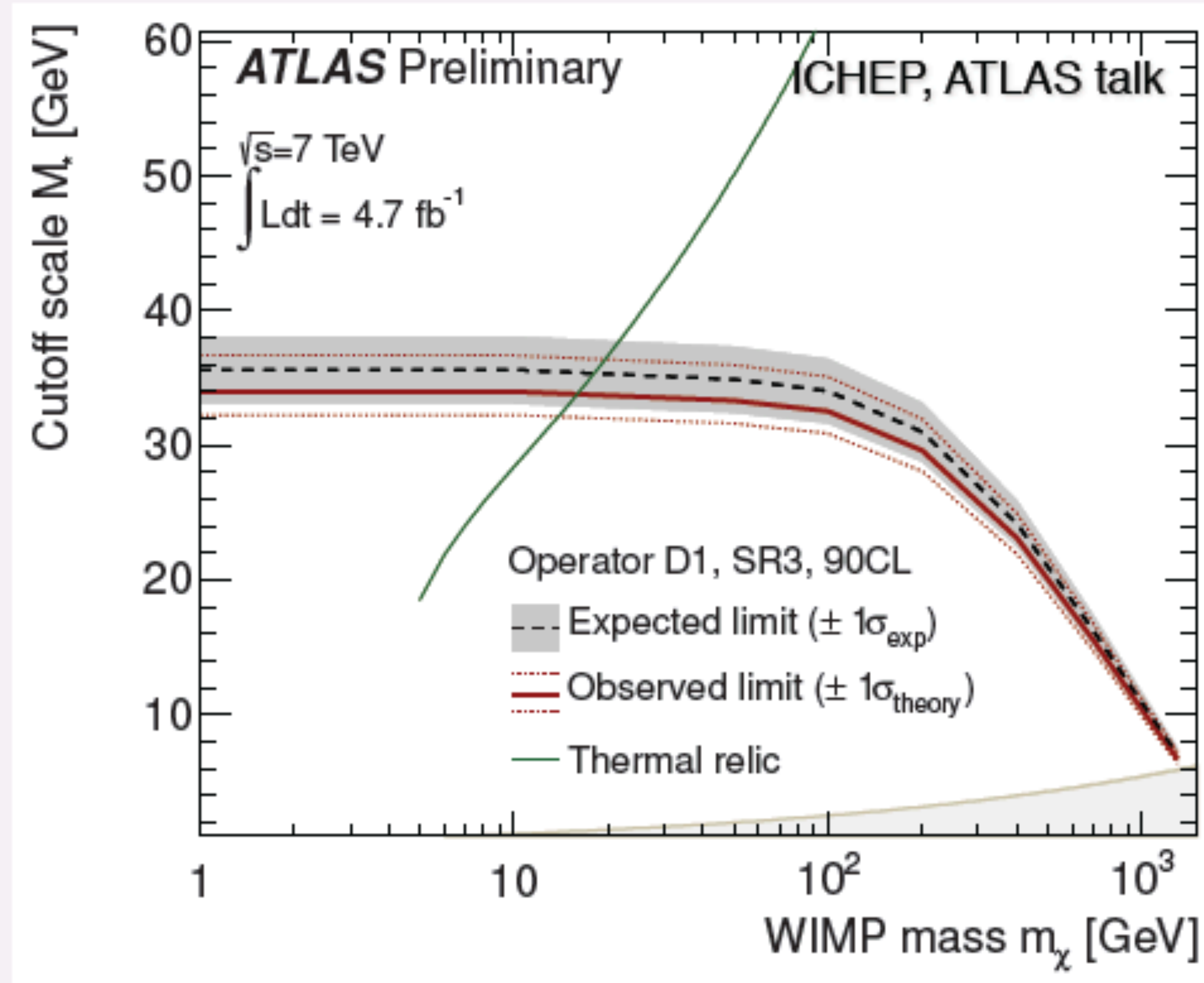

- one jet with P_T > 120/220 GeV
- MET > 350/500 GeV
- 3rd jet veto of P_T>30 GeV
- e (mu) veto of P_T > 20 (7) GeV

S. Su

No evidence for anomalous signal

Fermi Positron Fraction

- Fermi observes increase in positron fraction from 20 to 200GeV consistent with PAMELA
- Positron fraction measurement Uses the Earth's Magnetic Field

Fermi LAT Collaboration, PRL 108, 011103 (2012)

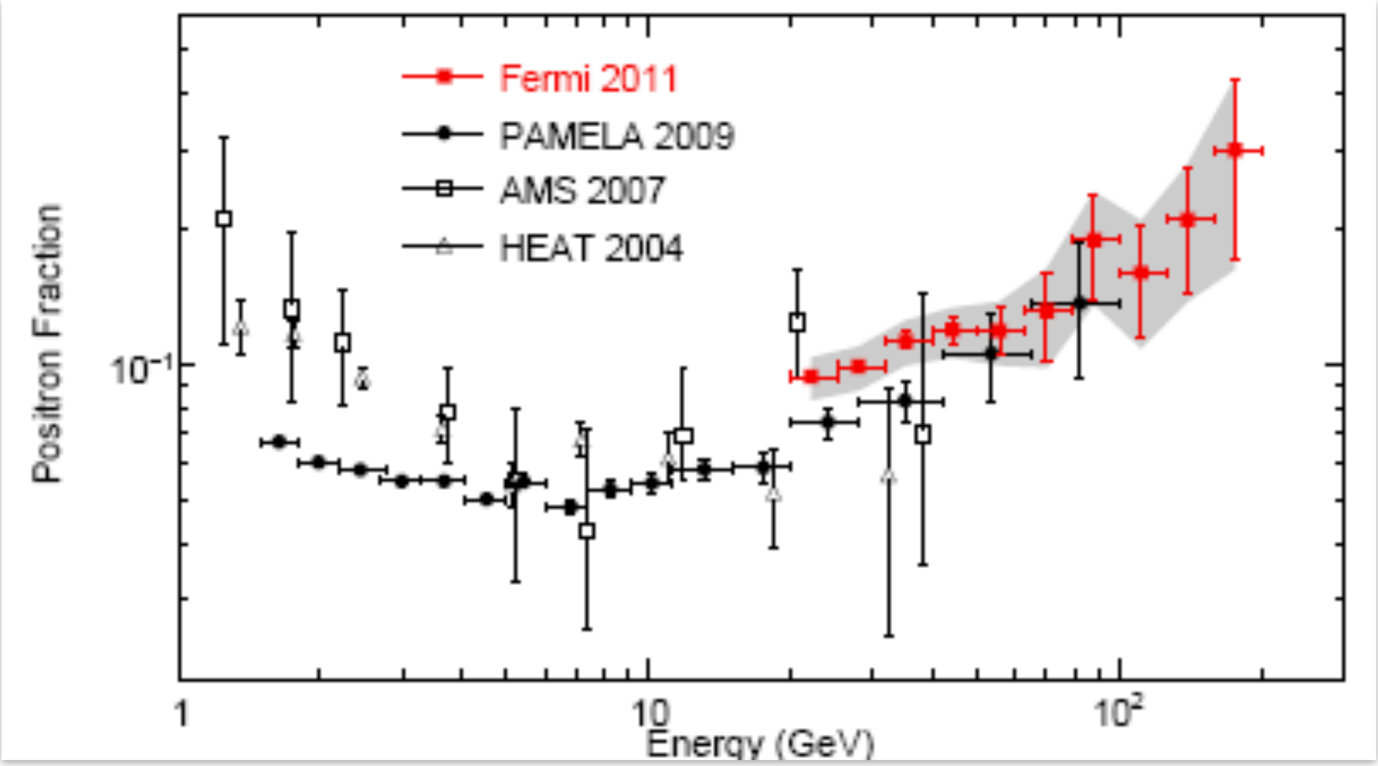

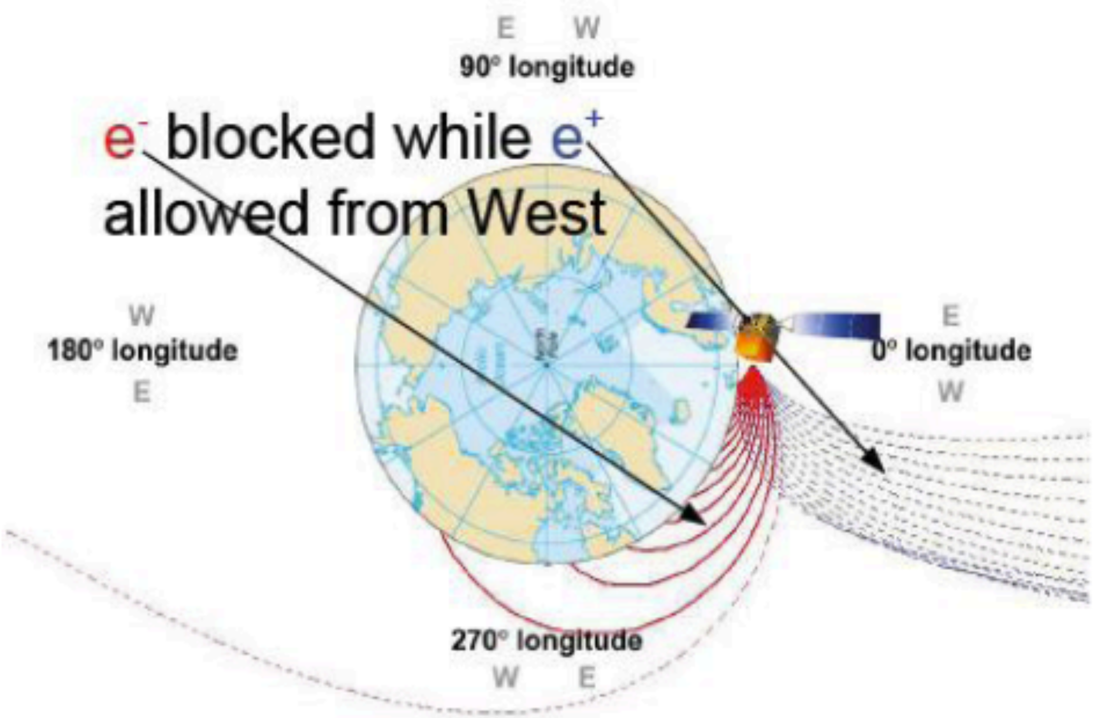

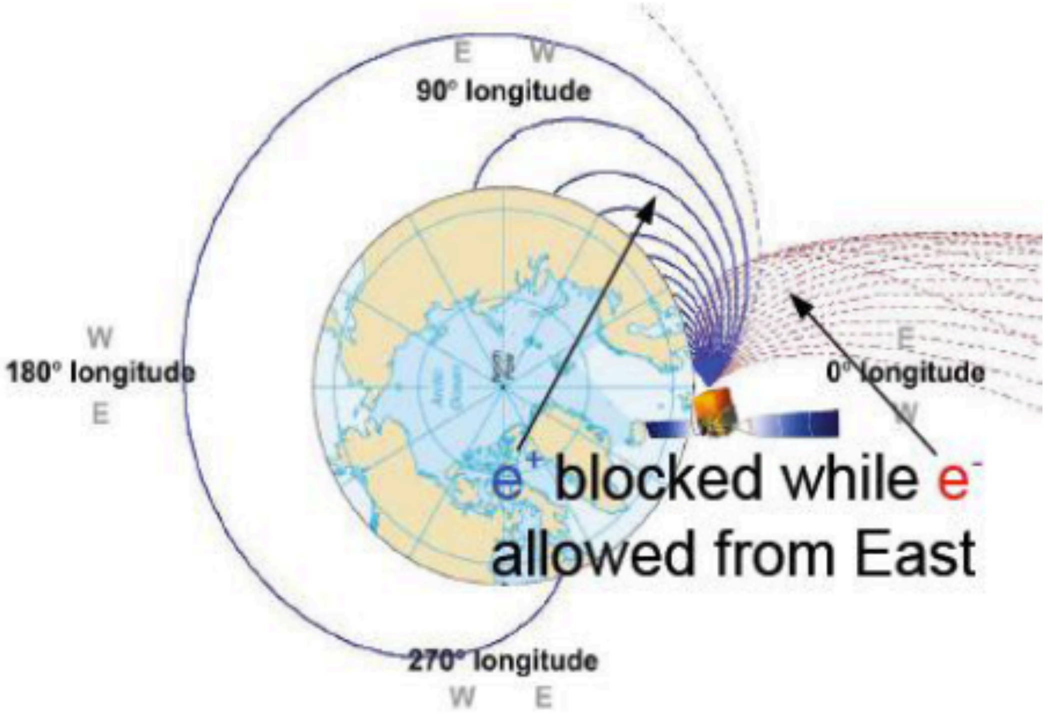

IC79 Solar WIMP

② Event Selection (Winter, High energy, 151days)

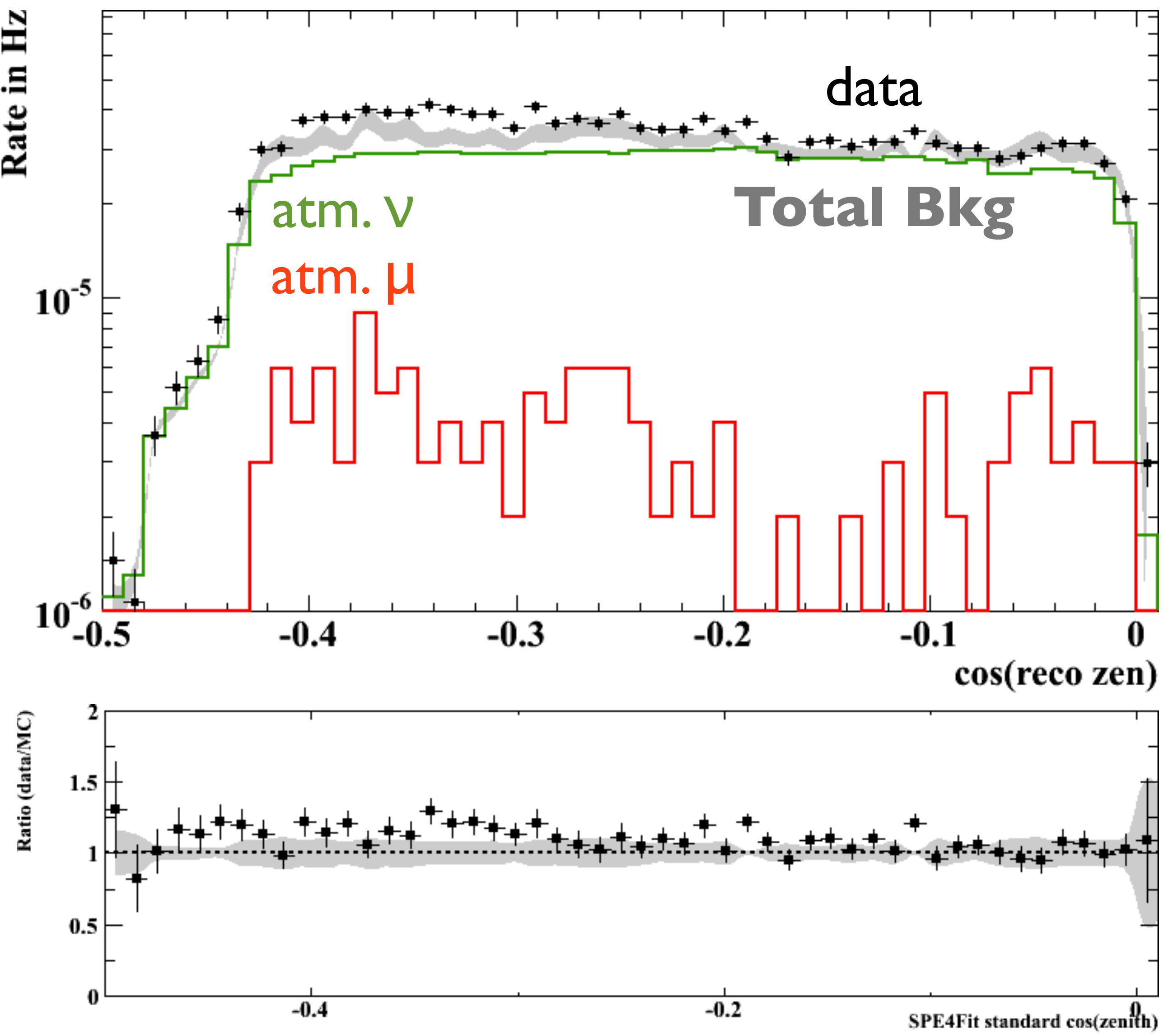

① Event Selection (Summer, Low energy, 166days)

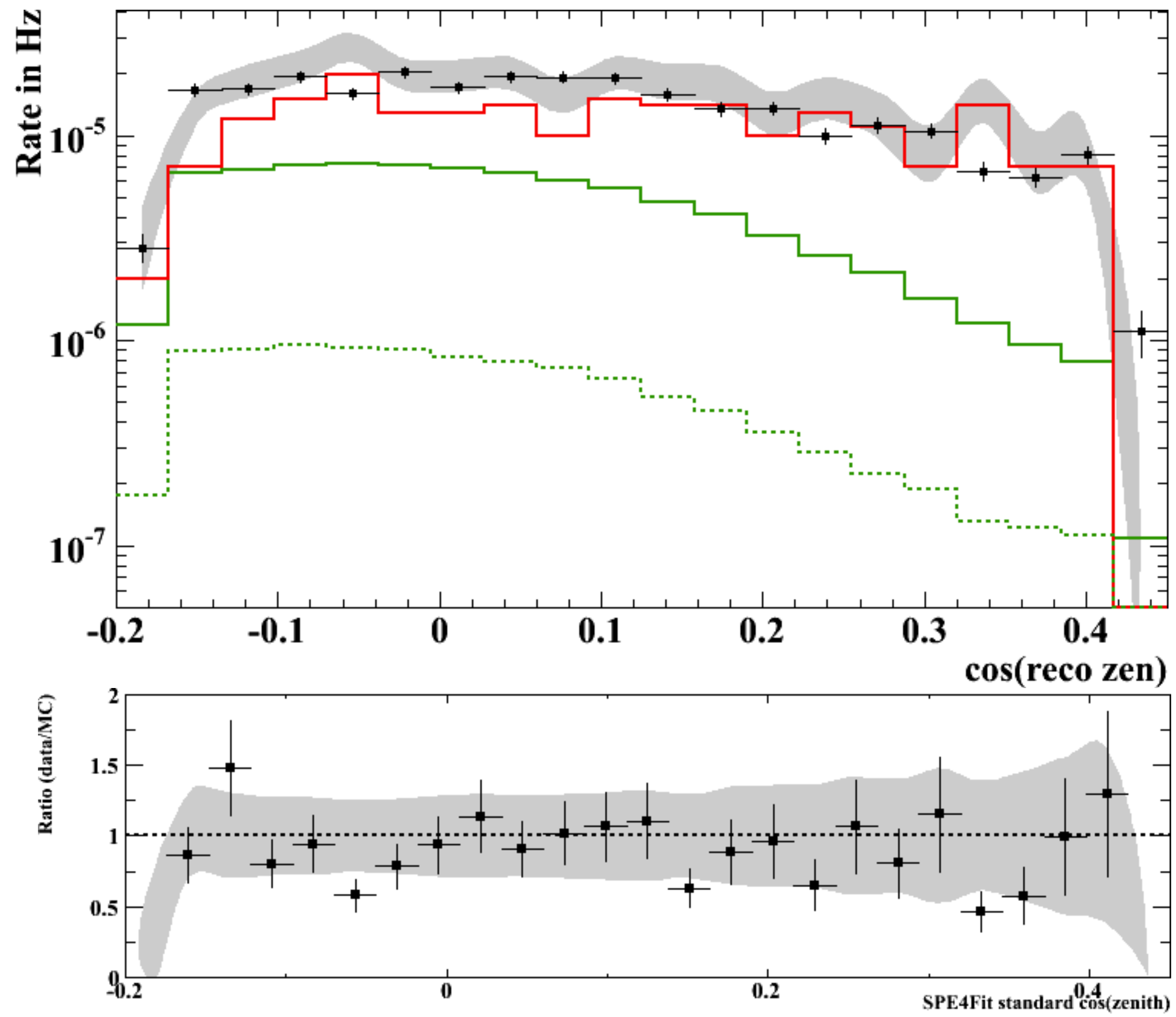

- Event selection with separate BDT
- Training on off-source data + signal simulation
- Optimized final cut on BDT output
  - run llh-analysis for various selection criteria to determine best sensitivity

Fermi Large Area Telescope (LAT)

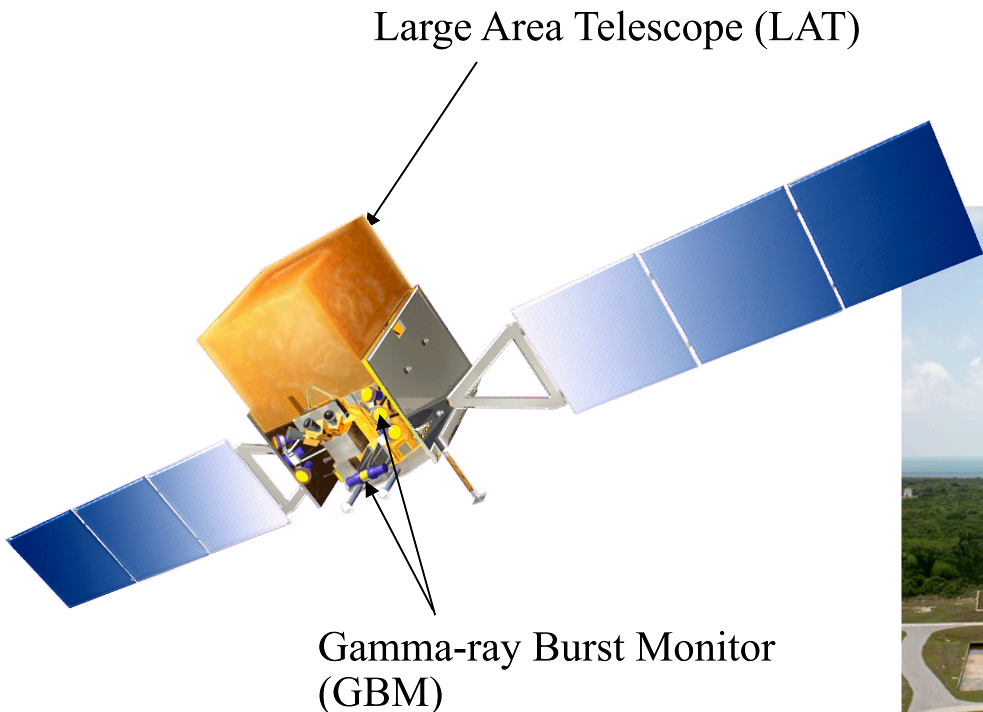

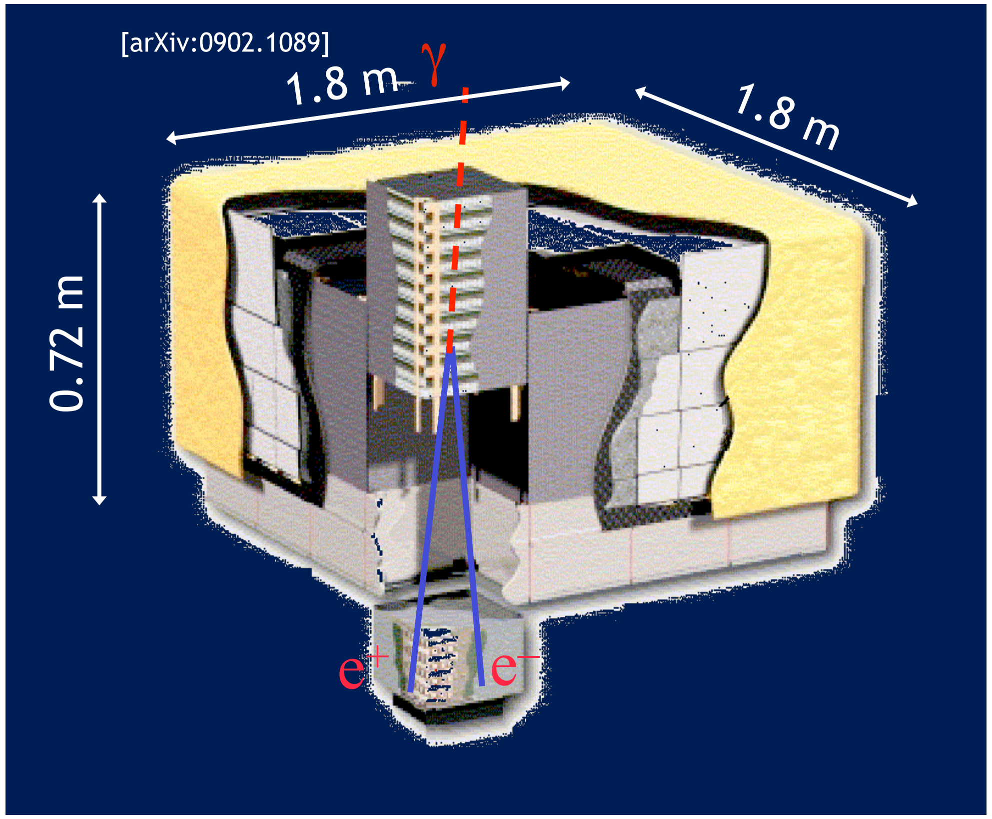

- Pair conversion telescope
- Launched June 11, 2008
- Energy range 20MeV - 300GeV
- γ-ray angular resolution ~0.1° (@10GeV) [~3.5° (@100MeV)]
- 2.5sr FoV
- Effective area ~ 1m^2

- Pair conversion telescope
- Tracking detector: 16 tungsten foils + 18 pairs of SI strip detectors
- Calorimeter: ~8.5 radiation length - 8 layers of CsI logs
- Anti-coincidence detector: 89 scintillating tiles ~99.97% efficient for MIPs

Fermi Large Area Telescope (LAT)

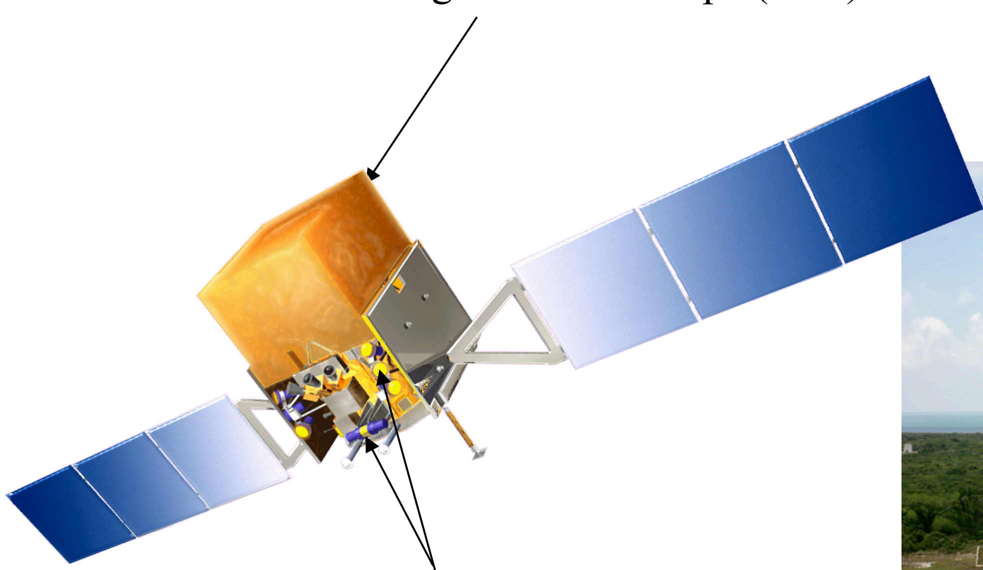

- Pair conversion telescope
- Launched June 11, 2008
- Energy range 20MeV - 300GeV
- γ-ray angular resolution ~0.1° (@10GeV) [~3.5° (@100MeV)]
- 2.5sr FoV
- Effective area ~ 1m^2

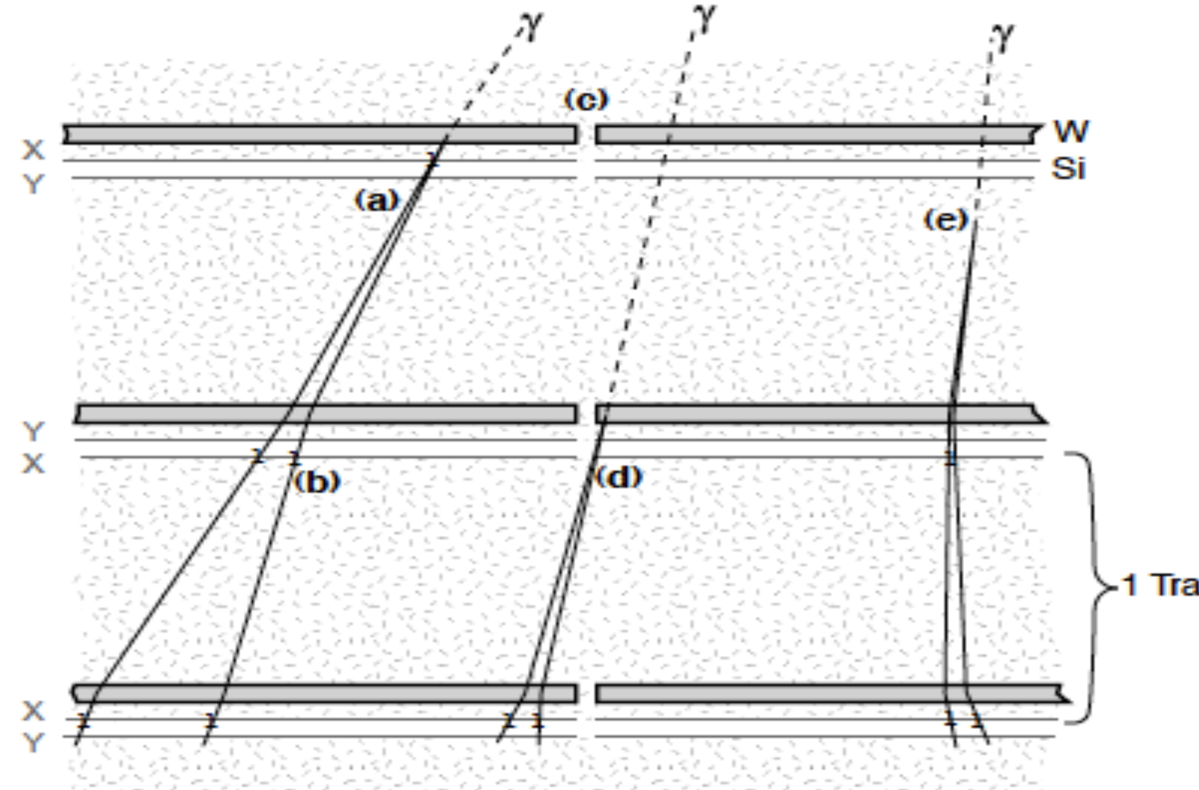

- Pair conversion telescope
- Tracking detector: 16 tungsten foils + 18 pairs of SI strip detectors
- Calorimeter: ~8.5 radiation length - 8 layers of CsI logs
- Anti-coincidence detector: 89 scintillating tiles ~99.97% efficient for MIPs

GAMMA-400

arXiv:1201.2490

- Energy range 100 MeV - 3 TeV
- Angular resolution ~1-2° (~0.01°) @100MeV (100GeV)
- Energy resolution ~1% at 100GeV
- Effective area of ~4m^2 at E_γ = 100 GeV
- Launch of the GAMMA-400 space observatory is planned in 2018

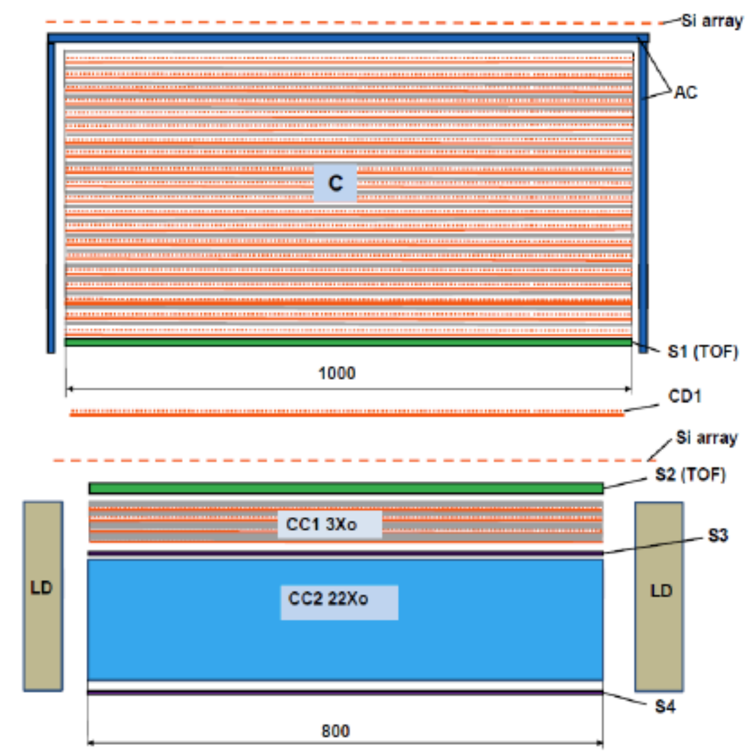

Table 1. A comparison of basic parameters of space-based and ground-based instruments

	SPACED-BASED					GROUND-BASED			
	EGRET	AGILE	Fermi	CALET	**GAMMA -400**	H.E.S.S.	MAGIC	VERITAS	CTA
Energy range, GeV	0.03-30	0.03-50	0.1-300	10-10000	**0.1-3000**	>100	>50	>100	>10
Angular resolution, deg (E_γ > 100 GeV)	0.2 $E_\gamma \sim$ 0.5 GeV	0.1 $E_\gamma \sim$ 1 GeV	0.1	0.1	**~0.01**	0.1	0.1	0.1	0.1
Energy resolution, % (E_γ > 100 GeV)	15 $E_\gamma \sim$ 0.5 GeV	50 $E_\gamma \sim$ 1 GeV	10	2	**~1**	15	20	15	15

Sommerfeld Enhancement

- DM annihilation cross section in the low velocity regime can be enhanced through the "Sommerfeld effect"
  - when non-relativistic particles interact through some kind of force, their wave function is distorted by the presence of a potential
    - In QFT this corresponds to contributions of "ladder" Feynman diagrams
      - gives rise to (non-perturbative) corrections to cross section

$$\sigma v = S \, \underline{(\sigma v)_0}$$

"Sommerfeld boost"

tree level cross section times velocity

http://arxiv.org/pdf/0812.0360

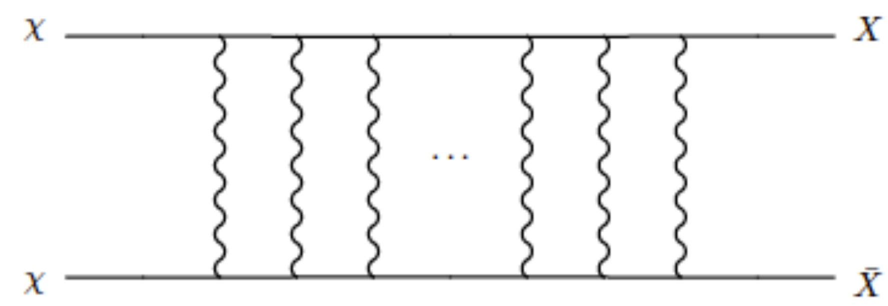

FIG. 1: Ladder diagram giving rise to the Sommerfeld enhancement for $\chi\chi \to X\overline{X}$ annihilation, via the exchange of gauge bosons.

- Simple case: a particle interacting through Yukawa potential:

Schroedinger Equation

$$\frac{1}{m}\frac{d^2\psi(r)}{dr^2} - V(r)\psi(r) = -m\beta^2\psi(r)$$

$\Psi(r)$ is reduced two-body wave function for s-wave annihilation

$V(r) = -\frac{\alpha}{r}e^{-m_V r}$ attractive Yukawa potential mediated by a boson of mass m_V

for m_V small the potential becomes Coulomb-like and Schrödinger equation can be solved analytically

$$S = \frac{\pi\alpha}{\beta}(1 - e^{-\pi\alpha/\beta})^{-1}$$ ~1/v

WIMP Nucleon Interaction

- The nucleon coupling of a slow-moving Majorana neutralino (or of any WIMP in the extreme non-relativistic limit) is characterized by two terms: spin-dependent (axial vector) and spin-independent (scalar).

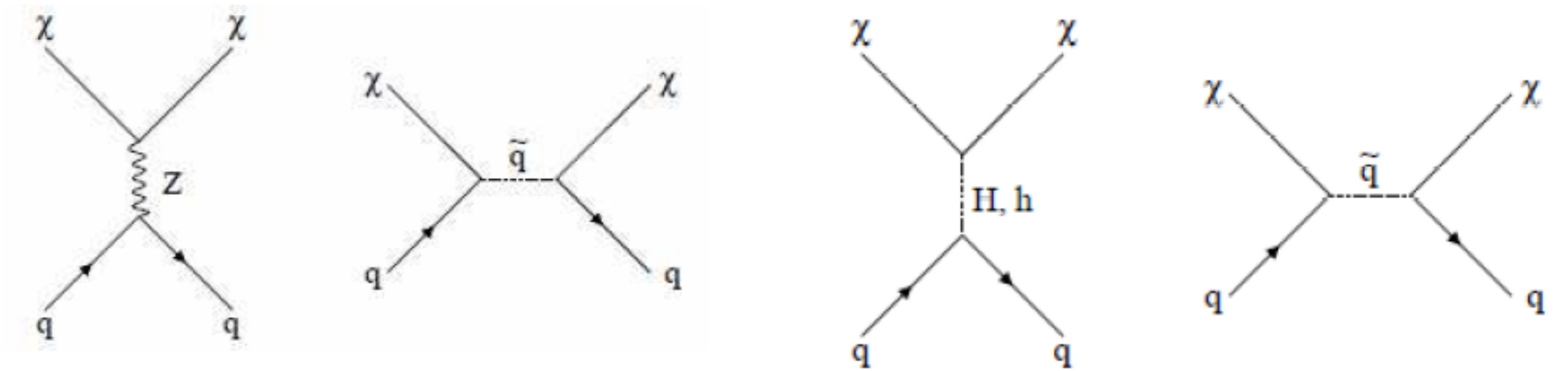

$$\sigma_{SD} = 32\frac{G_F^2\mu^2}{\pi}(a_p\{S_{p(N)}\} + a_n\{S_{n(N)}\})^2\frac{J+1}{J}$$

$$\mu = M_\chi M_N \ / \ M_\chi + M_N$$

- J - coupled angular momentum of the nucleus
- $\{S_{n(N)}\}$ spin of neutron in nucleus
- a_n ,a_p - coupling constants / G_F - Fermi constant

$$\sigma_{SI} = \frac{4\mu^2}{\pi}(Zf_p + (A-Z)f_n)^2F^2(q)$$

- f_p , f_n - coupling constants to proton and neutron
- F(q) form factor